Sugar Conjugates of 3-Hydroxy-4-pyridinones
Synthesis and Investigations into their Potential for Drug Delivery to the Brain.

Fuchs, Ferdinand Christian

Awarding institution:
King's College London

KING'S College LONDON

Sugar Conjugates of 3-Hydroxy-4-pyridinones: Synthesis and Investigations into their Potential for Drug Delivery to the Brain.

by

Ferdinand C. Fuchs

Supervisors: Dr. Gerd Wagner and Prof. Robert Hider

A thesis submitted in partial fulfillment for
the degree of Doctor of Philosophy

in the
Faculty of Life Sciences & Medicine
Institute of Pharmaceutical Science

Submitted:
25th November 2014

Corrections Submitted:
23rd April 2015

Declaration of Authorship

I, Ferdinand Christian Fuchs, declare that this thesis titled, "Sugar Conjugates of 3-Hydroxy-4-pyridinones: Synthesis and Investigations into their Potential for Drug Delivery to the Brain" and the work presented in it are my own. Where information has been derived from other sources, I confirm that this has been indicated in the thesis.

Signed: _____

Date: _____

"I have not failed. I've just found 10,000 ways that won't work."

Thomas A. Edison (attributed)

Abstract

Sugar Conjugates of 3-Hydroxy-4-pyridinones:
Synthesis and Investigations into their Potential
for Drug Delivery to the Brain.

by Ferdinand C. Fuchs

Parkinson's disease is the second most common neurodegenerative disease after Alzheimer's disease, with an incidence of 8-18 cases per 100,000 per year and currently about 125,000 cases in the UK. While lifestyle and genetic risk factors for Parkinson's disease have been identified, the aetiology remains unclear. The current treatment options are limited to the management of symptoms. Iron is misdistributed and accumulates in the affected brain regions (particularly the *substantia nigra*) as the disease progresses. Iron chelation has been identified as a treatment that slows down disease progression, demonstrating promising results in two clinical trials. Currently available iron chelators only enter the brain to a very limited extent, which restricts their use for the treatment of Parkinson's disease due to low effective doses achieved in the brain and potential systemic side effects. This thesis focused on the development of novel iron chelators that have been conjugated to sugars. In principle, this strategy could lead to the targeting of molecules to the brain and increase their penetration by facilitated transport across the blood-brain barrier by the glucose transporter GLUT1. The molecules are based on the 3-hydroxypyridin-4-one scaffold, which is the basis of the clinically used iron chelator deferiprone.

Hydroxypyridinone iron chelators could be linked to the sugars via ether, amide and triazole linkers, but the deprotection of the resulting conjugates could only be achieved for some molecules, while others could not be successfully deprotected without degradation of the desired conjugate.

Thirteen molecules were tested in blood-brain barrier assays based on primary cells from porcine brain endothelial microvessels. The tested chelators did not, however show greater blood-brain barrier permeability when compared to similar non-glycosylated chelators. Instead, permeability was low and correlated with the substances' lipophilicity. This indicates that glycosylation alone is not sufficient for the transport of the conjugates and may hinder permeability. In order to increase a compound's brain permeability by glucosylation, the transporter's substrate binding specificity needs to be considered.

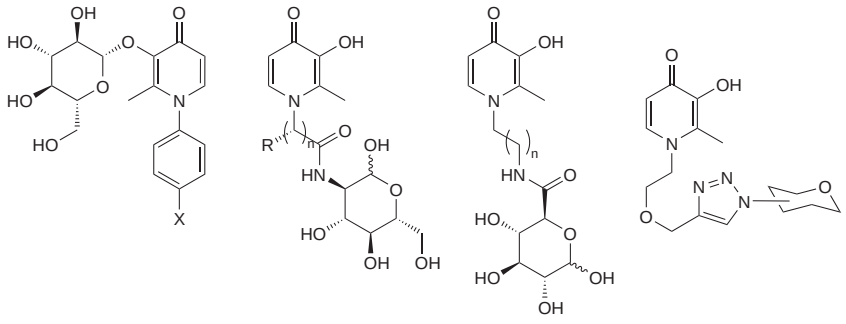

Acknowledgements

I am deeply grateful to my supervisors Dr Gerd Wagner and Prof Robert (Bob) Hider. They gave me the opportunity to work on this fascinating project and supported me with enthusiasm, patience, advice and encouragement, even at times when I had doubts myself. Big thanks also go to Dr Jane Preston for the opportunity to work on blood-brain barrier models guided by her expertise. She answered many questions in all related aspects and resolving any doubts about my data.

Thank you, to every past and present member of the laboratories (5.113/115/118) of the Medicinal Chemistry/Chemical Biology group, the Blood-Brain Barrier groups and all the PhD students on the fifth floor of FWB. First and foremost, I want to thank Dr Lauren Tedaldi, for brightening the lab with her indefatigable energy and upbeat persona, lending me an ear and engaging in many discussion, chemical and non-chemical. I am grateful to Drs Vincenzo Abbate and Yongmin Ma for helping me with any question I had about the mysteries of hydroxypyridinones. Anna Pöschl who always found time for me, in any case, whether it was for gossip, jokes or complaints, or activities after work.

Special thanks go to Ana Georgian, who introduced a chemist to the 'dark arts' of primary cell culture work, and was being helpful and accommodating beyond measure.

Shen Liu and Yongping Yu from Zheijang University, China, who supplied additional HPO-sugar conjugates for testing and gave advice on the synthesis.

Dr Neil Brown and Dr Piers Gaffney from Imperial College London who kindly provided access to a high pressure hydrogenation apparatus.

Erasmus students Anna Preisner, Sandra Pusch and particularly Chiara Maniaci shared part of the way with me during this project, became friends, but also challenged me with their questions, making me develop as a chemist but also as a teacher.

Words cannot describe how grateful I am to my girlfriend, who loved me, supported me and gave me the push I needed to carry on, and without whom I could not have produced this thesis.

I would like to thank my family, for their unconditional support and love throughout the whole of my PhD.

List of Contributions

Oral Presentations

KCL Chemical Biology Group Seminar Series	London	June 2011
APS International PharmSci Conference 2011	Nottingham	September 2011
London Iron Metabolism Group PhD/PostDoc Meeting	London	May 2012
KCL IPS Postgraduate Research Symposium	London	May 2013
KCL Chemical Biology Group Seminar Series	London	June 2013
KCL Britannia House Christmas Symposium	London	December 2013
KCL IPS PhD Student Seminar Series	London	February 2014

Poster Presentations

KCL IPS Postgraduate Research Symposium	London	May 2011
APS International PharmSci Conference 2011	Nottingham	September 2011
KCL IPS Postgraduate Research Symposium	London	May 2012
2nd UK & Ireland Early Career BBB Symposium	Liverpool	November 2012
5th IBIS BioIron Meeting	London	April 2013

Contents

List of Figures

List of Schemes

List of Tables

Abbreviations

3OMG	3-*O*-Methyl-D-glucose
ACN	Acetonitrile
AcOH	Acetic acid
AD	Alzheimer's Disease
AET	Active Efflux Transport
atm.	Atmosphere
AUC	Area Under the Curve
AZT	Azidothymidine (INN: Zidovudine)
BBB	Blood-Brain Barrier
Bn	Benzyl, $C_6H_5CH_2$–
BPDS	Bovine Plasma-Derived Serum
$CDCl_3$	Deuterated Chloroform
CD_3OD	Deuterated Methanol
CMT	Carrier-Mediated Transport
CNS	Central Nervous System
CuAAC	Copper Catalysed Azide-Alkyne Cycloaddition
DABCO	1,4-Diazabicyclo[2.2.2]octane
DCC	*N,N'*-Dicyclohexylcarbodiimide
DCM	Dichloromethane, Methylenechloride
DEAD	Diethyl azodicarboxylate
DMEM	Dulbecco's Modified Eagle's medium
DMF	*N,N*-Dimethylformamide
DMSO	Dimethylsulfoxide
DMSO−d_6	Deuterated Dimethylsulfoxide
EDC	1-Ethyl-3-(3-dimethylaminopropyl)carbodiimide hydrochloride
eq.	Equivalents

GLUT1	Glucose Transporter 1 (SLC2A1)
HBA	Hydrogen Bond Acceptor
HBD	Hydrogen Bond Donor
HBSS	Hank's Balanced Salt Solution
HEPES	4-(2-Hydroxyethyl)-1-piperazineethanesulfonic acid
HPLC	High Performance/Pressure Liquid Chromatography
HPO	3-Hydroxypyridin-4(1*H*)-one
HRMS	High Resolution Mass Spectrometry
L-DOPA	L-3,4-Dihydroxyphenylalanine
LAT1	Large Neutral Amino Acid Transporter (SLC3A2, SLC7A5)
m.p.	Melting Point
MCPBA	*meta*-Chloroperoxybenzoic acid
MFS	Major Facilitator Superfamily
MW	Molecular Weight
MPP+	1-methyl-4-phenylpyridinium
MPTP	1-Methyl-4-phenyl-1,2,3,6-tetrahydropyridine
MRP	Multidrug Resistance-Associated Protein
NBDG	6-Deoxy-*N*-(7-nitrobenz-2-oxa-1,3-diazol-4-yl)-aminoglucose
ND	Neurodegenerative Disorder
NHS	*N*-Hydroxysuccinimide
NMR	Nuclear Magnetic Resonance (Spectroscopy)
NSAID	Non-Steroidal Anti-Inflammatory Drug
NSI	Nanospray Ionisation
OATP	Organic Anion Transport Protein (SLCO1-6)
PBEC	Porcine Brain Endothelial Cell
PD	Parkinson's Disease
ppm	parts per million
PSA	Polar Surface Area
***p*-TsOH**	*para*-Toluenesulfonic acid, Tosylic acid
Py−SO_3	Sulfur trioxide-Pyridine complex
quant.	quantitative
RMT	Receptor-Mediated Transport

rt	Room Temperature
SEM	Standard Error of the Mean
SGLT	Sodium-Dependent Glucose Cotransporter
TBAB	Tetrabutylammonium bromide
TBAI	Tetrabutylammonium iodide
TBAS	Tetrabutylammonium hydrogen sulfate
tBuOH	*tert*-Butanol, 2-Methylpropan-2-ol
TEA	Triethylamine
TEAB	Triethylammonium bicarbonate
TEER	Transendothelial Electrical Resistance
Tf	Transferrin
TFA	Trifluoroacetic acid
TfR	Transferrin Receptor
THF	Tetrahydrofuran
TLC	Thin Layer Chromatography
TMS	Tetramethylsilane
TPP	Triphenylphospine
Trt	Trityl, Triphenylmethyl

Chapter 1

Introduction

1.1 Neurodegenerative Diseases

Neurological disorders are a class of disorders of the nervous system. They are a major burden on modern society, affecting one in four people worldwide.[1] In Europe, neurological disorders cause around 35% of years lost due to ill-health, disability or early death.[2] A subset of neurological disorders are called neurodegenerative, because they are linked to the progressive loss of neuronal function or structure. The primary risk factor for neurodegenerative diseases (ND) is age. This will exacerbate the healthcare burden of ND as the average age of the global population is expected to rise rapidly, especially in countries with a high or rising life expectancy (i.e. developed or newly industrialised countries).[3] This is particularly true for the most common neurodegenerative diseases: Alzheimer's disease (AD) and Parkinson's disease (PD).[4]

The underlying cause is only poorly understood in most ND, and the disease processes are also often unclear. The diagnosis is based on empirical clinical criteria, but a definitive diagnosis requires post-mortem autopsy.[5] Interestingly, certain hallmarks and patterns have been identified in the most important neurodegenerative diseases, including AD, PD, amyotrophic lateral sclerosis, prion diseases and Huntington's disease. They all show a characteristic progressive loss of specific, localised cell populations and the pathological accumulation and aggregation of certain proteins.[3,6–8]

1.1.1 Parkinson's Disease

1.1.1.1 Epidemiology

Parkinson's diseases was first described by James Parkinson in 1817[9] and is the second most common ND worldwide, after Alzheimer's disease.[7] The incidence rate of PD is

estimated to be 8-18 cases per 100,000 persons per year, but varies from country to country and is higher in populations with a higher average age.[10] The prevalence of PD in the UK was estimated to be around 125,000 cases in 2009, or 0.3% of the population.[11] The prevalence estimate is based on existing medical records, it is therefore likely that a significant number of undiagnosed cases exist in addition to these recorded cases.[11]
The biggest risk factor for Parkinson's disease is age, which is illustrated by the fact that over 90% of patients are aged 60 or older.[4,7,10] The average age at onset of the disease is 60 years. While some studies found that PD has a higher prevalence in men, others found no difference between sexes.[10] Most Western societies have a rapidly ageing population, which will lead to an increase in PD cases in the future. For the UK, studies expect a 50% increase of people aged 60 or over and accordingly a 25% increase of PD cases by 2020.[11] Similarly, the number of cases for 15 of the world's most populous nations is expected to double by 2030, driven by a pronounced increase of cases in developing and newly industrialised countries (China, India, Indonesia, Brazil, Pakistan, Bangladesh, Russia, Nigeria).[4] Other risk factors related to PD, such as a number of gene polymorphisms, have been identified, but only a small number of cases can be attributed to genetic factors. Mutations in genes such as SNCA (α-synuclein), LRRK2 (dardarin), PARK2 (parkin) or PINK1 have been shown to cause PD.[12] Nevertheless, over 90% of PD cases are idiopathic.[10,13] Environmental factors – such as smoking, diet, exposure to certain toxins, metals or herbicides – have been suggested as risk factors for PD, but their effect remains contested.[10,14]

1.1.1.2 Pathology and Symptoms

The pathology of PD is characterised by the loss of neurons in the nigrostriatal pathway,[7] and the presence of intracellular protein inclusions, so called Lewy bodies (see Figure 1.1).[15] The loss of neurons in PD is very specific and localised. It mainly affects the dopaminergic neurons projecting from the *substantia nigra* of the midbrain to the striatum. The neurons projecting into the putamen are lost preferentially over the caudate (Figure 1.1.A). At the time of death, up to 70-80% of neurons in that area are lost.[7,16] The neuronal loss leads to a depletion of dopamine in the striatum, interrupting the signal transduction to the areas responsible for motor control (Figure 1.1.B).[17] This causes the typical motor symptoms, such as resting tremors, stiffness and bradykinesia (slowness of

movement) – non-motor symptoms also exist but their cause is not as clear.[18] Interestingly, a large population of dopaminergic neurons is lost before the onset of symptoms.[7]

The exact cause of neuronal loss is unknown, but protein aggregation (Lewy bodies, Figure 1.1.C) and oxidative stress are known for their toxicity to cells, and both processes have been shown to occur in PD brains.[6,18,19] α-Synuclein is the main aggregating protein in PD, but the role of α-synuclein in health and disease is unclear. While it is neuroprotective for non-dopaminergic neurons, aggregates of soluble α-synuclein exhibit toxicity in the presence of dopamine.[20] Multiple mutations of the synuclein gene have been shown to cause PD, or to constitute a risk factor for sporadic PD.[12,16] Numerous markers of oxidative stress and oxidative damage have been found in Parkinsonian brains.[6,21–23] The natural dopamine metabolism and dopamine auto-oxidation produce highly reactive oxygen species, which cause oxidative stress. This requires a finely tuned anti-oxidative system to be in place in dopaminergic neurons.[18] Cell and animal models of PD are frequently induced by treatment with the chemicals 6-hydroxydopamine and 1-methyl-4-phenyl-1,2,3,6-tetrahydropyridine (MPTP). MPTP is metabolised to 1-methyl-4-phenylpyridinium (MPP+) in cells, which then acts as a complex I inhibitor in mitochondrial respiration.[24–26] MPP+ also reportedly opens the mitochondrial permeability transition pore, leading to the loss of membrane potential.[27] The cell's energy supply therefore depletes and oxidative damage of the mitochondria and the whole cell increases. MPP+ also appears to affect the dopamine release and re-uptake systems, which may play an additional role in the compound's toxicity to dopaminergic neurons.[28,29] Similarly, 6-hydroxydopamine also inhibits complex I of the mitochondrial respiratory chain and thus affects the energy metabolism of cells and increases oxidative damage, leading to cell death.[30–32]

Elevated levels of iron and other metals have been found in the *substantia nigra* of PD patients, often associated with protein aggregates, while the iron levels in other parts of the brain were not elevated.[21–23,33,34] Iron can participate in the Fenton reaction[35] to continually produce free radicals from hydrogen peroxide, which is mainly produced in mitochondria as a by-product of the natural metabolism.[36] The toxicity mediated by iron in cells appears at least partly linked to the accumulation of oxidative damage in the mitochondrial DNA, which leads to progressive mitochondrial dysfunction.[37] α-Synuclein misfolding and aggregation has also been shown to be enhanced by oxidative damage[38]

and the presence of iron.[39] It has been proposed that the dysregulated iron localisation in PD exacerbates the stress on dopaminergic neurons caused by protein aggregates and oxidative stress on multiple levels and may lead to the preferential death of dopaminergic cells.[3,7,18,21–23,33,36,37,40] The involvement of iron in these processes links it to Parkinson's disease and its progression. The removal of iron from PD brains therefore opens a novel way for the development of PD drugs, which could lead to disease modifying agents.

1.1.1.3 Current Treatments

At the present time, there is no cure for Parkinson's disease and existing treatment options only help to manage the symptoms.[16,18] The focus of current treatments is to alleviate the severity of motor symptoms. Multiple drugs are on the market, affecting different target proteins in order to increase the available dopamine in the striatum.[18]

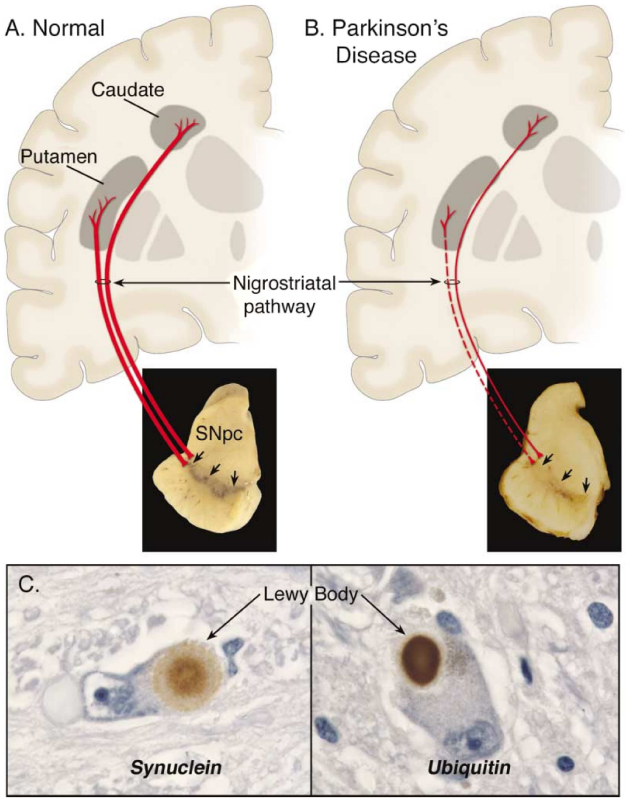

Figure 1.1: Pathology of Parkinson's Disease.
A. Normal nigrostriatal pathway in red. B. Nigrostriatal pathway in PD.
C. Immunostaining of Lewy Bodies in substantia nigra dopaminergic neurons.
(Reprinted by permission from Elsevier: Neuron, copyright 2003.)[7]

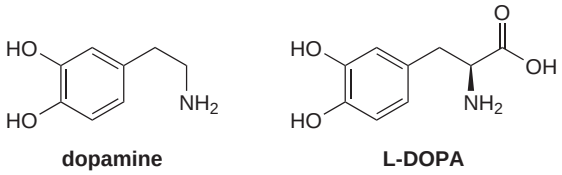

Figure 1.2: Structure of Dopamine and L-DOPA.

The primary treatment for PD patients is L-3,4-dihydroxyphenylalanine (L-DOPA, levodopa, Figure 1.2), which is orally administered and transported into the brain, where it is metabolised to dopamine.[18] L-DOPA is very effective, but when given over longer time periods, patients tend to show resistance to L-DOPA treatment,[7,18] or worse, start to develop dyskinesia with hyperkinetic movements.[41] Other drugs, such as dopamine agonists or monoamine oxidase B inhibitors, which inhibit dopamine metabolism, are also used for the management of PD.[16] Additionally, surgical treatments are available. These include lesioning of the affected brain regions or deep brain stimulation with electrodes, stimulating the neurons in the appropriate regions in order to facilitate the transduction of motoric signals.[16,18]

1.1.1.4 Emerging Treatment Options

Symptomatic treatments for PD have been successfully used since the early 1960s,[42] but drugs that affect the progression of the disease have not been developed yet. The involvement of iron in the pathological processes of PD via oxidative stress and increased protein aggregation[6,8,19,21–23,39] could be the basis for the development of the first class of disease modifying agents.[16,36,40]

A variety of studies investigated the effect of iron on neuronal cells *in vitro* and *in vivo*, as well as the effect of iron removal by chelation. Zheng et al. showed that iron chelators have an anti-oxidative effect on iron-mediated lipid-peroxidation in brain homogenate.[43] The group also found a marked neuroprotective effect of iron chelators against 6-hydroxydopamine insult – a method commonly used to induce parkinsonism in animal models – in an *in vitro* PD model, the pheochromocytoma cell line.[43] *In vivo* experiments performed by Dexter et al. showed that iron chelators were neuroprotective in rats after administration of 6-hydroxydopamine, attenuating the loss of dopamine

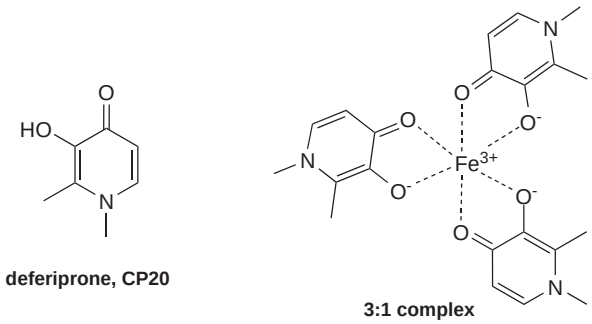

Figure 1.3: Structure of Deferiprone (**CP20**) and its Neutral 3:1 Complex with Fe^{3+}.

levels and tyrosine hydroxylase-positive* neuronal cells.[45] In this study, prior treatment with deferiprone (Figure 1.3) greatly reduced 6-hydroxydopamine induced loss of tyrosine hydroxylase positive neurons from 45% to only 15%, while other clinically used iron chelators protected to a lesser extent (desferal: 25%, desferrioxamine: 35%). The positive influence of deferiprone on iron-induced damage in cultured cortical neurons and human neuroblastoma SHSY-5Y cells *in vitro* was illustrated by Molina-Holgado et al.[46] They also reported over 50% protection against cell death (induced by treatment with 100 µM H_2O_2) by 100 µM deferiprone and a higher preservation of neuronal morphology than the neuroprotective compound 2,2'-dipyridyl. Deferiprone at 10 and 30 µM concentrations reduced cell death of SHSY-5Y cells caused by administation of 5 mM 1-methyl-4-phenyl-1,2,3,6-tetrahydropyridine (MPTP) 2-fold and 3-fold respectively. Similarly, the Bush group showed that iron chelation strategies in a MPTP-induced PD mouse model – either by administration of an orally available iron chelator, or by overexpression of ferritin – protect nigral dopaminergic neurons and rescues the levels of dopamine and dopamine metabolites.[47] Transgenic mice, overexpressing the ferritin heavy subunit, showed an increase in MRI signal intensity of ferric iron, while bioavailable ferrous iron was reduced by 22%. In transgenic mice, the harmful effect of MPTP administration on the number of dopaminergic neurons, oxidative stress levels or dopamine levels was prevented. Chemical chelation by a small molecular iron chelator clioquinol (30 mg/kg) reduced total *substantia nigra* iron content by about 30%, as determined by MRI and mass spectrometry. MPTP-mediated motor deficits and changes in oxidative stress (as measured by glutathione levels), number of dopaminergic neurons in *substantia nigra* and dopamine levels in the striatum were attenuated by clioquinol treatment.

*Tyrosine hydroxylase is an enzyme involved in the biosynthesis of dopamine. It hydroxylates tyrosine to L-DOPA using molecular oxygen.[44]

Based on these results and other studies,[8] two small clinical trials (40 and 22 patients) were recently conducted in Lille, France[48] and London, UK.[49] The trials were investigating the effect of deferiprone treatment in PD patients in placebo-controlled, double-blinded studies. The measured outcomes were removal of iron from the brain, as measured by the change of T2*/R2* times in MRI scans, personal well-being and motor indicators of disease progression. Both trials reported promising results for a 30 mg/kg per day dosing regime. In the French trial, the 40 patients' brain iron levels were monitored by MRI every 6 months. After 6 months of treatment, *susbtantia nigra* iron levels were significantly reduced and after 12 months, even more iron had been removed from the *substantia nigra*, and a significant change in putamen iron levels was also observed; serum and CSF ferritin levels were also reduced. Motor performance improved for patients in the deferiprone-treated group (change in UPDRS motor score of -2 points, compared to baseline at month 0), while it worsened in patients where the start of deferiprone treatment was delayed for 6 months. Deferiprone treatment also slowed the gradual worsening of motor performance over time. In the patient group which stopped treatment 6 months earlier than the rest, the motor performance deprecated more rapidly than for patients with prolonged treatment.[48] Additionally, patients improved in their motor scores and well-being even before a removal of iron from the brain could be observed by MRI.[50] These results prompted the French group to plan another trial with 300 to 400 patients.[50]

While deferiprone showed promising results in these trials, its known disadvantages are its relatively low brain penetration,[51] its fast metabolism –[52,53] and the occurrence of some dangerous – albeit rare and transient – side effects, such as agranulocytosis, which requires constant monitoring.[54] If the brain permeability of deferiprone could be improved, the impact of the rate of metabolism and the side effects would be reduced due to the lower drug concentrations needed in systemic circulation.

1.2 Delivery of Drugs to the Brain

Drugs active in the central nervous system (CNS) need to enter the brain to achieve their desired effect. Therefore, the delivery of drugs to the brain has been an important research area for many years.[55] The principle factor limiting the entry of drugs into the brain is the blood-brain barrier (BBB). Its existence was first experimentally confirmed by Goldmann in 1909.[56]

Only a small subset of drugs are able to penetrate the blood-brain barrier. In 1999, Ghose et al. analysed over 7000 drugs from the Comprehensive Medicinal Chemistry database and found that only 5% of them were CNS active drugs.[57] Of these drugs, all are used for the treatment of depression, schizophrenia and other mental disorders, but none for the treatment of neurodegenerative diseases.[57] CNS active drugs tend to be small, with a molecular weight (MW) <400 Da, but not all drugs with a low MW automatically enter the brain.[58] Drug molecules need to have a certain set of properties to enter the CNS,[59,60] which are dictated by the properties of the BBB. The development of efficient strategies for drug delivery to the brain therefore requires a profound understanding of the BBB.

1.2.1 The Blood-Brain Barrier

The blood-brain barrier is a multicellular structure (Figure 1.4) that exists in all species with a well developed CNS (all vertebrates and some invertebrates).[61] The BBB separates the brain from the systemic blood circulation and thus maintains homeostasis of the CNS for optimal neuronal function and synaptic signalling.[62,63] It functions as a combination of a physical, a transport and a metabolic barrier.

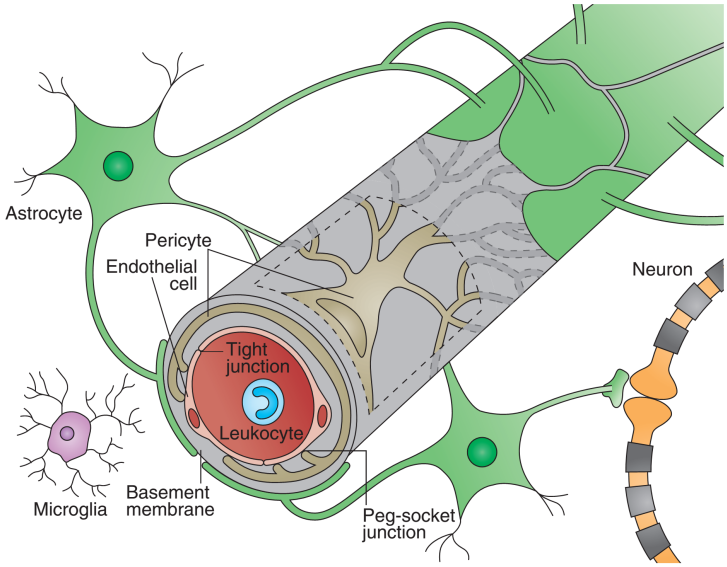

Figure 1.4: Cell Associations at the BBB. (Reprinted by permission from Macmillan Publishers Ltd: Nature Medicine, copyright 2013.)[63]

In mammals, the physical barrier of the BBB is formed by the endothelial cells of the cerebral capillaries.[61–63] In contrast to peripheral blood vessels, the endothelium of the brain vasculature is not leaky due to the lack of fenestrations and the formation of tight

junctions between the cells. These tight junctions prevent plasma proteins or other solutes in the blood from entering the brain by paracellular diffusion, i.e. via gaps between the cells.[64] Any substance that needs to get into or out of the brain therefore has to pass transcellularly through the endothelium (see Figure 1.5). The metabolic barrier of the BBB is comprised of metabolic enzymes in the cells of the BBB that degrade or detoxify potentially harmful substances during their transit, for example multiple cytochrome P450 enzymes, tranaminases, monoamine oxidases or UDP glucuronosyltransferases.[65] The transport barrier is comprised of transport systems (Figure 1.5), which efflux solutes entering endothelia back into the blood. These will be discussed in more detail in section 1.2.2.3.

Other CNS barriers – such as the blood-cerebrospinal fluid barriers at the choroid plexuses in cerebral ventricles and the arachnoid membrane under the dura mater – have a much smaller surface area and play a minor and more localised role in transport processes.[62]

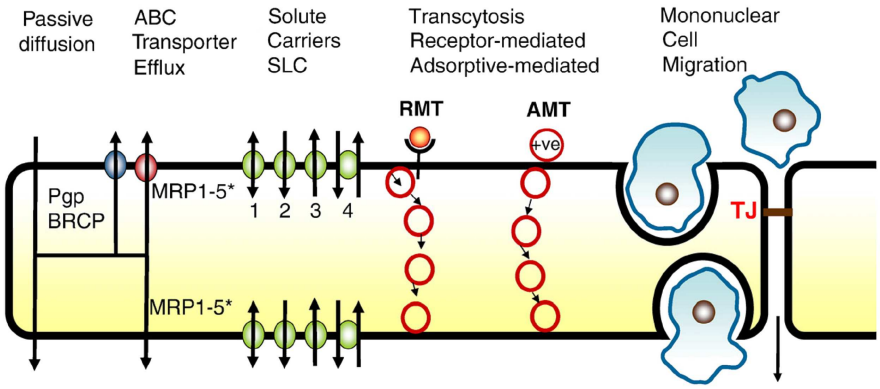

Figure 1.5: Transport Routes in the Blood-Brain Barrier. (Adapted by permission from Elsevier: Neurobiology of Disease, copyright 2010.)[62]

1.2.2 Overcoming the Blood-Brain Barrier

Multiple strategies to overcome the BBB exist includin for example, direct injection of drugs into the CNS (intrathecal) or nanoparticle carrier systems for large drug delivery, and chemical modification of drugs to improve small drug delivery. For small molecules such as deferiprone, the main strategies are either to modify the lipophilicity of molecules – thus changing their propensity to cross the BBB by passive diffusion – or to take advantage of the active or energy-independent transport systems at the BBB.[55]

1.2.2.1 Passive Diffusion

Passive diffusion across the blood brain barrier is limited by the molecules' ability to cross the lipid bilayers of the cell membrane. The movement of molecules is driven by the gradient between the extracellular and intracellular concentration.[66]

The permeability of molecules is mainly governed by their lipophilicity, polarity and size. Lipinski proposed a set of guidelines for drug discovery and development, termed the 'Rule of Five': 5 or fewer hydrogen bond donors, 10 or fewer hydrogen bond acceptors, a logP small than 5 and a molecular weight small than 500 (see Table 1.1).[66] Lipinski states, that poor oral absorption is more likely when the molecule breaks one or more of the rules.[66] While the 'Rule of Five' was developed to improve oral absorption of drugs, these parameters are often also applied as a guideline for CNS drug-delivery.[67,68] This principle is valid, because a main determinant of both oral absorption and CNS permeability is the ability to overcome cell membranes.[66,69]

Large molecules are unlikely to cross biological membranes by diffusion, because they need to displace a large number of lipid molecules in the membrane, which is energetically disfavoured.[70,71] The diffusion rate of molecules[†] is inversely related to their size[72] or cross-sectional area.[70] These properties can only be determined experimentally, while the molecular weight is easily calculated from the formula and thus used as a substitute for molecular size. Fischer et al. estimated the upper limit for the cross-sectional area for passive diffusion to be around 80 $Å^2$,[70] which corresponds to a molecular weight of 300–400 Da.[55] A molecular weight $\leq$ 500Da is suggested for good permeability by Lipinski and other groups.[66,73]

A hydrophilic molecule is unlikely to partition into the hydrophobic core of the membrane's lipid bilayer. High lipophilicity increases a molecule's membrane permeability,[74] but also reduces its solubility in aqueous media. It may also lead to low absorption and high plasma protein binding.[73,74] The free drug concentration in the plasma will therefore be low, resulting in a flat concentration gradient and slow diffusion rate.[74] Lipinski therefore suggests a logP ≤ 5 in order to achieve good bioavailability.[66]

The polarity of molecules, or rather polar surface area (PSA), is the sum of the surface of all polar atoms in a molecule. Hydrogen bond donors (HBD) and hydrogen bond acceptors (HBA) increase the polarity of a molecule and its solubility in water and polar

[†]Diffusion into and through the lipid bilayer, in this case.

environments, but limit its solubility in apolar environments, such as lipids.[68] Lipinski's rules suggest to limit the number of HBD and HBA to 10 and 5 respectively, for oral bioavailability.[66]

Table 1.1: Physicochemical Property Ranges Suggested for Increased CNS Permeability.

Property	Lipinski[66]	Hitchcock[73]
PSA (Å^2)	—	< 90
HBD	≤ 5	< 3
HBA	≤ 10	—
logP	≤ 5	2–5
MW (Da)	≤ 500	< 500

To increase BBB penetration, Hitchcock et al. suggested more stringent limits than specified in Lipinski's rules (see Table 1.1).[73] Norinder et al. reported another facile method to determine whether a molecule is likely to enter the CNS: the sum of nitrogen and oxygen atoms should be ≤ 5 and logP minus the sum of N+O atoms > 0.[60]

Even though violating these rules will negatively affect a molecule's ability to permeate the brain, they should be regarded as a 'rule of thumb', as compounds breaking one or more rules are known to enter the CNS.[75]

Habgood and colleagues found that the brain uptake of 3-hydroxypyridin-4-ones (HPOs) with varying chain length of the *N*-substituent correlated with their logP.[76] Lengthening the *N*-alkyl chain increased logP and thus brain penetration. In contrast, the introduction of an hydroxyl group almost entirely abolished the entry of HPOs into the brain, while non-hydroxylated derivatives with similar logP values entered the brain more easily.[76] The more lipophilic HPOs were not advanced further however, because their lipophilicity lead to higher partitioning into other organs such as the liver, where HPOs are rapidly metabolised and excreted.[52]

1.2.2.2 Prodrugs

Prodrugs are derivatives of drugs in which part of the active group is conjugated with a pro-moiety in order to avoid peripheral metabolism and/or improve uptake in the target tissue. The pro-moiety is then cleaved in the target tissue, releasing the active drug.[77,78]
A common strategy to improve the permeability of a drug is to mask their polar groups – these may act as hydrogen bond donors – with non-polar groups.[68,69,77] This increases the drug's lipophilicity, facilitating permeability across the BBB. The prodrug enters the brain and the active drug is released by bioconversion.[77,78]
Hydroxyl and acid groups are often masked as esters by reaction with acids or alcohol respectively, which can be cleaved by esterases in the brain.[68] One of the most successful example for this strategy is heroin, which is the diacetylated derivative of morphine. The diacetylation increases brain penetration, while esterase activity in the brain effectively locks in the deacetylated product (morphine) due to its lower lipophilicity.[74]
L-DOPA is a prodrug of dopamine – while dopamine does not enter the brain, L-DOPA is transported by the large neutral amino acid transporter 1 (LAT1).[73,79] It is then metabolised by DOPA decarboxylase to release dopamine.[73,80] A pro-moiety may also be used to direct the drug to its intended target via one of the endogenous transport systems.[78] Examples for this strategy will be discussed in section 1.2.2.3.

1.2.2.3 Transport Processes

The blood-brain barrier uses a multitude of different transport systems (Figure 1.6) to supply the brain with nutrients, remove metabolites and prevent the entry of foreign substances and toxins.[62,81] These transport systems are relevant for drug delivery and may even be targeted to increase drugs' BBB permeability.[82–85]

Active efflux transporters (AET) export molecules from the brain endothelium, often by using energy in the form of ATP or sodium-dependent co-transport.[55,62] Notable members are P-glycoprotein (P-gp), breast cancer resistance protein (BCRP) and the multidrug resistance-associated proteins (MRP 1–5). AETs preferentially transport lipophilic molecules and increasing lipophilicity makes molecules a more likely substrate of active efflux transporters.[67,78]

While AETs cannot be used to target molecules to the brain, they should be considered in the design of molecules, because AETs can severely limit a molecule's ability to reach effective concentrations in the brain.[85] Azidothymidine (AZT) and other drugs used in the treatment of AIDS are ineffective at penetrating the brain as a result of AET efflux, resulting in a sanctuary for HIV.[86] The responsible transporter was only identified in 2007 by Pan et al.[87] The group found that transfection of canine kidney cells with Bcrp1 (the mouse homologue of BCRP) significantly reduced the intracellular accumulation, as well as basolateral to apical flux of AZT and acabavir, when compared to wild-type cells. This effect was abolished by co-administration of BCRP inhibitors GF120918 or Ko143.[87]
AETs can also be used as a means to reduce undesirable brain penetration in peripheral drugs.[88] Loperamide is a opioid-receptor agonist, which is used for the treatment of diarrhoea. It is a Pgp substrate, which means that the brain is shielded from its CNS opioid effect under normal conditions.[89] When a Pgp inhibitor was co-administered, loperamide caused respiratory depression via its central opioid action.[89]

Receptor-mediated transcytosis (RMT). Large endogenous molecules, such as signalling peptides or proteins, may be transported across the BBB in vesicles by specific and non-specific transcytotic systems.[62] Non-specific transport occurs by adsorptive-mediated transcytosis (AMT), wherein a positively charged macromolecule adsorbs onto the cell membrane and the interaction with cell surface binding sites triggers the internalisation via the formation of a vesicle, which is then transported across the cell.[62] Contrarily,

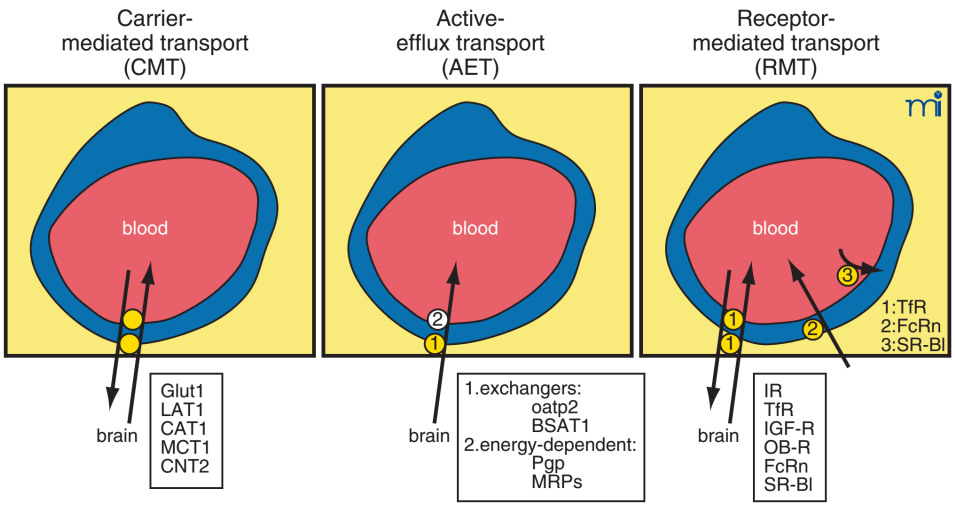

Figure 1.6: Transport Systems found in the BBB Endothelium. (Reprinted by permission from ASPET: Molecular Interventions, copyright 2003.)[55]

in receptor-mediated transcytosis (RMT), a specific ligand binds its receptor on the endothelial cell membrane and triggers the endocytosis of the ligand-receptor complex.[90,91] During RMT, a caveolus is formed, which internalises the ligand-receptor complex within a vesicle. This vesicle is transported across Receptor-ligand pairs undergoing RMT include insulin, transferrin, insulin-like growth factor and LDL.[55,62,67,78,81,84,92] This system can be used to transport drugs, in particular large molecules, as a 'Trojan horse' across the BBB. This Trojan horse can be the natural ligand of the receptor, which has been conjugated to the drug, or polypeptides, often a monoclonal antibody. These bind to an exofacial epitope of the receptor, distinct from the natural ligand-binding site and thus do not interfere with the transport of the endogenous ligand.[55,68]

The transferrin receptor (TfR) has been used for the delivery of molecules across the BBB using either strategy. Yan et al. studied fluorescence-labelled iron nanoparticles, which had been conjugated to transferrin (Tf). While the *in vivo* uptake of nanoparticles without Tf was very low, the Tf-coated nanoparticles entered the brain in abundance.[93] Niewoehner et al. produced constructs between anti-amyloid beta antibodies (mAb31) and monoclonal anti-TfR Fab fragments. Up to 50% of the given dose of these constructs passed the BBB in an *in vitro* model, and the constructs showed up to 55-fold higher binding of amyloid beta plaques than the untargeted antibody in mice after i.v. administration of the antibodies.[94]

Carrier mediated transport (CMT). In order to supply the brain with the nutrients it needs for metabolism, the brain endothelium contains an array of carrier proteins, which are specialised to transport specific classes of nutrients.[62,83,84] Transported substrates include glucose, amino acids, nucleosides, nucleotides and nucleobases, choline and thyroid hormone.[62,83] The transport can be facilitative, sodium-dependent or driven by an exchange with other ions.[62] Numerous drugs (Table 1.2) are known to enter the brain by CMT. These include L-DOPA, valproic acid, gabapentin, the lactone-opened metabolites of simvastatin and lovastatin, lidocaine or morphine glucuronide.[77,85,95]

The large neutral amino acid transporter 1 (LAT1) is one of few transporters which are already used for the drug delivery. LAT1 is involved in the transport of a number of drugs (Table 1.2).[97] These include L-DOPA,[98] phosphonoformate-tyrosine conjugate,[99] gabapentin,[100,101] melphalan[102] and 4-chlorokynurenine[103] (Figure 1.7).

LAT1 is a facilitative (sodium-independent, bidirectional) transporter found on the apical and basolateral membrane of the brain endothelium. LAT1 transports large α-amino

Table 1.2: Examples of Drugs Transported into the CNS by CMT (from Begley[85]).

Drug	Transporter
Valproic acid	MC fatty acid carrier[a]
DHA-taxol[b]	MC fatty acid carrier
DHA-dideoxycytidine	MC fatty acid carrier
L-DOPA	LAT1[c]
α-methyl-DOPA	LAT1
Melphalan	LAT1
Baclophen	LAT1
Gabapentin	LAT1
Acivicin	LAT1
D,L-NAM[d]	LAT1
Tyrosine-phosphonoformate	LAT1
Nitrosoarginine derivatives	LAT1
Simvastatin[e]	MCT1[f]
Lovastatin[e]	MCT1
Mepyramine	OCT family[g]
Diphenhydramine	OCT family
Diphenylpyraline	OCT family
Lidocaine	OCT family
Imipramine	OCT family
Propanolol	OCT family
Oxazolamine COR3224	Purine carrier
Abacivir	Nucleoside carrier
Morphine glucuronide	Hexose carrier

[a] Medium-chain fatty acid carrier.[96]
[b] DHA = Docosahexaenoic acid.
[c] Large neutral amino acid transporter 1.
[d] NAM = 2-Amino-7-bis[(2-chloroethyl)amino]-1,2,3,4-tetrahydro-2-naphthoic acid.
[e] Open lactone-form.
[f] Monocarboxylic acid transporter 1.
[g] Organic cation transporter.

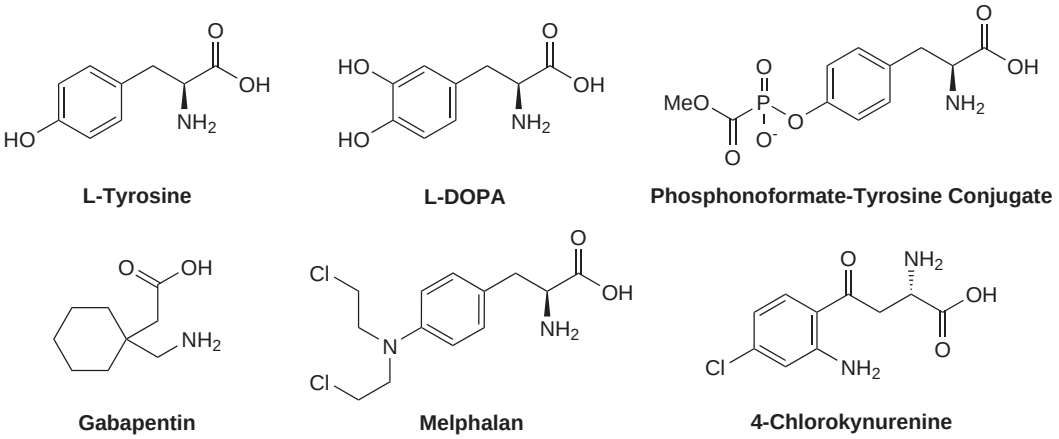

Figure 1.7: Structures of LAT1-transported molecules.

acids, such as tyrosine, phenylalanine or leucine.[62,68,97] Transported drugs, with the exception of gabapentin, are α-L-amino acids and therefore resemble the natural substrates. Gabapentin's cyclic structure and restricted conformation bring the amino and carboxy groups in close proximity however, allowing recognition and transport by LAT1.[84] Some of these drugs are only delivered to the brain, while others act as prodrugs that are metabolised to their active form in the brain and thus effectively trapped.[68,78] Examples include L-DOPA, which is decarboxylated to dopamine,[84] and 4-chlorokynurenine, which is cyclised to 7-chlorokynurenic acid.[103]

Other CMTs have also been suggested as facilitators of brain-directed drug delivery.[5,84,85,95] Attempts to utilise the glucose transporter GLUT1 will be discussed below.

1.2.3 GLUT1 Mediated Transport

1.2.3.1 Glucose transporter GLUT1

In mammalian cells, two groups of transporters are responsible for the transport of glucose. The sodium-dependent glucose co-transport proteins (SGLT) – responsible for dietary glucose uptake in the intestine and glucose reuptake in the nephron[104] – and the sodium-independent facilitative glucose transporters (GLUT).[104–106] Glucose transporter GLUT1 belongs to the latter family. In the brain, it is found almost exclusively and abundantly at the blood-brain barrier, while other members of the GLUT family are found in astrocytes and neurons.[106–109] GLUT1 is also localised in erythrocyte membranes, the retina, testes and the placenta.[110,111] The endogenous substrate of GLUT1 is D-glucose but not L-glucose.

L-Ascorbic acid is also transported by GLUT1 in its oxidised form (dehydroascorbic acid).[112,113]

Structure. GLUT1 is part of the major facilitator superfamily (MFS), a very large transporter superfamily.[110,114–116] Transporters of the MFS share a common core structure, comprised of 12 transmembrane domains.[115,117–119] This structure (Figure 1.8) has also been suggested for GLUT1 through sequence analysis,[105,120] CD spectroscopy[110] and comparison with bacterial homologues.[118,121]

The crystal structure of XylE, a bacterial homologue of GLUT1, was published in 2012 by Yan and coworkers.[122] This structure was then used as the basis to model the 3D structure of GLUT1. XylE is a xylose/H^+ symporter isolated from *Escherichia coli*. The protein has a sequence identity of around 30% with GLUT1–4 and sequence similarity around 50%.[122] This low identity may be excepted from the comparison of a bacterial and a mammalian protein. However, members of MFS are known to have high sequence difference to each other, while retaining homologous secondary structure and helical packing.[121] Most amino acid residues involved in substrate binding and a number of diseases-related residues in GLUT1 are invariant in XylE and GLUT1 (Figure 1.8),[122,123] which justifies the use of XylE as scaffold for the modelled structure of GLUT1. In early 2013, Quistgaard et al. reported two more crystal structures of XylE.[123] The protein was crystallised in the inward open and partially occluded inward open conformations. These supplement the structure by the Yan group, allowing closer study of the protein's transport cycle. The

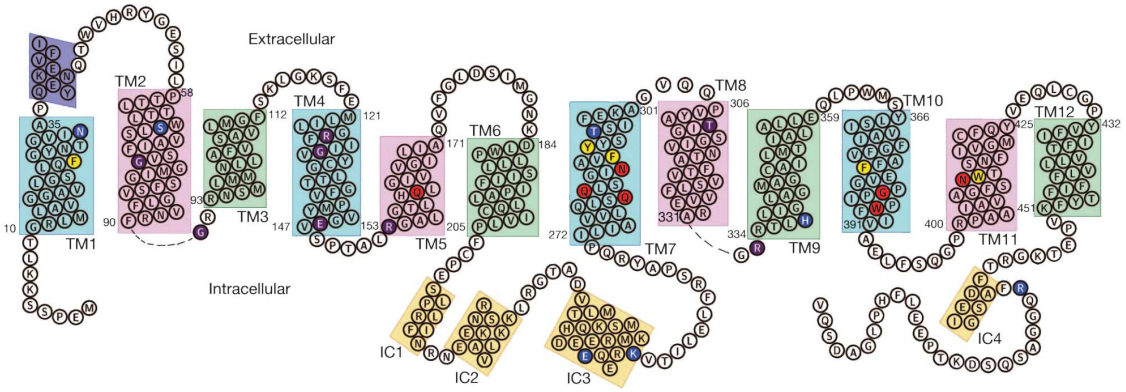

Figure 1.8: Predicted Secondary Structural Elements of GLUT1.
Polar and aromatic residues predicted to be involved in D-glucose binding are shaded red and yellow, respectively. The residues whose mutations were found in GLUT1 deficiency syndrome are shaded purple and blue for invariant and variant residues, respectively. (TM, Transmembrane Domain; IC, Intracellular Helix; Adapted by permission from Macmillan Publishers Ltd: Nature, copyright 2012.)[122]

crystal structures suggest a single binding site, which is alternatively accessible from the extracellular space in the outward open conformation and the intracellular space in the inward open conformation.[124]

In 2014, the Yan group finally reported the crystal structure of GLUT1, making it the first reported structure of a eukaryotic sugar transporter.[124] The protein was crystallised in the inward open conformation (Figure 1.9) and it closely matches the structure of XylE. The group found some differences in the length and arrangement of the intracellular helices (IC1–3, cf. Figure 1.8 and Figure 1.9) in the loop between transmembrane domains 6 and 7 and high similarity in the substrate binding transmembrane domains.[124] The intracellular helices between transmembrane domains 6 and 7 separate the protein into a C and a N domain. A central cavity is present in GLUT1, which appears to be the binding site for the co-crystallised nonyl-β-D-glucoside. The interactions of the protein with the glucoside includes multiple residues which are associated with GLUT1 deficiency syndrome.[124] GLUT1 is thought to transport substrates through the membrane by a series of conformation changes,[125] alternately making the substrate binding site available to one side of the membrane.[110,126] This is supported by the published crystal structures, which show a movement of the C and N domains relative to each other, exposing the binding site either to the extra- or intracellular side.[122–124] The intracellular helices are thought to close off access to the binding site during the transport cycle.[124]

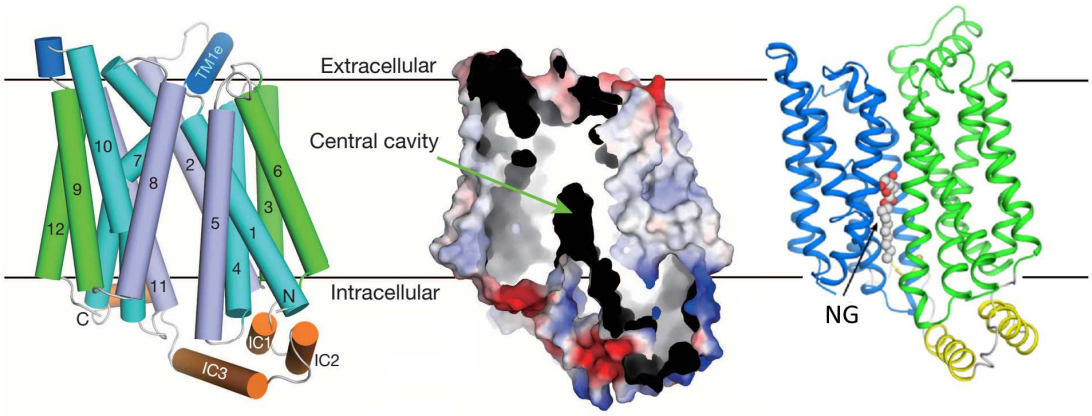

Figure 1.9: Overall Structure of the Human Glucose Transporter GLUT1.
The structure of full-length human GLUT1 containing two point mutations (N45T, E329Q) was determined in an inward-open conformation. The corresponding transmembrane segments in the four 3-helix repeats are coloured the same. A cut-open view of the surface electrostatic potential is shown in the centre, a ribbon schematic bound to nonyl-β-D-glucoside (NG) on the right. (IC, Intracellular Helix; Adapted by permission from Macmillan Publishers Ltd: Nature, copyright 2014.)[124]

Substrate Specificity. Studies of GLUT1 by Barnett et al. and Pardridge focused on the substrate binding properties and transport kinetics and inhibition.[127–129] These studies showed that the interactions of glucose derivatives with GLUT1 depend to a large extent on the position of the modification, as well as steric effects and hydrogen bonds (Table 1.3).[127–129]

Modifications in position 1 are badly tolerated. The β-fluoride is half as active as glucose (D-Glucose: $K_i = 8\,\text{mM}$), while the K_i for the α-fluoride is an order of a magnitude greater. 1-Alkylated derivatives lacking a hydroxyl group in position 1 have a 3–10 times higher K_i than glucose. This indicates that position 1 plays an important role in substrate recognition, leaving little room for modifications.

2-Deoxyglucose and 2-chloro-2-deoxyglucose have a similar K_i to glucose, while the C-2 epimer mannose is slightly less active. 2-*O*-Methylglucose is 15 times less active than glucose, indicating that substituents in position 2 are not tolerated due to steric hindrance.

For positon 3, a hydrogen bond acceptor in equatorial position appears to be required for high binding affinity. 3-Deoxyglucose had a high K_i of 70 mM and allose, the C-3 epimer, did not show any inhibitory effect. The K_i of 3-*O*-alkylglucoses decreased with increasing size of the substituent. The fluorine atom in 3-deoxy-3-fluoroglucose can accept a hydrogen bond and thus has a similar K_i to glucose, while the chloro and bromo derivatives are 4 times weaker inhibitors.

The introduction of alkyl substitutents in positions 4 and 6 appears to be well tolerated, with 6-*O*-pentylglucose, 6-*O*-pentylgalactose and 6-*O*-benzylgalactose showing a higher affinity for the transporter than glucose. The absence of a hydrogen bond in position 6 (6-deoxyglucose and xylose) increased the K_i over 9-fold, while a fluorine atom, which acts as hydrogen bond acceptor, but not donor, conferred a much lower K_i than glucose. The introduction of a cationic or anionic group (6-aminoglucose and glucose 6-phosphate, respectively), completely abolished inhibitory activity. Position 6 therefore apparently interacts with a mainly hydrophobic region of the binding pocket, which nevertheless requires the presence of a hydrogen bond acceptor for high affinity binding.

Galactose, the C-4 epimer, and its derivatives have a lower affinity than the respective glucose derivatives, indicating the requirement for the 4-hydroxyl group or its substituents to be in the equatorial position.

Table 1.3: GLUT1 Inhibition Constants (K_i) of Sugar Derivatives.[a]

Substrate	K_i (mM)	Reference	Substrate	K_i (mM)	Reference
Glucose 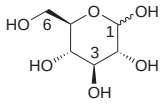	9	ref. [127]	3-Deoxy-3-fluoroglucose	7	ref. [128]
	7	ref. [128]	3-Chloro-3-deoxyglucose	33	ref. [128]
1-Deoxyglucose	77–81	ref. [128]	3-Bromo-3-deoxyglucose	33	ref. [128]
1,2-Dideoxyglucose	38	ref. [128]			
Glucal	27	ref. [128]	4-*O*-Propylglucose	10	ref. [128]
α-Glucopyranosyl fluoride	77–80	ref. [128]			
β-Glucopyranosyl fluoride	15	ref. [128]	6-Deoxyglucose	77–80	ref. [128]
Methyl α-glucopyranoside	ND[b]	ref. [128]	Xylose	70	ref. [128]
Methyl β-glucopyranoside	ND	ref. [128]	6-*O*-Propylglucose	17	ref. [129]
Propyl β-glucopyranoside	ND	ref. [129]		90[c]	ref. [129]
	9[c]	ref. [129]	6-*O*-Pentylglucose	1	ref. [129]
Phenyl β-glucopyranoside	6	ref. [129]	6-Amino-6-deoxyglucose	ND	ref. [128]
	0.5[c]	ref. [129]	Glucose 6-phosphate	ND	ref. [128]
			6-Deoxy-6-fluoroglucose	1	ref. [128]
2-Deoxyglucose	6	ref. [127]			
	3	ref. [128]	Galactose	40[d]	ref. [127]
Mannose	22[d]	ref. [127]		85–90	ref. [128]
	20	ref. [128]	Propyl β-galactopyranoside	ND	ref. [129]
2-*O*-Methylglucose	119	ref. [128]		90[c]	ref. [129]
2-Chloro-2-deoxyglucose	8	ref. [128]	6-Deoxygalactose	50	ref. [128]
			6-*O*-Methylgalactose	45	ref. [128]
3-Deoxyglucose	70	ref. [128]	6-*O*-Propylgalactose	17	ref. [129]
Allose	ND	ref. [128]		ND[c]	ref. [129]
3-*O*-Methylglucose	10	ref. [127]	6-*O*-Pentylgalactose	1.5	ref. [129]
	12–14	ref. [128]	6-*O*-Benzylgalactose	1.2	ref. [129]
	13	ref. [130]		6[c]	ref. [129]
3-*O*-Ethylglucose	48	ref. [128]	6-Deoxy-6-fluorogalactose	7	ref. [128]
3-*O*-Propylglucose	59	ref. [128]	6-Deoxy-6-iodogalactose	8	ref. [128]
3-*O*-Allylglucose	25	ref. [128]			

[a] Compounds were tested for the inhibition of i) L-sorbose entry into human erythrocytes[128,129] ii) brain uptake of D-[^{14}C]-glucose in rats[127] or iii) 3-*O*-[^{3}H]methyl-D-glucose uptake into a monolayer of bovine brain microvessel endothelial cells (BMEC).[130] All tested compounds were the D-isomer.

[b] No inhibition detected.

[c] Inhibitor present on intracellular side.

[d] $K_i \approx K_m$

Interestingly, the effect of derivatives was very different when they were present intracellularly, rather than on the outside.[129] Glucosides, which previously had a very limited effect, showed very high inhibitory activity inside the cell. This is in contrast to 6-alkylated sugars, which were very active outside the cell, but when applied to the inside, they show little to no inhibition to the transport activity of GLUT1. This data suggests that GLUT1 forms different interactions with glucose, depending on the orientation of the protein,[126,129] allowing alternating access to the substrate-binding site. Since the studies reported K_i and not K_m of the sugar derivatives, no direct assessment about the transportability can be made. A high inhibition constant signifies low binding and thus low likelihood of transport. The inverse assumption, that tightly bound compounds are better transported by GLUT1, is not true however, because the compounds may be non-transportable inhibitors. Nevertheless, binding is a prerequisite for transport.

The GLUT1 crystal structure (Figure 1.9) shows a central cavity – the putative binding site. It is accessible alternatively from the intra- or extracellular side.[124] Furthermore, GLUT1 was co-crystallised with nonyl-β-D-glucoside in an inward-facing conformation. The sugar was sitting in the binding pocket, with the nonyl-chain protruding towards the intracellular side.[124] All this information supports the described substrate-binding model and explains the distinct behaviour exhibited by 1- and 6-modified sugars. When the transporter is facing outwards, the 'front' of the sugar with position 1 is entering the binding pocket first, thus requiring an unsubstituted position 1 interacting with the transporter, while position 6 may have less interactions with the protein in this conformation. Conversely, in the inward facing conformation, position 6 is the first to interact with the binding pocket, while there remains space for substituents in position 1, e.g. the nonyl group in the crystal structure.

The information gained by these studies regarding the structural requirements for GLUT1 binding is therefore very useful for the design-considerations of GLUT1 transportable compounds.

1.2.3.2 Use of GLUT1 for Drug Targeting

Targeting glucose transporter GLUT1 has been suggested as potential strategy to deliver drugs to the CNS.[5,67,68,78,81,84,131]

Peptides. It has been speculated that glycosylation of peptides can improve their bioavailability and delivery to the brain.[68,131–133] A particular effort was made in the synthesis of glucosylated opioid peptides, such as enkephalins or dermorphin.[134–154] Two studies measured the *in vivo* pharmacological effect of these constructs.[137,138] They found improved bioavailability and CNS effects compared to the parent peptide, but did not attribute this to transport by GLUT1.[137,138] A recent study investigated the effect of enkephalin glycosylation on the permeability across a Caco-2 cell monolayer. The parent peptide did not cross the monolayer due to rapid degradation, while the glucosylated derivatives were able to cross the cell monolayer intact.[154] Only some Caco-2 cell clones express GLUT1, while all carry the sodium glucose co-transporter SGLT1.[104,155] Only a single study could be identified, which directly investigated the involvement of GLUT1 in the uptake process of a glucosylated peptide.[156] Williams et al. elegantly compared a D-glucosylated peptide with its L-glucose analogue using *in situ* rat brain perfusion of the radiolabelled peptides, while it was known that the unglycosylated peptide does not enter the brain. They found that this replacement did not affect CNS uptake, thus ruling out GLUT1 mediated transport. The Polt group speculated that glycopeptides are transported by adsorptive-mediated transcytosis.[137,138,147] The uptake mechanism for glycosylated peptides remains unclear and warrants further investigations.[68] Peptides are of lesser relevance to the present work, however, and will therefore not be discussed in more detail.[‡]

Small Molecules. Small molecules are the main focus of drug delivery efforts based on glycosylation. This strategy has been applied to develop or modify drugs from classes including chemotherapeutics, anti-inflammatory, anti-retroviral and PD drugs.

The delivery of anti-retroviral drugs to the brain is pursued, because the brain can serve as a reservoir for HIV.[157] Bonina et al. reported two glycosylated derivatives of azidothymidine (AZT, **1**, see Figure 1.11), a reverse-transcriptase inhibitor, and investigated the plasma concentration and release of free AZT in rats.[158] The total AUC was lower for both glycosylated drugs, but 6-galactosyl ester **1b** released AZT slower and over a longer period of time. Data on the drugs' brain penetration was not presented. Rouquayrol et al. synthesised 3-glucosyl esters of HIV protease inhibitors saquinavir (**2**), indinavir (**3**) and nelfinavir (**4**).[159] The group tested the permeability of the glucosylated drugs through a Caco-2 monolayer in both directions (apical to basolateral and basolateral to apical).[160]

[‡]For a review on glycosylated neuropeptides, see ref. [132].

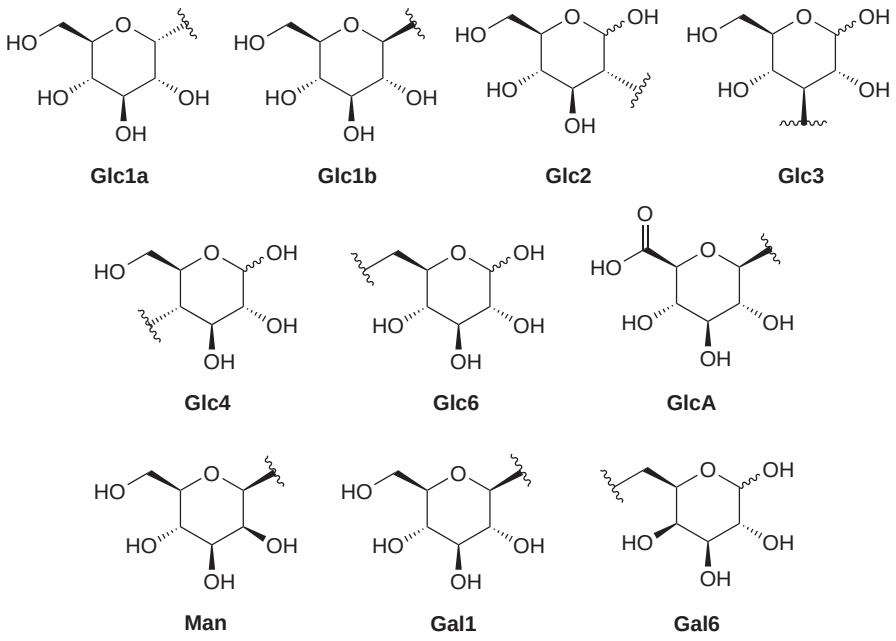

Figure 1.10: Sugar Fragments Used in Glycosylated Drugs. Wavy line indicates point of attachment.

Conjugates **3c** and **4a** showed comparable uptake to the respective parent drugs, while the uptake of the other conjugates that were tested (**2a**,**c** and **3a**) was much lower. Efflux rates were different to the uptake data, some were higher (**2c**), comparable (**4a**) or lower (**2a** and **3a**,**c**) than the parent drugs' efflux.[160] These results indicate that glucosylation does not improve the intestinal absorption of these anti-retroviral drugs, and its effect for transport by GLUT1 remains questionable.[160]

Recently, a number of glucosylated non-steroidal anti-inflammatory drugs (Figure 1.12) have been reported. Jacob and Tazawa synthesised a 3-glucosyl derivative of aspirin (**5**) and tested its cytotoxic effect against cancer cell lines, but did not report permeability data.[161] Chen et al. aimed to improve the brain drug delivery of ibuprofen by glucosylation. They formed an ester bond between ibuprofen and glucose in positions 2, 3, 4 and 6 (**6a**–**d**) and tested the resulting conjugates for their pharmacokinetic behaviour.[162] The tissue distribution of ibuprofen and the conjugates was measured 60 min after i.v. injection and about 15–25 µg/g was found in the brain for ibuprofen and ibuprofen conjugates **6a**–**c**, while the brain concentration of the 6-linked conjugate **6d** was found to be 55 µg/g. The group did not investigate whether GLUT1 is directly involved in the results they found, but explained their findings with GLUT1's substrate specificity and tolerance to modifications in certain positions.[162] The Gynther group reported the synthesis and investigation of the

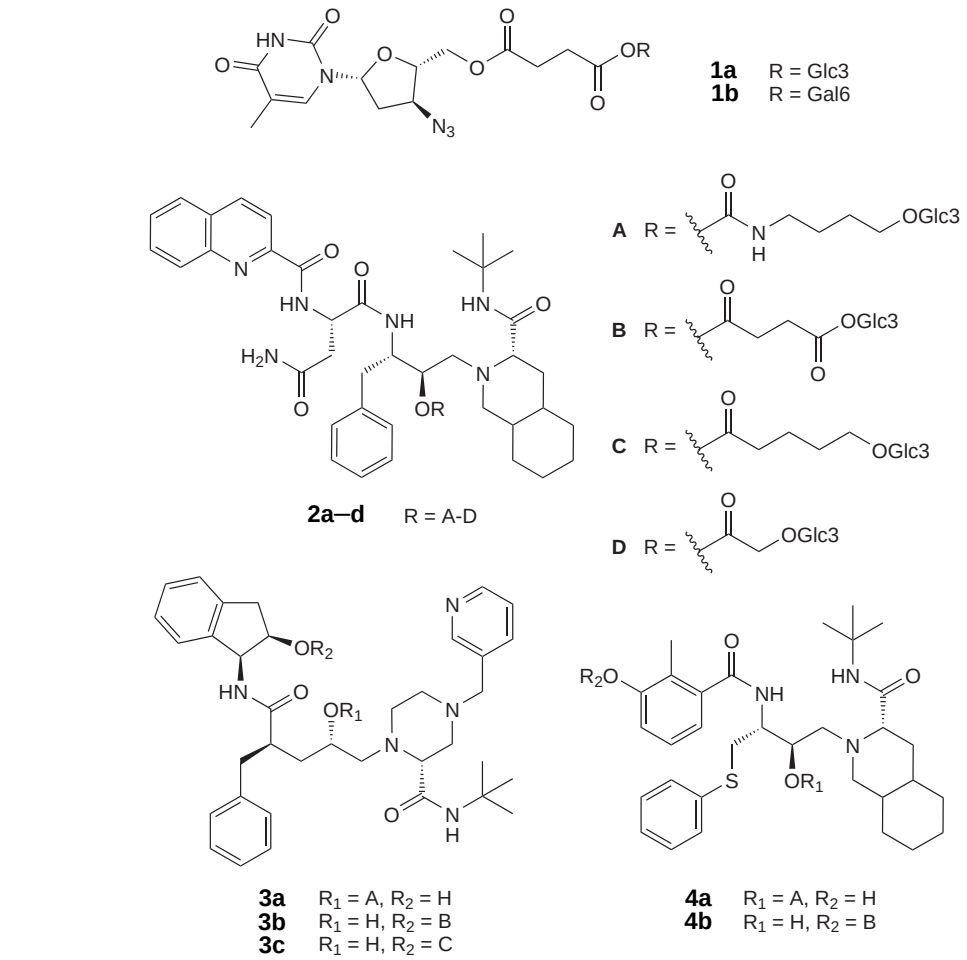

Figure 1.11: Structures of Glycosylated Anti-Retroviral Drugs. Azidothymidine (**1**), Saquinavir (**2**), Indinavir (**3**), Nelfinavir (**4**).

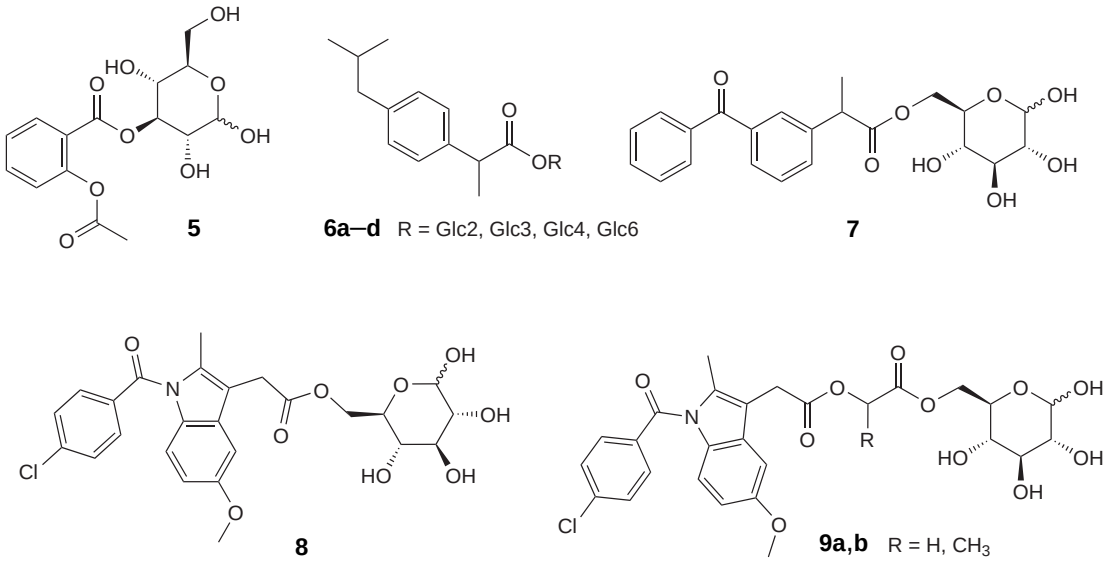

Figure 1.12: Structures of Glucosylated Non-Steroidal Anti-Inflammatory Drugs. Acetylsalicylic acid (Aspirin, **5**), Ibuprofen (**6**), Ketoprofen (**7**), Indomethacin (**8** and **9**).

brain uptake of ketoprofen and indomethacin 6-linked glucoconjugates (**7**, **8** and **9**).[163] *In situ* rat brain perfusion was used to study the brain uptake of ketoprofen derivative **7** and indomethacin derivative **8**. The uptake of the ketoprofen conjugate was reduced in the presence of 50 mM glucose, but no such effect was seen for the indomethacin conjugate. Incubation at 5 °C reduced the uptake of both glycoconjugates. Further experiments measured the inhibition of D-[^{14}C]glucose uptake in the presence of 20 mM glucose, compounds **7** and **8** (80 µM), at 5 °C or after preincubation with the conjugates followed by a wash step. Glucose, reduced temperature and ketoprofen derivative **7** all inhibited D-[^{14}C]glucose uptake by 75%, while the indomethacin derivative **8** inhibited over 95% of uptake. Inhibition was reversible, as washing the compounds from the capillaries restored D-[^{14}C]glucose uptake to 75–80% of the baseline. Furthermore, the IC_{50} values for **7** and **8** were determined to be 33 µM and 0.71 µM, respectively. These results indicate that 6-glucosylated ketoprofen **7** is transported into the brain by GLUT1. While the indomethacin derivative **8** has similarly high uptake into the brain, it is not inhibited by 50 mM glucose. This could signify that **8** is a non-transportable inhibitor and enters the brain via passive diffusion. It is, however, more probable that glucose does not inhibit the uptake of **8**, because of the compound's much higher affinity for the binding site compared to glucose.[163]

Halmos et al. studied glucose methanesulfonate esters as potential brain-targeted alkylating agents.[164] The compounds were tested for their inhibition (IC_{50}) of D-[^{14}C]glucose uptake by GLUT1. The IC_{50} values for glucose and its 3-mesylated, 4-mesylated, 6-mesylated, 3,6-dimesylated and 4,6-dimesylated derivatives were determined to be 10 mM, >100 mM, 32 mM, 52 mM, >100 mM and 42 mM, respectively. The study did not report whether the compounds enter the brain.[164] In an earlier study, Halmos et al. reported the synthesis of glucosylated chlorambucil derivatives (**10**, Figure 1.13) and their inhibition of D-[^{14}C]glucose transport by GLUT1.[165] The conjugates are 6-linked esters (**10a**) and amides (**10b**) of chlorambucil and glucose or methyl glucosides (**10c**,**d**). Conjugates were tested for their inhibition of D-[^{14}C]glucose uptake into erythrocytes. Both methyl glucosides (**10c**,**d**) had an IC_{50} of 3 mM, amide **10b** was inactive below 4 mM and ester **10a** was a strong inhibitor with an IC_{50} of 0.065 mM. This inhibition was determined to be reversible. Additionally, compound **10a** inhibited binding of [^{3}H]cytochalasin B, an allosteric GLUT1 inhibitor, to the transporter. The group also measured association

of carbon-14 labelled compound **10a** to erythrocytes and open erythrocyte membranes. The compound's binding was independent of the presence of cytochalasin B, and showed only a slight temperature dependence, while glucose transport was largely abolished by low temperatures.[165] The compound accumulated to the same extent in erthyrocytes and open erythrocyte membranes. These results taken together, indicate that compound **10a** is a high affinity, reversible, non-transported inhibitor of GLUT1. Uriel et al. conjugated keto-C-glycosides with various sugars and evaluated their potential as anti-cancer agents.[166] The compounds (**11**, Figure 1.13) were also tested for their inhibition of D-[^{14}C]glucose uptake into erythrocytes. The glucose and galactose derivatives had IC_{50} between 1.5 and 4.5 mM, while the xylose and L-rhamnose derivatives were much worse inhibitors. No permeability data was presented for these compounds.

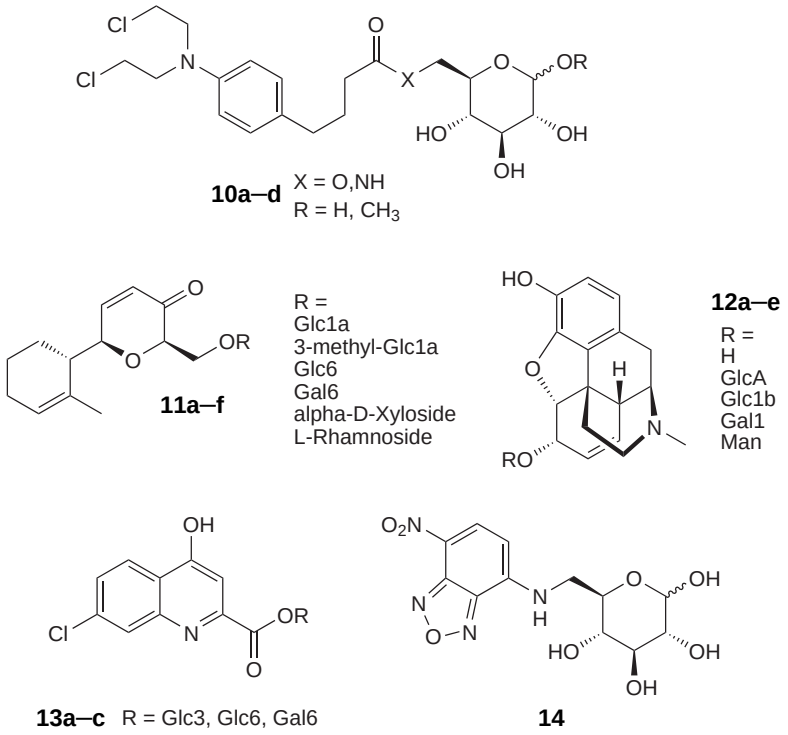

Figure 1.13: Structures of Other Glycosylated Molecules. Chlorambucil (**10**), Keto-C-glycosides **11**, Morphine (**12**), 7-Chlorokynurenic acid (**13**), 6-Deoxy-*N*-(7-nitrobenz-2-oxa-1,3-diazol-4-yl)-aminoglucose (NBDG, **14**).

Glucuronidation generally is used by the body to detoxify compounds, by increasing their solubility in blood and thus allowing excretion from the body via the kidneys. Glucuronidated substances were also found to be substrates of ATP-dependent efflux transporters, in particular the multidrug resistance-associated proteins (MRPs).[167,168] Several studies found an interplay between glucuronosyltransferase enzymes, in particular from the UDP

glucuronosyltransferase 1 family, and the expression and activity of MRPs.[169–171] In view of these findings, the glucuronidation of morphine has the interesting effect that it increases morphine's *in vivo* activity,[172] despite a 30-fold reduction of its brain uptake (%ID/g) in rats and a 60-fold reduction of its permeability surface area product (PS), compared to morphine.[173] Morphine (**12a**) and its glucuronide **12b**, glucoside **12c**, galactoside **12d** and other sugar derivatives have been studied regarding their opioid receptor binding and anti-nociceptive effect in rats.[174] The galactoside **12d** was much weaker, the glucuronide **12b** slightly weaker in their effect compared to morphine, while glucoside **12c** had a higher anti-nociceptive effect. The glucuronide and glucoside of 7,8-dihydromorphine showed the strongest anti-nociceptive effect.[174] A separate publication compared morphine mannoside **12e** to morphine and the glucuronide and found the mannoside to possess a much higher anti-nociceptive activity *in vivo*.[175] Neither of the studies tried to elucidate the mechanism of brain penetration, but a study by Bourasset et al. investigated the involvement of various transport proteins in morphine glucuronide (**12b**) brain uptake in mice.[176] The group found that knocking out mdr1a (PgP) did not affect the uptake of radiolabelled **12b**, but co-administration of glucose (30 mM), digoxin or PSC833 reduced the uptake to a third. Digoxin and PSC833 are inhibitors of PgP and the organic anion transport protein (OATP) family. These results indicate that **12b** is transported both by GLUT1 and a member of the OATP family.[176] In a more recent study however, Sattari et al. looked at the transport of **12b** in canine kidney cell lines MDCKII and MDCK-PGP (MDCK-MDR1), the latter of which over-expresses the PgP efflux transporter.[177] The group found that the transport of **12b** is increased by the PgP-inhibitor cyclosporin, in particular in MDCK-PGP cells, but reduced by PgP- and OATP-inhibitor digoxin. Treatment with probenecid, an inhibitor of OATP, did not have an effect, but partially inhibited by glucose. In summary, the authors of the study suggested, that morphine glucuronide **12b** is indeed subjected to PgP-efflux, but transported by GLUT1 and possibly members of the OATP transporter family.[177]

Sugar conjugates of 7-chlorokynurenic acid, a potential anti-convulsant, were reported by Battaglia et al.[178] The parent drug and the galactose derivative **13c** did not show anti-convulsant activity, while both glucose derivatives were active. Drug delivery to the brain was measured by continuous brain microdialysis in rats. Up to 1000-fold increased levels of conjugate **13b** and its metabolites were detected in the brain, when compared to unconjugated 7-chlorokynurenic acid, data for the other conjugates was not presented.[178]

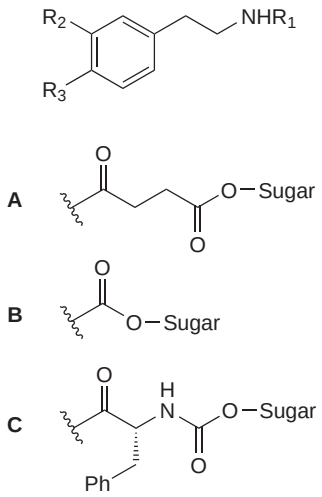

	R_1	R_2	R_3
dopamine	H	OH	OH
15a	A-Glc1b	OH	OH
15b	A-Glc3	OH	OH
15c	A-Glc4	OH	OH
15d	A-Glc6	OH	OH
15e	A-Gal6	OH	OH
16a	B-Glc1a	OH	OH
16b	B-Glc1b	OH	OH
16c	B-Glc3	OH	OH
16d	B-Glc6	OH	OH
16e	B-Glc6	OCH_3	OCH_3
16f	B-Glc6	OAc	OAc
16g	B-Glc6	methylenedioxy	
16h	B-Glc6	H	H
17	C-Glc6	OH	OH
18a	H	O-Glc1b	OH
18b	H	OH	O-Glc1b
18c	H	O-A-Glc6	OH
18d	H	OH	O-A-Glc6
18e	H	O-A-Glc6	O-A-Glc6

Figure 1.14: Structures of Dopamine-Sugar Conjugates.

A fluorescent glucose derivative, 6-deoxy-*N*-(7-nitrobenz-2-oxa-1,3-diazol-4-yl)-aminoglucose (**14**, NBDG) was first synthesised by Speizer et al.[179] The group found that NBDG (**14**) accumulates in erythrocytes and that its entry is inhibitied by glucose and cytochalasin B and is temperature dependent. This indicates transport by GLUT1.[179] Interestingly, its exit was uninfluenced by glucose but inhibited by cytochalasin B, while D- and L-glucose partially inhibit exit from erythrocyte ghosts. The authors speculated that uptake is in part mediated by GLUT1, while the exit was by passive diffusion.[179] Barros et al. showed that uptake of **14** is a slow process, which is due to a low transport rate.[180] A high binding affinity to GLUT1, which was calculated to be two orders of magnitude lower than glucose,[180] can explain the low inhibition by glucose, which was reported by Speizer. If the affinity of **14** to bind the inward facing conformation of GLUT1 is too low, it could be an explanation why it is not exported by GLUT1.

Dopamine and dopamine analogues have been conjugated to sugars in numerous ways (Figure 1.14, Figure 1.15). Bonina et al. synthesised dopamine and L-DOPA sugar conjugates **15b**,**e** and **19a**,**b** and evaluated them for their activity *in vivo*.[181] While dopamine normally does not enter the brain, its galactosyl derivative **15e** showed a higher activity than L-DOPA. The 3-glucosyl conjugate **15b** was also active, but to a lesser extent. The activity of L-DOPA, which is centrally active, was increased by conjugation to glucose

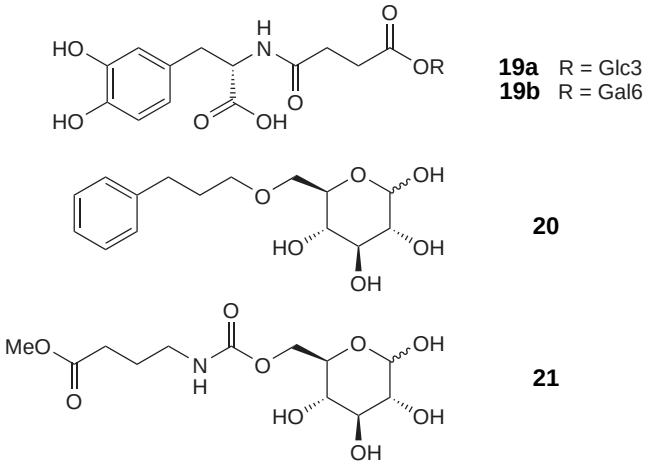

Figure 1.15: Structures of Glycosylated L-DOPA and Dopamine Analogues.

(**19a**), while the 6-galactosyl derivative **19b** had roughly the same activity as the parent drug.[181] The uptake of the compounds was not directly measured. Fernandez-Mayoralas and co-workers reported the synthesis of a large number of dopamine conjugates, including succinyl- (**15** and **18**), carbamate- (**16**) and peptide-linked (**17**) derivatives,[182–184] as well as structurally related sugar conjugates **20** and **21** (Figure 1.15).[184] The group determined the uptake into erythrocytes,[184] inhibition of glucose uptake by erythrocytes,[183] and the *in vivo* effect[182] of some of these conjugates. Compounds **15a**,**d**,**e** and **18a**,**b** were tested for their ability to recover motor activity in reserpinised mice.[182] The 6-linked derivative **15d** and β-glucoside **18b** were the most active compounds, but at the tested dose, they were only half as effective as amphetamine, while the other compounds showed even less modification of motor activity.[182] Compounds **15a**,**d**,**e**, **16a**–**d**, **17** and **18a** were tested for their effect on D-[^{14}C]glucose uptake into erythrocytes.[183] Glucosides **15a** and **18a** and galactose derivative **15e** were inactive, compounds **16a**–**c** had IC_{50} values of 50, 31 and 60 mM, respectively. Only conjugates that were linked in position 6 of glucose, had IC_{50} values around or lower than glucose: Values for **15d**, **16d** and **17** were 12, 1.5 and 2.2 mM, respectively.[183] The uptake into erythrocytes was evaluated for **16d**, along with 6-linked glucoconjugates **16e**–**h**, **20** and **21**.[184] No uptake was detected for the compound with the highest GLUT1 inhibition (**16d**), its *O*-acetyl derivative **16f** and compound **21**. Dopamine derivatives **16e**, **16g** and **16h** were taken up by erythrocytes (0.8, 1.8 and 2.5 mmol/l erythrocytes), as was compound **20** (4.9 mmol/l erythrocytes). Their uptake does not appear to be GLUT1 dependent, however, since co-incubation with reversible and irreversible GLUT1 inhibitors did not change the uptake of these compounds.[184]

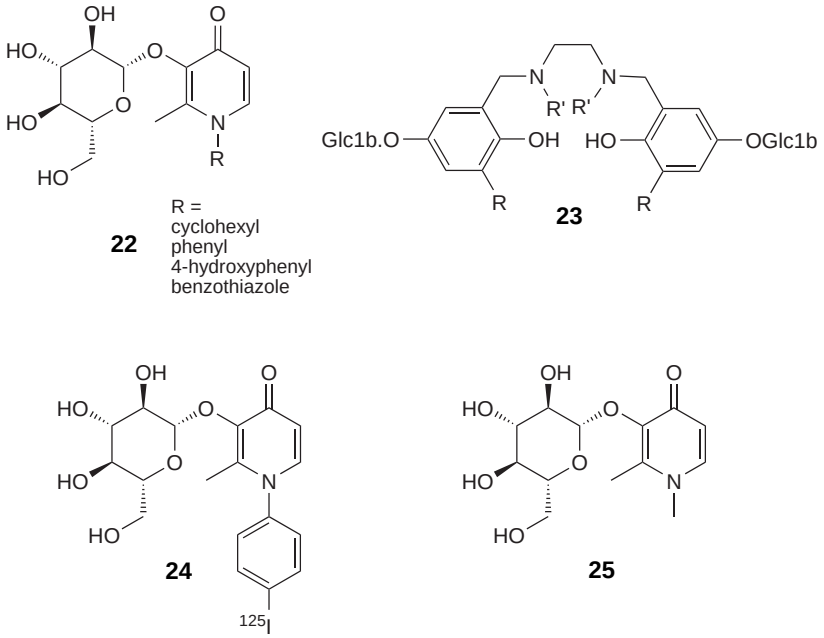

Figure 1.16: Structures of Glycosylated Metal Chelators.

Orvig and co-workers recently published the synthesis of glucosylated metal chelators of the hydroxypyridinone **22** and tetrahydrosalen **23** classes (Figure 1.16),[185–188] and speculated that this glucosylation results in directed uptake into the brain.[186,187] Hydroxypyridinone glucosides were tested for their use as prodrugs for the treatment of Alzheimer's disease by copper chelation. Furthermore, the uptake of radioiodinated compounds was tested in a rat brain perfusion assay.[186,187] The permeability of **24** was found to be $0.5\,\mu l\,s^{-1}\,g^{-1}$,[186] a structurally related radioiodinated glucoconjugate had a permeability of $0.9\pm0.4\,\mu l\,s^{-1}\,g^{-1}$, which is comparable to thiourea and lower than caffeine.[187] The group speculated that this uptake is due to GLUT1 transport.

Roy et al. synthesised glucosylated deferiprone (**25**), which is structurally closely related to pyridinone **24**. Brain uptake of **25** was measured by *in situ* brain perfusion of guinea pigs, but HPLC could not detect the compound in the brain.[51]

While many studies investigated the synthesis and activity of glycosylated molecules, which are purportedly transported by GLUT1, only few studies measured the compounds' interaction with and inhibition of the glucose transporter and even fewer measured the substances' uptake.

In the work published by the Orvig group, for example, rat brains were perfused via the common carotid artery with physiological perfusion fluid containing [^{3}H]-choline and the

radioiodinated HPO-glucoside **24** (Figure 1.16).[186,187] The brains were perfused for 60 seconds at 10 ml/min, resulting in an arterial pressure of 120 mmHg. After decapitation, the brains were isolated and cleaned of meningeal vessels and the arachnoid membrane. The perfused hemispheres were then dissected. The protocol mentions the digestion of 'brain regions' before scintillation counting, but no further details regarding the specific regions is given and only one permeability value is reported (presumably for the whole brain). The permeability was calculated (K_{in}) via the Crone-Renkin equation and corrected for the brain vascular space, which was estimated in separate experiments. While the design of the experiment is relatively solid, a more reliable K_{in} could have been calculated from linear regression if the uptake had been measured at multiple time points. Potentially, the radiolabel had partly dissociated [§] and diffused as iodide ion across the BBB, rather than the intact molecule, skewing the measured results towards a higher permeability. The direct measurement of a compound by HPLC/GC, or the use of stable radiolabels (tritium or carbon-14) would therefore be preferable. The main issue with these studies are that the presentation and interpretation of the data could be improved. The standard deviation or standard error or sample size for the experiments was not given, and the use of choline in the perfusion fluid is not explained or mentioned further. The authors of the studies interpret the uptake of the radioiodinated compound at levels lower than expected by passive diffusion as a sign that the compound is plausibly entering the brain through carrier-mediated transport. This conclusion is questionable, as GLUT1 transport or other carrier-mediated transport would increase the brain uptake of molecules in addition to their passive diffusion, rather than reduce the extent of passive diffusion. Active-efflux transport might be a better explanation for the low permeability found for the glucosylated compound.

In contrast, Halmos et al. studied glucosylated chlorambucil derivatives (**10**, Figure 1.13) in human erythrocytes and erythrocyte membranes.[165] Erythrocytes were isolated from fresh blood in citrate buffer by removal of platelets and leukocytes. The cells were washed by multiple centrifugation (2500 *g*) and resuspension steps in phosphate buffered saline and stored at a hematocrit of 30%. Erythrocyte membranes were prepared by hemolysis of erythrocytes in sodium phosphate solution followed by centrifugation (22000 *g*) and

[§]Iodinated compounds may dissociate due to the relatively low bond dissociation energy (under 60 kcal/mol for a carbon-iodine bond, carbon-bromine and carbon-hydrogen bonds are around 72 kcal/mol and 100 kcal/mol, respectively).[189]

multiple washings. The inhibition of [^{14}C]-glucose uptake (IC_{50}) into erythrocytes by glucose, methyl-β-glucopyranoside, 3-*O*-methylglucose and chlorambucil derivatives was determined at 8 seconds incubation time[¶] and stopped by an ice-cold buffer with inhibitors (phloretin, cytochalasin B and $HgCl_2$). The 6-amide-linked conjugate **10b** was found to have an IC_{50} value larger than the highest tested concentration (4 mM) and the 6-linked methylglucosides **10c**,**d** were relatively inactive (3.0±0.3 and 3.0±0.9 mM). The 6-ester-linked conjugate **10a**, however, was about 50-times better as an inhibitor of glucose uptake (IC_{50}: 65±15 µM). Conjugate **10a** was thus studied further. The inhibiton of glucose uptake by **10a** or cytochalasin B pre-incubation of 20 min was reversible by washing of the erythrocytes with PBS after the pre-incubation, eliminating the possibility that the inhibitory effect was due to alkylation of GLUT1. Similarly to the inhibiton of glucose uptake, the binding of tritium-labelled cytochalasin B to GLUT1 was inhibited by conjugate **10a** in a competitive manner. Finally, [^{14}C]-compound **10a** was incubated with erythrocytes over a range of times (up to 1 hour) and concentrations. The uptake of the compound was independent of saturating concentrations of glucose or cytochalasin B and independent of the temperature, thus suggesting non-specific binding to some component of the cells. This was confirmed by an experiment measuring the association of the compound to open erythrocyte membranes, which found the similar levels of binding as for intact erythrocytes. The authors therefore concluded that the conjugate **10a** interacts with GLUT1 as a non-transported inhibitor.[165] Halmos et al. tested the uptake of **10a** thoroughly, and drew the correct conclusions from the data that they had obtained from multiple well designed experiments, each with a specific intention.

Overall, certain trends in the literature could be identified. Sugars other than glucose are not very well tolerated by GLUT1. Inhibition of GLUT1 is not sufficient to indicate transport of the substance. All conjugates that were convincingly proven to be transported by GLUT1 are linked in position 6, and the drugs that have been linked are relatively small and lipophilic. The findings are in agreement with the studies on substrate specificity of GLUT1 (see 1.2.3.1).

The evidence base for GLUT1 transported drugs currently remains narrow, generalisations should therefore be avoided. Each compound class needs to be evaluated not through

[¶]Glucose uptake was previously determined to be linear up to this time point.

inference from other compound's results, but tested rigorously before conclusion about GLUT1-mediated transport are drawn.

1.3 Objectives

The use of iron chelators for the treatment of PD is a promising strategy, but the drugs currently being investigated rely on passive diffusion across the BBB. It was hypothesised that the conjugation of iron chelators with sugars could target them to the brain and enhance their uptake.

The aim of this project is therefore to investigate the BBB permeability of known and novel iron chelators of the 3-hydroxypyridin-4(1*H*)-one class. The focus is to study whether sugar conjugates can overcome the BBB, and whether this is facilitated by GLUT1.
The main objective is to investigate how different linkers, points of attachment on the HPO moiety and the sugar moiety affect the molecules' affinity for and transportability by GLUT1. Potential conjugates (Figure 1.17) can be linked in positions 1, 2 and 3 of the HPO moiety. Accessible linkers for the conjugation are amides, ester, ethers or triazoles, which could be linked in any position of the sugar. Due to the structural requirements for substrate recognition of GLUT1, conjugates linked in position 6 of the sugar are of particular interest.
Iron chelator glucosides have been reported previously, but the extent of their BBB permeability remains debated.[51,186] Further investigations into these conflicting findings are the second objective.
The third objective of this work is the development of a suitable cell-based assay, which can be used for the determination of BBB permeability, specifically with regards to the role of GLUT1 as facilitative transporter of sugar conjugates.

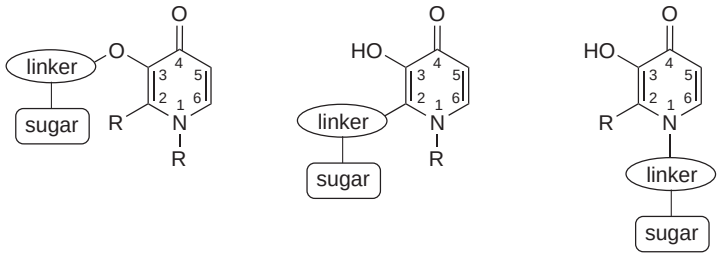

Figure 1.17: General Structure of Sugar-Hydroxypyridinone Conjugates.
Linker = Amide, Ester, Ether, Triazole.

Chapter 2

Synthesis of Glucoside-linked Conjugates

Reports regarding the blood-brain barrier permeability of HPO glucosides **24** and **25** (Figure 2.1) were published by Orvig's and Hider's groups, respectively.[51,186] Schugar et al. reported that the radiolabelled molecule **24** could be detected in the brain of rats by scintillation counting.[186] Roy et al. measured the permeability of *N*-methyl pyridinone **25** in guinea pigs, but could not detect any compound by HPLC analysis of the brain homogenate.[51]

In order to investigate this intriguing difference in BBB permeability further, the synthesis of the non-radiolabelled analogue of compound **24** and its close structural analogues **26** was attempted, and their permeability in a cell-based assay quantified directly by HPLC.

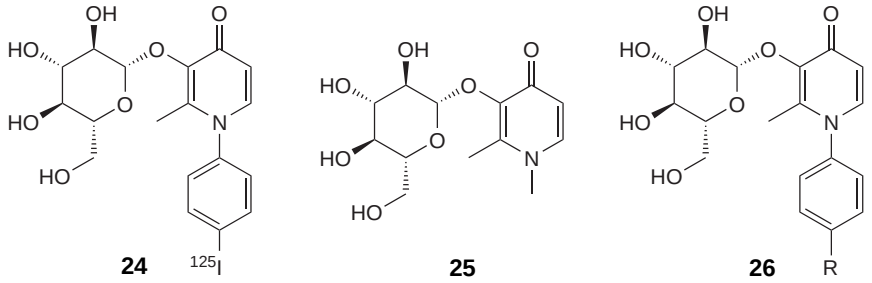

Figure 2.1: Structures of 3-(β-D-Glucopyranosyloxy)-pyridin-4-ones.[51,186]

Maltol (**27**, Scheme 2.1) was reacted with aniline (**28a**) and 4-bromoaniline (**28b**) to give *N*-arylpyridinones **29a** and **29b** in 60% and 33% yield, respectively. This difference in reactivity may be explained by the electronic effect the bromo-substituent has on the aromatic amine. Pyridinones **29** were then glucosylated with 2,3,4,6-tetra-*O*-acetyl-α-D-glucopyranosyl bromide (**30**, 1-bromo-α-D-glucose tetraacetate, which may be synthesised as described in Scheme 4.3) in the presence of sodium hydroxide in a biphasic reaction mixture, with tetrabutylammonium bromide or hydrogen sulfate as phase transfer agent. Protected glucosides **31a** and **31b** were obtained in 40% and 44% yield exclusively as

the β-anomers. This substitution reaction proceeds via elimination of the bromide and attack by the carbonyl oxygen of the adjacent acetyl group. The resulting α-configured oxocarbenium ion is attacked by the alcohol, resulting in the β-configuration of the product.[190] This is also confirmed by the ^{1}H-NMR signal of the anomeric proton. In α-configured glucosyl bromide **30**, the signal is at δ 6.61 ppm and the coupling constant is 4.0 Hz, while in glucosides **31a** and **31b** the coupling constant is 7.9 Hz (chemical shift: 5.70 ppm and 5.69 ppm respectively). These values match the coupling constants for β-configured glucopyranoses (around 8 Hz), which have been determined experimentally,[191] while the anomeric proton of α-configured glucopyranoses has a coupling constant around 4 Hz.[191] Deprotection of the sugar with sodium methoxide in dry methanol finally gave the desired glucosides **26a** in 74% yield and **26b** in 60% yield. The purity of these compounds was found to be >99%, as determined by HPLC.

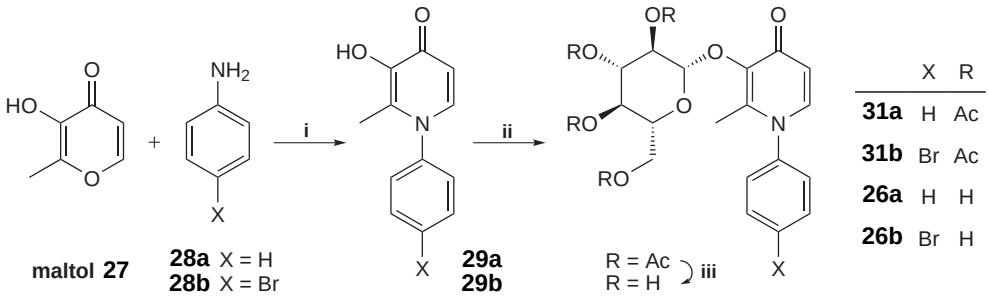

Scheme 2.1: Synthesis of 3-(β-D-Glucopyranosyloxy)-1-phenylpyridin-4-ones. Reagents and Conditions: i) HCl, H_2O, reflux, **29a**: 60%, **29b**: 33%; ii) 1-bromo-α-D-glucose tetraacetate **30**, TBAB or TBAS, NaOH, DCM/H_2O, 35 °C, **31a**: 40%, **31b**: 44%; iii) NaOMe, dry MeOH, rt, **26a**: 74%, **26b**: 60% .

Following the procedure for the synthesis of [^{125}I]pyridinone **24**, described by Schugar et al., the 4-brominated glucoside **31b** was transformed to arylstannane **31c** with bis(tributyltin) and tetrakis(triphenylphosphine)palladium in 13% yield (Scheme 2.2, literature:[186] 38%). A potential reason for the lower yield could be that the anhydrous reaction conditions were not maintained as rigorously as it might be necessary. The next step, replacement of the tributylstannyl group with the radioisotope – or 'cold' iodine in this case – was effected by sodium iodide, chloramine T and dilute phosphoric acid. Schugar et al. report the successful transformation to the radioiodinated product and its subsequent deprotection to glucoside **24**. Despite exactly replicating the reported procedure, the reaction did not yield the desired **31d**, but rather starting materials and decomposition products. After column chromatography, some decomposition products could be identified as (partially)

deacetylated starting material due to their NMR spectra, which showed one or two acetyl signals fewer than the starting material's spectrum.

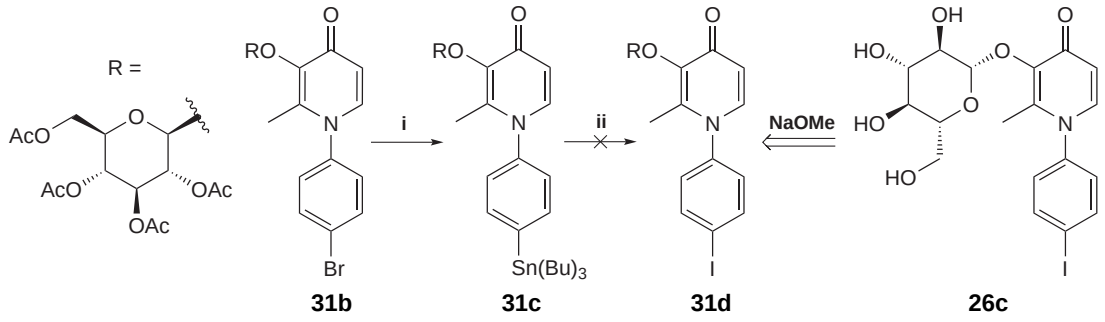

Scheme 2.2: Attempted Synthesis of 3-(2,3,4,6-Tetra-*O*-acetyl-β-D-glucopyranosyloxy)-1-(4-iodophenyl)-2-methylpyridin-4(1*H*)-one. Reagents and Conditions: i) Bis(tributyltin), $Pd(PPh_3)_4$, dry toluene, N_2 atmosphere, reflux, 13%; ii) NaI, chloramine T, H_2PO_4, $EtOH/H_2O$, rt.

Alternative Routes to 1-(4-Iodophenyl)-Pyridin-4-ones

Attempts were made to obtain **31d** via other synthetic routes. The reaction conditions, which were previously used for the double Michael addition of an aromatic amine to maltol (Scheme 2.1), gave the expected pyridinones **29a** and **29b** from aniline and 4-bromoaniline. When 4-iodoaniline (**28c**) was used as reagent however (Scheme 2.3), extensive polymerisation was observed and no product could be identified or isolated, while unreacted maltol was partly recovered. Reversal of the reaction steps, thus glucosylating maltol first, yielded pyranone **32** (30%). The double Michael addition of 4-iodoaniline under acidic conditions again resulted in polymerisation of 4-iodoaniline and some decomposition of glucoside **32** (partial deacetylation of the glucoside). Saghaie et al. reported that the reaction between pyranone and aniline proceeds without addition of acid, but at high temperatures (150 °C to 160 °C) in a sealed pressure tube.[192] Under these conditions, no reaction was observed even after prolonged reaction times, and the unmodified starting materials were recovered (Scheme 2.3).

After reactions with 4-iodoaniline did not yield iodinated pyridinones, other possibilities to introduce iodine to an aromatic ring were investigated. Buchwald's group published a facile and high yielding method for the exchange of aromatic bromides via an aromatic Finkelstein reaction.[193] For this, the aromatic bromide, sodium iodide, a catalytic amount of copper(I) iodide and a simple diamine ligand are heated to reflux in a protic or non-protic, polar solvent (or solvent mixture), generally for 12–24 hours.[193]

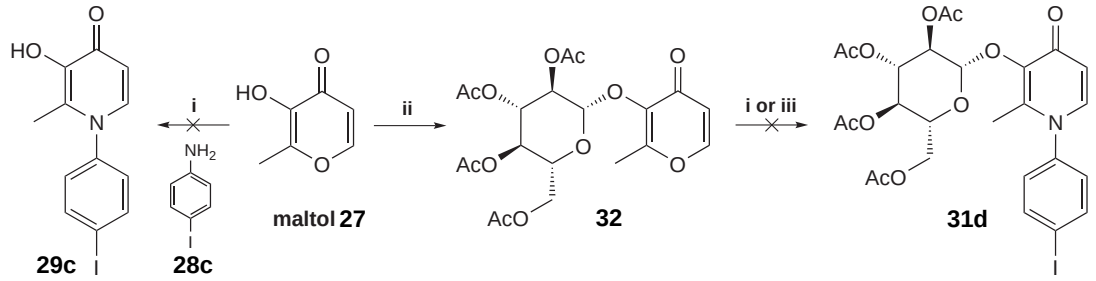

Scheme 2.3: Attempted Synthesis of 1-(4-Iodophenyl)-pyridin-4-ones. Reagents and Conditions: i) 4-iodoaniline **28c**, HCl, MeOH/H_2O, reflux; ii) glucosyl bromide **30**, TBAB, NaOH, DCM/H_2O, 35 °C, 30%; iii) 4-iodoaniline **28c**, MeOH/H_2O, 150 °C, sealed tube.

The feasibility of this reaction was explored in a set of trial experiments using less complex starting materials. HPOs have a high affinity to chelate copper,[194,195] which would lead to the chelation of the catalyst for the transhalogenation. The iron chelating part of the molecule (3-hydroxy and 4-oxo groups) therefore had to be masked to prevent chelation of the catalyst. Benzylated maltol **33** (Scheme 2.4) was thus synthesised from maltol and benzyl bromide in excellent yield. Pyranone **33** was then transformed to pyridinone **34a** by reaction with 4-bromoaniline (yield: 79%), as described for the non-benzylated pyridinones **29**. The transhalogenation reaction was then attempted on benzylated bromopyridinone **34a**. For this, the pyridinone **34a**, sodium iodide, copper(I) iodide, *N,N'*-dimethylethylenediamine and dioxane were added to a sealed tube and heated to 110 °C for 24 hours. The crude product was isolated and analysed by ^{1}H-NMR spectroscopic analysis, which showed that the reaction successfully produced **34b**, but some unreacted starting material remained (5/1 ratio **34b**/**34a**; yield by NMR: 64%). The product was identified by the change of the ^{1}H-NMR shift of the phenyl ring protons (*ortho* and *meta* to

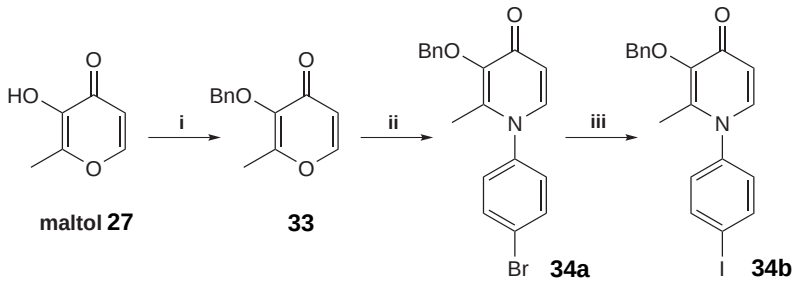

Scheme 2.4: Synthesis of 3-(Benzyloxy)-1-(4-iodophenyl)-2-methylpyridin-4(1*H*)-one. Reagents and Conditions: i) Benzyl bromide, NaOH, MeOH/water, reflux, 92%; ii) 4-bromoaniline **28b**, HCl, MeOH/H_2O, reflux, 79%; iii) NaI, CuI, *N,N'*-dimethylethylenediamine, dry dioxane, 110 °C, sealed tube, 64%.

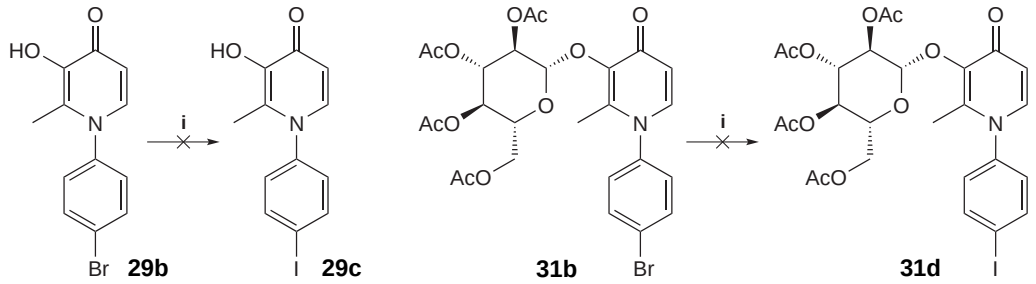

Scheme 2.5: Attempted Transhalogenation of 1-(4-Bromophenyl)-pyridin-4-ones. Reagents and Conditions: i) NaI, CuI, *N,N'*-dimethylethylenediamine, dry dioxane, 110 °C, sealed tube.

the halogen substituent). In the 4-bromo substituted HPO **34a**, these signals are doublets with a chemical shift of 7.73 ppm and 7.28 ppm, while the iodinated product **34b** lacks these peaks and shows doublets at 7.83 ppm and 6.93 ppm, instead, which can be explained by the stronger electronic effect of the iodine substituent.

When the same reaction conditions were used for the transhalogenation of 3-hydroxy-pyridinone **29b** (Scheme 2.5), no reaction was observed, however, and the starting materials were recovered. This result was expected as the compound presumably sequestered the copper catalyst, preventing any reaction. In the glucosylated pyridinone **31b**, the glucoside masks the 3-hydroxy group, which should prevent chelation of the catalyst. Surprisingly, after column chromatography we mainly isolated unreacted **31b**, some partially deacetylated starting material and other unidentified side products. This lack of reactivity could not be explained in view of the previous experiments, however.

At this point, no further attempts towards the synthesis of pyridinone **26c** (Scheme 2.2) were made, and the blood-brain barrier permeability assays were carried out with the non-iodinated analogues **26a** and **26b**.

Spectroscopic Investigations

The spectroscopic investigations for the structure elucidation of glucoside **26a** (Figure 2.2) and full assignment of all ^{1}H- and ^{13}C-resonances – and ^{1}H,^{1}H-coupling constants where possible – are presented here (Table 2.1), in order to demonstrate the general approach taken to ascertain that the isolated compounds are of the expected structure.

Reliable and unambiguously assigned chemical shift data are important reference material for NMR prediction programs, such as CSEARCH[196]/NMRPREDICT[197] (part of the

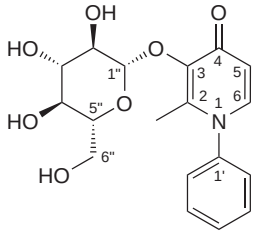

26a

Figure 2.2: Structure and Numbering of Glucoside **26a**.

Mnova package) and ACD/NMR Predictors.[198] NMR prediction programs have become very popular in the last few years, particularly for predicting ^{13}C-NMR chemical shifts. However, the quality of such predictions is highly dependent on the availability of authentic reference data from related structures.

Glucoside **26a** is a pale tan solid, which decomposes at 198 °C. High resolution mass spectrometry found the parent ion plus chloride ([M+Cl$^-$]) at m/z 398.1007/400.0973 amu, which is within ±0.01 amu of the calculated values for expected parent ion plus chloride. This indicates, that the molecule has the same molecular formula as the expected product ($C_{18}H_{21}NO_7$+Cl$^-$).

Multiple NMR spectra of **26a** in deuterated methanol were recorded for the structure elucidation: ^{1}H-NMR, proton decoupled ^{13}C-NMR, DEPT135, ^{1}H,^{13}C-HSQC, ^{1}H,^{13}C-HMBC and ^{1}H,^{1}H-COSY. Certain signals are unique in this compound and can be assigned directly, such as the singlet at 2.25 ppm (2-CH_3) and the two doublets at 7.75 and 6.57 ppm, which are the pyridinone ring hydrogens (H-5 and H-6). The COSY spectrum allows the assignment of the network of hydrogen atoms that couple with each other. Starting from proton signals which are very distinct, such as the doublet of H-1" (4.73 ppm), the anomeric centre of the sugar, the remaining signals of the sugar part of the molecule (between 3 and 4 ppm) are easily assigned (Table 2.1). The signals of the phenyl ring appear as two multiplets: 7.63–7.57 ppm for H-3',4',5' and 7.47–7.41 ppm for H-2',6'.

The proton decoupled ^{13}C-NMR spectrum shows all carbon signals, while the DEPT135 spectrum shows only carbon atoms which are bonded to at least one hydrogen atom. DEPT135 also shows whether a carbon is connected to an even or odd number of hydrogen atoms. Signals that do not appear in the DEPT135 spectrum, but are present in the decoupled carbon NMR spectrum, must stem from quaternary carbon atoms. The HSQC spectrum allows the assignment of the proton signals to the carbon atoms to which the

protons are attached to, so that the quaternary carbon signals are the only signals that have not been assigned at this point (Table 2.1).

The ^{1}H,^{13}C-HMBC spectrum contains a large amount of information about the connectivity within a molecule and is a very powerful and important NMR technique for structure elucidation. Since the signal at 145.91 ppm correlates with the signal of H-1" (4.73 ppm), this carbon must be C-3 (Figure 2.3.a). H-5 may also be identified from its correlation with the signal from C-3, and its shift is therefore 6.57 ppm. C-3 also correlates with the 2-methyl group (2.25 ppm). The other quaternary carbon (146.76 ppm) the 2-methyl group has a correlation with, must thus be C-2 (Figure 2.3.b). The correlation of C-2 with the signal of H-6 (7.75 ppm) confirms the previous assignment of H-5. H-5 and H-6 both correlate with the carbonyl signal at 174.86 (C-4, Figure 2.3.c), while only H-6 correlates with C-1' of the *N*-phenyl ring. Three-bond correlations were observed (H-2',6' with C-4' (131.16 ppm), H-3',5' with C-1' and H-4' with C-2',6'), while two-bond correlations were too weak to be observed.

To summarise, a combination of standard 1D and 2D NMR techniques was sufficient to fully and unambiguously assign all carbon and proton signals of glucoside **26a**.

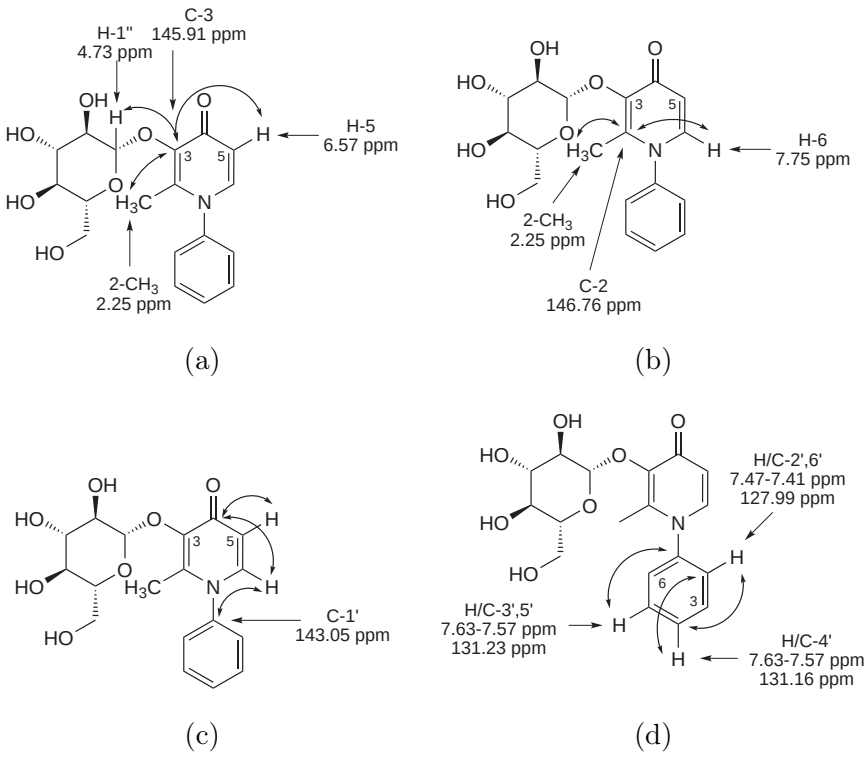

Figure 2.3: HMBC Correlations in Glucoside **26a**.

Table 2.1: Proton and Carbon NMR Signals of **26a** in CD_3OD. Shifts given as δ ppm, relative to TMS.

Position	^{1}H Shift	^{13}C Shift	Signal Type[a]
2	–	146.76	Cq
3	–	145.91	Cq
4	–	174.86	Cq
5	6.57	116.89	CH, d
6	7.75	142.3	CH, d
2-CH_3	2.25	15.74	CH_3, s
1’	–	143.05	Cq
2’,6’	7.47–7.41	127.99	CH, m
3’,5’	7.63–7.57	131.23	CH, m
4’	7.63–7.57	131.16	CH, m
1”	4.73	107.06	CH, d
2”	3.47–3.40	75.58	CH, m
3”	3.47–3.40	78.48	CH, m
4”	3.34	71.11	CH, ‘t’
5”	3.27	78.72	CH, ddd
6a”	3.84	62.63	CH, dd
6b”	3.66	62.63	CH, dd

[a] Type of carbon signal: Cq – quaternary carbon. Multiplicity: s – singlet, d – doublet, t – triplet, m – multiplet.

Chapter 3

Synthesis of Amide-linked Conjugates

The second aim of this project – in addition to the preparation of HPO-glucosides **26** discussed in the previous chapter – was to obtain conjugates which are linked in other positions, particularly positions 2 and 6 of the sugar moiety. These positions are expected to facilitate the recognition and transport of sugar conjugates by GLUT1, as discussed in Section 1.2.3.2.

In this chapter, the synthesis of amide-linked conjugates is described. Amide-linked conjugates were designed, because amides are relatively facile to form, while at the same time stable enough to withstand the esterases and general milieu found in blood. The starting materials for the formation of an amide are commonly a carboxylic acid and an amine. This allows two distinct strategies for HPO-sugar conjugates (Figure 3.1). On the one hand an amino sugar could be coupled with an HPO with a carboxylic acid moiety, and on the other hand a sugar bearing an acid group could be attached to an HPO with a free amino group. Both routes are described in this chapter.

Additionally, 3-hydroxypyridin-4-ones can be conveniently functionalised on two parts of the molecule: A substituent with the desired functional group may be introduced on the nitrogen of the pyridinone ring or any of the ring carbons.

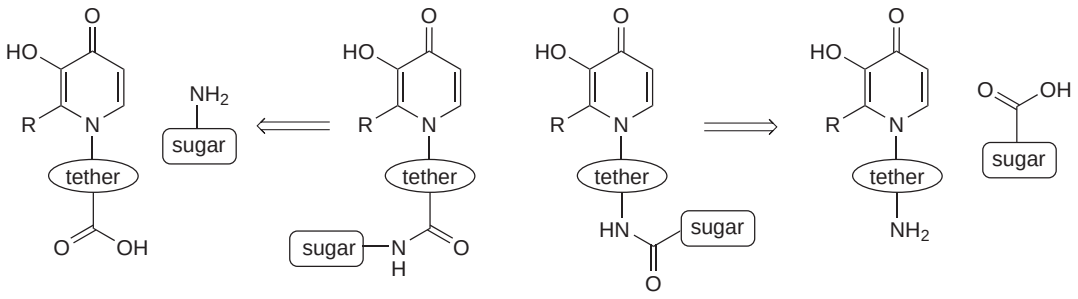

Figure 3.1: Routes towards Amide-linked Conjugates.

3.1 Preparation of Conjugates with Glucosamine

3.1.1 Synthesis of ω-(4-Oxopyridin-1-yl)carboxylic acids

This section covers the preparation of HPOs with *N*-alkyl substituents bearing a carboxylic acid group.

Maltol (**27**), protected maltol **35** or other pyran-4-ones are readily transformed into their respective pyridin-4-ones **36** (Scheme 3.1) via a double Michael addition of alkylamines, amino alcohols, amino acids and most other aliphatic primary amines under basic conditions, as demonstrated by Dobbin et al.[199] Alternatively, *N*-unsubstituted HPOs **37** may be alkylated or acylated with the appropriate alkyl or acid halides.[200,201]

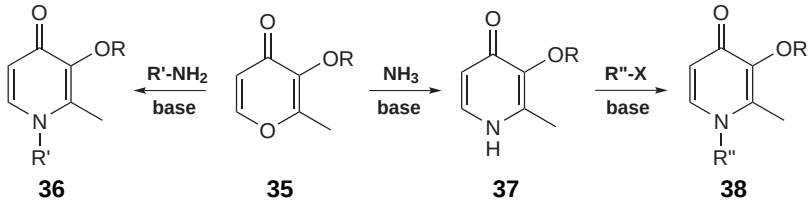

Scheme 3.1: Synthesis of *N*-substituted 3-Hydroxypyridin-4-ones.[199–201] Reagents and Conditions: R = H, Me, Bn; R' = alkyl, hydroxyalkyl, carboxylic acid, aminoalkyl; R'' = alkyl, acyl.

In order to obtain the desired HPOs, the protocol described by Dobbin et al. was followed. The 3-hydroxy group of maltol was first benzylated to give pyranone **33** in 92% yield (Scheme 3.2). Reaction of this intermediate with glycine, β-alanine or γ-aminobutyric acid transformed the protected pyranone into pyridinones **39a**, **39b** and **39c**, respectively, in good to excellent yield (71–98%). This reaction proceeds via a double Michael addition under basic conditions (Scheme 3.3), as described by Elkaschef and Nosseir.[202]

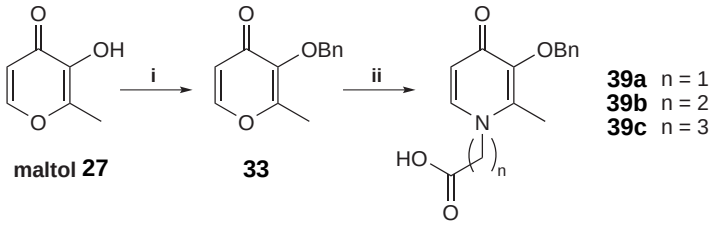

Scheme 3.2: Synthesis of ω-(4-Oxopyridin-1-yl)carboxylic acids. Reagents and Conditions: i) Benzyl bromide, NaOH, MeOH/water, reflux, 92%; ii) glycine or β-alanine or γ-aminobutyric acid, NaOH, MeOH/water, reflux, **39a**: 94%, **39b**: 71%, **39c**: 98% .

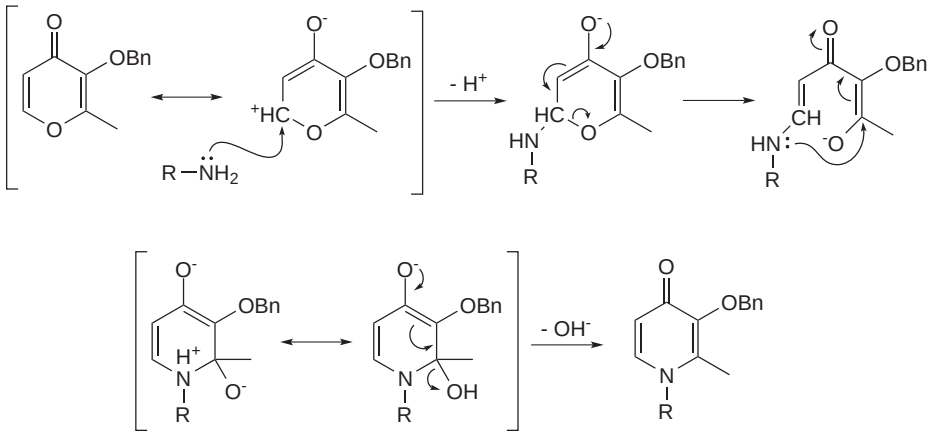

Scheme 3.3: Reaction Mechanism of Double Michael Addition to Pyran-4-ones.

3.1.2 Preparation of 2-Carboxypyridin-4-ones

HPOs bearing functional groups in position 2 have been described in the literature, but their synthesis typically involved numerous steps to introduce an oxygen on the substituent on position 2, which was then oxidised further.

For example, Liu et al. prepared pyromeconic acid (**40**, R=H, Scheme 3.4) from furfuryl alcohol in 4 steps (40% overall yield).[203] Pyromeconic acid or its 6-substituted analogues were then reacted with an aldehyde, in a reaction analogous to an aldol condensation. This was followed by the protection of both hydroxy groups as a benzylidene acetal, to give pyranones **41**. These intermediates were transformed to the respective pyridinone **42** via double Michael addition of a primary amine R"-NH_2. The 2-hydroxyalkyl group was then deprotected by catalytic hydrogenolysis to furnish pyridinones **43**.[203] Such pyridinones **43**, where R'=H, are suitable starting materials for the further oxidation of the alcohol functionality in position 2 to the respective carboxylic acids, as described below (Scheme 3.5).

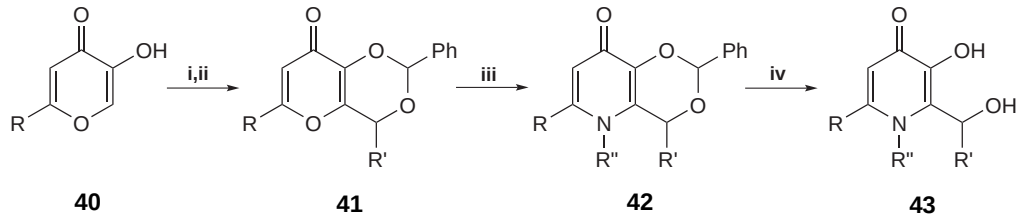

Scheme 3.4: Published Synthesis of 2-(1'-Hydroxyalkyl)-3-hydroxypyridin-4-ones.[203] Reagents and Conditions: i) R'-CHO, water, pH 10.5, rt, then HCl, 47%; ii) benzaldehyde dimethyl acetal, *p*-TsOH, DMF, 80 °C, 82%; iii) R"-NH_2, 2M NaOH, EtOH/water (1/1), 70 °C, 40–79%; iv) Pd/C (5%), H_2, EtOH, pH 1, rt, 73–88%.

An alternative route for the synthesis of HPOs with a carboxy group in position 2 was reported by Piyamongkol et al. and starts from maltol (Scheme 3.5).[204] First, the 3-hydroxy group was benzylated, followed by the double Michael addition of ammonia to furnish pyridinone **44**. The carbonyl group in position 4 was then benzylated in a Mitsunobu reaction using benzyl alcohol to give 3,4-bis(benzyloxy)-2-methylpyridine, which in turn was oxidised to its *N*-oxide **45** with *m*-chloroperoxybenzoic acid in DCM. The *N*-oxide was acetylated with acetic anhydride, which re-arranges to give ester **46**. The ester was hydrolysed and the resulting hydroxide transformed to the aldehyde with a Parikh-Doering oxidation. 3,4-Bis(benzyloxy)picolinic acid (**47**) is finally obtained in 14% overall yield by oxidation with sodium chlorite and sulfamic acid.[204]

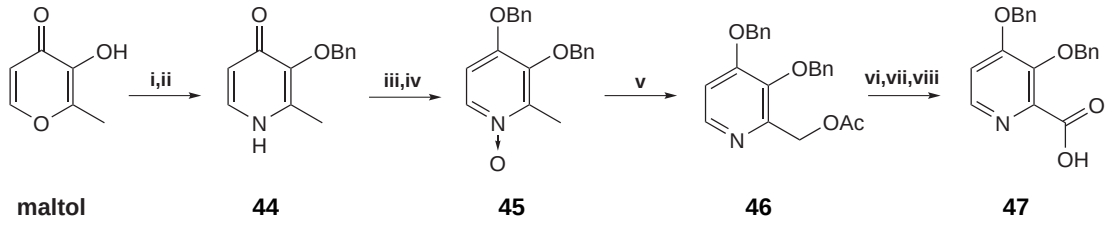

Scheme 3.5: Synthesis of 3,4-Bis(benzyloxy)picolinic acid.[204] Reagents and Conditions: i) BnBr, NaOH, EtOH, reflux, 80%; ii) NH3, EtOH, reflux, 75%; iii) TPP, DEAD, BnOH, THF, reflux, 79%; iv) MCPBA, DCM, rt, 77%; v) acetic anhydride, reflux; vi) 2M NaOH, reflux, 81% (two steps); vii) DMSO, Py−SO_3, TEA, chloroform, rt, 62%; viii) $NaClO_2$, H_2NSO_3H, acetone/water (1/1), rt, 77%.

In general, the desired carboxylic acid (**48**, see Scheme 3.6) could be obtained from the oxidation of pyridinone **49** or from the double Michael addition of methylamine to an oxidised pyranone, e.g. carboxylic acid **50**. The latter route was chosen, avoiding the potential problems with the selective oxidation of one methyl group over the other in **49**.

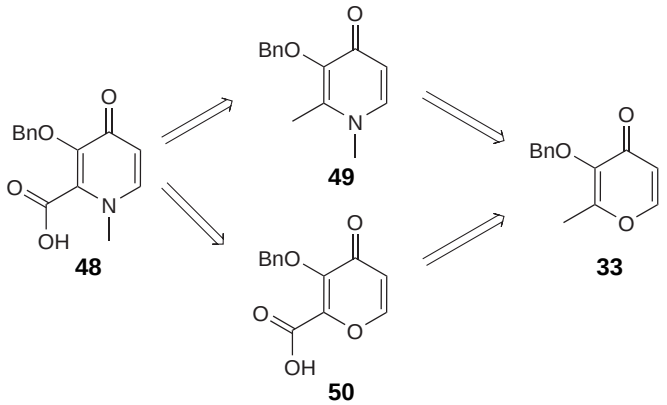

Scheme 3.6: Retrosynthetic Analysis of 3-(Benzyloxy)-2-carboxypyridin-4-one.

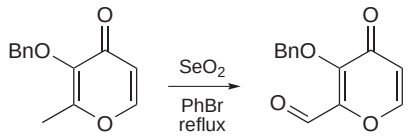

33 **51**

Scheme 3.7: Synthesis of 3-(Benzyloxy)-2-formylpyran-4-one.[205]

Pace et al. reported the facile oxidation of 3-benzyloxy maltol (**33**) with selenium dioxide in refluxing bromobenzene in good yield (Scheme 3.7).[205]

Replicating the published procedure, the reaction proceeded without side products, but full conversion of the starting material could not be achieved – about half the starting material remained unreacted. The product **51** has a very similar R_f value (R_f = 0.50, Ethyl acetate/Hexane: 2/1) to the starting material (R_f = 0.54) on thin layer chromatographic (TLC) plates, which made the purification by column chromatography difficult. Numerous eluent mixtures were investigated, but none allowed a significantly better separation than ethyl acetate/hexane mixtures.

Therefore, attempts were made to optimise the reaction (see Table 3.1). First, the influence of temperature was investigated (entries 1–5). The crude material was analysed by ^{1}H-NMR and the amount of aldehyde quantified via the intensity of the characteristic signal of the aldehyde proton at δ 9.87 ppm. At low temperatures (20 °C and 40 °C), no peak could be observed. The peak was only detected at higher temperatures: barely noticeable at 80 °C and 120 °C, but distinct and strong at reflux temperature (160 °C). However, even when the reaction was heated to reflux, only half of the material had been converted to the desired aldehyde **51** and the other half was the unchanged starting material, as determined by NMR. Varying the amount of selenium dioxide used in the reaction did not seem to have a large effect, where reactions with around 2 equivalents (entries 6–8) gave yields between 35–43%, while 4 equivalents (entry 9) reduced the yield to 20% and multiple additions of reagent (entry 10) also appeared to have a detrimental effect. The choice of solvent seemed to be limited to bromobenzene, because the use of other solvents, which had previously been reported to work with selenium dioxide, prevented the formation of product in this instance: When refluxing acetic acid/acetic anhydride was used,[206] no turnover was observed, while refluxing DMF[207] led to a complex mixture, which could not be purified. DABCO and copper(I)bromide-dimethylsulfide complex (entry 13), which had been published by Wang et al. as reagent for the oxidation of heteroaromatic methyl

groups,[208] did not result in any turnover of starting material.

Because no significant improvement had been achieved at this point, it was decided to purify the aldehyde **51** by repeated column chromatography and proceed by converting **51** into pyridinone **52** (Scheme 3.8). Unexpectedly, the usual reaction conditions (as described for compounds **39**, Scheme 3.2) only returned the unreacted starting material. The electronic effect of the aldehyde group may interfere with the double Michael addition, which could explain that the reaction did not proceed. Thus, the aldehyde group was protected as dimethyl acetal **53**, which gave pyridinone **54** in 75% yield by reaction with methylamine. The deprotection of the pyridinone acetal to aldehyde **52** was attempted with a range of acidic conditions (e.g. HCl or TFA), but no reaction was observed, when monitored by TLC.

Instead, maltol aldehyde **51** was oxidised to pyranone acid **50** with sodium chlorite and sulfamic acid in fair yield (Scheme 3.9), following the protocol by Piyamongkol.[204] Then, the transformation of acid **50** into pyridinone acid **48** via double Michael addition was attempted. The reaction did not proceed when heated to reflux at atmospheric pressure, but only when heated to high temperatures (110 °C) in a sealed tube. This afforded the desired carboxylic acid **48** in 70% yield. An advantage of this route is that the troublesome purification of aldehyde **51** is not necessary, because the crude product could be directly oxidised to carboxylic acid **50**. Any remaining benzylated maltol (**33**) was readily removed during work up, when the product was washed with acetone.

Overall, this synthetic route shortens the 8-step synthesis by Piyamongkol et al. to a 4-step route. All steps are synthetically facile, do not require exclusion of moisture of air and do not involve purification by column chromatography – only the first intermediate **33** is purified by recrystallisation. The overall yield is comparable to the published procedure (14% vs 17%), but could be greatly increased, if full conversion in the oxidation with selenium dioxide was achieved.

3.1.3 Formation of Selectively Protected Glucosamine Derivatives

Glucosamine was chosen as the amino sugar for the coupling with HPO carboxylic acids, as it is cheap and commercially available, while other amino sugars are not readily available (in particular aminoglucose derivatives). The use of an *O*-protected amino sugar may be advantageous for the formation of the amide bond, precluding side reactions leading to the

Table 3.1: Optimisation of the Oxidation of 3-(Benzyloxy)maltol with SeO_2.

Entry	Reagent	Eq.	Solvent	Temp.	Time (h)	Ratio **51**/**33**[a]
1	SeO_2	2	PhBr	20 °C	22	no reaction
2	SeO_2	2	PhBr	40 °C	22	no reaction
3	SeO_2	2	PhBr	80 °C	22	1/625
4	SeO_2	2	PhBr	120 °C	22	1/72
5	SeO_2	2	PhBr	160 °C	22	1/1

Entry	Reagent	Eq.	Solvent	Temp.	Time (h)	Yield **51**	Yield **33**[b]
6	SeO_2	1.5	PhBr	160 °C	20	40%	20%
7	SeO_2	2	PhBr	160 °C	22	35%	21%
8	SeO_2	2.5	PhBr	160 °C	19	43%	36%
9	SeO_2	4	PhBr	160 °C	21	20%	51%
10	SeO_2	2[c]	PhBr	160 °C	20	30%	30%
11	SeO_2	2	$AcOH/Ac_2O$	80 °C	4	—	100%
12	SeO_2	2	DMF	120 °C	22	complex mixture	
13[d]	$CuBr{\cdot}SMe_2$ DABCO	0.15 1	DMSO	100 °C	29	—	100%

[a] Determined by NMR. [b] Remainder to 100% isolated as mixture of **51** and **33**. [c] Added in portions over 2 hours. [d] Under O_2 atmosphere.

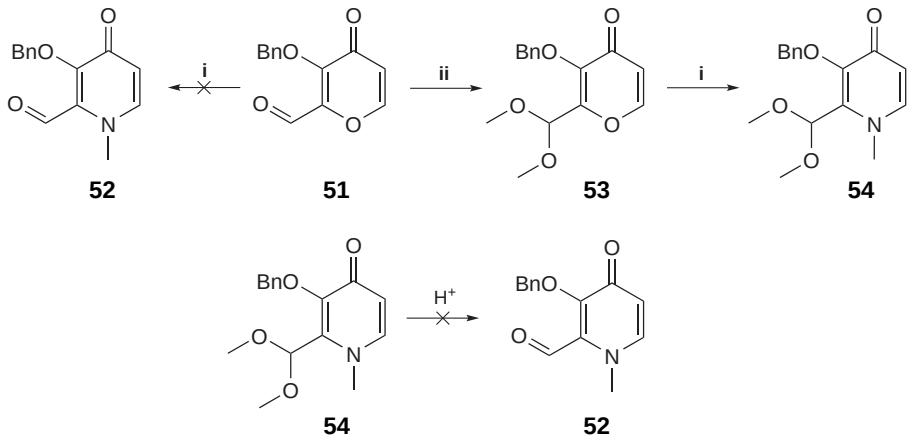

Scheme 3.8: Attempted Synthesis of 3-(Benzyloxy)-2-formylpyridin-4(1*H*)-one. Reagents and Conditions: i) Methylamine, NaOH, $MeOH/H_2O$, reflux, 75% (**53**→**54**); ii) trimethyl orthoformate, TsOH, dry MeOH, reflux, 89%.

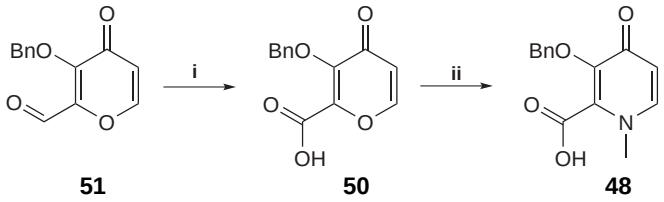

Scheme 3.9: Synthesis of 2-Carboxypyridin-4-one. Reagents and Conditions: i) sulfamic acid, $NaClO_2$, acetone/H_2O, rt, 48%; ii) methylamine, H_2O, 110 °C, sealed tube, 70%.

formation of esters with the carbohydrate hydroxyl groups. Therefore, glucosamine hydrochloride was selectively protected as its tetra-*O*-acetyl derivative **58** (see Scheme 3.10). This reaction was first described by Bergmann and Zervas in 1931,[209] while this work is using a modified procedure that was described by Myszka et al.[210]

Briefly, glucosamine was reacted with anisaldehyde under neutral reaction conditions to give imine **56** (yield: 84%). This was acetylated with acetic acid and pyridine to give fully protected sugar **57** in very good yield, which was quantitatively deprotected by hydrolysis of the imine group with hydrochloric acid, furnishing tetra-*O*-acetylated glucosamine **58**.

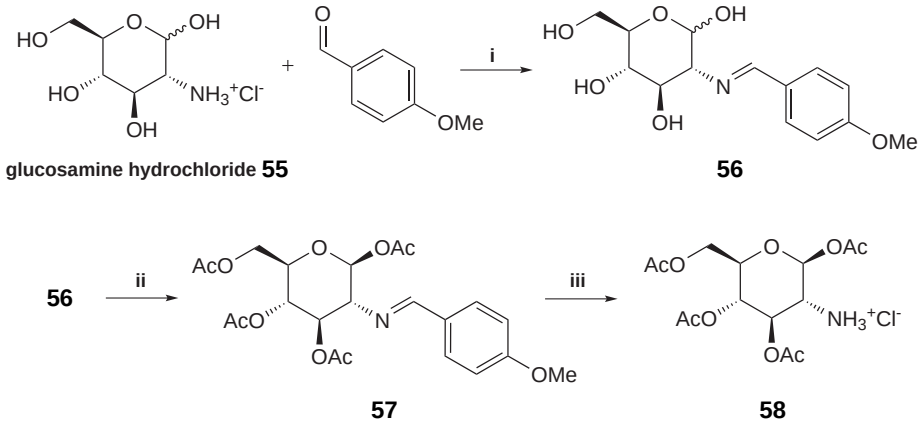

Scheme 3.10: Synthesis of 1,3,4,6-Tetra-*O*-acetyl-β-D-glucosamine hydrochloride. Reagents and Conditions: i) NaOH, rt, 84%; ii) acetic anhydride, pyridine, 0 °C, then rt, 81%; iii) 5M HCl, acetone, reflux, quantitative.

3.1.4 Formation of Amides with Glucosamine Derivatives

Glycine derivative **39a** (Scheme 3.11) was activated as its *N*-hydroxysuccinimide ester **61a** from the reaction of acid **39a** with DCC and *N*-hydroxysuccinimide (NHS) in dry DMF in 45% yield. The reaction proceeds via the *O*-acylisourea **62**, which reacts quickly with NHS to give the more stable NHS-ester **61a** and *N,N'*-dicylcohexylurea. The activated ester can be separated from the formed urea by filtration and unreacted acid may be

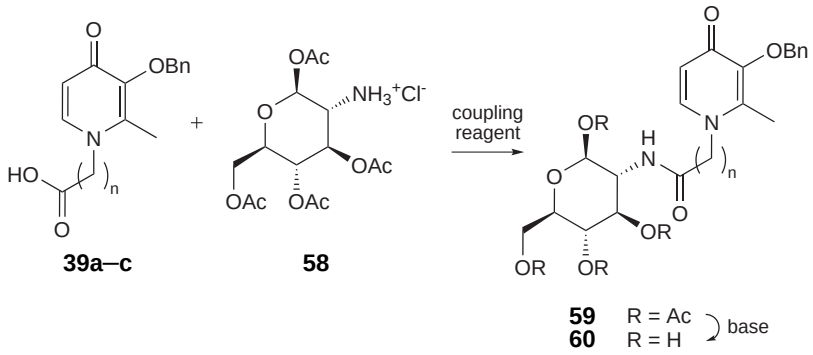

Scheme 3.11: Synthesis of 1-(β-D-Glucopyranos-2-yl)-ω-(4-oxopyridin-1-yl)acylamides.

removed by extraction if necessary. Ester **61a** was reacted with protected glucosamine **58** in dry DMF in the presence of diisopropylethylamine to yield the desired amide **63a** in good yield (34% from **39a**). For the synthesis of β-alanine derivative **63b**, protected glucosamine **58**, acid **39b** was reacted with 1-hydroxybenzotriazole and EDC (1-ethyl-3-(3-dimethylaminopropyl)carbodiimide hydrochloride) in aqueous DMF at 80 °C to give the desired amide **63b** in 22% yield after prolonged reaction time.

The synthesised amides **59** were subjected to common deprotection conditions.[211] Methanolic sodium methoxide or aqueous sodium hydroxide solutions were used to deprotect the amides, but the desired products could not be isolated from the crude material, because significant quantities of decomposition products (i.e. fragments from the cleavage of the amide bond) hampered the purification. Side products co-eluted with the deprotected products when purified by column chromatography, so that no deacetylated amides **60** could be obtained in sufficient purity for further use. The purification of the synthesised amides was ultimately abandoned in favour of different amide conjugates described below.

3.2 Preparation of Glucuronamides

In addition to the amides described in the previous section, amide-linked conjugates were investigated, where the amine- and acid-bearing moieties are reversed, i.e. a sugar bearing a carboxylic acid being linked to an HPO with a free amino group (Scheme 3.12). The necessary HPO may be readily obtained from the reaction of maltol and a diaminoalkane, whereas various sugar acids could be used as starting material.

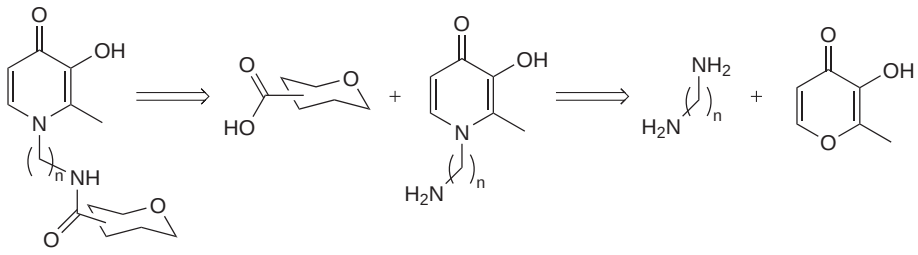

Scheme 3.12: Retrosynthetic Analysis of Conjugates of Sugar Acids and HPOs.

3.2.1 Synthesis of Protected Glucurono-6,3-lactone

Glucuronic acid was selected as sugar acid, allowing ready access to conjugates that are linked on position 6 of the sugar, thus expanding the diversity of the linked positions. The glucuronic acid derivative glucurono-6,3-lactone (**64**) was chosen as starting point, because the 5-membered lactone should activate the acid moiety sufficiently to forego additional activation steps. Fieser et al. demonstrated the viability of this idea by synthesising glucuronamides from long chain alkylamines and glucurono-6,3-lactone.[212] In order to prevent side reactions of the amino group with the anomeric centre of the sugar, the sugar hydroxyl groups in positions 1 and 2 had to be protected. 1,2-*O*-Protected glucurono-6,3-lactones have been described previously and the most commonly used are acetonide protected lactone **65** and the analogous benzylidene derivative **66** (see Scheme 3.13).[212–215] The preparation of the acetonide derivative was first described by Owen at al. in 1941,[213] but herein the modification by Fieser et al. was used.[212] Glucurono-6,3-lactone (**64**) was dissolved in acetone with addition of a catalytic amount of sulfuric acid to convert it into its 1,2-*O*-acetonide **65** in excellent yield (Scheme 3.13).

Similarly, glucuronolactone was protected as its 1,2-*O*-benzylidene derivative **66**, which can be deprotected by hydrogenation.[215] This should allow the deprotection of the conjugate in one step, rather than a two step procedure, which will be necessary for the acetonide protected conjugates (deprotection of the sugar, followed by deprotection of the HPO part). Reaction of glucurono-6,3-lactone with neat benzaldehyde in the presence of zinc chloride gave 1,2-benzylidene protected sugar **66** in 59% yield. The product was an epimeric mixture of *S*- and *R*-stereoisomers in a 4/1 ratio, as determined by NMR. The assignment of the main constituent as the *S*-isomer was based on a recent paper by Jenkinson et al., who purified the main reaction product and determined its absolute configuration by X-ray crystallographic analysis.[216] The ^{13}C-NMR spectrum reported by

Csuk et al. for the *S*-isomer matches the spectrum of the mixture's major component,[214] confirming the assignment made.

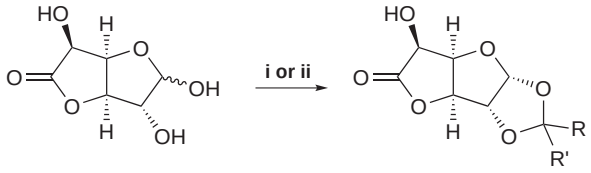

64

65 R = R' = CH_3
66 R = Ph, R' = H

Scheme 3.13: Preparation of 1,2-Protected Glucurono-6,3-lactones. Reagents and Conditions: i) Acetone, H_2SO_4, rt, 93%; ii) Benzaldehyde, $ZnCl_2$, rt, 59% (Ratio S/R: 41).

3.2.2 Preparation of 1-(ω-Aminoalkyl)-pyridin-4-ones

Following the general protocol described for the synthesis of *N*-substituted HPOs by Dobbin et al.,[199] benzylated maltol **33** was reacted with a slight excess of diaminoalkanes of varying chain lengths (1.1 equivalents) to form the desired aminoalkyl-HPOs **67**. The reaction with ethylenediamine dihydrochloride gave pyridinone **67a** in 38% yield, wheras the butane derivative **67b** and the previously undescribed hexane derivative **67c** were obtained in 62% and 64% yield, respectively. The novel octane derivative **67d** was obtained almost quantitatively. During work up, an unexpected precipitate was isolated from the

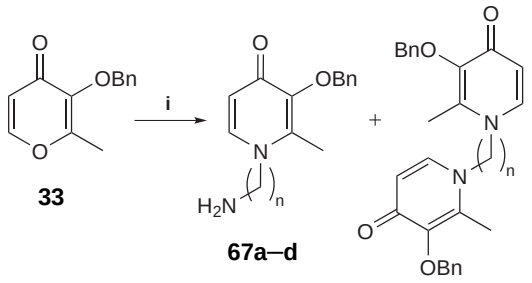

33

67a–d

68a–d

n	**67**	Yield	**68**	Yield
2	**a**	38%	**a**	N/I[a]
4	**b**	62%	**b**	26%
6	**c**	64%	**c**	36%
8	**d**	99%	**d**	N/I[a]

[a] N/I – not isolated

Scheme 3.14: Synthesis of 1-(ω-Aminoalkyl)-pyridin-4-ones. Reagents and Conditions: i) 1,2-Diaminoethane dihydrochloride or 1,4-diaminobutane or 1,6-diaminohexane or 1,8-diaminooctane, NaOH, EtOH/water, reflux.

reactions where n=4 or n=6. This precipitate was the dimer **68b** and **68c**, which resulted from the addition of a second molecule of protected maltol **33** to the desired product **67**. The dimer was identified by high resolution mass spectrometry and NMR spectroscopy, showing the peaks and integration pattern which would be expected for a dimeric molecule.

The formation of such dimers is facilitated by a high ratio of pyranone **33** to amine and could have been avoided by addition of the diamine in larger excess.

Interestingly, an almost quantitative (combined) yield was observed for the longer chain diaminoalkanes, while the shortest diaminoalkane (n=2) had a significantly lower yield of products. In contrast, the longest diaminoalkane (n=8) yielded no dimer, while the shorter diamines did give significant amounts of dimer. These differences could potentially be due to the increased length and flexibility of the side chain, allowing the formation of an intramolecular hydrogen bond, which would not be possible in the shorter chained analogues. Any dimer that had formed for n=2 was not isolated however, because it did not precipitate during work up.

3.2.3 Preparation of *N*-(ω-(4-Oxopyridin-1-yl)alkyl)glucuronamides

The use of protected glucuronolactones for the synthesis of emulsifiers has been described by Fieser et al., where the lactone was reacted directly with the respective amines, yielding the desired long chained amides.[212] In a first set of trial experiments (Scheme 3.15), protected glucuronolactone **65** was reacted with pentylamine or 5-amino-1-pentanol in DMF at room temperature or 40 °C. The reaction mixtures were evaporated and analysis of the crude material by ^{1}H- and ^{13}C-NMR spectroscopy showed full conversion to the respective amides **69** and **70**, as determined by the shift of the methylene protons adjacent to the amine/amide nitrogen atom.

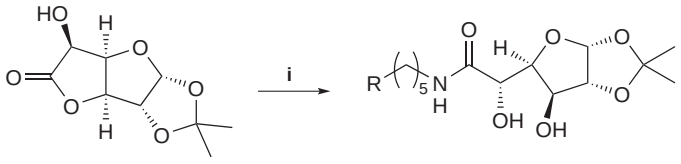

65 **69** R = H **70** R = OH

Scheme 3.15: Reaction of Protected Glucuronolactone with Alkylamines. Reagents and Conditions: i) Pentylamine or 5-amino-1-pentanol, DMF, rt or 40 °C, quantitative by NMR.

Based on these results, lactones **65** and **66** were reacted with aminoalkyl HPOs **67b** and **67c** in dry DMF at room temperature. After extraction and column chromatography, the desired protected amides **71b**, **71c**, **72b** and **72c** were obtained in fair yields (61–78%, see Scheme 3.16).

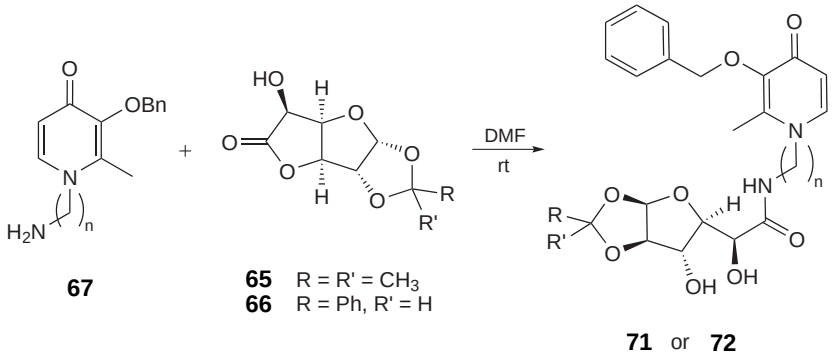

Scheme 3.16: Preparation of *N*-(ω-(4-Oxopyridin-1-yl)alkyl)glucuronamides.

Cmpd	n	R	R'	Yield	Cmpd	n	R	R'	Yield
71a	2	CH_3	CH_3	—[a]	**72a**	2	Ph	H	—[a]
71b	4	CH_3	CH_3	65%	**72b**	4	Ph	H	78%
71c	6	CH_3	CH_3	61%	**72c**	6	Ph	H	70%
71d	8	CH_3	CH_3	—[a]	**72d**	8	Ph	H	—[a]

[a] Synthesis not attempted in this work.

According to Fieser et al., glucuronamides protected as 1,2-acetonide may be deprotected under acidic conditions.[212] In a first set of experiments, the deprotection of the acetonide-protected lactone **65** was thus attempted with a range of acidic conditions (Table 3.2). 1,2-*O*-Isopropylideneglucurono-6,3-lactone (**65**) was treated with 90% acetic acid or trifluoroacetic acid at room temperature, but the reaction did not proceed, even with prolonged reaction times. When heating the lactone in aqueous acetic acid solutions to elevated temperatures, it was deprotected after few hours. Similarly, Amberlite (H^+ form) did not deprotect the lactone at 40 °C, but did so when heating the reaction mixture to 80 °C. Dilute hydrochloric acid was able to deprotect the lactone under reflux in less than one hour. The deprotection of the sugar and thus the presence of a free anomeric centre was tested with Fehling's test. An aliquot of the reaction mixture was treated with Fehling's solution (copper(II)sulfate and sodium tartrate) and heated – the formation of a reddish copper(I) oxide precipitate indicated the presence of an (reducing) aldehyde group, which is only present in the unprotected sugar.

Reaction conditions that successfully deprotected glucuronolactone **65** (Table 3.2) were then used for the deprotection of the full conjugates **71** and the reactions were monitored in regular intervals by TLC. The reaction mixtures were evaporated and analysed by NMR, to check the outcome of the reaction. The use of 60% acetic acid at 95 °C resulted in extensive cleavage of the amide bond. When the temperature was reduced to 60 °C and

reaction time to 6 hours, the main constituent of the crude product was the unreacted amide, besides traces of the desired product. Increasing the acid concentration from 60% to 70% however, signs of cleavage of the amide bond were observed, while substantial amounts of starting material remained. A similar result was observed with Amberlite at 80 °C after 36 hours, while at shorter time points, no reaction could be observed. Dilute hydrochloric acid (0.45M HCl) did not deprotect the glucuronamide after 30 minutes, while the use of 1M hydrochloric acid for 45 minutes resulted in substantial cleavage of the starting material and/or desired product.

These results suggest that a very narrow window exists for the deprotection of glucuronamides **71**, where the 1,2-protecting group is hydrolysed before cleavage of the amide bond occurs, which might make it impossible to isolate the final product in substantial yield. Efforts were therefore focused on the hydrogenation of benzylidene protected amides **72**.

Table 3.2: Acidic Deprotection of Glucuronolactones and Glucuronamides.

Cmpd	Reagent	Solvent	Temp.	Time (h)	Result
65	90% AcOH[a]	H_2O	20 °C	48	no reaction
65	90% TFA[b]	H_2O	20 °C	48	no reaction
65	60% AcOH	H_2O	95 °C	24	positive[c]
65	60% AcOH	H_2O	60 °C	6	positive
65	70% AcOH	H_2O	60 °C	6	positive
65	Amberlite[d]	MeOH/H_2O	40 °C	19	no reaction
65	Amberlite	dioxane/H_2O	80 °C	24	positive
65	0.45M HCl	H_2O	90 °C	30 min	positive
65	1M HCl	MeOH/H_2O	100 °C	45 min	positive
71	60% AcOH	H_2O	95 °C	24	cleavage[e]
71	60% AcOH	H_2O	60 °C	6	partial[f]
71	70% AcOH	H_2O	60 °C	6	partial, cleavage
71	Amberlite	dioxane/H_2O	80 °C	36	partial, cleavage
71	0.45M HCl	H_2O	90 °C	30 min	no reaction
71	1M HCl	MeOH/H_2O	100 °C	45 min	cleavage

[a] Acetic acid. [b] Trifluoroacetic acid. [c] Positive Fehling's test. [d] Amberlite Resin H^+ form. [e] Cleavage of amide bond observed. [f] Starting materials remaining.

Like acetonides, benzylidene-protected diols may be deprotected under acidic conditions, but they are also commonly deprotected by catalytic hydrogenation.[211,215] Similar to the acetonide protected molecules, various conditions were first tried on benzylidene glucuronolactone **66** (see Table 3.3) before applying them to the full conjugates (**72**).

1,2-*O*-Benzylidene glucuronolactone (**66**) was shaken with palladium on charcoal (Pd/C) under hydrogen atmosphere. Hydrogenation under high pressure (9 bar, 3 days) was previously shown by Weymouth-Wilson et al. to deprotect a modified glucuronic acid.[215] The same conditions were used for lactone **66**, but the reaction did not proceed and only starting material was recovered, as was determined by NMR spectroscopy of the recovered material. Based on previous reports that a mixture of palladium on charcoal and palladium hydroxide on charcoal ($Pd(OH)_2/C$) may serve as a better catalyst for debenzylation,[217] the effect of the palladium mixture was investigated for the present reaction. The mixture did successfully deprotect lactone **66** to lactone **64** when used in methanol – hydrogenolysis in DMF did not proceed. This surprising difference between Pd/C and the catalyst mixture was further investigated by using $Pd(OH)_2/C$ on its own, which also deprotected the lactone. These results highlighted an interesting difference in reactivity between Pd/C and $Pd(OH)_2/C$ in this particular case.

Having identified methods that are suitable for the removal of the benzylidene in sugar **66** by hydrogenolysis, these were then applied to the deprotection of conjugate **72** (Table 3.3). As seen for the lactone, Pd/C is not sufficient for the removal of the benzylidene protecting group, but the 1/1 mixture of palladium catalysts was also found to be inactive, when used in methanol, THF or DMF. The use of rhodium catalyst also could not effect deprotection of the diol.

Unfortunately, catalysts that allowed the deprotection of glucuronamides **72** could not be identified. Interestingly, the hydrogenolysis of the 3-benzyloxy group on pyridinones usually proceeds readily under these conditions (Pd/C is commonly used as catalyst),[199] but for pyridinones **72** this reaction was not detected in any of the hydrogenations. The author therefore speculates that the lipophilic nature of the protected conjugates prevented adsorption onto the catalyst surface, thus ultimately forestalling the reaction.

Neither the deprotection of acetonide protected amides **71** nor benzylidene protected amides **72** was successful. Thus, another method for the deprotection or an alternative route for the synthesis need to be investigated. A possible route could be the coupling of glucuronic acid to HPO amines **67** by conventional amidation protocols.

Table 3.3: Hydrogenation of Glucuronolactones and Glucuronamides.[a]

Cmpd	Catalyst	w/w	H_2 Pressure	Time (d)	Result
66	10% Pd/C	20%	2.5 bar	3.5	no reaction
66	10% Pd/C	20%	9 bar	3	no reaction
66	Pd mixture[b]	30%	2.5 bar	3	full conversion
66	Pd mixture	30%	2.5 bar	4	no reaction[c]
66	20% $Pd(OH)_2$/C	30%	2.5 bar	2	full conversion
72	10% Pd/C	20%	2.5 bar	3	no reaction
72	Pd mixture	30%	2.5 bar	3	no reaction
72	Pd mixture	30%	2.5 bar	3	no reaction[c]
72	Pd mixture	30%	2.5 bar	3	no reaction[d]
72	5% Rh/C	20%	2.5 bar	3	no reaction

[a] All reactions were suspensions in methanol. After hydrogenation, reactions were filtered through celite and evaporated to dryness. [b] 1/1 Mixture of 10% Pd/C and 20% $Pd(OH)_2$/C. [c] Reaction was performed in DMF. [d] Reaction was performed in THF.

Chapter 4

Synthesis of Triazole-linked Conjugates

4.1 Formation of Triazoles by Click Chemistry

The use and synthetic application of 1,3-dipolar cycloadditions, which can be used for the synthesis of various 5-membered heterocycles, was mainly developed by Huisgen from the 1950s (for a review see ref. [218]). The reactions were not common, except for the preparation of triazoles, and even for these, the reaction requires high temperatures and forms mixtures of 1,4- and 1,5-substituted 1,2,3-triazoles.[218]

About 40 years later, Meldal[219] and Sharpless[220] independently developed a copper catalysed variant, which proceeds under mild conditions and also in aqueous medium. This copper catalysed azide-alkyne cycloaddition (CuAAC) gained considerable attention due to its wide applicability, robustness and biocompatibility and its stereoselectivity for 1,4-substituted triazoles, allowing even the labelling of molecules *in vivo*.*

The CuAAC links azides and alkynes to form 1,4-substituted triazoles via a copper catalysed reaction (Scheme 4.1). In the first step, copper (or a copper-ligand complex) coordinates with the acetylene π-electrons, which lowers the pK_a of the terminal proton. Then the proton is abstracted and the acetylide is formed. Whether one copper atom or more are directly involved in this acetylide complex remains unclear, but crystal structures of alkyne-copper complexes suggest the involvement of two copper atoms, both at an angle to the C-C bond.[221] The acetylide-copper complex then coordinates the azide on the carbon-bound oxygen, allowing attack of the terminal nitrogen on the non-terminal acetylene carbon. This results in the formation of a 6-membered metallocycle, which could account for the regioselectivity for the formation of 1,4-substituted triazoles. The triazole is formed by further rearrangement, first bound to the copper-complex, which is finally released by

*For a review of CuAAC, see Meldal et al.[221]

protonation, yielding the free copper-ligand complex and the 1,4-substituted triazole. Sugars and other biomolecules are frequently used in CuAAC, but it also finds applications in material sciences and other areas, demonstrating the wide range of possible substrates and tolerance of reaction media, while maintaining specificity and reliability.[222]

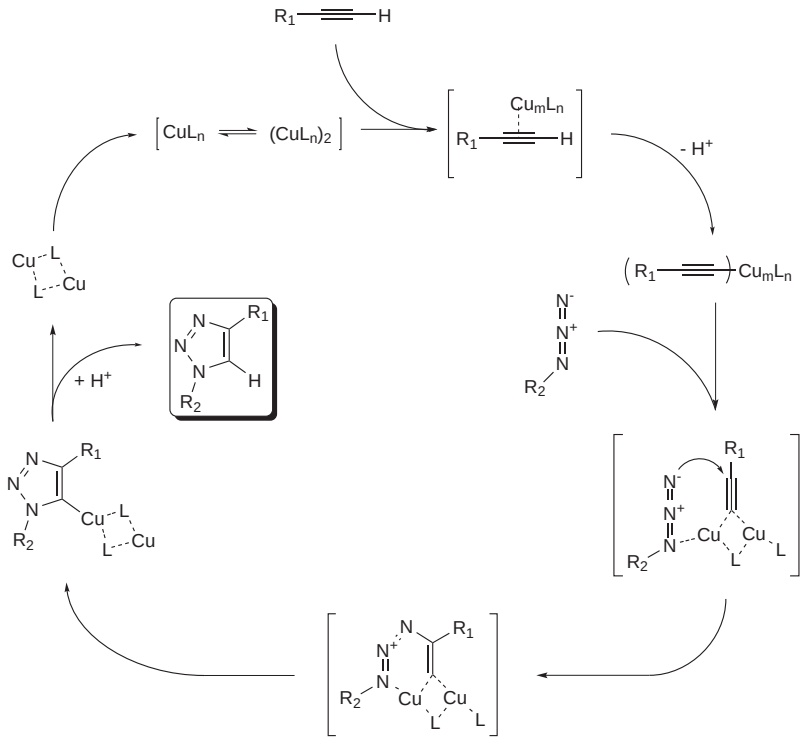

Scheme 4.1: Plausible Mechanism for the Cu(I) Catalysed Reaction between Organic Azides and Terminal Alkynes. (Adapted from Meldal et al.[221])

The application of azide-alkyne click chemistry has since been developed further, with the advent of copper-free reactions.[221] On the one hand, McNulty and co-workers described the preparation of 1,4-substituted triazoles utilising silver(I) complexes instead of copper,[223,224] which has recently been expanded to the synthesis of pyrroles.[225] The Bertozzi group published a metal-free variant in 2007, which is based on the reaction of cyclooctynes with azides.[226] Here, the reaction proceeds due to the relief of steric strain of the cyclic alkyne. Another variant of the CuAAC was developed by the Fokin group, where ruthenium(II) complexes catalyse the formation of 1,4-substituted triazoles.[227] Interestingly, 1,5-substituted triazoles are selectively formed, when the ruthenium catalyst is complexed by cyclopentadienyl ligands.[228,229]

4.2 Design of Triazole-linked Conjugates

In view of the instability of the amide-linked conjugates under deprotection conditions discussed in the previous chapter, a strategy to obtain conjugates with a more stable linkage had to be found. Triazoles are stable under most conditions and readily prepared from an azide and an alkyne in an atom-efficient and clean reaction and thus an attractive alternative to amides. Triazole-tethered HPO-sugar conjugates were therefore designed.
For the synthesis of the triazole-linked HPO-sugar conjugates, HPO-azides and alkyne bearing carbohydrates or alternatively, azidosugars and HPO-alkynes (Scheme 4.2) are required. The preparation of both alkyne- and azido-HPOs is straightforward, and azidosugars are readily prepared either from commercial starting materials or in few steps.[230,231] Contrarily, the synthesis of alkyne bearing carbohydrates takes several steps and often require expensive starting materials.[232–235]

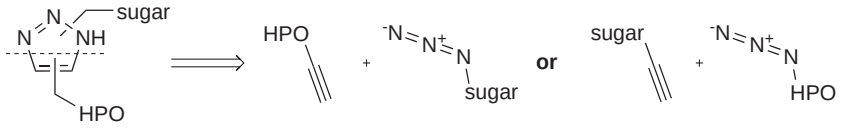

Scheme 4.2: Retrosynthetic Analysis of Triazole-linked HPO-sugar Conjugates.

4.3 Preparation of Azidosugars

Azidosugars have previously been used in click chemistry reactions.[236] For the present work, the synthesis of triazoles based on 1-,2- and 6-azidoglucose derivatives (Figure 4.1) was planned.

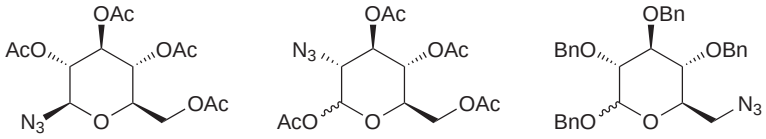

73 **74** **75**

Figure 4.1: Structures of Used Azidoglucose Derivatives.

For the synthesis of 1-azidoglucose, a rapid route had been described, where acetobromo glucose **30** is reacted with sodium azide to give the desired azidosugar **73**.[237] Acetobromo glucose is commercially available, or it may be synthesised from glucose in 2 steps. First, glucose was per-*O*-acetylated with acetic anhydride in pyridine to yield pentaacetyl glucose

76 (74%, Scheme 4.3), which was then brominated with hydrobromic acid in acetic acid. This gave 2,3,4,6-tetra-*O*-acetyl-α-D-glucopyranosyl bromide (**30**) in almost quantitative yield. Glucosyl bromide **30** was transformed to the azide in an exchange reaction with sodium azide, tetrabutylammonium iodide and sodium bicarbonate in a biphasic reaction mixture, yielding acetylated 1-azido-β-D-glucopyranoside **73** (69% yield). The β-conformation was determined by NMR spectroscopy – as described in chapter 2 – in particular by analysis of the coupling constant for the ^3J coupling between the anomeric proton and the proton in position 2 with 9.0 Hz which is in agreement with published data for this compound,[238] and β-configured glucopyranoses in general.[191]

Goddard-Borger et al. described the facile synthesis of 2-azidoglucose from glucosamine.[230] To this end, an efficient diazotransfer reagent had been synthesised.[230] Following this synthetic strategy, imidazole was reacted with azidosulfonyl chloride, which was prepared *in situ* from sulfuryl chloride and sodium azide (Scheme 4.4). The resulting diazotransfer reagent **77** was not isolated due to its potentially explosive nature,[239] but rather obtained as the stable sulfate salt in 61% yield. The reagent **78** was then used to transfer a diazo group onto the nitrogen of glucosamine (Scheme 4.5), a reaction which is catalysed by copper(II) sulfate in the presence of potassium carbonate.[230,239] This azide was directly protected with acetic anhydride in pyridine for ease of handling and use. The desired acetylated 2-azidoglucose **74** was obtained in 23% yield. This result is in stark contrast to the published yield of 92%,[230] and could be due to a low yielding acetylation reaction.

6-Azidoglucose was synthesised mainly following the route for the selective protection of glucose by Amigues et al.[231] Glucose was reacted with triphenylmethyl chloride in pyridine to give 6-tritylglucose **79** in good yield (Scheme 4.6 The remaining hydroxy groups were benzylated with benzyl bromide and sodium hydride as base in 76% yield. Aluminium trichloride in DCM/Et_2O achieved the selective deprotection of fully protected sugar **80**, yielding 6-hydroxy sugar **81** (72%).

The introduction of the azido group followed the general protocol reported by Tagamose et al.[240] In a one-pot reaction, the 6-hydroxy group was first mesylated to give compound **82** with methanesulfonyl chloride and triethylamine, which was subsequently transformed to the desired azide **75** with sodium azide in DMF containing trace water[241] (66% yield over both steps). The yield was improved however, when the mesylate **82** (89%) was isolated and the azide introduced in a separate step (**75** 91%, 81% over both steps).

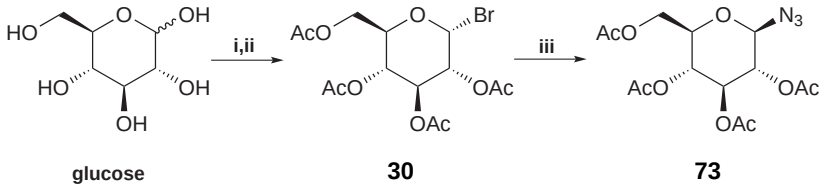

Scheme 4.3: Synthesis of 2,3,4,6-Tetra-*O*-acetyl-α-D-glucopyranosyl azide. Reagents and Conditions: i) Ac_2O, pyridine, 0 °C→rt, 74%; ii) HBr in AcOH, DCM, 0 °C→rt, 93%; iii) NaN_3, $NaHCO_3$, TBAI, DCM/H_2O, rt, 69%.

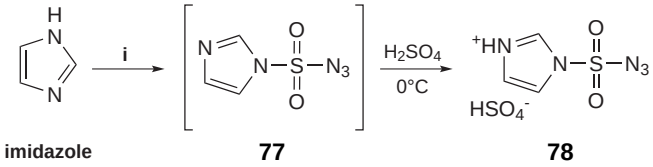

Scheme 4.4: Synthesis of 3-(Azidosulfonyl)-3*H*-imidazol-1-ium hydrogen sulfate. Reagents and Conditions: i) NaN_3, SO_2Cl_2, dry ACN, 0 °C→rt, then 0 °C, imidazole, 0 °C→rt; overall: 61%.

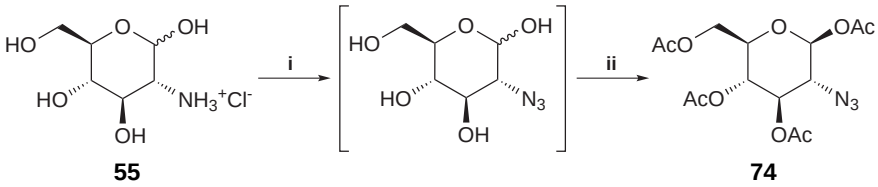

Scheme 4.5: Synthesis of 2-Azido-2-deoxy-D-glucopyranose 1,3,4,6-tetra-*O*-acetate. Reagents and Conditions: i) Imidazole-1-sulfonyl azide **78**, K_2CO_3, $CuSO_4$, MeOH, rt; ii) Ac_2O, pyridine, rt, 23%.

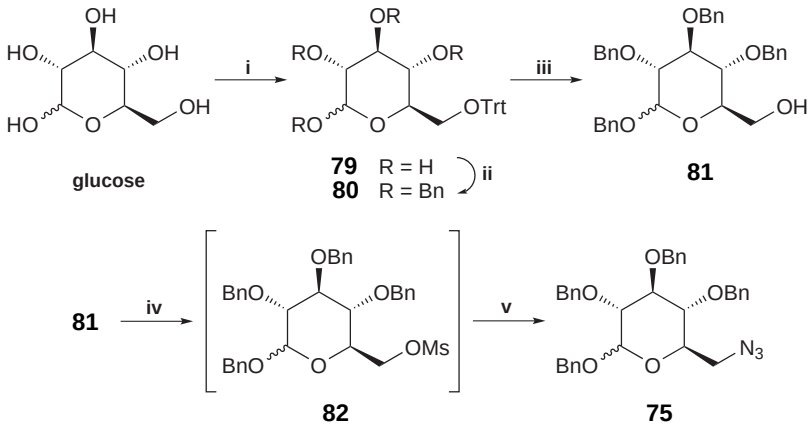

Scheme 4.6: Synthesis of 6-Azido-1,2,3,4-tetra-*O*-benzyl-6-deoxy-D-glucopyranose. Reagents and Conditions: i) Triphenylmethyl chloride, pyridine, 75 °C, 72%; ii) BnBr, NaH, TBAI, dry DMF, N_2 atmosphere, 0 °C→rt, 76%; iii) $AlCl_3$, dry DCM, dry Et_2O, rt, 72%; iv) mesyl chloride, TEA, dry DCM, N_2 atmosphere, −10 °C to 0 °C, 89%; v) NaN_3, DMF, 110 °C, 91%.

4.4 Preparation of Alkynes

The most convenient way to obtain an alkyne derivative of HPOs is the double Michael addition of propargylamine (Scheme 4.7) to a pyranone, following to the previously described method (Chapter 3). Benzylated maltol **33** was reacted with propargylamine under basic reaction conditions, but a very complicated reaction mixture was obtained, which could not be purified by column chromatography. Alternatively, benzylated maltol was reacted with ethanolamine to give pyridinone **83** (56% yield). The alkyne functionality was introduced by alkylation of the hydroxyl group with propargyl bromide in DMF, obtaining the desired alkyne **84** in 65% yield, easily identified because of the presence of a characteristic triplet of the terminal alkyne proton at δ 2.43 ppm.

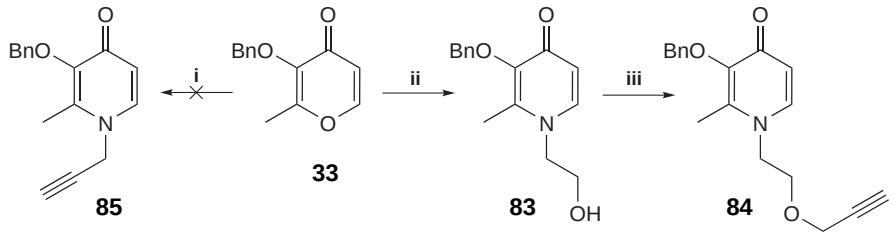

Scheme 4.7: Synthesis of Alkyne-substituted HPOs. Reagents and Conditions: i) Propargylamine, NaOH, MeOH/H_2O, reflux; ii) ethanolamine, NaOH, MeOH/H_2O, reflux, 56%; iii) propargyl bromide, NaH, TBAI, dry DMF, N_2 atm., −10 °C→rt, 65%.

4.5 Formation of Triazole-Linker

The formation of triazoles from alkynes and azides via a copper-catalysed click reaction has been well studied and numerous reaction conditions have been published (for a review see ref. [221]).

A small set of different conditions (see Table 4.1) was selected for trial reactions on a small scale. HPO alkyne **84** and 1-azidosugar **73** were reacted in the presence of copper(II) sulfate and ascorbic acid in DMF and water (Table 4.1, entry 1). Even after prolonged reaction times and repeated addition of copper and reducing agent, no reaction was observed and the starting material could be recovered. In the reaction in dry DMF, catalysed by copper(I) iodide and triethylamine (entry 2), the quick appearance of multiple weak spots on TLC was observed, but no further progress was observed after 5 days reaction time and additional catalyst and base.

Table 4.1: Reactions Conditions for Triazole-Formation.[a]

Entry	Alkyne	Azide	Cu Species (eq.)	Reductant (eq.)	Solvent	Time
1[b]	**84**	**73**	$CuSO_4$ (0.75)	Asc. (1.66)	DMF/H_2O	12 d
2[b]	**84**	**73**	CuI (0.7)[c]	—	dry DMF	5 d
3	**84**	**73**	$CuSO_4$ (0.5)	NaAsc (1+0.5)[d]	DCM/H_2O	4 d
4	**84**	**74**	$CuSO_4$ (0.5)	NaAsc (1+0.5)[d]	DCM/H_2O	4 d
5	**86**	NaN_3	$CuSO_4$ (0.75)	Asc. (1.66)	DCM/H_2O	1 d
6	**86**	NaN_3	$CuSO_4$ (0.5)	NaAsc (1)	DCM/H_2O	1 d
7	**86**	NaN_3	CuI (0.5)[e]	—	dry DMF	1 d

[a] All reactions were performed at room temperature. [b] Catalyst and reductant/base were added in portions over the reaction time. [c] Triethylamine (4 eq.) was added to the reaction. [d] Second portion added after 3 days. [e] Triethylamine (0.5 eq.) was added to the reaction.

Since many publications use sodium ascorbate, rather than ascorbic acid,[221] further reactions (entries 3 and 4) were therefore performed with copper(II) sulfate and sodium ascorbate (prepared from ascorbic acid and aqueous sodium hydroxide). Interestingly, upon addition of the sodium ascorbate solution, the reaction mixtures changed to a brownish colour and partly gelled. This gel dissolved over time, but no formation of product could be observed.

In order to eliminate potential problems, phenyl propargyl ether **86** (Figure 4.2) and sodium azide were used as structurally simple starting materials (entries 5–7) and subjected to all previously used reaction conditions. No reaction was observed for entries 5 and 6, but the reaction with copper(I) iodide as reagent did show the disappearance of the starting material, a new spot on TLC. Upon work-up, NMR of the crude material only showed unchanged starting material **86**, however.

While similar to the previously used methods, a protocol published by Sharpless et al.[242] in 2005, applied light heat (60 °C) and aqueous *tert*-butanol as solvent. A model reaction with phenyl propargyl ether (**86**) and benzyl azide (**87**, see Table 4.2, entry 1) gave 1-benzyl-4-(phenoxymethyl)-1*H*-1,2,3-triazole (**88**) in 84% yield. Reaction of phenyl propargyl ether with 1-azidoglucose **73** gave the appropriate triazole **89** in excellent yield (93%), but required longer reaction times for completion.

Applying these reaction conditions to couple HPO alkyne **84** with benzyl azide gave 1-{2-[(1-benzyl-1*H*-1,2,3-triazol-4-yl)methoxy]ethyl}-3-(benzyloxy)-2-methylpyridin-4(1*H*)-one

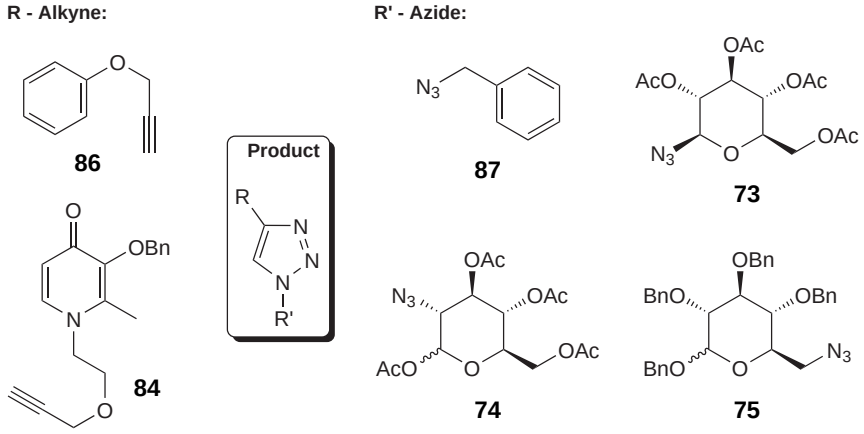

Figure 4.2: Structures of Alkynes, Azides and Products.

(**90**) in good yield (87%). HPO alkyne **84** was linked with 1-azidoglucose **73** in good yield under the described reaction conditions, despite some partially insoluble starting materials at the beginning of the reaction. In a separate experiment (entry 5), chloroform was added to the reaction mixture until the starting materials were fully dissolved. Surprisingly, this reaction did not proceed as smoothly as entry 4. After 18 hours, the reaction showed only partial turnover of alkyne **84**, while the reaction without added chloroform (entry 4) had gone to completion. The reactions linking HPO alkyne **84** with the prepared azidosugars **74** and **75** (Figure 4.2 and Table 4.2, entries 6 and 7) – performed without additional chloroform – furnished the desired triazoles **92** and **93** in 84 and 66% yield, respectively.

Table 4.2: Synthesis of Triazoles.[a]

Entry	Alkyne	Azide	Time (h)	Product	Yield
1	**86**	**87**	1	**88**	84
2	**86**	**73**	22	**89**	93
3	**84**	**87**	20	**90**	87
4	**84**	**73**	18	**91**	85
5[b]	**84**	**73**	18	**91**	inc.[c]
6	**84**	**74**	23	**92**	84
7	**84**	**75**	20	**93**	66

[a] Alkyne (1 eq.), azide (1 eq.), ascorbic acid (0.1 eq.), 1M NaOH (0.1 eq.), 1M $CuSO_4$ (0.05 eq.), tBuOH/H_2O 1/1, sealed tube. [b] $CHCl_3$ added for solubility. [c] Incomplete turnover.

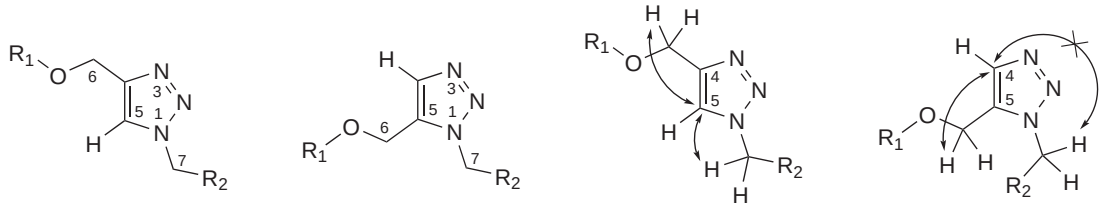

(a) Structures and Numbering.

(b) Possible HMBC Correlations between Substituent Protons and the Unsubstituted Triazole Carbon.

Figure 4.3: Possible 1,4- and 1,5-substituted Triazole Isomers.

In order to confirm that the desired 1,4-substituted triazoles were synthesised and not the 1,5-substituted isomers, the 1D and 2D NMR studies, which were performed, are described here. ^{1}H-NMR, decoupled ^{13}C-NMR, DEPT135, HSQC and HMBC spectra were recorded for all compounds (except **88**), ^{1}H,^{1}H-COSY spectra were recorded where necessary. With these spectra, all ^{1}H- and ^{13}C-NMR signals – including ^{1}H,^{1}H-coupling constants – were assigned in full and unambiguously.

DEPT135, HSQC and HMBC spectra were recorded in order to determine which structural isomer was produced by the click reactions. The carbon signals at ∼145 ppm and ∼122 ppm were analysed (for exact shifts, see Table 4.3). DEPT135 and HSQC allowed the assignment of the CH and the quaternary carbon of the triazole ring as the signals at ∼122 ppm and ∼145 ppm, respectively. The carbon shift of the triazole-CH signal lies around 120 ppm in 1,4-substituted triazoles, while in 1,5-substituted triazoles the signal is around 133 ppm.[243–245] This suggests, that the isolated compounds are indeed the 1,4-substituted isomers, as would be expected from the reported stereoselectivity of the CuAAC. HMBC data confirms this assignment, because correlation peaks from H-6 and H-7 with the triazole-CH carbon were observed. The latter correlation (H-7 to triazole-CH) would not be expected in the 1,5-substituted isomer **94** (Figure 4.3). Additionally, NOESY experiments could have shown the close spatial proximity of the protons in position 6 and 7 in the 1,5-substituted, but not in the 1,4-substituted triazoles.[246]

Table 4.3: NMR Chemical Shift Data of Triazoles (δ ppm in $CDCl_3$).

Compound	**H-5**	**C-5**	**C-4**
89	7.86	121.03	145.11
90	7.22	122.48	144.55
91	7.58	121.000	144.93
92	7.56/7.44[a]	122.15/122.09[a]	144.93
93	7.43	124.62/124.34[a]	143.88

[a] β isomer/α isomer

4.6 Deprotection of Triazole-linked Conjugates

Conjugates **91**, **92** and **93** were then deprotected to obtain their differentially protected derivatives. The 1-linked conjugate **91** was debenzylated by hydrogenolysis over Pd/C to give 3-hydroxy pyridinone **96** in 71% yield (Scheme 4.8), while selective deacetylation was achieved with sodium methoxide in methanol, quantitatively yielding the desired **97**. The fully deprotected pyridinone **98** was obtained in quantitative yield as its HCl salt by hydrogenolysis of **97** over Pd/C at pH 1.

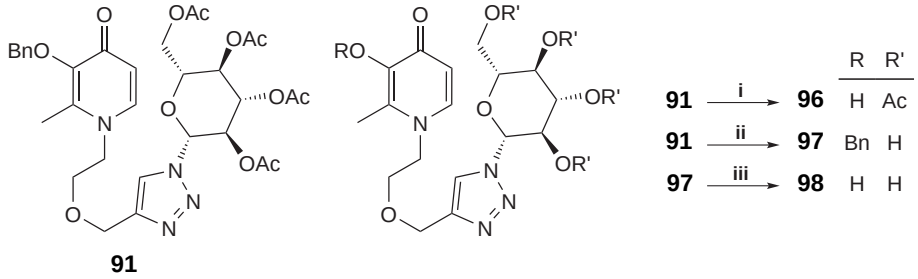

Scheme 4.8: Deprotection of 1-(2-{[1-(β-D-Glucopyranosyl)-1,2,3-triazol-4-yl]methoxy}ethyl)pyridinones. Reagents and Conditions: i) Pd/C (10%), 2 bar H_2, MeOH, rt, 71%; ii) NaOMe, dry MeOH, rt, quant.; iii) Pd/C (10%), HCl, 2 bar H_2, MeOH, rt, quant. as HCl salt.

Similarly, 2-linked conjugate **92** was debenzylated by hydrogenolysis over Pd/C to give its respective 3-hydroxy pyridinone **99** (quantitative). Deacetylation of **92** with sodium methoxide in dry methanol yielded pyridinone **100** in surprisingly poor yield (27%). Finally, fully deprotected pyridinone **101** could be obtained by hydrogenation of fully protected conjugate **92** over Pd/C with HCl over 3 days (92% yield).

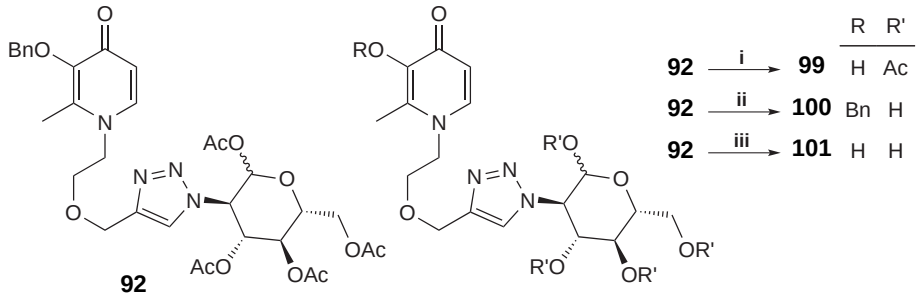

Scheme 4.9: Deprotection of 1-(2-{[1-(2-Deoxy-D-glucopyranos-2-yl)-1,2,3-triazol-4-yl]methoxy}ethyl)pyridinones. Reagents and Conditions: i) Pd/C (10%), 2 bar H_2, MeOH, rt, quant.; ii) NaOMe, dry MeOH, rt, 27%; iii) Pd/C (10%), HCl, 2 bar H_2, MeOH, rt, 92%.

Selective deprotection the 6-linked conjugate **93** (Scheme 4.10) – as it was achieved for the other triazole-linked HPO conjugates – is impossible, because the compound is fully benzylated, rather than protected with multiple different protecting groups. Benzyl protecting groups are usually removed by hydrogenolysis,[211] but after hydrogenation of the conjugate **93** with Pd/C, only unreacted starting material was recovered.

Boron tribromide has previously been used to debenzylate HPOs in excellent yields in the presence of amide bonds,[247] which indicates a selectivity for benzyl groups over other functionalities.

Conjugate **93** was reacted with boron tribromide in dry DCM. Full consumption of the starting material was observed, but purification of the reaction mixture by reverse phase chromatography did not give the desired product **102**. The only products that could be isolated were *N*-(hydroxyethyl)pyridinone **83** and its 3-hydroxy derivative, indicating that the ether bond of the tether was preferentially cleaved over the benzyl ethers.

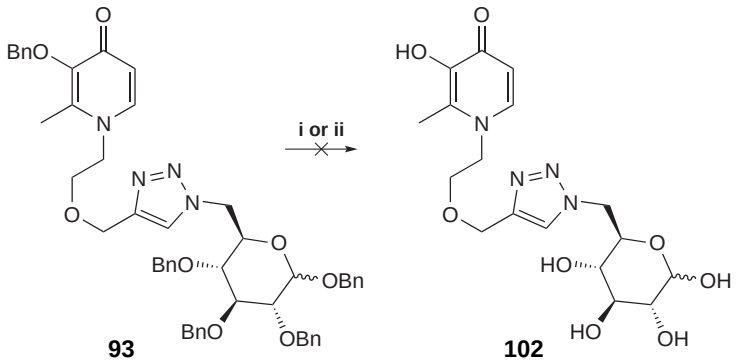

Scheme 4.10: Deprotection of 1-(2-{[1-(6-Deoxy–D-glucopyranos-6-yl)-1,2,3-triazol-4-yl]methoxy}ethyl)pyridinones. Reagents and Conditions: i) Pd/C (10%), 2 bar H_2, MeOH/$CHCl_3$, rt; ii) BBr_3, dry DCM, N_2 atmosphere, 0 °C→rt.

In summary, the desired triazoles derived from 1- and 2-azidoglucose in diversely protected forms were successfully prepared, as well as the triazole derived from 6-azidoglucose in its protected form. The purity of **98** and **101** was determined by HPLC to be above 98% and therefore pure enough to be used in the uptake and permeability assays.

It may be necessary to find another route to obtain fully deprotected 6-linked conjugates. This may be achieved by the use of different protecting groups, or by avoiding the ether bond in the tether. A potential route could be the reaction of *N*-unsubstituted pyridinone **44** with propargyl bromide to give **85**, which could then be clicked to azidoglucose **75**.

Chapter 5

Interaction of Glycoconjugates with GLUT1

Studies that discussed glycosylated compounds usually did not report biological data relating to their brain permeability, while only a number of them measured the interaction of the glycosylated compounds with GLUT1. This was generally done by inhibition studies of GLUT1 transportable substrates in erythrocytes. The transport of glycosylated compounds was only measured directly in select studies, either based on the accumulation of compounds into erythrocytes, or by *in vivo/in situ* brain perfusion, as has been discussed in Section 1.2.3. Due to these shortcomings in experimental design, incorrect conclusions have been drawn, regarding the effect of glycosylation on molecules' brain permeability. It is therefore necessary to measure the movement and distribution of compounds directly, rather than making assumptions about a molecule's behaviour based on indirect measurements (e.g. pharmacological effect or inhibition of another molecules' transport). A number of *in vitro* models of the BBB have been developed previously, based on primary or immortalised cell lines from various species.[248–254]

In this work, the permeability of glucosylated compounds (Figure 5.1) and their interaction with GLUT1 were studied in assays based on primary porcine brain endothelial cells (PBECs).[255] The model was chosen, because primary cells are the closest representation of the properties the BBB has *in vivo* and are expected to express the relevant range of transport systems. The PBEC system used has previously been characterised and expresses tight junction proteins, both uptake and efflux transport systems and has a high transendothelial electrical resistance, which indicates the formation of a tight barrier.[256,257]

For the determination of uptake and interaction with GLUT1, the previously synthesised compounds (described in the preceding chapters) were complemented by compounds kindly supplied by Shen Liu and Yongping Yu from Zheijang University, China. These additional compounds are amides of glucosamine or methyl 6-amino-6-deoxy-α-D-mannoside. All

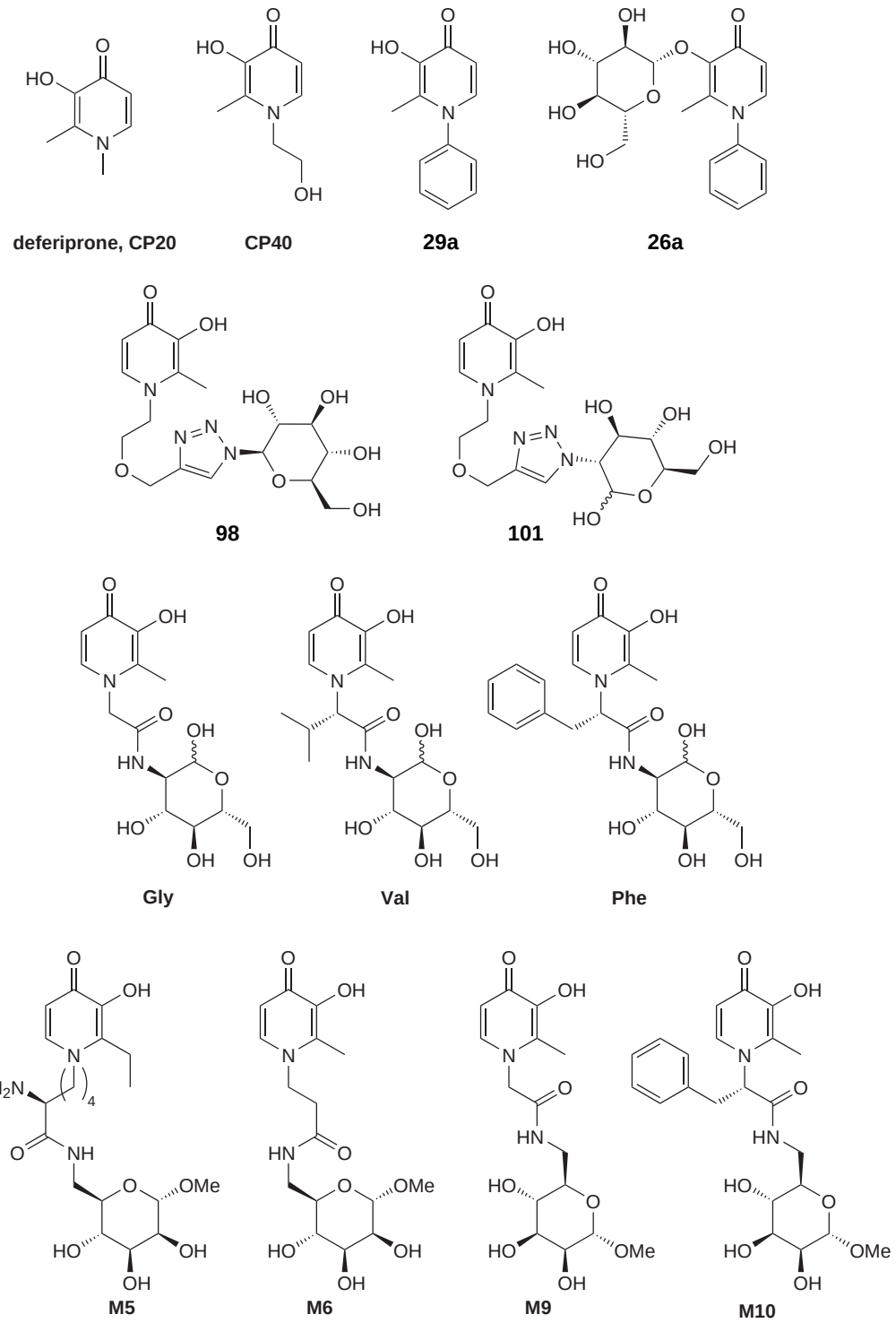

Figure 5.1: Structures of Tested Compounds.
The synthesis of compounds **26a**, **29a**, **98** and **101** is described in the preceding chapters; **Gly**, **Val**, **Phe** and **M5**–**10** were procured from collaborators.

tested compounds were quantified directly by HPLC (see Experimental Chapter), as opposed to indirect measurements.

5.1 Uptake of Compounds into a PBEC Monolayer

In a first set of experiments, PBECs were cultured as a confluent monolayer in microplates (96-, 24-, or 12-well) and used to (a) determine the uptake of the test compounds (Figure 5.2) into the cells, or (b) determine the inhibitory effect of the test compounds on the uptake of GLUT1 transported non-metabolised sugar [^{3}H]3-*O*-methylglucose (3OMG). A microplate format was initially chosen, because it allows a higher throughput than other assay formats.

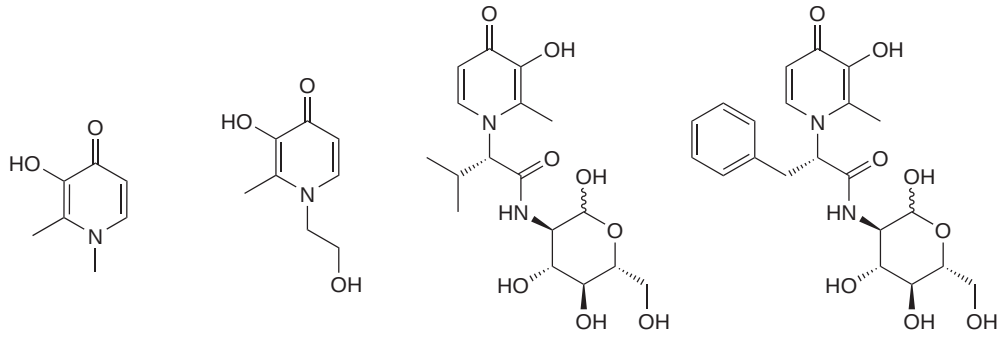

Figure 5.2: Structures of Compounds Used in Experiments Performed on Microplates.

Uptake of Hydroxypyridinones. PBECs were incubated with 500 µM **CP20** or 500 µM **Phe** in the presence or absence of 5 mM glucose in a 96-well plate format (200 µl) for 1, 4 or 24 hours. At the end of the incubation time, the washed cells were lysed (200 µl water or 100 µl Triton X-100 solution) and the lysate analysed by HPLC. **CP20** and **Phe** could be detected in the incubation medium, but not in the cell lysate for any test condition.

Inhibition of [^{3}H]3-*O*-Methylglucose Uptake by Hydroxypyridinones. Glycosylated and non-glycosylated HPOs (**CP20**, **CP40**, **Val**, **Phe**; Figure 5.2) were tested at a range of concentrations (0–500 µM) for their inhibition of 3OMG uptake in a 96-well plate setup. The cells were co-incubated with 3OMG (0.3 µCi per well) and a compound for either 10 or 20 minutes, then washed and lysed. The result of the experiments could not be interpreted due to very low and variable counts from the scintillation counter (Data not shown).

Further optimisation steps were then carried out. **CP20** and **Phe** at 500 µM were tested for their inhibition of 3OMG (1.5 µCi/ml) uptake in 24-well plates for 15 and 60 minutes. Glucose (5 mM) was tested for its effect on 3OMG (1.5 µCi/ml) uptake in 24- and 12-well plates for 15 seconds. In order to deplete any intracellular glucose, which could affect the transport of 3OMG, the cells were pre-incubated with (glucose free) assay buffer for 30 minutes. At the end of the experiment, the cells were washed with an equal volume stopping buffer containing mercuric chloride (1 µM) and phloretin (100 µM) to inhibit potential efflux of 3OMG by GLUT1 before lysis. When corrected for the extracellular component using [^{14}C]sucrose (0.15 µCi/ml), the intracellular radioactivity counts were below zero, indicating no uptake of 3OMG, even under control conditions (Data not shown).

These results may be explained by the extremely small cellular volume of brain endothelial cells. The thickness of brain endothelial cells is less than 0.5 µm.[258] The surface area of a single well on a 96-, 24- and 12-well microplate is 0.32, 1.9 and 3.8 cm^2, respectively. A confluent monolayer of PBECs would therefore have an approximate total cell volume of 16, 95 and 190 nl. The concentration of the compounds that might have been taken up by the cells falls below the level of detection and/or quantification of the HPLC after the lysis of the cells and the consequent dilution, this limitation should have been accounted for, when the experiment was designed.*

The shortfall of this experimental setup might be overcome by the use of cells with a larger cellular volume (e.g. erythrocytes), or by using a different assay setup, in which the compounds can accumulate in a larger volume. In this work, a Transwell assay was chosen, where the compounds can cross the monolayer and accumulate in basolateral compartment.

5.2 Transport of Compounds across a PBEC Monolayer

Transwells are microporous filter membranes, on which cells are grown. The membranes can be inserted into multiwell plates, which allows access for the independent manipulation of the apical and basolateral compartments.

Patabendige et al. recently reported the use of PBECs in a Transwell setup and showed its applicability for permeability studies. The group tested molecules that cross a PBEC

*For a compound that reaches a 500 µM concentration within the cells of a 24-well plate, the lysis and dilution into 100 µl would result in a 0.5 µM concentration in the lysate. The level of quantification for the tested compounds lies around 1–2 µM.

monolayer by passive diffusion, LAT-1 transport or are subject to active efflux.[257] The BBB permeability of glycosylated drugs has not been determined in an *in vitro* assay based on brain endothelial cells before (1.2.3.2), making this a novel method, which is closer to the natural processes at the BBB than the erythrocyte based assays that have been used by other groups.

PBECs in a Transwell-based assay closely model the *in vivo* properties of the BBB, which has been demonstrated by Abbott and co-workers.[257] The cells were shown to grow in a monolayer and retain their morphology, also forming tight junctions – resulting in relatively high TEER (transendothelial electrical resistance). PBECs express efflux transporters, which are found at the BBB,[256,257] and also express GLUT1 express high levels[256]

5.2.1 Transendothelial Electrical Resistance.

The transendothelial electrical resistance is a good indicator for the tightness of the cell monolayer,[259] and has been determined to be around 1800 $\Omega\,cm^2$ *in vivo*.[260]

In this work, the TEER values were very dependent on the particular isolation batch (Figure 5.3). The values for inserts after 3 days of growth and 2 days of treatment with induction medium ranged from 84 to 1537 $\Omega\,cm^2$. Within a batch, values were generally consistent, while the batch to batch variation was large. Batch 25 had significantly higher TEER values, than all other batches, with a mean of $948 \pm 35\ \Omega\,cm^2$. Batches 23 and 26 had lower TEER values than batch 25 – $700 \pm 36\ \Omega\,cm^2$ and $698 \pm 46\ \Omega\,cm^2$, respectively – and their TEER values did not differ significantly. The remaining batches 4, 22, 24 and 24 SF had much low TEER values (192, 218, 198 and 134 $\Omega\,cm^2$, respectively; Table 5.1). The supplementation with (batch 24) or without serum (batch 24 SF) did not have a significant impact on the cells (see B24 vs B24 SF in Table 5.1), but in cells with higher TEERs, serum supplementation on the apical side may have a measurable effect.

The TEER on day one of supplementation is a good indication of the insert's final TEER value. Inserts with low values (<150 $\Omega\,cm^2$) showed no significant improvement the next day (Table 5.2), medium TEER inserts (150–350 $\Omega\,cm^2$) showed an increase of up to 100 $\Omega\,cm^2$, while inserts with a high TEER (>350 $\Omega\,cm^2$, e.g. batches 23, 25 and 26) improved significantly on the second day (increase by 200–300 $\Omega\,cm^2$).

Sodium fluorescein is a small fluorescent molecule, which has previously been used as a marker for paracellular permeability.[261,262] PBECs with a low TEER (<150 $\Omega\,cm^2$) are

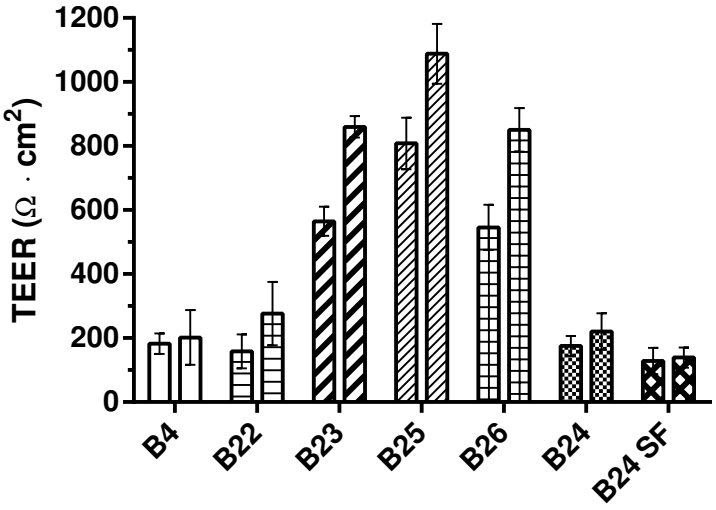

Figure 5.3: Comparison of Transendothelial Electrical Resistance (TEER) for Batches Isolated on Different Days. All batches were measured after one and two days of treatment with supplements (left and right bar, respectively). (SF = serum free induction medium on both sides; Error bars = SEM)

lacking barrier tightness and thus were found to be much more permeable for sodium fluorescein than cells with TEERs above 300 $\Omega\,\mathrm{cm}^2$ (Figure 5.4). The permeability of cells with a very low TEER is similar to filter inserts without cells.

Table 5.1: Statistical Results of Batch-to-Batch Comparison of TEERs (2-Way ANOVA).

Batch	n	B4	B22	B23	B25	B26	B24	B24 SF
B4	8	X	ns[a]	****	****	****	ns	ns
B22	38		X	****	****	****	ns	ns
B23	46			X	****	ns	****	****
B25	68				X	***	****	****
B26	14					X	****	****
B24	36						X	ns
B24 SF	12							X

[a] ns = not significant, * = $p < 0.05$, *** = $p < 0.001$, **** = $p < 0.0001$.

Table 5.2: Comparison of TEERs after 1 or 2 days of Supplementation.

Batch	n	1d vs 2d
B4	4	ns[a]
B22	19	ns
B23	21	****
B25	34	****
B26	7	*
B24	18	ns
B24 SF	6	ns

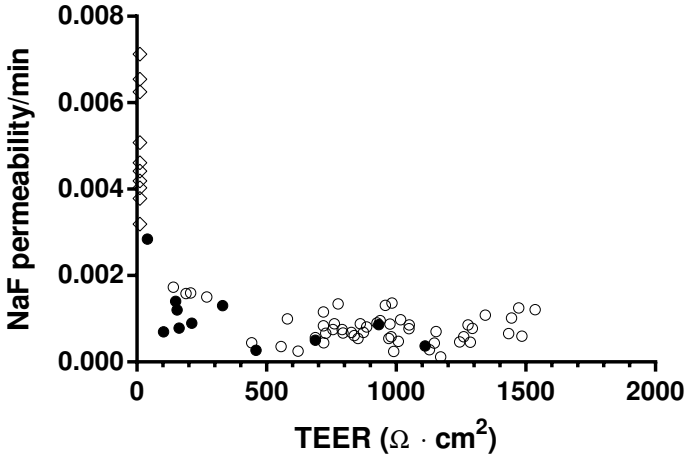

Figure 5.4: Correlation of Sodium Fluorescein Permeability with TEER. (○, 60 min; ●, 30 min; ◇, blank insert; NaF, sodium fluorescein; each point represents one well)

5.2.2 Inhibition of 3OMG Transport by Glycosylated Compounds

An assay based on the Transwell format allows the collection of two sets of data at the same time. On the one hand, the permeability of compounds can be determined by HPLC and on the other hand one can measure the inhibitory effect the compound has on the transport of 3OMG by liquid scintillation. The large volume of the receiver compartment allows sufficient test compound for quantification by HPLC (see Experimental Chapter). In the setup that was used, [^{14}C]sucrose was used as marker for paracellular permeability. Compounds **26a**, **CP20**, **Val**, **Phe** (all 500 µM, Figure 5.5) and glucose (5 mM) were tested for their inhibitory effect on the transport of [^{3}H]3-*O*-methylglucose by GLUT1 when (a) present on both sides or (b) on the apical side only. The incubation time was 30, 60 or 120 minutes.

All samples contained both radioisotopes ([^{14}C]sucrose and 3OMG), which posed problems for the scintillation reading. The emission energies of tritium and carbon-14 overlap (Figure 5.6), the program thus takes a correction factor into account using stored standard curves. But because the ratio of tritium to carbon-14 shifts over time in these experiments, any single correction factor would only be correct for a small subset of analysed samples. Therefore, the scintillator could not calculate the correct quantities of both isotopes and no information about the inhibition of 3OMG transport could be extracted from these experiments. In addition, the donor and receiver compartments were analysed by HPLC. The measured permeability could not be corrected for paracellular permeability, due to the

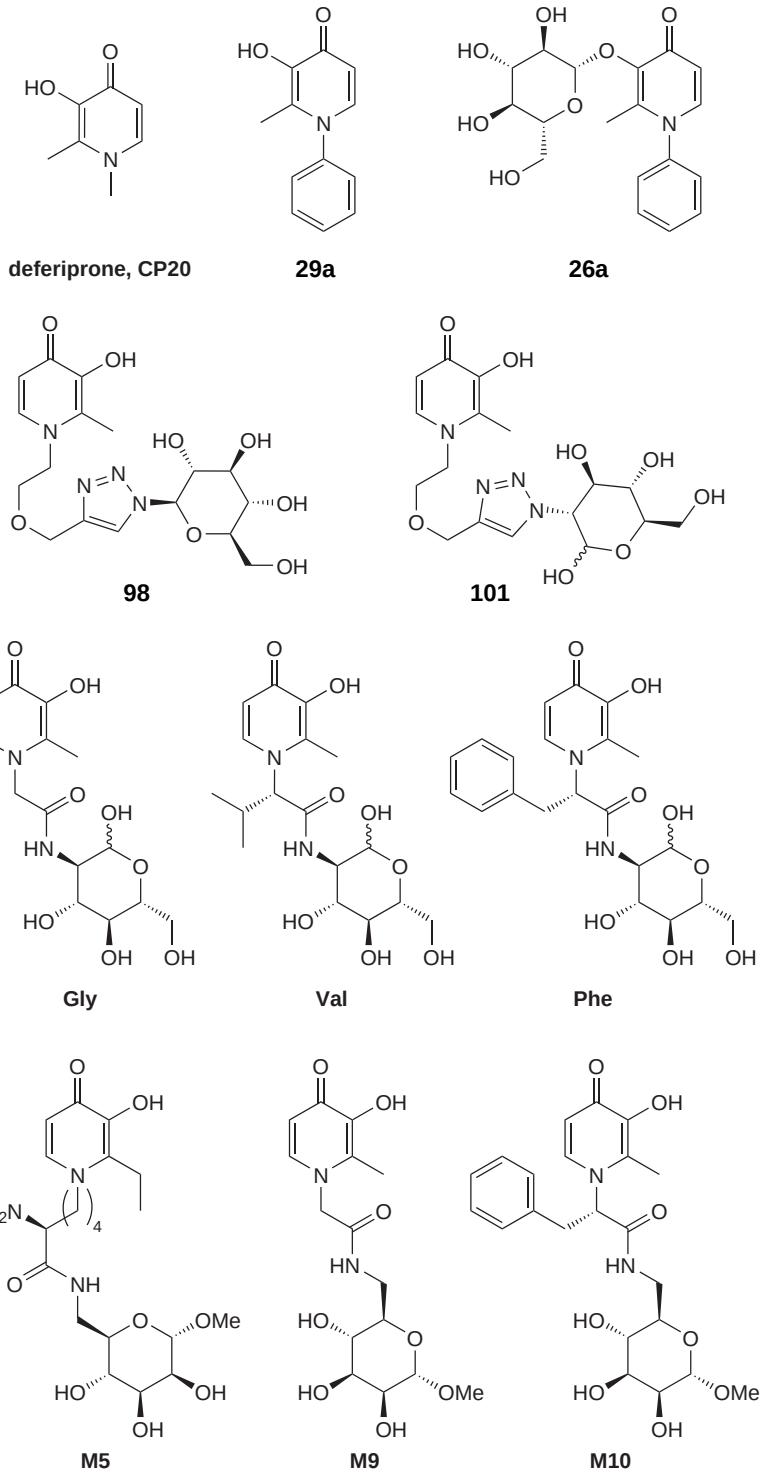

Figure 5.5: Structures of Compounds Used in Transwell Experiments.

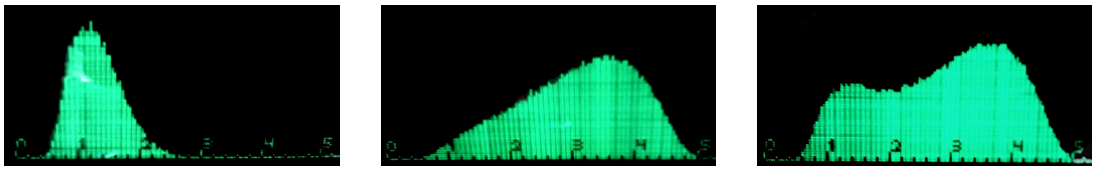

(a) [^{3}H]3-*O*-Methyl-D-glucose (b) D-[^{14}C]Sucrose (c) 1:1 Mixture of both

FIGURE 5.6: Overlapping Energy Emission Profiles of [^{3}H]3OMG and [^{14}C]sucrose. x-Axis is the Energy of the Detected Photons and the y-Axis the Number of Counts.

same problems with [^{14}C]sucrose quantification. A different, non-radioactive paracellular marker was therefore required to avoid these problems.

Another set of experiments was performed with sodium fluorescein as paracellular marker, instead of [^{14}C]sucrose. [^{3}H]3OMG transport over 30 minutes was tested in the presence of 5 mM glucose, 250 µM phloretin (a GLUT1 inhibitor), **CP20**, **26a**, **Phe**, **M6** or **M10** (all 500 µM). The apparent permeability (P_{app}) of 3OMG was calculated according to the equation given by Youdim et al.[263] It was found that the P_{app} of 3OMG (3.72±0.35 $\times 10^{-5}$cm s^{-1}, Figure 5.7) was not affected by any of the compounds. Glucose and the GLUT1 inhibitor phloretin also had no effect, while M10 appeared to increase the transport of 3OMG, rather than inhibit it.

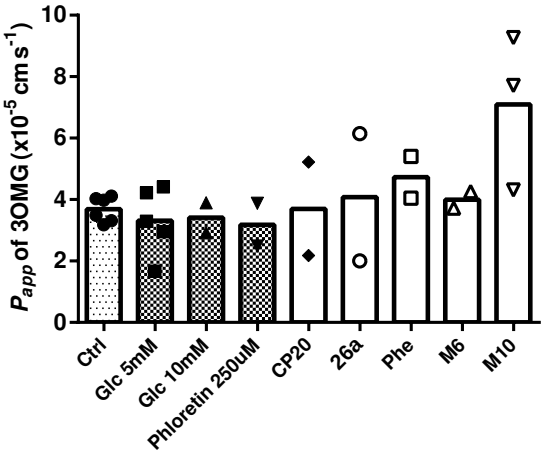

P_{app} $\times 10^{-5}$ cm s^{-1}		± SEM
3OMG	3.72	0.35
+ Glc 5mM	3.19	0.48
+ Glc 10mM	3.41	0.49
+ Phloretin 250uM	2.95	0.60
+ **CP20**	3.70	0.91
+ **26a**	4.08	1.37
+ **Phe**	4.95	0.46
+ **M6**	4.08	0.28
+ **M10**	7.66	0.94

FIGURE 5.7: Competitive Inhibition of [^{3}H]3OMG. P_{app} after 30 min Incubation in Transwells. (All data points shown)

The penetration of the test compounds across the monolayer was determined by HPLC (Figure 5.8). The P_{app} of **CP20** was about 1.00±0.05 $\times 10^{-5}$cm s^{-1}, while permeability of all the glycosylated compounds was lower (0.53–0.72 $\times 10^{-5}$cm s^{-1}) and phloretin was comparable with 1.01±0.05 $\times 10^{-5}$cm s^{-1}.

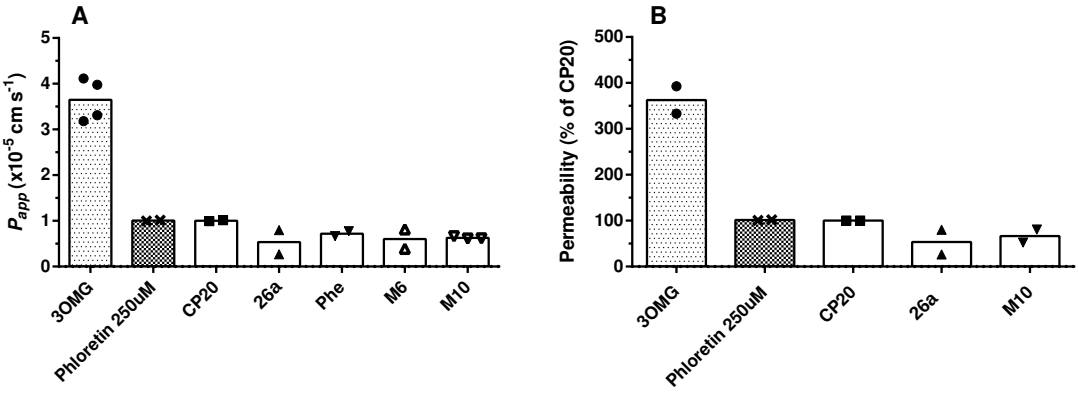

Figure 5.8: Permeability Assay, 30 min Incubation Time. A) P_{app} of Tested Compounds. B) Permeability of Tested Compounds, Normalised to CP20. (All data points shown)

The tested compounds have a much lower permeability than the known GLUT1 substrate 3OMG, which indicates, that the other substances are either not transported by GLUT1, or much worse substrates for the transport protein than 3OMG. Both, the P_{app} of radiolabelled sugar 3OMG in the presence of compounds (Figure 5.7) and the HPLC-determined permeability of compounds (Figure 5.8), exhibited a relatively high variability, which makes definitive statements about the brain permeability of the compounds or interactions with GLUT1 impossible. A large portion of inserts had TEER values between 150–200 $\Omega\,\mathrm{cm}^2$. The permeability in low TEER cells tends to be higher, even after correction for paracellular permeability, which could explain the high variability.

5.2.3 Transport of Glycosylated Compounds by GLUT1

Ten hydroxypyridinones (Figure 5.5: **CP20**, **26a**, **29a**, **98**, **101**, **Gly**, **Val**, **Phe**, **M5** and **M9**) were selected to investigate their BBB permeability in the Transwell setup. Only cells with a TEER value $>400\ \Omega\,\mathrm{cm}^2$ were used, in order to reduce variability. Incubation time was prolonged to 60 minutes to achieve higher concentrations in the receiver compartment. The permeability of compounds was determined by HPLC analysis of both compartments. Since the experiment was performed over a longer timescale without removal of accumulated compound, the possibility of non-linear uptake existed due to a reduced concentration gradient across the monolayer. The permeability of the compounds was low enough, however, that this did not have a marked effect on the results of these experiments.

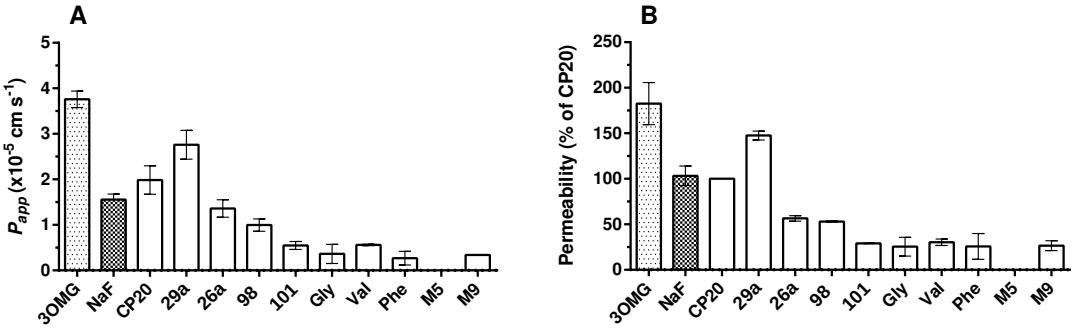

Figure 5.9: Permeability Assay, 60 min Incubation Time. (n = 2–11, Error bars = SEM) A) P_{app} of Tested Compounds. B) Permeability of Tested Compounds, Normalised to **CP20**.

The apparent permeability (P_{app}) of **CP20** was 1.99±0.31 $\times 10^{-5}$cm s^{-1} (Figure 5.9.A and Table 5.3), about twice as high as the P_{app} in the previous experiments (Figure 5.8). While there was a significant difference between the P_{app} of **CP20** and 3OMG, **Gly, Val, Phe, M5, M9** or **101**, no significant difference was observed between **CP20** and **26a**, **29a** or **98** (1.36±0.19, 2.76±0.32 and 1.00±0.13 $\times 10^{-5}$cm s^{-1}, respectively; see Table 5.3).
The results from each experiment were normalised to **CP20** as 100%, in order to account for day-to-day variability (Figure 5.9.B). A highly significant difference ($p < 0.001$) was found between the permeability of **CP20** and all other compounds except sodium fluorescein (NaF): **29a** showed the highest permeability (147%±5), followed by NaF (103%±11), **CP20** (100%), **26a** (56%±3) and **98** (53%±1). The other compounds had a permeability of 0–30% of **CP20**.

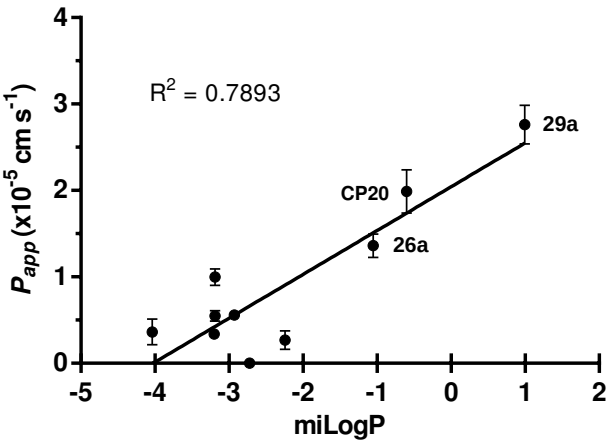

Figure 5.10: P_{app} of Tested Compounds Plotted Against their milogP. (Error bars = SEM)

Glucosylation did not enhance the BBB permeability, but rather had the opposite effect of a drastic reduction in permeability (147% vs 56% for the non-glycosylated **29a** vs the glycosylated derivative **26a**). Interestingly, the permeability of the compounds appears to correlate linearly with the compounds' lipohilicity (Figure 5.10, Table 5.3, $R^2 = 0.79$). Compound **29a** had the highest BBB permeability and is also the most lipophilic compound with a milogP[†] of 0.996. **CP20** is less lipophilic (milogP -0.601) and **26a** is even less than **CP20** (milogP -1.052). The iodinated derivative **26c** has a higher milogP than **26a**, and thus would be expected to permeate the BBB at a higher rate, possibly close to, or even higher than **CP20**. A milogP around -1.2 appears to be the threshold for permeability, because all compounds with a lower logP value barely penetrated the BBB. This finding indicates that the tested HPOs do not cross the BBB by GLUT1 mediated transport, but rather by passive diffusion. In view of the information on substrate specificity of GLUT1 (Section 1.2.3.1) that exists, it is not too surprising that the glycosylated HPOs were not transported by the transporter. All conjugates were linked in position 1 or 2 of the sugar, or – in the case of the 6-linked mannosides – had a modification in position 1. These positions in particular had been identified to be critical for substrate recognition for the outward facing conformation.

While the author was aware of GLUT1 selectivity, the preparation of more suitable substrates for the transport protein, namely 6-linked glucoconjugates, was unfortunately unsuccessful despite several methodological trials (see Chapter 4).

[†]milogP are a predicted clogP values, calculated using the physicochemical property calculator provided online by Molinspiration.[264]

Table 5.3: Physicochemical Properties of Tested Compounds.[a]

Cpd	MW	milogP	HBD	HBA	PSA	P_{app} [c]	± SEM
CP20	139	−0.601	1	3	42.2	1.99	0.31
29a	201	0.996	1	3	42.2	2.76	0.32
26a	363	−1.052	4	8	121.4	1.36	0.19
26c[b]	489	0.031	4	8	121.4	–	–
98	412	−3.19	5	12	172.3	1.00	0.13
101	412	−3.19	5	12	172.3	0.55	0.09
Gly	344	−4.036	6	10	161.5	0.36	0.21
Val	386	−2.927	6	10	161.5	0.56	0.02
Phe	434	−2.245	6	10	161.5	0.27	0.15
M5	443	−2.72	7	11	176.5	0.00	0.00
M6	372	−2.931	5	10	150.5	–	–
M9	358	−3.202	5	10	150.5	0.34	0.00
M10	448	−1.411	5	10	150.5	–	–

[a] MW = Molecular Weight, milogP = clogP calculated by Molinspiration (http://www.molinspiration.com/), HBD = Hydrogen Bond Donors, HBA = Hydrogen Bond Acceptors, PSA = Polar Surface Area.
[b] Compound not tested.
[c] P_{app} in $\times 10^{-5}$ cm s^{-1} after 60 min.

Chapter 6

Conclusions and Future Work

The aim of this work was to investigate the BBB permeability of 3-hydroxypyridin-4-one iron chelators and whether glycosylation can improve the molecules' permeability by utilising the glucose transporter GLUT1 for facilitated transport across the BBB.

6.1 Synthetic Chemistry

Glucosides of *N*-phenyl and *N*-4-bromophenyl substituted HPOs (**26a**,**b**, Figure 6.1) were synthesised from maltol, the respective aniline and a glycosyl donor. The 4-iodophenyl analogue (**26c**) could not be synthesised, however. The published procedure (Scheme 2.2),[186] and other routes described in this work (Scheme 2.3 and Scheme 2.5) did not yield the desired product **26c**. The copper catalysed transhalogenation of 1-(4-bromophenyl)-3-

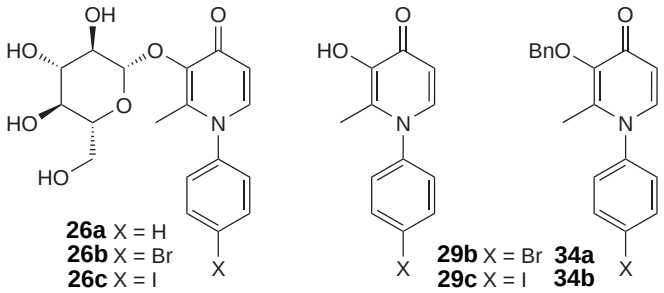

Figure 6.1: Structures of *N*-Phenyl hydroxypyridinones.

hydroxy-2-methylpyridin-4-one **29b** did not proceed, while masking of the 3-hydroxy group allowed the successful transformation of **34a** into the 4-iodophenyl derivative **34b**. This indicates that the copper catalyst was chelated by the hydroxypyridinone part of the molecule, which is known as an iron and copper chelator, thus preventing the transhalogenation of the 3-hydroxy derivative. While the 3-hydroxy group in glucoside **31b** is also masked, the reaction mainly furnished unreacted starting material and some side

products. Attempts to directly obtain iodinated pyridinones by using 4-iodoaniline did not yield any products due to extensive polymerisation. It is the opinion of the author that the relatively high reactivity of aromatic iodine atoms, compared to bromine, is the cause of these side reactions. The author believes that further optimisations of the transhalogenation protocol will afford the 4-iodophenyl derivative **26c**.

Pyridinones bearing carboxylic acid substituents on the ring nitrogen were readily prepared from maltol and amino acids in good yields. Pyridinone **48** (Figure 6.2), with a carboxyl group in position 2 of the ring, was obtained from a much shorter synthesis than previously published routes (4 steps instead of 8), additionally foregoing any chromatographic purifications. Amide-linked conjugates were prepared from the HPOs derived from amino acids, which were coupled with protected glucosamine after optimisation of the coupling protocol. The final products could not be isolated, however. Decomposition occurred during treatment with base when attempting to deacetylate the compounds. Glucuronamides of *N*-alkylamine HPOs (Figure 6.2) were prepared from 1,2-acetonide or 1,2-benzylidene protected glucuronolactones and the respective HPOs. The resultant amides were subjected to varying deprotection conditions. Acidic conditions led to decomposition of the amide bond, while hydrogenation of the benzylidene protected compounds did not proceed at all, even at very high pressures. While the deprotection under acidic conditions might be improved, the author believes that the coupling with unprotected glucuronic acid or glucuronolactone is a better alternative to obtain the desired HPO-glucuronamide conjugates.

Conjugation using a triazole-tether (Figure 6.2) was achieved by reaction of an alkyne-HPO with an azido-sugar via copper catalysed alkyne-azide cycloaddition. Azidosugars

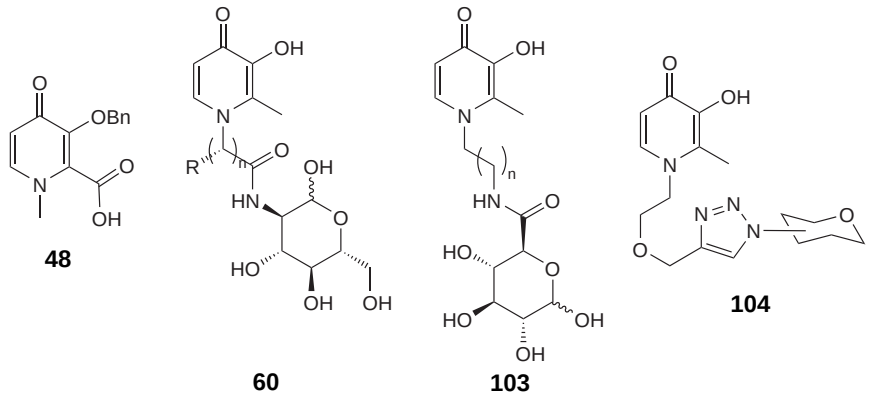

Figure 6.2: Structures of Amide and Triazole-linked Conjugates.

were prepared from glucose or glucosamine and linked to an alkyne-HPO after optimisation of the coupling protocol. The resultant acetylated triazole-conjugates were deprotected by the action of sodium methoxide, followed by hydrogenation. The 6-linked conjugate was fully benzylated, and subjecting it to the same conditions gave only starting materials, while the use of boron tribromide resulted in decomposition. The deprotection of the 6-linked conjugate could not be investigated further due to time constraints, but should be pursued in future work, because the literature suggests that 6-linked glycoconjugates are most likely to be transported by GLUT1.
Overall, the deprotection of various conjugates posed the biggest problems in this work. Hydrogenation of the benzyl protected triazole derivatives, or the benzylidene protected glucuronamides did not proceed, while other derivatives were readily hydrogenated. The author believes, that the compounds may have been too lipophilic and thus could not be adsorbed onto the catalyst, preventing hydrogenation. It may therefore be necessary to substitute overly lipophilic protecting groups for smaller and/or more polar groups.

In conclusion, the synthesis of some novel sugar conjugates of 3-hydroxypyridin-4-ones has been successful, while others could not be obtained due to problematic syntheses and time constraints. Unfortunately, 6-linked glucoconjugates, which were expected to have the highest chance to be transported by GLUT1, could not be synthesised, limiting the study to 1- and 2-linked gluconjugates.

6.2 Biological Data

The conjugates that had been synthesised, and additional conjugates that were supplied by Shen Liu and Yongping Yu from Zheijang University, China, were tested for their behaviour in blood-brain barrier models based on PBECs. Multiple call based assays were evaluated for their use to determine the uptake into or permeability across a PBEC monolayer. The models were further used to investigate the compounds' interaction with the BBB glucose transporter GLUT1.
The uptake experiments did not give interpretable results, because the cell monolayer was found to be too thin to accumulate measurable quantities of the tested compounds. The same problem persisted for the inhibition assay in a multiwell plate setup. This problem could have been circumvented by using higher compound concentrations, however. The

interpretation of results generated in the Transwell format was complicated by problems with the scintillation counter. This was due to the overlapping emission energy profiles of the used radioisotopes.

The permeability assay was performed using cells grown on a permeable Transwell filter membrane. Due to the high density of GLUT1 found in the BBB, a substrate of GLUT1 would be expected to have a higher permeability than its non-glycosylated analogue, which can permeate merely by passive diffusion. When tested directly and quantified by HPLC, rather than through indirect measurements as in previous studies, none of the tested HPO-sugar conjugates had a higher permeability than the tested non-glycosylated parent HPOs. The compounds with the highest lipophilicity were able to cross the BBB the most, while the permeability of compounds with a milogP lower -1 was very limited. There is therefore no evidence that the tested molecules were transported by GLUT1, as the permeability of the molecules was not influenced by the absence or presence of a sugar moiety, except for the sugar's effect on lipophilicity. The sugar moiety hindered – rather than enhanced – permeability due to its high hydrophilicity and multiple hydrogen bond donors and acceptors. It thus appears imperative to design transportable glucose conjugates in order to facilitate their brain penetration, compared to their parent molecules. However, the study did identify a non-conjugated molecule, **29b**, with superior permeability compared to **CP20**. This molecules is not fully characterised in terms of its iron-chelating and neuroprotection capabilities, but warrants further studies.

6.3 Ideas for Future Work

Future areas for development of this work would include the synthesis and testing of additional HPO-sugar conjugates, in particular those that are linked in position 6 of the sugar moiety. The only conjugates that have previously been shown by Gynther et al. to utilise GLUT1 transporter to enter the brain, have been linked in position 6.[163]

A potential route towards the synthesis of 6-linked triazole derivatives could proceed via 1,2,3,4-tetraacetylated glucose **105** (Scheme 6.1), which could be prepared from compound **79** via acetylation and selective deprotection of position 6 by catalytic hydrogenation. Alternatively, the primary alcohol of glucose could be selectively silylated with *tert*-butyldimethylsilyl chloride (TBDMSCl).[211] Acetylation, followed by the removal of the silyl group with tetrabutylammonium fluoride, would furnish 6-hydroxysugar **105**.

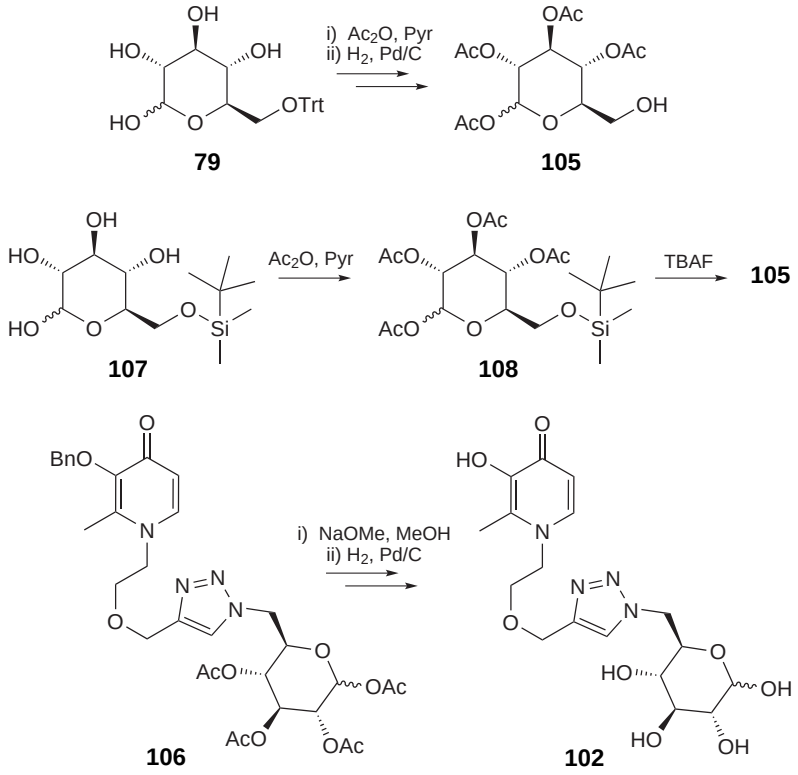

Scheme 6.1: Possible Reaction Pathway towards 6-linked Triazole Conjugates.

Introduction of the azido group on the sugar and triazole formation, following the syntheses described in chapter 4, gives protected sugar conjugate **106**. This could be deprotected similarly to 1- and 2-linked triazoles by hydrogenation and deacetylation, giving the desired 6-linked triazole **102**. Amides linked in position 6 could be obtained directly from carboxylic acids and this 6-azido sugar via Staudinger ligation, or by classic amide formation, following the reduction of the azide.

In order to efficiently investigate the permeability of glucose conjugates, the author suggests two different screening methods. The preliminary screening of the membrane permeability could be achieved in an assay investigating the uptake into erythrocytes, which are readily available, uncomplicated to handle and express GLUT1 on their cell membrane. A facile assay determining the uptake into erythrocytes in the presence and absence of GLUT1 inhibitor would serve as primary screening method. Promising candidates should then be evaluated further in the PBEC-based BBB assay that was used in the present work. This assay allows the reliable detection and quantification of a compounds BBB permeability by common methods such as HPLC, and it closely reflects the barrier and transport properties of the blood-brain barrier (Section 1.2.3.1, Chapter 5 and references

therein). Modifications and optimisations are possible, such as studying the effect of glucose (substrate inhibition), a GLUT1 inhibitor (e.g. phloretin or cytochalasin B) and reduced temperature on the permeability of the candidate. These experiments would indicate if, and to what extent, GLUT1 is involved in the compound's transport across the BBB. It could be worthwhile to study the levels of GLUT1 expression in different batches of PBECs, as this could also shed some light on the variability of 3OMG transport that was seen in some experiments.

For a better understanding of the interactions of GLUT1 with its natural and non-natural substrates, the author recommends that potential candidates molecules should be screened *in silico*, before testing them *in vitro*. Studying molecules by docking them into the recently published crystal structures of GLUT1[124] and its bacterial homologue XylE[122,123] should provide a better understanding of the exact interactions of GLUT1 with its substrates, and may highlight where modifications are tolerated by the protein, thus allowing a more focused approach to the design of novel glycoconjugates.

The identification of a successful candidate could allow the expansion of the glycosylation strategy to other substance classes, such as anti-retroviral or chemotherapeutic drugs, as discussed in Chapter 1, in order to allow a more targeted therapy reducing global side-effects or to gain access the brain with drugs which had previously not been able to penetrate the BBB. This is of particular importance in diseases such as HIV or parasite infections, where the brain serves as a reservoir for the pathogens which cannot be reached with conventional drugs.[157,265,266]

Further avenues include the design of cleavable linkers, so that the drug is released in the brain, otherwise the formed iron complex may not be able to cross the blood-brain barrier back into the blood, effectively trapping the complexed iron within the brain. A first approach could be the use of ester-linked molecules, which may even turn out to be too labile to reach the blood-brain barrier intact.

Much more work remains to be done in order to develop successful glycoconjugation strategies for the delivery of drugs via GLUT1 and the author hopes that the present work will be built upon in future studies.

Chapter 7

Experimental

7.1 Synthetic Procedures

7.1.1 General

Melting points were determined on an Electrothermal apparatus and are uncorrected. IR spectra were recorded on a Perkin Elmer Spectrum Two FT-IR spectrophotometer. ^{1}H- and ^{13}C-NMR spectra were recorded on a Bruker Avance 400 spectrometer at 298 K (400.13 MHz for ^{1}H, 100.62 MHz for ^{13}C). The spectra were referenced against TMS where present, or the centre of the solvent signal was used as an internal standard, which was related to TMS according to Gottlieb *et al.*[267] The digital resolution was 0.13 Hz/data point in the ^{1}H- spectra and 0.37 Hz/data point in the ^{13}C-NMR spectra. Chemical shifts (δ) are given as parts per million (ppm), coupling constants as Hertz (Hz). The EPSRC National Mass Spectrometry Facility Swansea kindly recorded all mass spectra on a Thermofisher LTQ Orbitrap XL.

All reagents were obtained from major suppliers (Sigma-Aldrich, Alfa Aesar, VWR International, Thermo Fisher Scientific) and were used as received and without further purification, unless stated otherwise. For chromatographic separations, silica gel 60 (pore size 60 Å, 230-400 mesh, Sigma-Aldrich) was used. For thin layer chromatography, silica coated aluminium plates (silica gel 60, UV indicator 254 nm, Merck KGaA) were used. Room temperature indicates a temperature in the range 16 °C to 22 °C.

Where possible, systematic names were generated by ChemDraw (PerkinElmer, Inc., Waltham, MA, USA) The numbering within chemical structures is used to aid the unambiguous assignment of NMR signals and is unrelated to the systematic names of substances.

Purity determination by HPLC. The purity of all compounds tested in cell assays was determined on a Waters HPLC system (600 controller, 626 pump, 996 PDA detector, 717 autosampler; Waters Corp, Milford, MA, USA) and found to be 98% or higher. A

reverse-phase polymer column (PLRP-S 150 x 4.6 mm, pore size 300 Å, particle size 8 µm) with a flow rate of 1 ml/min was used for separation with gradient elution. Acetonitrile, water and 1-heptanesulfonic acid (all HPLC grade) were obtained from Thermo Fisher Scientific. The mobile phase was composed of a buffer (5 mmol 1-heptanesulfonic acid in water, adjusted to pH 2 with HCl) and acetonitrile.
A gradient of 2-35% acetonitrile was run for 20 min, followed by 5 min at 35% acetonitrile and a 5 min post-run period at 2% acetonitrile. The total time per sample was 31 min, samples were injected twice or thrice (100 µl per injection). Sample components were detected by UV absorption at 280 nm. Chromatograms were processed and exported with Millennium32 (Waters Corp).

7.1.2 General Reactions

α-D-Glucopyranose 1,2,3,4,6-penta-*O*-acetate

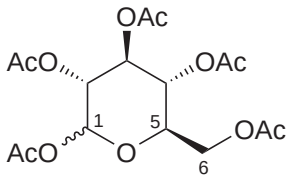

76

Glucose (9.0 g, 50 mmol) was added to an ice-cooled solution of acetic anhydride (25 ml) in pyridine (75 ml). The reaction mixture was allowed to warm to room temperature and stirred over night, then poured onto ice-water and stirred for 2 hours. The formed precipitate was collected by vacuum filtration to give fully acetylated sugar **76** as a white powder (14.4 g, 36.9 mmol, 74%, ratio α/β: >10).

All analytical data is in good agreement with published data for the α isomer.[268]

^{1}H-NMR ($CDCl_3$, 400 MHz): δ 6.33 (d, ^3J(H1,H2) = 3.8 Hz, 1H, H-1), 5.47 ('t', ^3J = 9.9 Hz, 1H, H-3), 5.14 ('t', ^3J = 10.1 Hz, 1H, H-4), 5.10 (dd, ^3J(H2,H3) = 10.4 Hz, ^{H2}J(H1, ,) = 3.8 Hz 1H, H-2), 4.27 (dd, ^2J(H6a,H6b) = 12.7 Hz, ^3J(H6a,H5) = 4.5 Hz, 1H, H-6a), 4.14–4.11 (m, 1H, H-5), 4.09 (dd, ^2J(H6b,H6a) = 12.7 Hz, ^3J(H6b,H5) = 2.4 Hz, 1H, H-6b), 2.18 (s, 3H, CH_3), 2.09 (s, 3H, CH_3), 2.04 (s, 3H, CH_3), 2.03 (s, 3H, CH_3), 2.02 (s, 3H, CH_3).

^{13}C-NMR ($CDCl_3$, 100 MHz): δ 170.65 (C=O), 170.24 (C=O), 169.67 (C=O), 169.40 (C=O), 168.77 (C=O), 89.07 (C-1), 69.83 (C-3,C-5), 69.19 (C-2), 67.87 (C-4), 61.45 (C-6), 20.91 (CH_3), 20.72 (CH_3), 20.69 (CH_3), 20.59 (CH_3), 20.48 (CH_3).

2,3,4,6-Tetra-*O*-acetyl-α-D-glucopyranosyl bromide

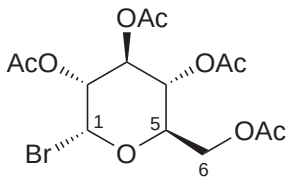

30

Peracetyl glucose **76** (2.0 g, 5.1 mmol) was dissolved in DCM (10 ml) and cooled to 0 °C, then hydrobromic acid (45% w/v in acetic acid, 3 ml) was added and the reaction mixture stirred on ice for 1 hour and at room temperature for 4 hours. The reaction mixture was diluted with DCM (20 ml) and poured onto ice water. The organic phase was washed with saturated $NaHCO_3$ solution and brine, then dried and evaporated. The residue was recrystallised from ethanol and the precipitate collected on a filter and washed with cold ethanol to yield 2,3,4,6-tetra-*O*-acetyl-α-D-glucopyranosyl bromide (**30**) as white crystals (1.95 g, 4.74 mmol, 93%).

All analytical data is in good agreement with published data.[269]

^{1}H-NMR ($CDCl_3$, 400 MHz): δ 6.61 (d, ^3J(H1,H2) = 4.0 Hz, 1H, H-1), 5.56 ('t', ^3J(H3, H2) = 10.0 Hz, ^3J(H3,H4) = 9.5 Hz, 1H, H-3), 5.17 ('t', ^3J(H4,H5) = 10.1 Hz, ^3J(H4,H3) = 9.5 Hz, 1H, H-4), 4.84 (dd, ^3J(H2,H3) = 10.0 Hz, ^3J(H2,H1) = 4.0 Hz, 1H, H-2), 4.33 (dd, ^2J(H6a,H6b) = 12.3 Hz, ^3J(H6a,H5) = 3.7 Hz, 1H, H-6a), 4.30 (ddd, ^3J(H5,H4) = 10.0 Hz, ^3J(H5,H6a) = 3.7 Hz, ^3J(H5,H6b) = 1.9 Hz, 1H, H-5), 4.13 (dd, ^2J(H6b,H6a) = 12.3 Hz, ^3J(H6b,H5) = 1.9 Hz, 1H, H-6b), 2.11 (s, 3H, CH_3), 2.10 (s, 3H, CH_3), 2.06 (s, 3H, CH_3), 2.04 (s, 3H, CH_3).

7.1.3 Synthesis of Glucoside-linked Conjugates

3-Hydroxy-2-methyl-1-phenylpyridin-4(1*H*)-one

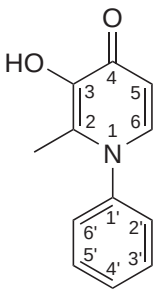

29a

Maltol (12.6 g, 100 mmol) and aniline (18.2 ml, 200 mmol) were suspended in 0.5M HCl (250 ml). The reaction mixture was heated to reflux for 72 hours, then cooled and kept at 4 °C over night. The formed precipitated was collected by vacuum filtration and washed with cooled water to give 3-hydroxy-2-methyl-1-phenylpyridin-4(1*H*)-one (**29a**) as yellow needles (12.0 g, 59.6 mmol, 60%).

Analytical data is in agreement with published data.[270,271]

Melting point: m.p. 212−213 °C (lit. m.p. 222 °C).[272]

^{1}H-NMR (CD_3OD, 400 MHz): δ 7.61–7.57 (m, 4H, H-6,3',4',5'), 7.42–7.39 (m, 2H, H-2',6'), 6.48 (d, ^3J(H5,H6) = 7.2 Hz, 1H, H-5), 2.11 (s, 3H, CH_3).

^{13}C-NMR (CD_3OD, 100 MHz): δ 171.54 (C-4), 146.85 (C-2), 143.20 (C-1'), 139.31 (C-6), 132.95 (C-3), 131.07 (C-3',5'), 130.87 (C-4'), 127.96 (C-2',6'), 112.55 (C-5), 13.77 (CH_3).

1-(4-Bromophenyl)-3-hydroxy-2-methylpyridin-4(1*H*)-one

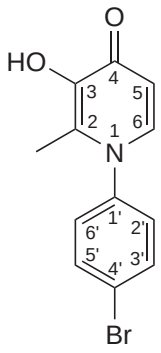

29b

Maltol (5.04 g, 40 mmol) and 4-bromoaniline (13.76 g, 80 mmol, 2 eq.) were dissolved in methanol (40 ml) and 0.5M HCl (100 ml) and heated to reflux for 48 hours. The reaction mixture was kept at 4 °C for 3 days, the formed precipitate was then collected by vacuum filtration and washed with cold water and cold methanol to give 1-(4-bromophenyl)-3-hydroxy-2-methylpyridin-4(1*H*)-one (**29b**) as pale brown crystals (3.72 g, 13.3 mmol, 33%).

Analytical data is in agreement with published data.[186]

^{1}H-NMR (CD_3OD, 400 MHz): δ 7.76 (d, ^3J = 8.7 Hz, 2H, H-3',5'), 7.59 (d, ^3J = 7.3 Hz, 1H, H-6), 7.36 (d, ^3J = 8.7 Hz, 2H, H-2',6'), 6.47 (d, ^3J = 7.3 Hz, 1H, H-5), 2.13 (s, 3H, CH_3).

3-Hydroxy-1-(4-iodophenyl)-2-methylpyridin-4(1*H*)-one

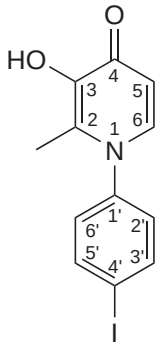

29c

Maltol (1.0 g, 8 mmol) and 4-iodoaniline (3.5 g, 16 mmol, 2 eq.) were dissolved in methanol (8 ml) and water (20 ml). Concentrated HCl (37%, 0.5 ml) was added and the reaction mixture heated to reflux for 49 hours. The reaction mixture was neutralised with 1M NaOH, then extracted with ethyl acetate. The organic phase was washed with brine, then dried over Na_2SO_4 before evaporation. The residue was purified by column chromatography (ethyl acetate/hexane: 2/1), but only decomposition products could be isolated.

3-(Benzyloxy)-2-methyl-4*H*-pyran-4-one

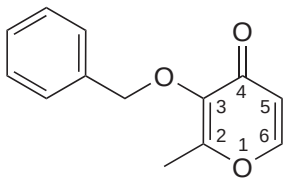

33

A solution of NaOH (3.5 g, 88 mmol) in water (10 ml) was added to a solution of maltol (10.1 g, 80 mmol) in methanol (10 ml). The resulting solution was heated to reflux while benzyl bromide (10.5 ml, 88 mmol) was added via a dropping funnel. The reaction mixture was heated to reflux for 18 hours, then concentrated *in vacuo*, diluted with water (50 ml) and extracted with ethyl acetate (2×). The combined organic phases were washed with 1M NaOH and brine twice, then dried over Na_2SO_4 and evaporated to give the crude product as brown oil. The crude residue crystallised upon addition of a seed crystal and was recrystallised from Et_2O to give 3-(benzyloxy)-2-methyl-4*H*-pyran-4-one (**33**) as pale pink needles (15.9 g, 74 mmol, 92%).

All analytical data is in good agreement with published data.[273]

Melting point: m.p. 51−52 °C (lit. m.p. 53−55 °C).[199]

IR (neat) cm^{-1}: 1641, 1425, 1250, 1181.

^{1}H-NMR ($CDCl_3$, 400 MHz): δ 7.59 (d, ^3J(H6,H5) = 5.6 Hz, 1H, H-6), 7.40 (dd, ^3J = 7.7 Hz, ^3J = 1.8 Hz, 2H, Ph H-3,5), 7.37–7.32 (m, 3H, Ph H-2,4,6), 6.36 (d, ^3J(H5,H6) = 5.6 Hz, 1H, H-5), 5.16 (s, 2H, O−*CH*$_2$−Ph), 2.08 (s, 3H, CH_3).

^{13}C-NMR ($CDCl_3$, 100 MHz): δ 175.10 (C-4), 159.74 (C-2), 153.42 (C-6), 143.77 (C-3), 136.86 (Ph C-1), 129.04 (Ph C-3,5), 128.43 (Ph C-2,6), 128.32 (Ph C-4), 117.18 (C-5), 73.54 (O−*CH*$_2$−Ph), 14.79 (CH_3).

NSI-MS *m/z* (%): 455 (29, [2M+Na^+]), 433 (22, [2M+H^+]), 239 (14, [M+Na^+]), 217 (100, [M+H^+]).

HRMS-NSI *m/z*: Calc. for $C_{13}H_{13}O_3$ [M+H^+]: 217.0859; found: 217.0862.

3-(Benzyloxy)-1-(4-bromophenyl)-2-methylpyridin-4(1*H*)-one

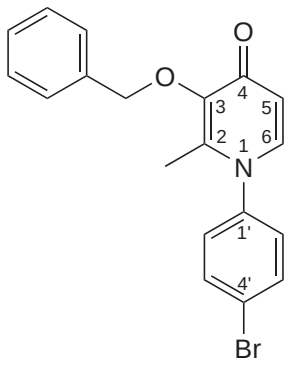

34a

3-(Benzyloxy)-2-methyl-4*H*-pyran-4-one (**33**) (1.08 g, 5 mmol) and 4-bromoaniline (1.72 g, 10 mmol, 2 eq.) were dissolved in methanol (10 ml) and 0.5M HCl (10 ml). The resulting mixture was heated to reflux for 60 hours and then concentrated *in vacuo* and extracted with DCM (3×). The combined organic phases were washed with 1M NaOH and water, then dried over Na_2SO_4. Evaporation gave the crude product as a brown oil (2.1 g), which was purified by column chromatography (chloroform/methanol: 50/1 → 20/1 → 9/1). 3-(Benzyloxy)-1-(4-bromophenyl)-2-methylpyridin-4(1*H*)-one was isolated as pale yellow crystals (1.46 g, 3.9 mmol, 79%).

Melting point: m.p. 144−145 °C.

IR (neat) cm^{-1}: 3017, 2966, 1622, 1576, 1488, 1356, 1280, 1169, 961.

^{1}H-NMR (CD_3OD, 400 MHz): δ 7.73 (d, ^{3}J(H3',5',H2',6') = 8.6 Hz, 2H, H-3',5'), 7.67 (d, ^{3}J(H6,H5) = 7.4 Hz, 1H, H-6), 7.44–7.41 (m, 2H, Ph H-3,5), 7.38–7.32 (m, 3H, Ph H-2,4,6), 7.28 (d, ^{3}J(H2',6',H3',5') = 8.6 Hz, 2H, H-2',6'), 6.54 (d, ^{3}J(H5,H6) = 7.4 Hz, 1H, H-5), 5.13 (s, 2H, O−CH_2−Ph), 1.89 (s, 3H, CH_3).

^{13}C-NMR (CD_3OD, 100 MHz): δ 175.67 (C-4), 146.78 (C-1'), 144.84 (C-2), 142.05 (C-3), 141.31 (C-6), 138.46 (Ph C-1), 134.31 (C-3',5'), 130.25 (Ph C-3,5), 129.89 (Ph C-2,6), 129.43 (C-2',6'), 129.40 (Ph C-4), 124.83 (C-4'), 117.21 (C-5), 74.58 (O−CH_2−Ph), 14.79 (CH_3).

NSI-MS *m/z* (%): 743 (10, [2M+H$^+$]), 741 (21, [2M+H$^+$]), 739 (10, [2M+H$^+$]), 372 (98, [M+H$^+$]), 370 (100, [M+H$^+$]).

HRMS-NSI *m/z*: Calc. for $C_{19}H_{17}BrNO_2$ [M+H$^+$]: 370.0437, 372.0417; found: 370.0441, 372.416.

3-(Benzyloxy)-1-(4-iodophenyl)-2-methylpyridin-4(1*H*)-one

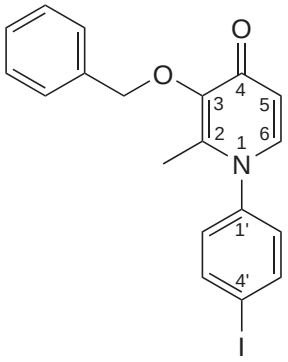

34b

A pressure tube was charged with 3-(benzyloxy)-1-(4-bromophenyl)-2-methylpyridin-4(1*H*)-one (**34a**) (741 mg, 2.0 mmol), sodium iodide (604 mg, 4.0 mmol, 2 eq.) and copper(I) iodide (24.0 mg, 125 µmol, 6.25%mol) and flushed with nitrogen. *N,N'*-Dimethylethylenediamine (21.6 µl, 200 µmol, 10%mol) and dry dioxane (2 ml) were added and the tube sealed before heating to 110 °C for 24 hours. The reaction mixture was diluted with aqueous ammonia (20 ml), then poured onto water (40 ml) before extraction with DCM (3× 25 ml). The combined organic phases were dried over Na_2SO_4 and evaporated to afford a pale olive green oil (640 mg) which solidified on cooling. The crude product was found to be a mixture of the desired 3-(benzyloxy)-1-(4-iodophenyl)-2-methylpyridin-4(1*H*)-one (**34b**) and starting material **34a** in a 5:1 ratio (determined by NMR), and was not purified further (Product: 534 mg, 1.28 mmol, 64%).

Melting point: m.p. 129−132 °C.

IR (neat) cm^{-1}: 2967 (w), 2949 (w), 2783 (br), 1622, 1568, 1484, 1453, 1391, 1350, 1283, 1160, 1010, 947.

^{1}H-NMR ($CDCl_3$, 400 MHz): δ 7.83 (d, ^3J(H3',5',H2',6') = 8.6 Hz, 2H, H-3',5'), 7.44 (dd, ^3J(Ph H2,6,Ph H3,5) = 7.7 Hz,^4J(Ph H2,6,Ph H4) = 1.7 Hz, 2H, Ph H-2,6), 7.36–7.29 (m, 3H, Ph H-3,4,5), 7.20 (d, ^3J(H6,H5) = 7.5 Hz, 1H, H-6), 6.93 (d, ^3J(H2',6',H3',5') = 8.6 Hz, 2H, H-2',6') 6.47 (d, ^3J(H5,H6) = 7.5 Hz, 1H, H-5), 5.27 (s, 2H, O−*CH*$_2$−Ph), 1.81 (s, 3H, CH_3).

NSI-MS *m/z* (%): 835 (8, [2M+H^+]), 418 (100, [M+H^+), 372/370 (9, [$C_{19}H_{16}BrNO_2$+H^+]).

HRMS-NSI *m/z*: Calc. for $C_{19}H_{17}INO_2$ [M+H^+]: 418.0298; found: 418.0296.

3-(2,3,4,6-Tetra-*O*-acetyl-β-D-glucopyranosyloxy)-2-methylpyran-(4*H*)-one

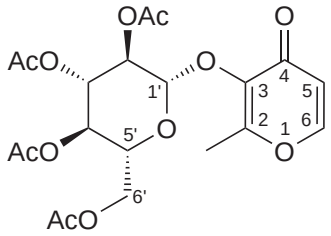

32

Maltol (3.79 g, 30 mmol), glucopyranosyl bromide **30** (4.11 g, 10 mmol) and tetrabutylammonium bromide (3.19 g, 9.9 mmol) were dissolved in DCM (40 ml) and 1M NaOH (40 ml). The resulting solution was stirred vigorously and heated to 35 °C for 4.5 hours, before extraction with ethyl acetate (300 ml). The organic phase was washed twice with 1M NaOH, water and brine, before drying over Na_2SO_4. Evaporation gave a slowly crystallising orange oil (2.45 g) which was purified by column chromatography (ethyl acetate/hexane: 2/1) to give an off-white solid. Recrystallisation from water gave 3-(2,3,4,6-tetra-*O*-acetyl-β-D-glucopyranosyloxy)-2-methylpyran-(4*H*)-one (**32**) as colourless needles (1.35 g, 2.96 mmol, 30%).

All analytical data is in good agreement with published data.[51,274]

^{1}H-NMR ($CDCl_3$, 400 MHz): δ 7.63 (d, ^3J(H6,H5) = 5.7 Hz, 1H, H-6), 6.34 (d, ^3J(H5, H6) = 5.7 Hz, 1H, H- H-5), 5.35 (d, ^3J(H1',H2') = 7.9 Hz, 1H, H-1'), 5.29 ('t', ^3J(H3', H2') = 9.6 Hz, ^3J(H3',H4') = 9.2 Hz, 1H, H-3'), 5.18 (dd, ^3J(H2',H3') = 9.6 Hz, ^3J(H2', H1') = 7.9 Hz, 1H, H-2'), 5.11 ('t', ^3J(H4',H5') = 10.1 Hz, ^3J(H4',H3) = 9.2 Hz, 1H, H-4'),

4.20 (dd, ^2J(H6a',H6b') = 12.3 Hz, ^3J(H6a',H5') = 4.5 Hz, 1H, H-6a'), 4.12 (dd, ^2J(H6b', H6a') = 12.3 Hz, ^3J(H6b',H5') = 2.6 Hz, 1H, H-6b'), 3.65 (ddd, ^3J(H5',H4') = 10.1 Hz, ^3J(H5',H6a') = 4.5 Hz, ^3J(H5',H6b') = 2.6 Hz, 1H, H-5), 2.31 (s, 3H, 2-CH_3), 2.13 (s, 3H, 2'-CH_3), 2.04 (s, 3H, 6'-CH_3), 2.02 (s, 3H, 4'-CH_3), 2.02 (s, 3H, 3'-CH_3).

^{13}C-NMR ($CDCl_3$, 100 MHz): δ 173.81 (C-4), 170.62 (6'-C=O), 170.26 (2'-C=O), 170.19 (3'-C=O), 169.68 (4'-C=O), 161.45 (C-2), 153.86 (C-6), 141.38 (C-3), 117.47 (C-5), 99.53 (C-1'), 72.65 (C-3'), 71.93 (C-5'), 71.46 (C-2'), 68.58 (C-4'), 61.68 (C-6'), 21.01 (2'-CH_3), 20.80 (6'-CH_3), 20.76 (3'-CH_3, 4'-CH_3), 15.38 (2-CH_3).

NSI-MS *m/z* (%): 935 (22, [2M+Na^+]), 930 (16, [2M+NH_4^+]), 479 (14, [M+Na^+]), 457 (100, [M+H^+]), 331 (9, [M-pyranone]$^+$).

HRMS-NSI *m/z*: Calc. for $C_{20}H_{25}O_{12}$ [M+H^+]: 457.1341; found: 457.1339.

3-(2,3,4,6-Tetra-*O*-acetyl-β-D-glucopyranosyloxy)-2-methyl-1-phenylpyridin-4(1*H*)-one

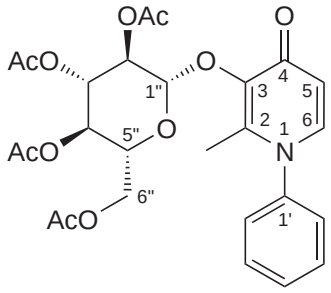

31a

2,3,4,6-Tetra-*O*-acetyl-α-D-glucopyranosyl bromide **30** (616 mg, 1.5 mmol), pyridinone **29a** (608 mg, 3 mmol, 2 eq.), and tetrabutylammonium hydrogensulfate (517 mg, 1.52 mmol) were taken up in DCM (5 ml) and 1M NaOH (5 ml). Stirring vigorously, the biphasic reaction mixture was heated to 35 °C over night, then diluted with ethyl acetate (50 ml) and washed with 1M NaOH (3×), water and brine before drying over Na_2SO_4. Evaporation gave the crude product as dark brown solid (605 mg), which was purified by column chromatography (ethyl acetate/methanol: 9/1) to yield glucoside **31a** as pale beige plates (317 mg, 0.60 mmol, 40%).

Melting point: m.p. 173−175 °C.

IR (neat) cm^{-1}: 1746, 1634, 1580, 1367, 1219, 1180, 1036.

^{1}H-NMR ($CDCl_3$, 400 MHz): δ 7.55–7.50 (m, 3H, H-3',4',5'), 7.35–7.26 (m, 1H, H-2'/6'), 7.28 (d, ^3J(H6,H5) = 7.6 Hz, 1H, H-6), 7.25–7.17 (m, 1H, H6'/2'), 6.43 (d, ^3J(H5,H6) = 7.6 Hz, 1H, H-5), 5.70 (d, ^3J(H1",H2") = 7.9 Hz, 1H, H-1"), 5.34 ('t', ^3J(H3",H2") = 9.7 Hz, ^3J(H3",H4") = 9.5 Hz, 1H, H-3"), 5.22 (dd, ^3J(H2",H3") = 9.7 Hz, ^3J(H2",H1") = 7.9 Hz, 1H, H-2"), 5.13 ('t', ^3J(H4",H5") = 9.9 Hz, ^3J(H4",H3") = 9.5 Hz, 1H, H-4"), 4.22 (dd, ^2J(H6a",H6b") = 12.3 Hz, ^3J(H6a",H5") = 4.5 Hz, 1H, H-6a"), 4.13 (dd, ^2J(H6b",H6a") = 12.3 Hz, ^3J(H6b",H5") = 2.5 Hz, 1H, H-6b"), 3.68 (ddd, ^3J(H5",H4") = 10.0 Hz, ^3J(H5", H6a") = 4.4 Hz, ^3J(H5",H6b") = 2.6 Hz, 1H, H-5"), 2.16 (s, 3H, CH_3), 2.05 (s, 3H, 2-CH_3), 2.03 (s, 3H, CH_3), 2.02 (s, 3H, CH_3), 2.01 (s, 3H, CH_3).

^{13}C-NMR ($CDCl_3$, 100 MHz): δ 172.75 (C-4), 171.05 (C=O), 170.48 (C=O), 170.40 (2 C=O), 143.01 (C-2), 142.63 (C-1'), 139.02 (C-3), 138.96 (C-6), 130.00 (C-3',5'), 129.61 (C-4'), 126.82 (C-2',6'), 117.32 (C-5), 98.83 (C-1"), 72.77 (C-3"), 71.69 (C-5"), 71.61 (C-2"), 68.54 (C-4"), 61.57 (C-6"), 20.95 (CH_3), 20.78 (CH_3), 20.58 (CH_3), 20.38 (CH_3), 14.79 (2-CH_3).

NSI-MS *m/z* (%): 532 (100, [M+H^+]), 202 (36, [$C_{12}H_{11}NO_2$+H^+]).

HRMS-NSI *m/z*: Calc. for $C_{26}H_{30}NO_{11}$ [M+H^+]: 532.1813; found: 532.1809.

3-(2,3,4,6-Tetra-*O*-acetyl-β-D-glucopyranosyloxy)-1-(4-bromophenyl)-2-methyl-pyridin-4(1*H*)-one

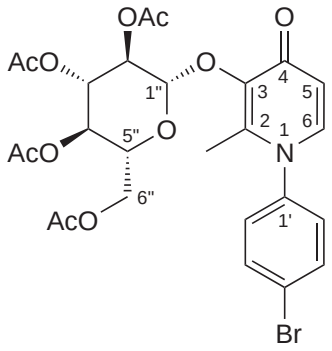

31b

Pyridinone **29b** (2.80 g, 10 mmol) was reacted with sugar **30** (1.84 g, 4.5 mmol) and tetrabutylammonium bromide (1.77 g, 5.5 mmol) in DCM (10 ml) and 1M NaOH (15 ml) as described for the synthesis of **31a**. Column chromatography (ethyl acetate/methanol: 9/1) gave the glycoside **31b** as off-white solid (1.20 g, 1.97 mmol, 44%).

^{1}H-NMR data is in agreement with published data.[186]

IR (neat) cm^{-1}: 1749, 1631, 1576, 1488, 1366, 1295, 1215, 1035.

^{1}H-NMR ($CDCl_3$, 400 MHz): δ 7.67 (d, ^3J(H2',6',H3',5') = 8.5 Hz, 2H, H-2',6'), 7.24 (d, ^3J(H6,H5) = 7.6 Hz, 1H, H-6), 7.11 (br, 2H, H-3',5'), 6.42 (d, ^3J(H5,H6) = 7.6 Hz, 1H, H-5), 5.69 (d, ^3J(H1",H2") = 7.9 Hz, 1H, H-1"), 5.33 ('t', ^3J(H3",H2") = 9.7 Hz, ^3J(H3", H4") = 9.3 Hz, 1H, H-3"), 5.21 (dd, ^3J(H2",H3") = 9.7 Hz, ^3J(H2",H1") = 7.9 Hz, 1H, H-2"), 5.13 ('t', ^3J(H4",H5") = 10.0 Hz, ^3J(H4",H3") = 9.4 Hz, 1H, H-4"), 4.21 (dd, ^2J(H6a", H6b") = 12.2 Hz, ^3J(H6a",H5") = 4.3 Hz, 1H, H-6a"), 4.14 (dd, ^2J(H6b",H6a") = 12.2 Hz, ^3J(H6b",H5") = 2.6 Hz, 1H, H-6b"), 3.67 (ddd, ^3J(H5",H4") = 10.1 Hz, ^3J(H5",H6a") = 4.1 Hz, ^3J(H5",H6b") = 2.7 Hz, 1H, H-5"), 2.15 (s, 3H, CH_3), 2.04 (s, 3H, 2-CH_3), 2.03 (s, 3H, CH_3), 2.02 (s, 3H, CH_3), 2.01 (s, 3H, CH_3).

^{13}C-NMR ($CDCl_3$, 100 MHz): δ 172.96 (C-4), 170.80 (C=O), 170.58 (C=O), 170.45 (C=O), 170.22 (C=O), 143.21 (C-3), 142.62 (C-2), 140.37 (C-1'), 138.95 (C-6), 133.48 (C-2',6'), 128.70 (C-3',5'), 117.63 (C-5), 116.72 (C-4'), 98.77 (C-1"), 72.81 (C-3"), 71.97 (C-5"), 71.69 (C-2"), 68.75 (C-4"), 61.60 (C-6"), 21.14 (CH_3), 21.13 (CH_3), 20.88 (CH_3), 20.80 (CH_3), 15.02 (2-CH_3).

NSI-MS *m/z* (%): 634/632 (14, [M+Na^+]), 612/610 (100, [M+H^+]), 282/280 (27, [$C_{12}H_{10}BrNO_2$+H^+]).

HRMS-NSI *m/z*: Calc. for $C_{26}H_{29}BrNO_{11}$ [M+H^+]: 612.0903/610.0918; found: 612.0897/610.0919.

3-(2,3,4,6-Tetra-*O*-acetyl-β-D-glucopyranosyloxy)-1-(4-iodophenyl)-2-methylpyridin-4(1*H*)-one

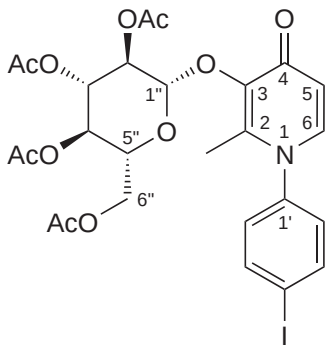

31d

Method A: From maltol glucoside – acidic reaction conditions Glucoside **32** (92 mg, 200 µmol) and 4-iodoaniline (88 mg, 400 µmol) were dissolved in methanol (1.5 ml) and 0.2M HCl (1 ml) and heated to reflux for 24 hours, then neutralised with $NaHCO_3$. The reaction mixture was diluted with water and extracetd with ethyl acetate. The organic phase was washed with brine, dried over Na_2SO_4 and evaporated. Only starting material and decomposed materials could be isolated after column chromatography (ethyl acetate/hexane: 2/1).

Method B: From maltol glucoside – sealed tube Glucoside **32** (92 mg, 200 µmol) and 4-iodoaniline (89 mg, 400 µmol) were dissolved in methanol (2 ml) and water (2 ml) and heated to 150 °C in a sealed tube for 24 hours. Work up as described for method A yielded only unreacted starting material.

Method C: Transhalogenation 4-Bromo glucoside **31b** (1.22 g, 2 mmol), copper(I) iodide (40 mg, 0.2 mmol, 10%mol) and sodium iodide (600 mg, 4 mmol, 2 eq.) were added to dry dioxane (3 ml) under nitrogen atmosphere. *N,N'*-dimethylethylenediamine (43 µl, 0.4 mmol, 20%mol) was added to the solution and the tube sealed tightly before heating to 110 °C for 18 hours. The reaction mixture was diluted with water (20 ml) and dilute ammonia (10 ml) and extracted with DCM. The organic phase was dried over Na_2SO_4, then evaporated to give a dark brown residue (2 g). Column chromatography (ethyl acetate/methanol: 9/1) gave multiple fractions, which did not contain the desired product.

Method D: *Via* Stannane 4-Bromo glucoside **31b** (550 mg, 0.9 mmol) and tetrakis(triphenylphosphine)palladium(0) (110 mg, 95 µmol, 10.5%mol) were added to a flask under nitrogen atmosphere. Dry toluene (15 ml) and bis(tributyltin) (2.27 ml, 4.5 mmol, 5 eq.) were added to the flask and the reaction mixture heated to reflux under nitrogen for 20 hours. The reaction mixture was filtered through celite, washed thoroughly with DCM and evaporated *in vacuo*. The residue was dissolved in acetonitrile (15 ml) and washed with hexane (3× 30 ml). The acetonitrile layer was evaporated and and purified by column chromatography (ethyl acetate/methanol: 20/1) to give 3-(2,3,4,6-tetra-*O*-acetyl-β-D-glucopyranosyloxy)-2-methyl-1-(4-(tributylstannyl)phenyl)pyridin-4(1*H*)-one (**31c**) as a pale yellow glass (94 mg, 115 µmol, 13%).
Stannane **31c** (16 mg, 20 µmol), sodium iodide (15 mg, 100 µmol, 5 eq.) and dilute phosphoric acid (0.05N, 100 µl) were dissolved in ethanol (3 ml). A fresh aqueous solution of chloramine T (50 mg, 180 µmol, 9 eq. in 2 ml) was added and the reaction mixture stirred at room temperature for 1 hour. The reaction was monitored by TLC (ethyl acetate/methanol: 20/1), which showed consumption of the starting materials, but after work-up, no product could be isolated.

3-(2,3,4,6-tetra-*O*-acetyl-β-D-glucopyranosyloxy)-2-methyl-1-(4-(tributylstannyl) phenyl)pyridin-4(1*H*)-one (31c)

^{1}H-NMR data is in agreement with published data, the corrected assignment for the stannylbutyl substituents is reported below.

Melting point: m.p. 46−48 °C.

IR (neat) cm^{-1}: 2956 (w), 2926 (w), 1748, 1633, 1578, 1367, 1287, 1215, 1036.

^{1}H-NMR ($CDCl_3$, 400 MHz): δ 7.57 (d, ^3J(H3',5',H2',6') = 7.9 Hz, 2H, H-3',5'), 7.28 (d, ^3J(H6,H5) = 7.6 Hz, 1H, H-6), 7.23–7.07 (br d, 2H, H-2',6'), 6.41 (d, ^3J(H5,H6) = 7.6 Hz, 1H, H-5), 5.66 (d, ^3J(H1",H2") = 8.0 Hz, 1H, H-1"), 5.32 ('t', ^3J(H3",H2") = 9.7 Hz, ^3J(H3", H4") = 9.3 Hz, 1H, H-3"), 5.20 (dd, ^3J(H2",H3") = 9.7 Hz, ^3J(H2",H1") = 8.0 Hz, 1H, H-2"), 5.10 ('t', ^3J(H4",H5") = 10.1 Hz, ^3J(H4",H3") = 9.3 Hz, 1H, H-4"), 4.20 (dd, ^2J(H6a", H6b") = 12.1 Hz, ^3J(H6a",H5") = 4.4 Hz, 1H, H-6a"), 4.10 (dd, ^2J(H6b",H6a") = 12.1 Hz, ^3J(H6b",H5") = 2.4 Hz, 1H, H-6a"), 3.67 (ddd, ^3J(H5",H4") = 10.1 Hz, ^3J(H5",H6a") = 4.3 Hz, ^3J(H5",H6b") = 2.5 Hz, 1H, H-5"), 2.14 (s, 3H, CH_3), 2.04 (s, 3H, 2-CH_3), 2.01 (s, 3H, CH_3), 2.00 (s, 3H, CH_3), 1.99 (s, 3H, CH_3), 1.63–1.43 (m, 6H, $SnCH_2\mathit{CH_2}C_2H_5$), 1.32 ('sex', ^3J = 7.3 Hz, 6H, $SnC_2H_4\mathit{CH_2}CH_3$), 1.09 ('t', ^3J = 8.1 Hz, 6H, $Sn\mathit{CH_2}C_3H_7$), 0.88 (t, $^3J(CH_3,CH_2)$ = 7.3 Hz, 9H, $SnC_3H_6\mathit{CH_3}$).

^{13}C-NMR ($CDCl_3$, 100 MHz): δ 172.56 (C-4), 170.57 (C=O), 170.47 (C=O), 170.13 (C=O), 169.72 (C=O), 145.14 (C-4'), 142.91 (C-3), 142.67 (C-2), 141.46 (C-1'), 139.18 (C-6), 137.84 (C-3',5'), 125.93 (C-2',6'), 117.23 (C-5), 98.95 (C-1"), 72.82 (C-3"), 71.74 (C-5"), 71.67 (C-2"), 68.76 (C-4"), 61.70 (C-6"), 29.10 ($SnCH_2\mathit{CH_2}C_2H_5$), 27.41 ($SnC_2H_4\mathit{CH_2}CH_3$), 21.08 ($CH_3$), 20.80 ($CH_3$), 20.74 (2 CH_3), 15.00 (2-CH_3), 13.76 ($SnC_3H_6\mathit{CH_3}$), 9.85 ($Sn\mathit{CH_2}C_3H_7$).

NSI-MS *m/z* (%): 822 (100, [M+H$^+$]), 820 (78, [M+H$^+$]), 818 (40, [M+H$^+$]), 279 (20, [P(O)Ph_3+H+]).

HRMS-NSI *m/z*: Calc. for $C_{39}H_{56}NO_{11}Sn$ [M+H$^+$]: 822.2878; found: 822.2868.

3-(β-D-Glucopyranosyloxy)-2-methyl-1-phenylpyridin-4(1*H*)-one

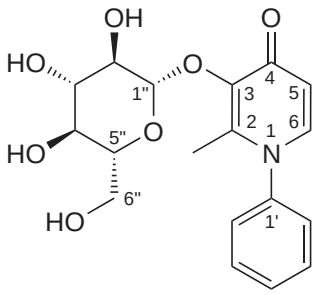

26a

Glucoside **31a** (714 mg, 1.34 mmol) was dissolved in dry methanol (7.5 ml), then 1M sodium methoxide (1.0 ml, 1 mmol) was added and the reaction mixture was stirred at room temperature for 1 hour. The solution was neutralised with 2M HCl and evaporated to dryness. The residue was purified by column chromatography (chloroform/methanol: 20/1→6/1) to yield 3-(β-D-glucopyranosyloxy)-2-methyl-1-phenylpyridin-4(1*H*)-one (**26a**) as a pale tan solid (360 mg, 0.99 mmol, 74%).

NMR data is in good agreement with published data.[188] Melting point data does not match the published data.[275]

Melting point: Decomposition at 198 °C (lit. m.p. 230−231 °C).[275]

IR (neat) cm^{-1}: 3318 (w), 3187 (br), 1622, 1545, 1492, 1274, 1083, 1059, 1028.

^{1}H-NMR (CD_3OD, 400 MHz): δ 7.75 (d, ^3J(H6,H5) = 7.4 Hz, 1H, H-6), 7.63–7.57 (m, 3H, H-3',4',5'), 7.47–7.41 (m, 2H, H-2',6'), 6.57 (d, ^3J(H5,H6) = 7.4 Hz, 1H, H-5), 4.73 (d, ^3J(H1",H2") = 7.4 Hz, 1H, H-1"), 3.84 (dd, ^2J(H6a",H6b") = 11.9 Hz, ^3J(H6a",H5") = 2.1 Hz, 1H, H-6a"), 3.66 (dd, ^2J(H6b",H6a") = 11.9 Hz, ^3J(H6b",H5") = 5.5 Hz, 1H, H6b"), 3.47–3.40 (m, 2H, H-2",3"), 3.34 ('t', ^3J = 9.1 Hz, 1H, H-4"), 3.27 (ddd, ^3J(H5",H4") = 9.4 Hz, ^3J(H5",H6b") = 5.4 Hz, ^3J(H5",H6a") = 2.1 Hz, 1H, H-5"), 2.25 (s, 3H, 2-CH_3).

^{13}C-NMR (CD_3OD, 100 MHz): δ 174.86 (C-4), 146.76 (C-2), 145.91 (C-3), 143.05 (C-1'), 142.30 (C-6), 131.23 (C-3',5'), 131.16 (C-4'), 127.99 (C-2',6'), 116.89 (C-5), 107.06 (C-1"), 78.72 (C-5"), 78.48 (C-3"), 75.58 (C-2"), 71.11 (C-4"), 62.63 (C-6"), 15.74 (2-CH_3).

NSI-MS *m/z* (%): 761 (32, [2M+Cl^-]), 400 (34, [M+Cl^-]), 398 (100, [M+Cl^-]).

HRMS-NSI *m/z*: Calc. for $C_{18}H_{21}NO_7Cl$ [M+Cl^-]: 398.1012/400.0983; found: 398.1007/400.0973.

1-(4-Bromophenyl)-3-(β-D-glucopyranosyloxy)-2-methylpyridin-4(1*H*)-one

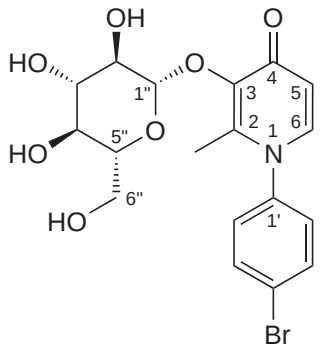

26b

Glucoside **31b** (220 mg, 360 µmol) was dissolved in dry methanol (5 ml), then 1M sodium methoxide (150 µl, 150 µmol) was added and the solution was allowed to stir for 8 hours, then further sodium methoxide (300 µl) was added. The reaction mixture was stirred for further 20 hours (28 hours total) before neutralisation with 2M HCl and evaporation to dryness. The residue was purified by column chromatography (chloroform/methanol: 6/1) to give 1-(4-bromophenyl)-3-(β-D-glucopyranosyloxy)-2-methylpyridin-4(1*H*)-one (**26b**) as a pale brown solid (108 mg, 242 µmol, 67%).

Melting point: Decomposition at 174 °C.

IR (neat) cm^{-1}: 3265 (br), 1623, 1552, 1485, 1282,1195, 1066, 1011.

^{1}H-NMR (CD_3OD, 400 MHz): δ 7.76 (d, ^3J(H2',6',H3',5') = 8.2 Hz, 2H, H-2',6'), 7.75 (d, ^3J(H6,H5) = 7.4 Hz, 1H, H-6), 7.40 (d, ^3J(H3',5',H2',6') = 8.2 Hz,2H, H-3',5'), 6.56 (d, ^3J(H5,H6) = 7.4 Hz, 1H, H-5), 4.73 (d, ^3J(H1",H2") = 7.4 Hz, 1H, H-1"), 3.84 (dd, ^2J(H6a",H6b") = 11.9 Hz, ^3J(H6a",H5") = 1.8 Hz, 1H, H-6a"), 3.66 (dd, ^2J(H6b",H6a") = 11.9 Hz, ^3J(H6b",H5") = 5.5 Hz, 1H, H6b"), 3.47–3.38 (m, 2H, H-2",3"), 3.34 ('t', ^3J = 8.9 Hz, 1H, H-4"), 3.27 (ddd, ^3J(H5",H4") = 9.4 Hz, ^3J(H5",H6b") = 5.5 Hz, ^3J(H5",H6a") = 2.0 Hz, 1H, H-5"), 2.25 (s, 3H, 2-CH_3).

^{13}C-NMR (CD_3OD, 100 MHz): δ 174.94 (C-4), 146.51 (C-3), 145.84 (C-2), 143.05 (C-1'), 142.30 (C-6), 134.32 (C-2',6'), 130.01 (C-3',5'), 124.95 (C-4'), 117.01 (C-5), 106.86 (C-1"), 78.65 (C-5"), 78.35 (C-3"), 75.44 (C-2"), 71.03 (C-4"), 62.51 (C-6"), 15.71 (2-CH_3).

NSI-MS *m/z* (%): 502/500 (14), 488/486/484 (23/29/30), 478/476 (100/73, [M+Cl^-]), 442/440 (18, [M-H^+]).

HRMS-NSI *m/z*: Calc. for $C_{18}H_{19}BrNO_7$ [M−H^+]$^-$: 440.0350/442.0330; found: 440.0354/442.0332.

7.1.4 Synthesis of Amide-linked Conjugates

ω-(3-(Benzyloxy)-2-methyl-4-oxopyridin-1-(4*H*)-yl)carboxylic acids

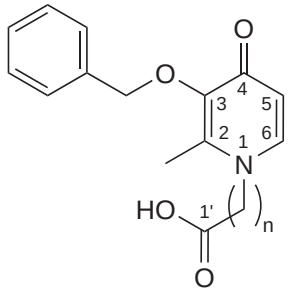

39a n = 1
39b n = 2
39c n = 3

cpd **33**		amino acid	g	mmol	product	g	Yield
g	mmol						
5.4	25.0	glycine	4.7	62.6	**39a**	6.43	94%
10.0	46.2	β-alanine	5.0	56.1	**39b**	9.36	71%
15.0	69.4	GABA	8.3	80.5	**39c**	20.55	98%

Benzyl maltol **33** (5.4 g, 25 mmol) and glycine (4.7 g, 62.6 mmol, 2.5 eq.) were dissolved in methanol (50 ml) and 1M NaOH (60 ml). The resulting solution was heated to reflux for 22 hours, then concentrated *in vacuo* and diluted with water. The solution was extracted with ethyl acetate, the organic phase discarded and the aqueous phase acidified with HCl to pH 4, then cooled to 4 °C over night. The formed precipitate was collected by vacuum filtration to give 2-(3-(benzyloxy)-2-methyl-4-oxopyridin-1-(4*H*)-yl)propanoic acid (**39a**) as a pale tan powder (6.43 g, 23.5 mmol, 94%).
An analogous procedure using β-alanine and γ-aminobutyric acid (GABA) gave 3-(3-(benzyloxy)-2-methyl-4-oxopyridin-1-(4*H*)-yl)propanoic acid (**39b**) and 4-(3-(benzyloxy)-2-methyl-4-oxopyridin-1-(4*H*)-yl)butanoic acid (**39c**) respectively.

2-(3-(Benzyloxy)-2-methyl-4-oxopyridin-1-(4*H*)-yl)acetic acid (39a)

Melting point: m.p. 191−194 °C.

IR (neat) cm^{-1}: 3050 (br), 2348 (br), 1893 (br), 1616, 1497, 1375, 1360, 1299, 1271, 1250, 968.

^{1}H-NMR (CD_3OD, 400 MHz): δ 7.77 (d, ^3J(H6,H5) = 7.4 Hz, 1H, H-6), 7.42–7.39 (m, 2H, Ph H-3,5), 7.37–7.31 (m, 3H, Ph H-2,4,6), 6.62 (d, ^3J(H5,H6) = 7.4 Hz, 1H, H-5), 5.09 (s, 2H, O−*CH*$_2$−Ph), 4.84 (s, 2H, H-2'), 2.16 (s, 3H, CH_3).

^{13}C-NMR (CD_3OD, 100 MHz): δ 173.36 (C-4), 170.44 (C-1'), 147.08 (C-2), 146.42 (C-3), 142.70 (C-6), 138.19 (Ph C-1), 130.17 (Ph C-3,5), 129.51 (Ph C-2,6), 129.42 (Ph C-4), 116.37 (C-5), 75.05 (O−*CH₂*−Ph), 56.66 (C-2'), 13.02 (CH_3).

NSI-MS *m/z* (%): 545 (49, [2M-H$^+$]), 272 (100, [M-H$^+$]).

HRMS-NSI *m/z*: Calc. for $C_{15}H_{14}NO_4$ [M−H$^+$]$^-$: 272.0928; found: 272.0928.

3-(3-(Benzyloxy)-2-methyl-4-oxopyridin-1-(4*H*)-yl)propanoic acid (39b)

NMR data is in good agreement with published data.[273]

Melting point: m.p. 160−161 °C (lit. m.p. 170−171 °C).[199]).

IR (neat) cm^{-1}: 2454 (w), 1913 (w), 1699, 1621, 1534, 1496, 1259, 1224, 1056, 1006.

^{1}H-NMR (CD_3OD, 400 MHz): δ 7.77 (d, ^3J(H5,H6) = 7.5 Hz, 1H, H-6), 7.40–7.32 (m, 5H, Ph H-2–6), 6.47 (d, ^3J(H5,H6) = 7.5 Hz, 1H, H-5), 5.07 (s, 2H, O−*CH₂*−Ph), 4.25 (t, ^3J(H3',H2') = 6.9 Hz, 2H, H-3'), 2.70 (t, ^3J(H2',H3') = 6.9 Hz, 2H, H-2'), 2.20 (s, 3H, 2-CH_3).

^{13}C-NMR (CD_3OD, 100 MHz): δ 174.68 (C-4), 173.49 (C-1'), 147.00 (C-2), 145.32 (C-3), 141.60 (C-6), 138.38 (Ph C-1), 130.27 (Ph C-3,5), 129.43 (Ph C-2,6), 129.37 (Ph C-4), 117.15 (C-5), 74.58 (O−*CH₂*−Ph), 50.87 (C-3'), 35.40 (C-2'), 12.77 (2-CH_3).

4-(3-(Benzyloxy)-2-methyl-4-oxopyridin-1-(4*H*)-yl)butanoic acid (39c)

NMR data is in good agreement with published data.[276]

Melting point: m.p. 154−156 °C (lit. m.p. 169−170 °C).[199]

IR (neat) cm^{-1}: 3395 (br), 2498 (br), 1892 (br), 1688 (w), 1615, 1531, 1497, 1453, 1324, 1219, 1155, 1038 (w).

^{1}H-NMR (CD_3OD, 400 MHz): δ 7.69 (d, ^3J(H6,H5) = 7.4 Hz, 1H, H-6), 7.40–7.31 (m, 5H, Ph H-2–6), 6.48 (d, ^3J(H5,H6) = 7.4 Hz, 1H, H-5), 5.08 (s, 2H, O−*CH₂*−Ph), 4.00 (tt, ^3J(H4',H3') = 7.6 Hz, ^4J(H4',H2') = 1.7 Hz, 2H, H-4'), 2.33 (t, ^3J(H2',H3') = 6.9 Hz, 2H, H-2'), 2.19 (s, 3H, 2-CH_3), 1.91 (tt, ^3J(H4',H3') = 7.6 Hz, ^3J(H4',H3') = 6.9 Hz, 2H, H-3').

^{13}C-NMR (CD_3OD, 100 MHz): δ 176.20 (C-4), 174.79 (C-1'), 146.98 (C-2), 145.30 (C-3), 141.19 (C-6), 138.38 (Ph C-1), 130.36 (Ph C-3,5), 129.41 (Ph C-2,6), 129.39 (Ph C-4), 117.39 (C-5), 74.48 (O−*CH₂*−Ph), 54.46 (C-4'), 31.23 (C-2'), 26.83 (C-3'), 12.75 (2-CH_3).

3-(Benzyloxy)-1,2-dimethylpyridin-4(1*H*)-one

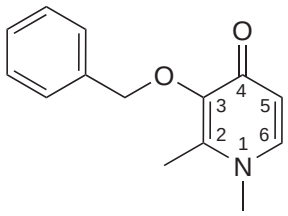

49

Benzyl maltol **33** (540 mg, 2.5 mmol) and aqueous methylamine (40% w/v, 344 µl, 4.0 mmol) were dissolved in methanol (4 ml) and 1M NaOH (0.5 ml). The solution was heated to reflux for 2 hours, then evaporated to near dryness and resuspended in methanol. 1M HCl was added dropwise until no more precipitate formed. The suspension was heated to reflux, Et_2O was added until the solution turned slightly cloudy. The precipitate, which had formed after refrigeration, was collected by vacuum filtration and washed with Et_2O to give 3-(benzyloxy)-1,2-dimethylpyridin-4(1*H*)-one (**49**) as off-white flakes (542 mg, 2.0 mmol, 82%).

^{1}H-NMR (CD_3OD, 400 MHz): δ 8.25 (d, ^3J(H6,H5) = 7.1 Hz, 1H, H-6), 7.46–7.43 (m, 2H, Ph H-3,5), 7.40–7.36 (m, 3H, Ph H-2,4,6), 7.17 (d, ^3J(H5,H6) = 7.1 Hz, 1H, H-5), 5.17 (s, 2H, O−*CH₂*−Ph), 4.00 (s, 3H, 1-CH_3), 2.48 (s, 3H, 2-CH_3).

^{13}C-NMR (CD_3OD, 100 MHz): δ 165.66 (C-4), 151.75 (C-2), 144.62 (C-3), 143.62 (C-6), 137.18 (Ph C-1), 130.03 (Ph C-3,5), 129.88 (Ph C-4), 129.67 (Ph C-2,6), 113.59 (C-5), 76.18 (O−*CH₂*−Ph), 45.00 (2-CH_3), 13.96 (1-CH_3).

NSI-MS *m/z* (%): 459 (32, [2M+H^+]), 230 (100, [M+H^+]).

HRMS-NSI *m/z*: Calc. for $C_{14}H_{16}NO_2$ [M+H^+]: 230.1176; found: 230.1174.

3-(Benzyloxy)-2-formyl-4*H*-pyran-4-one

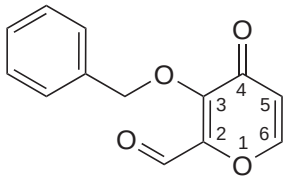

51

Benzyl maltol **33** (1085 mg, 5 mmol) and selenium dioxide (117 mg, 10 mmol, 2 eq.) were suspended in bromobenzene (20 ml) and heated to reflux for 20 hours. The reaction mixture was filtered through a pad of celite and washed with water and DCM. The filtrate was extracted with DCM, the organic phase dried over Na_2SO_4 and evaporate to give the crude product as brown oil. Purification by column chromatography (hexane/ethyl acetate: 2/1) yielded unreacted starting material **33** (224 mg, 1 mmol) and 3-(benzyloxy)-2-formyl-4*H*-pyran-4-one (**51**) as a pale orange oil (400 mg, 1.7 mmol, 35%).

All analytical data is in good agreement with published data.[277]

^{1}H-NMR ($CDCl_3$, 400 MHz): δ 9.82 (s, 1H, 2-CHO), 7.69 (d, ^3J(H6,H5) = 5.7 Hz, 1H, H-6), 7.36–7.26 (m, 5H, Ph H-2–6), 6.45 (d, ^3J(H6,H5) = 5.7 Hz, 1H, H-5), 5.46 (s, 2H, O−*CH*$_2$−Ph).

^{13}C-NMR ($CDCl_3$, 100 MHz): δ 182.63 (2-CHO), 176.96 (C-4), 154.26 (C-6), 151.84 (C-3), 149.31 (C-2), 135.02 (Ph C-1), 129.22 (Ph C-3,5), 129.18 (Ph C-4), 128.90 (Ph C-2,6), 118.37 (C-5), 74.98 (O−*CH*$_2$−Ph).

NSI-MS *m/z* (%): 547 (47, [2M+2MeOH+Na^+]), 525 (12, [2M+2MeOH+H^+]), 285 (23, [M+MeOH+Na^+]), 263 (100, [M+MeOH+H^+]), 231 (8, [M+H^+]).

HRMS-NSI *m/z*: Calc. for $C_{13}H_{11}O_4$ [M+H^+]: 231.0652, found: 231.0654; calc. for $C_{14}H_{15}O_5$ [M+MeOH+H^+]: 263.0914, found: 263.0917.

3-(Benzyloxy)-2-(dimethoxymethyl)-4*H*-pyran-4-one

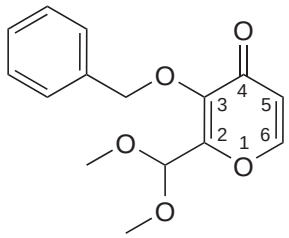

53

Aldehyde **51** (345 mg, 1.5 mmol) and tosylic acid (5 mg, catalytic) were dissolved in dry methanol (7.5 ml), trimethyl orthoformate (250 µl, 2.3 mmol) was added and the reaction mixture heated to reflux for 3 hours under anhydrous conditions. The reaction mixture was evaporated to dryness, diluted with water and extracted with ethyl acetate. The organic phase was washed with brine, dried over Na_2SO_4 and evaporated to give 3-(benzyloxy)-2-(dimethoxymethyl)-4*H*-pyran-4-one (**53**) as a brown oil (367 mg, 1.33 mmol, 89%).

^{1}H-NMR ($CDCl_3$, 400 MHz): δ 7.72 (d, ^3J(H6,H5) = 5.6 Hz, 1H, H-6), 7.41–7.33 (m, 5H, Ph H-2–6), 6.43 (d, ^3J(H5,H6) = 5.6 Hz, 1H, H-5), 5.24 (s, 1H, 2-$CH(OCH_3)_2$), 5.22 (s, 2H, O−*CH_2*−Ph), 3.29 (s, 6H, O−CH_3).

^{13}C-NMR ($CDCl_3$, 100 MHz): δ 175.64 (C-4), 154.96 (C-2), 154.15 (C-6), 144.41 (C-3), 136.39 (Ph C-1), 129.32 (Ph C-3,5), 128.71 (Ph C-2,4,6), 117.56 (C-5), 97.28 (2-$CH(OCH_3)_2$), 74.26 (O−*CH_2*−Ph), 55.23 (O−CH_3).

3-(Benzyloxy)-2-(dimethoxymethyl)-1-methylpyridin-4(1*H*)-one

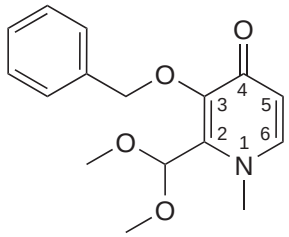

54

Pyranone **53** (135 mg, 490 µmol) and aqueous methylamine (40% w/v, 70 µl, 810 µmol) were dissolved in methanol (2 ml). 1M NaOH (200 µl) was added and the reaction mixture heated to reflux for 4 hours. The reaction mixture was diluted with water and extraced with ethyl acetate and the organic phase was washed with brine. Evaporation and drying *in vacuo* gave 3-(benzyloxy)-2-(dimethoxymethyl)-1-methylpyridin-4(1*H*)-one (**54**) as a brown oil (106 mg, 366 µmol, 75%).
The product was subjected to a range of deprotection conditions, but none of these could successfully reconstitute the aldehyde.

IR (neat) cm^{-1}: 2932 (w, br), 1623, 1566, 1454 (w), 1250, 1207, 1100, 1065, 952.

^{1}H-NMR ($CDCl_3$, 400 MHz): δ 7.33–7.31 (m, 2H, Ph H-3,5), 7.29–7.22 (m, 3H, Ph H-2,4,6), 7.09 (d, ^3J(H6,H5) = 7.5 Hz, 1H, H-6), 6.33 (d, ^3J(H5,H6) = 7.5 Hz, 1H, H-5), 5.44 (s, 1H, 2-$CH(OCH_3)_2$), 5.18 (s, 2H, O−*CH_2*−Ph), 3.65 (s, 3H, 1-CH_3), 3.14 (s, 6H, O−CH_3).

^{13}C-NMR ($CDCl_3$, 100 MHz): δ 173.65 (C-4), 146.96 (C-3), 141.12 (C-6), 138.03 (C-2), 137.12 (Ph C-1), 129.07 (Ph C-3,5), 128.41 (Ph C-2,6), 128.13 (Ph C-4), 117.26 (C-5), 100.10 (2-$CH(OCH_3)_2$), 73.64 (O−*CH_2*−Ph), 55.99 (O−CH_3), 42.18 (1-CH_3).

NSI-MS *m/z* (%): 601 (22, [2M+Na^+]), 290 (100, [M+H^+]), 230 (23).

HRMS-NSI *m/z*: Calc. for $C_{16}H_{20}NO_4$ [M+H^+]: 290.1387; found: 290.1389.

3-(Benzyloxy)-2-carboxy-4*H*-pyran-4-one

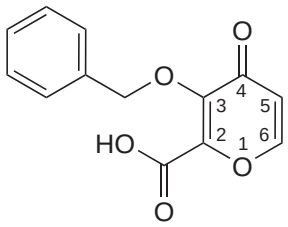

50

Aldehyde **51** (230 mg, 1 mmol), sulfamic acid (107 mg, 1.1 mmol) and sodium chlorite (80% w/w, 124 mg, 1.1 mmol) were suspended in acetone/water (5 ml). The reaction mixture was stirred over night at room temperature, then filtered and the residue was washed with water and a small quantity of acetone to give carboxylic acid **50** as a white powder. More product could be isolated by concentrating the filtrate (117 mg, 475 µmol, 48%).

NMR data is in good agreement with published data.[278]

Melting point: m.p. 138−140 °C (lit. m.p. 150−152 °C).[278]

IR (neat) cm^{-1}: 2414 (br), 1896 (br), 1712, 1620, 1583, 1286, 1199, 1050, 973.

^{1}H-NMR (DMSO−d_6, 400 MHz): δ 8.21 (d, ^3J(H6,H5) = 5.6 Hz, 1H, H-6), 7.48–7.31 (m, 5H, Ph H-2–6), 6.55 (d, ^3J(H6,H5) = 5.6 Hz, 1H, H-5), 5.11 (s, 2H, O−CH_2−Ph).

NSI-MS *m/z* (%): 419 (29, [2M-H$^+$]), 245 (100, [M-H$^+$]).

HRMS-NSI *m/z*: Calc. for $C_{13}H_9NO_5$ [M-H$^+$]$^-$: 245.0455; found: 245.0455.

3-(Benzyloxy)-2-carboxypyridin-4(1*H*)-one

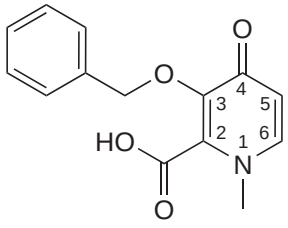

48

Pyranone **50** (82 mg, 333 µmol) was added to a solution of aqueous methylamine (40% w/v, 200 µl, 2.3 mmol) in water (3 ml). The reaction mixture was heated to 110 °C in a

sealed tube for 20 hours, then diluted with water (10 ml) and acidified to pH 2 with HCl and stirred for 10 min. The formed precipitate was collected by vacuum filtration and washed with water and acetone to give 3-(benzyloxy)-2-carboxy-4*H*-pyran-4-one (**48**) as off-white powder (60.5 mg, 233 µmol. 70%).

Melting point: m.p. 120−122 °C.

IR (neat) cm^{-1}: 3065 (br, w), 1678, 1633, 1544 (w), 1454, 1435, 1360, 1260, 1182 (w), 972.

^{1}H-NMR (CD_3OD, 400 MHz): δ 8.01 (d, ^3J(H6,H5) = 7.1 Hz, 1H, H-6), 7.52–7.49 (m, 2H, Ph H-2,6), 7.37–7.28 (m, 3H, Ph H-3,4,5), 6.96 (d, ^3J(H5,H6) = 7.1 Hz, 1H, H-5), 5.14 (s, 2H, O−*CH*$_2$−Ph), 3.97 (s, 3H, 1-CH_3).

^{13}C-NMR (CD_3OD, 100 MHz): δ 173.85 (C-4), 169.53 (2-CO_2H), 149.92 (C-3), 142.23 (C-6), 137.84 (Ph C-1), 136.42 (C-2), 129.80 (Ph C-2,6), 129.34 (Ph C-3–5), 115.37 (C-5), 76.53 (O−*CH*$_2$−Ph), 44.01 (1-CH_3).

NSI-MS *m/z* (%): 519 (33, [2M+H^+]), 260 (100, [M+H^+]).

HRMS-NSI *m/z*: Calc. for $C_{14}H_{14}NO_4$ [M+H^+]: 260.0917; found: 260.0917.

***N*-(4-Methoxybenzylidene)-D-glucosamine**

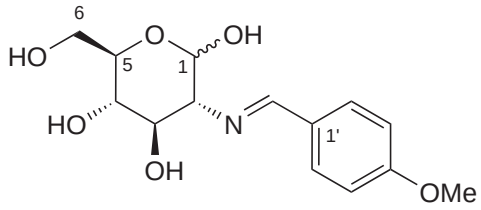

56

Anisaldehyde (8.5 ml, 70 mmol, 1.2 eq.) was added to a solution of glucosamine hydrochloride (12.5 g, 58 mmol) in 1M NaOH (60 ml). The mixture was stirred vigorously for 10 min and a large amount of precipitate formed after a few minutes. The reaction mixture was cooled to 4 °C over night, and the solid collected by vacuum filtration, washed with cold water, then Et_2O/ethanol (2/1 v/v) to give *N*-(4-methoxybenzylidene)-D-glucosamine (**56**) as a white powder. Concentrating the mother liquor yielded additional product. (14.2 g, 48 mmol, 84%).

All analytical data is in good agreement with published data.[279]

^{1}H-NMR (DMSO−d_6, 400 MHz): δ 8.11 (s, 1H, N=CH), 7.68 (d, ^3J(H2',6',H3',5') = 8.8 Hz, 2H, H-2',6'), 6.98 (d, ^3J(H3',5',H2',6') = 8.8 Hz, 2H, H-3',5'), 6.53 (d, ^3J(OH,H1)

= 6.8 Hz, 1H, 1-OH), 4.94 (d, ^3J(OH,H4) = 5.3 Hz, 1H, 4-OH), 4.82 (d, ^3J(OH,H3) = 5.6 Hz, 1H, 3-OH), 4.69 ('t', ^3J(H1,H2) = 7.9 Hz, ^3J(H1,OH) = 6.8 Hz, 1H, H-1), 4.56 (t, ^3J(OH,H6) = 5.7 Hz, 1H, 6-OH), 3.80 (s, 3H, 4'-OCH_3), 3.72 (ddd, ^2J(H6a,H6b) = 11.5 Hz, ^3J(H6a,OH) = 5.7 Hz, ^3J(H6a,H5) = 1.9 Hz, 1H, H-6a), 3.50 (dd, ^2J(H6b,H6a) = 11.5 Hz, ^3J(H6b,OH) = 5.7 Hz, 1H, H-6b), 3.46–3.40 (m, ^3J(H3,H2) = 9.0 Hz, ^3J(H3,OH) = 5.6 Hz, 1H, H-3), 3.26–3.21 (m, 1H, H-5), 3.17–3.12 (m, ^3J(H4,OH) = 5.3 Hz, 1H, H-4), 2.78 (dd, ^3J(H2,H3) = 9.0 Hz, ^3J(H2,H1) = 7.9 Hz, 1H, H-2).

^{13}C-NMR (DMSO−d_6, 100 MHz): δ 161.23 (N=CH), 161.06 (C-4'), 129.64 (C-2',6'), 129.12 (C-1'), 113.91 (C-3',5'), 95.64 (C-1), 78.20 (C-2), 76.88 (C-5), 74.60 (C-3), 70.36 (C-4), 61.27 (C-6), 55.29 (4'-OCH_3).

NSI-MS *m/z* (%): 671 (7, [2M+Na^+]), 320 (9, [M+Na^+]), 298 (100, [M+H^+]).

HRMS-NSI *m/z*: Calc. for $C_{14}H_{20}NO_6$ [M+H^+]: 298.1285; found: 298.1288.

***N*-(4-Methoxybenzylidene)-β-D-glucosamine 1,3,4,6-tetra-*O*-acetate**

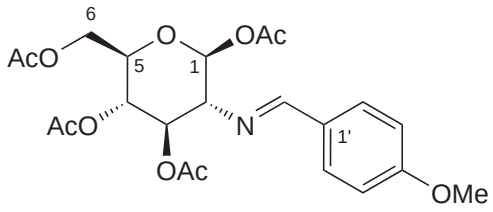

57

Benzylidene **56** (10.0 , 33.6 mmol) was added to an ice-cooled mixture of pyridine (55 ml) and acetic anhydride (30 ml). The reaction mixture was allowed to warm to room temperature and stirred over night, then poured onto ice-water (250 ml) and stirred for 30 min. The formed precipitate was collected by vacuum filtration and washed liberally with cold water and dried over P_2O_5, giving *N*-(4-methoxybenzylidene)-β-D-glucosamine 1,3,4,6-tetra-*O*-acetate (**57**) as a white to cream coloured powder (12.5 g, 27.3 mmol, 81%).

All analytical data is in good agreement with published data.[279]

^{1}H-NMR ($CDCl_3$, 400 MHz): δ 8.15 (s, 1H, N=CH), 7.67 (d, ^3J(H2',6',H3',5') = 8.6 Hz, 2H, H-2',6'), 6.92 (d, ^3J(H3',5',H2',6') = 8.8 Hz, 2H, H-3',5'), 5.95 (d, ^3J(H1,H2) = 8.3 Hz, 1H, H-1), 5.43 (t, ^3J(H3,H2) = 9.7 Hz, ^3J(H3,H4) = 9.5 Hz, 1H, H-3), 5.14 ('t', ^3J(H4,H5) = 10.1 Hz, ^3J(H4,H3) = 9.5 Hz, 1H, H-4), 4.38 (dd, ^2J(H6a,H6b) = 12.4 Hz, ^3J(H6a,H5) = 4.5 Hz, 1H, H-6a), 4.13 (dd, ^2J(H6b,H6a) = 12.4 Hz, ^3J(H6b,H5) = 2.0 Hz, 1H, H-6b), 3.97 (ddd, ^3J(H5,H4) = 10.1 Hz ^3J(H5,H6a) = 4.5 Hz, ^3J(H5,H6b) = 2.0 Hz, 1H, H-5),

3.84 (s, 3H, 4'-OCH_3), 3.46 (dd, ^3J(H2,H3) = 9.7 Hz, ^3J(H2,H1) = 8.3 Hz, 1H, H-2), 2.10 (s, 3H, $COCH_3$), 2.03 (s, 3H, $COCH_3$), 2.02 (s, 3H, $COCH_3$), 1.88 (s, 3H, $COCH_3$).

^{13}C-NMR ($CDCl_3$, 100 MHz): δ 170.85 (C=O), 170.05 (C=O), 169.70 (C=O), 168.89 (C=O), 164.51 (N=CH), 162.46 (C-4'), 130.43 (C-2',6'), 128.25 (C-1'), 114.26 (C-3',5'), 93.26 (C-1), 73.38 (C-3), 73.13 (C-2), 72.91 (C-5), 68.17 (C-4), 61.96 (C-6), 55.58 (OCH_3), 20.97 ($COCH_3$), 20.92 ($COCH_3$), 20.84 ($COCH_3$), 20.67 ($COCH_3$).

NSI-MS *m/z* (%): 953 (8, [2M+Na^+]), 931 (17, [2M+H^+]), 488 (7, [M+Na^+]), 466 (100, [M+H^+]).

HRMS-NSI *m/z*: Calc. for $C_{22}H_{28}NO_{10}$ [M+H^+]: 466.1708; found: 466.1697.

1,3,4,6-Tetra-*O*-acetyl-β-D-glucosamine hydrochloride

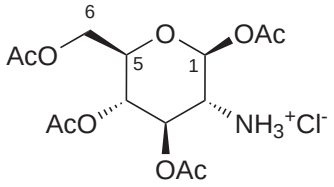

58

Fully protected sugar **57** (11.6 g, 25.4 mmol) was dissolved in warm acetone (80 ml) and the solution heated to reflux. To the refluxing solution, 5M HCl (6 ml, 30 mmol) was added, immediately turning the reaction mixture solid. The solid was broken up mechanically and stirred for 2 hours after addition of Et_2O, then cooled to 4 °C over night. The solid was collected by vacuum filtration and washed with Et_2O to give the selectively protected sugar 1,3,4,6-tetra-*O*-acetyl-β-D-glucosamine hydrochloride (**58**) as a white solid (10 g, quantitative).

All analytical data is in agreement with published data.[279]

^{1}H-NMR (D_2O, 400 MHz): δ 5.89 (d, ^3J(H1,H2) = 8.8 Hz, 1H, H-1), 5.41 (dd, ^3J(H3, H2) = 10.5 Hz, ^3J(H3,H4) = 9.1 Hz, 1H, H-3), 5.13 ('t', ^3J(H4,H5) = 10.0 Hz, ^3J(H4,H3) = 9.1 Hz, 1H, H-4), 4.40 (dd, ^2J(H6a,H6b) = 12.9 Hz, ^3J(H6a,H5) = 4.1 Hz, 1H, H-6a), 4.24–4.18 (m, 2H, H-5,6b), 3.61 (dd, ^3J(H2,H3) = 10.5 Hz, ^3J(H2,H1) = 8.8 Hz, 1H, H-2), 2.23 (s, 3H, CH_3), 2.15 (s, 3H, CH_3), 2.111 (s, 3H, CH_3), 2.105 (s, 3H, CH_3).

^{13}C-NMR (D_2O, 100 MHz): δ 176.54 (C=O), 176.11 (C=O), 175.73 (C=O), 174.41 (C=O), 94.39 (C-1), 75.01 (C-5), 74.82 (C-3), 71.08 (C-4), 64.42 (C-6), 55.65 (C-2), 23.12 (2× CH_3), 22.99 (CH_3), 22.96 (CH_3).

NSI-MS *m/z* (%): 835 (29, [M+Starting material+Na^+), 717 (68, [2M+Na^+]), 695 (12, [2M+H^+]), 488 (31, [Starting material+Na^+]), 466 (17, [Starting material+H^+]), 370 (100, [M+Na^+]), 348 (33, [M+H^+]).

HRMS-NSI *m/z*: Calc. for $C_{14}H_{22}NO_9$ [M+H^+]: 348.1289; found: 348.1294.

1-(1,3,4,6-Tetra-*O*-acetyl-2-deoxy-β-D-glucopyranos-2-yl)-2-(3-(benzyloxy)-2-methyl-4-oxopyridin-1(4*H*)-yl)acetamide

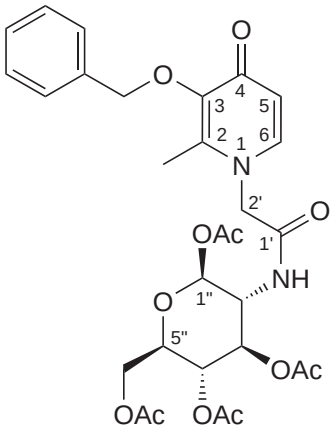

59a

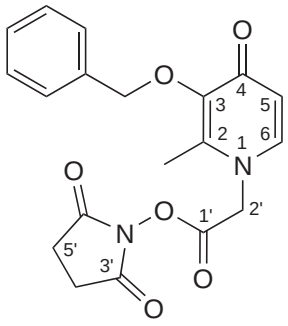

61a

Pyridinone **39a** (957 mg, 3.5 mmol) was dissolved in dry DMF (20 ml) under nitrogen atmosphere and combined with solutions of *N,N'*-dicyclohexylcarbodiimide (825 mg, 4 mmol, 1.14 eq.) and *N*-hydroxysuccinimide (407 mg, 3.5 mmol) in dry DMF (5 ml). The resulting solution was stirred under nitrogen for 21 h, then filtered and the filtrate evaporated to give a pale orange residue. The residue was dissolved in DCM and few drops of Et_2O and filtered. The filtrate was diluted with Et_2O and the formed precipitate was collected by vacuum filtration and washed with diethyl ether and little DCM to give 2,5-dioxopyrrolidin-1-yl 2-(3-(benzyloxy)-2-methyl-4-oxopyridin-1(4*H*)-yl)acetate (**61a**) as a white powder (720 mg, 3:1 mixture with unreacted acid **39a**). The crude intermediate product (592 mg, 1.56 mmol, 45%) was used directly and without further purification. 1,3,4,6-Tetra-*O*-acetyl-β-D-glucosamine hydrochloride (**58**) (385 mg, 1.0 mmol) and *N,N'*-diisopropylethylamine (350 µl, 2 mmol) were added to a solution of activated acid **61a** (1.1 mmol, 700 mg crude intermediate) in dry DMF (15 ml). The resulting solution was stirred for 21 hours at room temperature, then evaporated to dryness and the residue dissolved in DCM (25 ml) and washed with dilute HCl (pH 5). The formed precipitate was removed by filtration. The aqueous layer was exctracted with DCM, and the combined organic layers washed with HCl (pH 5), water and aqueous $NaHCO_3$ (pH 8.5). Drying over

Na_2SO_4 and evaporation gave 1-(1,3,4,6-tetra-*O*-acetyl-2-deoxy-β-D-glucopyranos-2-yl)-2-(3-(benzyloxy)-2-methyl-4-oxopyridin-1(4*H*)-yl)acetamide (**59a**) as a yellow gum (458 mg, 0.76 mmol, 76%, 34% over both steps).

2,5-Dioxopyrrolidin-1-yl 2-(3-(benzyloxy)-2-methyl-4-oxopyridin-1(4*H*)-yl) acetate (61a)

^{1}H-NMR (DMSO−d_6, 400 MHz): δ 7.69 (d, ^3J(H6,H5) = 7.6 Hz, 1H, H-6), 7.42–7.39 (m, 2H, Ph H-3,5), 7.37–7.30 (m, 3H, Ph H-2,4,6), 6.21 (d, ^3J(H5,H6) = 7.6 Hz, 1H, H-5), 5.48 (s, 2H, H-2'), 5.01 (s, 2H, O−*CH*$_2$−Ph), 2.83 (s, 4H, H-4',5'), 2.15 (s, 3H, 2-CH_3).

^{13}C-NMR (DMSO−d_6, 100 MHz): δ 172.47 (C-4), 169.87 (C-3',6'), 165.20 (C-1'), 145.30 (q), 140.86 (q), 140.37 (q), 137.58 (q, Ar), 128.41 (Ph C-2,6), 128.25 (Ph C-3,5), 127.88 (Ph C-4), 116.36 (C-5), 71.98 (O−*CH*$_2$−Ph), 51.56 (C-2'), 25.51 (C-4',5'), 11.72 (2-CH_3).

1-(1,3,4,6-Tetra-*O*-acetyl-2-deoxy-β-D-glucopyranos-2-yl)-2-(3-(benzyloxy)-2-methyl-4-oxo-pyridin-1(4*H*)-yl)acetamide (59a)

^{1}H-NMR (CD_3OD, 400 MHz): δ 7.55 (d, ^3J(H6,H5) = 7.5 Hz, 1H, H-6), 7.42–7.38 (m, 2H, Ph H-3,5), 7.37–7.29 (m, 3H, Ph H-2,4,6), 6.46 (d, ^3J(H5,H6) = 7.4 Hz, 1H, H-5), 5.84 (d, ^3J(H1",H2") = 8.8 Hz, 1H, H-1"), 5.32 (dd, ^3J(H3",H2") = 10.4 Hz, ^3J(H3",H4") = 9.3 Hz, 1H, H-3"), 5.06 (s, 2H, O−*CH*$_2$−Ph), 5.05 (dd, ^3J(H4",H5") = 10.1 Hz, ^3J(H4",H3") = 9.3 Hz, 1H, H-4"), 4.63 (s, 2H, H-2'), 4.27 (dd, ^2J(H6a",H6b") = 12.5 Hz, ^3J(H6a",H5") = 4.5 Hz, 1H, H-6a"), 4.09 (dd, ^2J(H6b",H6a") = 12.5 Hz, ^3J(H6a",H5") = 2.1 Hz, 1H, H-6b"), 4.05 (dd, ^3J(H2",H3") = 10.4 Hz, ^3J(H2",H1") = 8.8 Hz, 1H, H-2"), 3.92 (ddd, ^3J(H5",H4") = 10.1 Hz, ^3J(H5",H6a") = 4.5 Hz, ^3J(H5",H6b") = 2.2 Hz, 1H, H-5"), 2.05 (s, 6H, CH_3, 2-CH_3), 2.04 (s, 3H, CH_3), 2.01 (s, 3H, CH_3), 1.96 (s, 3H, CH_3).

^{13}C-NMR (CD_3OD, 100 MHz): δ 175.14 (C-4), 172.13 (C=O), 171.69 (C=O), 171.05 (C=O), 170.45 (C=O), 168.53 (C-1'), 146.88 (C-3), 145.00 (C-2), 142.32 (C-6), 138.35 (Ph C-1), 129.94 (Ph C-2,6), 129.40 (Ph C-3,5), 129.23 (Ph C-4), 117.11 (C-5), 92.93 (C-1"), 74.56 (O−*CH*$_2$−Ph), 73.54 (C-3"), 73.48 (C-5"), 69.41 (C-4"), 62.76 (C-6"), 56.66 (C-2'), 54.46 (C-2"), 20.78 (CH_3), 20.73 (CH_3), 20.66 (CH_3), 20.62 (CH_3), 12.88 (2-CH_3).

NSI-MS *m/z* (%): 1227 (6, [2M+Na^+]), 625 (27, [M+Na^+]), 603 (100, [M+H^+]).

HRMS-NSI *m/z*: Calc. for $C_{29}H_{35}N_2O_{12}$ [M+H^+]: 603.2185; found: 603.2179.

1-(1,3,4,6-Tetra-*O*-acetyl-2-deoxy-β-D-glucopyranos-2-yl)-3-(3-(benzyloxy)-2-methyl-4-oxopyridin-1(4*H*)-yl)propanamide

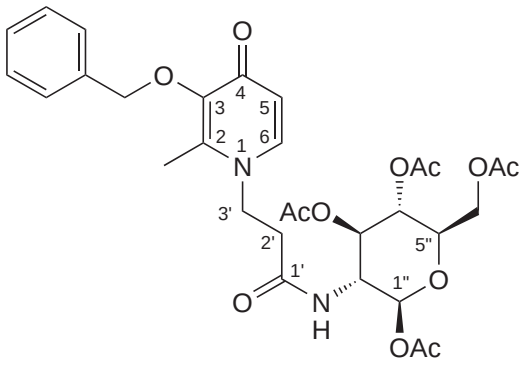

59b

Pyridinone **39b** (570 mg, 2 mmol), 1-hydroxybenzotriazole hydrate (100 mg, 0.6 mmol) and 1-ethyl-3-(3-dimethylaminopropyl)carbodiimide hydrochloride (EDC, 422 mg, 2.2 mmol) were dissolved in DMF (15 ml) and water (5 ml) and stirred for 5 min. Selectively protected glucosamine **58** (763 mg, 2 mmol) and *N,N'*-diisopropylethylamine (380 µl, 4 mmol) were added, and the reaction mixture heated to 80 °C for 40 hours. The reaction mixture was concentrated, then diluted with water and extracted with chloroform (3×). The combined organic phases were washed with sodium acetate buffer (pH 4) and 1M NaOH, then dried over Na_2SO_4. Evaporation gave 1-(1,3,4,6-tetra-*O*-acetyl-2-deoxy-β-D-glucopyranos-2-yl)-3-(3-(benzyloxy)-2-methyl-4-oxopyridin-1(4*H*)-yl)propanamide (**59b**) as a tan foam (274 mg, 0.44 mmol, 22%).

Melting point: m.p. 74−87 °C.

IR (neat) cm^{-1}: 2925 (br, w), 1744, 1679 (w), 1625, 1554, 1366, 1213, 1033.

^{1}H-NMR ($CDCl_3$, 400 MHz): δ 8.16 (d, ^3J(NH,H2") = 8.9 Hz, 1H, NH), 7.39–7.31 (m, 5H, Ph H-2–6), 7.26 (d, ^3J(H6,H5) = 7.4 Hz, 1H, H-6), 6.23 (d, ^3J(H5,H6) = 7.4 Hz, 1H, H-5), 5.89 (d, ^3J(H1",H2") = 8.8 Hz, 1H, H-1"), 5.33 ('t', ^3J(H3",H2") = 10.2 Hz, ^3J(H3", H4") = 9.2 Hz, 1H, H-3"), 5.10 (s, 2H, O−CH_2−Ph), 5.08 ('t', ^3J(H4",H5") = 10.2 Hz, ^3J(H4",H3") = 9.2 Hz, 1H, H-4"), 4.25 (dd, ^2J(H6a",H6b") = 12.5 Hz, ^3J(H6a",H5") = 4.4 Hz, 1H, H-6a"), 4.11 (ddd, ^3J(H2",H3") = 10.1 Hz, ^3J(H2",NH) = 9.0 Hz, ^3J(H2",H1") = 8.8 Hz, 1H, H-2"), 4.06 ('t', ^3J(H3',H2') = 7.0 Hz, 2H, H-3'), 4.03 (dd, ^2J(H6b",H6a") = 12.5 Hz, ^3J(H6b",H5") = 2.2 Hz, 1H, H-6b"), 3.74 (ddd, ^3J(H5",H4") = 10.3 Hz, ^3J(H5", H6a") = 4.3 Hz, ^3J(H5",H6b") = 2.2 Hz, 1H, H-5"), 2.50–2.44 (m, 2H, H-2'), 2.12 (s, 3H, 2-CH_3), 2.07 (s, 3H, CH_3), 2.02 (s, 3H, CH_3), 2.01 (s, 3H, CH_3), 1.96 (s, 3H, CH_3).

^{13}C-NMR ($CDCl_3$, 100 MHz): δ 173.02 (C-4), 170.67 (C=O), 169.58 (C=O), 169.40 (C=O), 169.09 (C=O), 168.03 (C-1'), 145.92 (C-3), 141.69 (C-2), 138.80 (C-6), 137.06 (Ph C-1), 129.02 (Ph C-3,5), 128.43 (Ph C-2,6), 128.27 (Ph C-4), 116.80 (C-5), 92.07 (C-1"), 73.11 (O−*CH*$_2$−Ph), 72.69 (C-3"), 72.26 (C-5"), 68.07 (C-4"), 61.53 (C-6"), 53.32 (C-2"), 49.44 (C-3'), 36.38 (C-2'), 20.89 (CH_3), 20.71 (CH_3), 20.69 (CH_3), 20.60 (CH_3), 12.38 (2-CH_3).

1,2-*O*-Isopropylidene-α-D-glucofuranurono-6,3-lactone

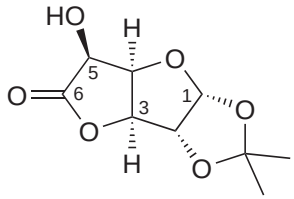

65

Concentrated H_2SO_4 (2 ml) was added to a solution of glucuronolactone **64** (10 g, 57 mmol) in acetone (250 ml) and the reaction mixture stirred for 24 hours at room temperature. The yellow solution was neutralised with 6M NaOH and the formed precipitate removed by filtration. Evaporation of the filtrate gave 1,2-*O*-isopropylidene-D-glucofuranurono-6,3-lactone (**65**) as off-white solid (11.5 g, 53 mmol, 93%).

All analytical data is in good agreement with published data.[214,280]

Melting point: m.p. 114−116 °C (lit. m.p. 118−119 °C).[280]

IR (neat) cm^{-1}: 3436, 2974 (w), 1172, 1377, 1230, 1158, 1126, 1090, 1019, 948, 900.

^{1}H-NMR (DMSO−d_6, 400 MHz): δ 6.13 (d, ^3J(OH,H5) = 7.5 Hz, 1H, OH), 5.96 (d, ^3J(H1,H2) = 3.8 Hz, 1H, H-1), 4.82 (d, ^3J(H3,H4) = 2.8 Hz, 1H, H-3), 4.80 (d, ^3J(H2,H1) = 3.8 Hz, 1H, H-2), 4.77 (dd, ^3J(H4,H5) = 4.3 Hz, ^3J(H4,H3) = 2.9 Hz, 1H, H-4), 4.62 (dd, ^3J(H5,OH) = 7.5 Hz, ^3J(H5,H4) = 4.3 Hz, 1H, H-5), 1.43 (s, 3H, CH_3), 1.27 (s, 3H, CH_3).

^{13}C-NMR (DMSO−d_6, 100 MHz): δ 174.74 (C-6), 111.97 ($C(CH_3)_2$), 106.21 (C-1), 82.06 (C-2), 80.99 (C-3), 79.00 (C-4), 69.56 (C-5), 26.62 (CH_3), 26.39 (CH_3).

1,2-*O*-Benzylidene-α-D-glucofuranurono-6,3-lactone

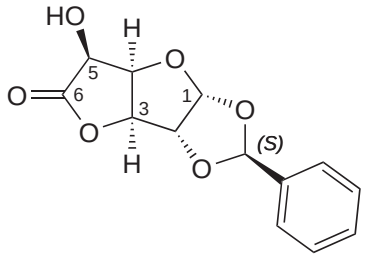

66

Glucuronolactone **64** (1.0 g, 5.7 mmol) and zinc chloride (970 mg, 7.15 mmol, 1.25 eq.) were added to benzaldehyde (5 ml, 49 mmol) and stirred at room temperature for 48 hours. The reaction mixture was diluted with Et_2O (30 ml) and washed twice with water (30 ml). The organic phase was dried over Na_2SO_4 and evaporated, the residue taken up in methanol (30 ml) and washed twice with hexane. The methanolic phase was evaporated and the residue taken up hexane/ethyl acetate (4/1, 5 ml) and stirred vigorously. The pale yellow precipitate was collected by vacuum filtration to give 1,2-*O*-benzylidene-α-D-glucofuranurono-6,3-lactone (**66**) as mixture of stereoisomers (894 mg, 3.4 mmol, 59%, Ratio S/R:[216] 4/1).

All analytical data is in agreement with published data for the *S* isomer.[214]

Melting point: m.p. 135−138 °C (lit. m.p. 168−169 °C (*S* isomer)).[281]

IR (neat) cm^{-1}: 3475 (br), 3321 (br), 1780, 1463 (w), 1395 (w), 1308 (w), 1218 (w), 1170, 1137, 1112, 1098, 1022, 956.

^{1}H-NMR ($CDCl_3$, 400 MHz): δ 7.50–7.37 (m, 25H, *S*/*R*, Ph H-2–6), 6.16 (d, ^3J(H1,H2) = 3.5 Hz, 4H, *S*, H-1), 6.15 (d, ^3J(H1,H2) = 3.7 Hz, 1H, *R*, H-1), 6.07 (s, 1H, *R*, *CH*-Ph), 6.05 (s, 4H, *S*, *CH*-Ph), 5.04–4.96 (m, 12H, *S*, H-2,3,4), 4.93 (d, ^3J(H2,H1) = 3.8 Hz, 1H, *R*, H-2), 4.85 (d, ^3J(H3,H4) = 2.6 Hz, 1H, *R*, H-3), 4.70 (dd, ^3J(H4,H5) = 4.1 Hz, ^3J(H4, H3) = 2.6 Hz, 1H, *R*, H-4), 4.57 (d, ^3J(H5,H4) = 3.7 Hz, 4H, *S*, H-5), 4.46 (d, ^3J(H5,H4) = 4.3 Hz, 1H, *R*, H-5).

^{13}C-NMR ($CDCl_3$, 100 MHz): δ 173.48 (*S*/*R*, C-6), 135.74 (*R*, Ph C-1), 135.40 (*S*, Ph C-1), 130.32 (*S*, Ph C-4), 130.05 (*R*, Ph C-4), 128.76 (*R*, Ph C-3,5), 128.73 (*S*, Ph C-3,5), 126.63 (*S*, Ph C-2,6), 126.25 (*R*, Ph C-2,6), 106.78 (*R*, C-1), 106.34 (*S*, C-1), 106.03 (*R*, *CH*-Ph), 106.00 (*S*, *CH*-Ph), 83.73 (*R*, C-2), 83.36 (*S*, C-2), 81.29 (*R*, C-3), 81.17 (*S*, C-3), 80.04 (*S*, C-4), 78.64 (*R*, C-4), 71.06 (*S*, C-5), 70.60 (*R*, C-5).

1-(ω-Aminoalkyl)-3-(benzyloxy)-2-methylpyridin-4(1*H*)-ones (67)
1,1'-(Alkane-1,ω-diyl)bis[3-(benzyloxy)-2-methylpyridin-4(1*H*)-one]s (68)

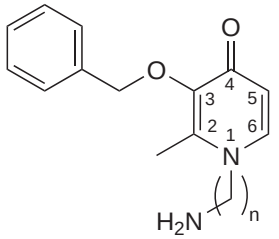

67a n = 2
67b n = 4
67c n = 6
67d n = 8

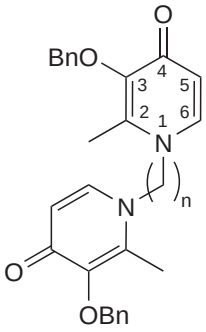

68a n = 2
68b n = 4
68c n = 6
68d n = 8

n	cpd **33**		cpd **109**		product	mg	Yield	dimer	mg	Yield
	g	mmol	mg	mmol						
2	2.0	9.2	1330	10	**67a**	780	38%	**68a**	—	—
4	1.0	4.6	441	5	**67b**	814	62%	**68b**	289	26%
6	1.0	4.6	581	5	**67c**	870	64%	**68c**	420	36%
8	1.0	4.6	721	5	**67d**	1553	99%	**68d**	—	—

Benzyl maltol **33** and diamine **109** (1.1 eq., n=2 as dihydrochloride) were dissolved in ethanol (2 ml/mmol) and water (2 ml/mmol, n=2: 1 ml), then 1M NaOH (0.2 ml/mmol, n=2: 2 ml/mmol) was added and the reaction mixture heated to reflux over night. The solution was acidified to pH 1 with HCl and concentrated *in vacuo*. Any formed precipitate (for n = 3 and 5) was collected by filtration to yield the dimers **68b** and **68c**, respectively, as pale tan powder. The filtrate was extracted with Et_2O, the organic phase discarded and the aqueous phase adjusted to pH 12 with 10M NaOH before extraction with DCM (3×). The combined organic phases were washed with water, dried over Na_2SO_4 and evaporated. The desired *N*-aminoalkyl pyridinone **67** was obtained as orange syrup.

1-(2-Aminoethyl)-3-(benzyloxy)-2-methylpyridin-4(1*H*)-one (67a)

NMR data is in good agreement with published data.[282]

^{1}H-NMR ($CDCl_3$, 400 MHz): δ 7.41–7.28 (m, 5H, Ph H-2–6), 7.29 (d, ^3J(H6,H5) = 7.7 Hz, 1H, H-6), 6.40 (d, ^3J(H5,H6) = 7.5 Hz, 1H, H-5), 5.20 (s, 2H, O−*CH₂*−Ph), 3.83 (t, ^3J(H1',H2') = 6.2 Hz, 2H, H-1'), 2.95 (t, ^3J(H2',H1') = 6.2 Hz, 2H, H-2'), 2.10 (s, 3H, 2-CH_3).

^{13}C-NMR ($CDCl_3$, 100 MHz): δ 173.36 (C-4), 146.00 (C-3), 140.78 (C-2), 138.77 (C-6), 137.48 (Ph C-1), 129.13 (Ph C-3,5), 128.21 (Ph C-2,6), 127.98 (Ph C-4), 117.04 (C-5), 72.93 (O−*CH₂*−Ph), 55.90 (C-1'), 41.85 (C-2'), 12.57 (2-CH_3).

NSI-MS *m/z* (%): 539 (56, [2M+Na^+]) 517 (17, [2M+H^+]) 457 (19, [Dimer+H^+]), 281 (37, [M+Na^+]), 259 (100, [M+H^+]).

HRMS-NSI *m/z*: Calc. for $C_{15}H_{19}N_2O_2$ [M+H^+]: 259.1441; found: 259.1444.

1-(4-Aminobutyl)-3-(benzyloxy)-2-methylpyridin-4(1*H*)-one (67b)

NMR data is in general agreement with published data.[283]

^{1}H-NMR ($CDCl_3$, 400 MHz): δ 7.42–7.28 (m, 5H, Ph H-2–6), 7.21 (d, ^3J(H6,H5) = 7.5 Hz, 1H, H-6), 6.41 (d, ^3J(H5,H6) = 7.5 Hz, 1H, H-5), 5.21 (s, 2H, O−*CH₂*−Ph), 3.76 (t, ^3J(H1',H2') = 7.5 Hz, 2H, H-1'), 2.95 (t, ^3J(H4',H3') = 6.9 Hz, 2H, H-4'), 2.10 (s, 3H, 2-CH_3) 1.68 (tt, ^3J(H2',H3') = 7.9 Hz, ^3J(H2',H1') = 7.5 Hz, 2H, H-2'), 1.44 (tt, ^3J(H3', H2') = 7.9 Hz, ^3J(H3',H4') = 6.9 Hz, 2H, H-3').

^{13}C-NMR ($CDCl_3$, 100 MHz): δ 173.26 (C-4), 146.03 (C-3), 140.61 (C-2), 138.77 (C-6), 137.54 (Ph C-1), 129.11 (Ph C-3,5), 128.20 (Ph C-2,6), 127.93 (Ph C-4), 117.25 (C-5), 72.90 (O−*CH₂*−Ph), 53.59 (C-1'), 41.29 (C-4'), 29.62 (C-3'), 28.14 (C-2'), 12.38 (2-CH_3).

NSI-MS *m/z* (%): 595 (18, [2M+Na^+]) 573 (27, [2M+H^+]) 485 (32, [Dimer+H^+]), 329 (13), 309 (22, [M+Na^+]), 287 (100, [M+H^+]).

HRMS-NSI *m/z*: Calc. for $C_{17}H_{23}N_2O_2$ [M+H^+]: 287.1754; found: 287.1759.

1-(6-Aminohexyl)-3-(benzyloxy)-2-methylpyridin-4(1*H*)-one (67c)

IR (neat) cm^{-1}: 3279 (br), 2931, 2858 (w), 1623, 1556, 1498, 1247, 1217, 1037.

^{1}H-NMR ($CDCl_3$, 400 MHz): δ 7.43–7.28 (m, 5H, Ph H-2–6), 7.18 (d, ^3J(H6,H5) = 7.5 Hz, 1H, H-6), 6.42 (d, ^3J(H5,H6) = 7.5 Hz, 1H, H-5), 5.22 (s, 2H, O−*CH₂*−Ph), 3.73 (t, ^3J(H1',H2') = 7.5 Hz, 2H, H-1'), 2.70 (t, ^3J(H4',H3') = 6.9 Hz, 2H, H-6'), 2.07 (s, 3H, 2-CH_3) 1.63 (tt, ^3J(H2',H1') = 7.5 Hz, ^3J(H2',H3') = 7.4 Hz,2H, H-2'), 1.45 (tt, ^3J(H5', H4') = 7.4 Hz, ^3J(H5',H6') = 6.9 Hz, 2H, H-5'). 1.39–1.24 (m, 4H, H-3',4').

^{13}C-NMR ($CDCl_3$, 100 MHz): δ 173.32 (C-4), 146.08 (C-3), 140.59 (C-2), 138.13 (C-6), 137.62 (Ph C-1), 129.17 (Ph C-3,5), 128.23 (Ph C-2,6), 127.96 (Ph C-4), 117.30 (C-5), 72.94 (O−*CH₂*−Ph), 53.74 (C-1'), 41.83 (C-6'), 33.11 (C-5') 30.71 (C-2'), 26.42 (C-3' or 4'), 26.19 (C-3' or 4'), 12.41 (2-CH_3).

NSI-MS *m/z* (%): 513 (12, [Dimer+H^+]), 315 (100, [M+H^+]).

HRMS-NSI *m/z*: Calc. for $C_{19}H_{27}N_2O_2$ [M+H^+]: 315.2067; found: 315.2073.

1-(8-Aminooctyl)-3-(benzyloxy)-2-methylpyridin-4(1*H*)-one (67d)

IR (neat) cm^{-1}: 3302 (br), 2931, 2857 (w), 1623, 1548, 1506, 1248, 1218, 1030.

^{1}H-NMR ($CDCl_3$, 400 MHz): δ 7.42–7.29 (m, 5H, Ph H-2–6), 7.17 (d, ^3J(H6,H5) = 7.5 Hz, 1H, H-6), 6.41 (d, ^3J(H5,H6) = 7.5 Hz, 1H, H-5), 5.23 (s, 2H, O−*CH₂*−Ph), 3.72 (t, ^3J(H1',H2') = 7.5 Hz, 2H, H-1'), 2.68 (t, ^3J(H8',H7') = 7.0 Hz, 2H, H-8'), 2.07 (s, 3H, 2-CH_3) 1.61 (tt, ^3J(H2',H1') = 7.5 Hz, ^3J(H2',H3') = 6.9 Hz,2H, H-2'), 1.43 (tt, ^3J(H7', H6') = 7.2 Hz, ^3J(H7',H8') = 6.9 Hz, 2H, H-7'). 1.35–1.21 (m, 8H, H-3'–6').

^{13}C-NMR ($CDCl_3$, 100 MHz): δ 173.34 (C-4), 146.16 (C-3), 140.54 (C-2), 138.06 (C-6), 137.64 (Ph C-1), 129.18 (Ph C-3,5), 128.22 (Ph C-2,6), 127.94 (Ph C-4), 117.32 (C-5),

72.94 (O−*CH₂*−Ph), 53.80 (C-1'), 42.15 (C-8'), 33.63 (C-7') 30.75 (C-2'), 29.27 (C-3' or 4'), 29.12 (C-3' or 4'), 26.75 (C-5' or 6'), 26.29 (C-5' or 6'), 12.40 (2-CH_3).

NSI-MS *m/z* (%): 541 (76, [Dimer+H^+]), 343 (100, [M+H^+]).

HRMS-NSI *m/z*: Calc. for $C_{21}H_{31}N_2O_2$ [M+H^+]: 343.2380; found: 343.2383.

1,1'-(Butane-1,4-diyl)bis[3-(benzyloxy)-2-methylpyridin-4(1*H*)-one] (68b)

NMR data is in agreement with published data.[284]

^{1}H-NMR (CD_3OD, 400 MHz): δ 8.36 (d, ^3J(H6,H5) = 7.2 Hz, 1H, H-6), 7.45–7.36 (m, 5H, Ph H-2–6), 7.21 (d, ^3J(H5,H6) = 7.1 Hz, 1H, H-5), 5.20 (s, 2H, O−*CH₂*−Ph), 4.37 ('t', ^3J(H1',H2') = 6.5 Hz, 2H, H-1'), 2.52 (s, 3H, 2-CH_3), 1.90–1.85 (m, 2H, H-2').

^{13}C-NMR (CD_3OD, 100 MHz): δ 165.74 (C-4), 151.35 (C-2), 144.97 (C-3), 143.09 (C-6), 137.27 (Ph C-1), 130.16 (Ph C-3,5), 129.95 (Ph C-4), 129.72 (Ph C-2,6), 114.14 (C-5), 76.27 (O−*CH₂*−Ph), 57.01 (C-1'), 27.81 (C-2'), 13.69 (2-CH_3).

NSI-MS *m/z* (%): 991 (26, [2M+Na^+]), 969 (14, [2M+H^+]), 507 (100, [M+Na^+]), 485 (70, [M+H^+]).

HRMS-NSI *m/z*: Calc. for $C_{30}H_{33}N_2O_4$ [M+H^+]: 485.2435; found: 485.2426.

1,1'-(Hexane-1,6-diyl)bis[3-(benzyloxy)-2-methylpyridin-4(1*H*)-one] (68c)

^{1}H-NMR (CD_3OD, 400 MHz): δ 8.33 (d, ^3J(H6,H5) = 7.2 Hz, 1H, H-6), 7.45–7.35 (m, 5H, Ph H-2–6), 7.18 (d, ^3J(H5,H6) = 7.1 Hz, 1H, H-5), 5.19 (s, 2H, O−*CH₂*−Ph), 4.37 ('t', ^3J(H1',H2') = 7.7 Hz, 2H, H-1'), 2.47 (s, 3H, 2-CH_3), 1.84–1.75 (m, 2H, H-2'), 1.45–1.38 (m, 2H, H-3').

^{13}C-NMR (CD_3OD, 100 MHz): δ 165.84 (C-4), 150.75 (C-2), 144.65 (C-3), 143.06 (C-6), 137.27 (Ph C-1), 130.26 (Ph C-3,5), 129.95 (Ph C-4), 129.72 (Ph C-2,6), 114.11 (C-5), 76.21 (O−*CH*$_2$−Ph), 57.68 (C-1'), 30.99 (C-'), 26.70(C-'), 13.64 (2-CH_3).

NSI-MS *m/z* (%): 535 (100, [M+Na^+]), 513 (37, [M+H^+]).

HRMS-NSI *m/z*: Calc. for $C_{32}H_{37}N_2O_4$ [M+H^+]: 513.2748; found: 513.2846.

N-{ω-[3-(Benzyloxy)-2-methyl-4-oxopyridin-1(4*H*)-yl]alkyl}-1,2-*O*-isopropylidene-α-D-glucofuranuronamides

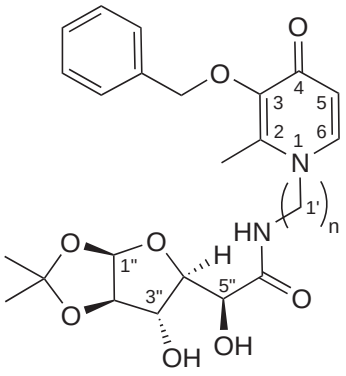

71a n = 2
71b n = 4
71c n = 6
71d n = 8

The lactone **65** (973 mg, 4.5 mmol) and pyridinone **67b** (859 mg, 3 mmol) were dissolved in dry DMF (30 ml) and stirred at room temperature for 3 days. The reaction mixture was evaporated and the residue taken up in DCM. The solution was washed twice with water, then dried over Na_2SO_4 and evaporated. The resulting dark brown syrup was then purified by column chromatography (DCM/methanol: 6/1) to give the desired product *N*-{4-[3-(benzyloxy)-2-methyl-4-oxopyridin-1(4*H*)-yl]butyl}-1,2-*O*-isopropylidene-α-D-glucofuranuronamide (**71b**) as a pale yellow glass (982 mg, 1.95 mmol, 65%).
An analogous procedure reacting pyridinone **67c** (943 mg, 3 mmol) with lactone **65** gave *N*-{6-[3-(benzyloxy)-2-methyl-4-oxopyridin-1(4*H*)-yl]hexyl}-1,2-*O*-isopropylidene-α-D-glucofuranuronamide (**71c**) as a light brown glass (971 mg, 1.83 mmol, 61%).

N-{4-[3-(Benzyloxy)-2-methyl-4-oxopyridin-1(4*H*)-yl]butyl}-1,2-*O*-isopropylidene-α-D-glucofuranuronamide (71b)

IR (neat) cm^{-1}: 3317 (br), 2934, 1797 (w), 1623, 1542, 1509, 1455, 1374, 1249, 1216, 1163, 1069, 1010.

^{1}H-NMR (CD_3OD, 400 MHz): δ 7.66 (d, ^3J(H6,H5) = 7.4 Hz, 1H, H-6), 7.45–7.35 (m, 5H, Ph H-2–6), 6.46 (d, ^3J(H5,H6) = 7.4 Hz, 1H, H-5), 5.83 (d, ^3J(H1",H2") = 3.6 Hz, 1H, H-1"), 5.04 (s, 2H, O−*CH*$_2$−Ph), 4.46 (d, ^3J(H2",H1") = 3.6 Hz, 1H, H-2"), 4.33 (d,

^3J(H5",H4") = 6.4 Hz, 1H, H-5"), 4.22 (dd, ^3J(H4",H5") = 6.4 Hz, ^3J(H4",H3") = 2.7 Hz, 1H, H-4"), 4.19 (d, ^3J(H3",H4") = 2.7 Hz, 1H, H-3"), 3.93 (t, ^3J(H1',H2') = 7.7 Hz, 2H, H-1'), 3.26 (t, ^3J(H4',H3') = 6.4 Hz, 2H, H-4'), 2.16 (s, 3H, 2-CH_3), 1.66 ('quint', ^3J(H2', H1') = 7.7 Hz, ^3J(H2',H3') = 7.5 Hz, 2H, H-2'), 1.51 (tt, ^3J(H3',H2') = 7.5 Hz, ^3J(H3', H4') = 6.4 Hz, 2H, H-3'), 1.38 (s, 3H, CH_3), 1.25 (s, 3H, CH_3).

^{13}C-NMR (CD_3OD, 100 MHz): δ 174.77 (C-6"), 174.51 (C-4), 146.87 (C-3), 145.00 (C-2), 141.16 (C-6), 138.35 (Ph C-1), 130.17 (Ph C-3,5), 129.37 (Ph C-2,6), 129.29 (Ph C-4), 117.32 (C-5), 112.75 ($C(CH_3)_2$), 106.31 (C-1"), 86.42 (C-2"), 82.48 (C-4"), 75.65 (C-3"), 74.37 (O−CH_2−Ph), 70.73 (C-5"), 54.76 (C-1'), 39.01 (C-4'), 28.50 (C-2'), 27.13 (CH_3), 27.05 (C-3'), 26.44 (CH_3), 12.83 (2-CH_3).

NSI-MS *m/z* (%): 1003 (19, [2M-H$^+$]), 547 (23), 501 (100, [M-H$^+$]).

HRMS-NSI *m/z*: Calc. for $C_{26}H_{33}N_2O_8$ [M-H$^+$]: 501.2242; found: 501.2238.

N-{6-[3-(Benzyloxy)-2-methyl-4-oxopyridin-1(4*H*)-yl]hexyl}-1,2-*O*-isopropylidene-α-D-glucofuranuronamide (71c)

Melting point: m.p. 67−72 °C.

IR (neat) cm^{-1}: 3251 (br), 2933, 2860 (w), 1622, 1546, 1510, 1455, 1373, 1248, 1217, 1163, 1069, 1010.

^{1}H-NMR ($CDCl_3$, 400 MHz): δ 7.39–7.27 (m, 5H, Ph H-2–6), 7.22 (d, ^3J(H6,H5) = 7.5 Hz, 1H, H-6), 7.06 (d, ^3J(NH,H6') = 5.8 Hz, 1H, NH), 6.41 (d, ^3J(H5,H6) = 7.4 Hz, 1H, H-5), 5.93 (d, ^3J(H1",H2") = 3.6 Hz, 1H, H-1"), 5.14 (s, 2H, O−CH_2−Ph), 4.52 (d, ^3J(H2",H1") = 3.6 Hz, 1H, H-2"), 4.48 (d, ^3J(H5",H4") = 4.6 Hz, 1H, H-5"), 4.39 (dd, ^3J(H4",H5") = 4.7 Hz, ^3J(H4",H3") = 3.0 Hz, 1H, H-4"), 4.33 (d, ^3J(H3",H4") = 3.0 Hz, 1H, H-3"), 3.74 (t, ^3J(H1',H2') = 7.4 Hz, 2H, H-1'), 3.36–3.19 (m, ^3J(H6',NH) = 5.8 Hz, 2H, H-6'), 2.08 (s, 3H, 2-CH_3), 1.60 ('quint', ^3J(H2',H1') = 7.4 Hz, ^3J(H2',H3') = 6.8 Hz, 2H, H-2'), 1.52–1.45 (m, 2H, H-5'), 1.44 (s, 3H, CH_3), 1.34–1.22 (m, 7H, CH_3, H-3',4').

^{13}C-NMR ($CDCl_3$, 100 MHz): δ 173.18 (C-4), 172.28 (C-6"), 145.98 (C-3), 141.52 (C-2), 138.53 (C-6), 137.22 (Ph C-1), 129.05 (Ph C-3,5), 128.28 (Ph C-2,6), 128.11 (Ph C-4), 116.92 (C-5), 111.79 ($C(CH_3)_2$), 105.16 (C-1"), 85.41 (C-2"), 81.47 (C-4"), 75.36 (C-3"), 73.07 (O−CH_2−Ph), 70.18 (C-5"), 54.00 (C-1'), 38.82 (C-6'), 30.28 (C-2'), 29.05 (C-5'), 26.92 (CH_3), 26.30 (CH_3), 26.04 (C-3' or 4'), 25.78 (C-3' or 4'), 12.42 (2-CH_3).

NSI-MS *m/z* (%): 1083 (8, [2M+Na$^+$]), 1062 (6, [2M+H$^+$]), 553 (13, [M+Na$^+$]), 531 (100, [M+H$^+$]).

HRMS-NSI *m/z*: Calc. for $C_{28}H_{39}N_2O_8$ [M+H$^+$]: 531.2701; found: 531.2688.

1,2-*O*-Benzylidene-*N*-{ω-[3-(benzyloxy)-2-methyl-4-oxopyridin-1(4*H*)-yl]alkyl}-α-D-glucofuranuronamides

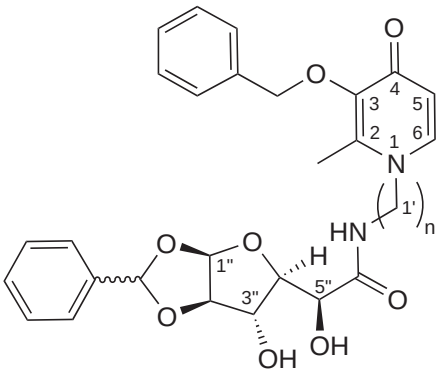

72a n = 2
72b n = 4
72c n = 6
72d n = 8

The lactone **66** (119 mg, 0.45 mmol) and pyridinone **67b** (86 mg, 0.3 mmol) were dissolved in dry DMF (5 ml) and stirred at room temperature for 3 days. The reaction mixture was evaporated and the residue taken up in DCM. The solution was washed twice with water, then dried over Na_2SO_4 and evaporated. The resulting dark brown oil was purified by column chromatography (DCM/methanol: 6/1) to give 1,2-*O*-benzylidene-*N*-{4-[3-(benzyloxy)-2-methyl-4-oxopyridin-1(4*H*)-yl]butyl}-α-D-glucofuranuronamide (**72b**) as pale yellow glass (128 mg, 233 µmol, 78%).

An analogous procedure using pyridinone **67c** (943 mg, 3 mmol) gave 1,2-*O*-benzylidene-*N*-{6-[3-(benzyloxy)-2-methyl-4-oxopyridin-1(4*H*)-yl]hexyl}-α-D-glucofuranuronamide (**72c**) as pale tan solid (121 mg, 209 µmol, 70%).

7.1.5 Synthesis of Triazole-linked Conjugates

2,3,4,6-Tetra-*O*-acetyl-α-D-glucopyranosyl azide

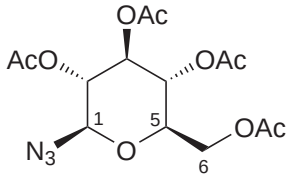

73

2,3,4,6-Tetra-*O*-acetyl-α-D-glucopyranosyl bromide (**30**) (1.4 g, 3.3 mmol) was dissolved in DCM (20 ml), then sodium azide (1.3 g, 20 mmol, 6 eq.), tetrabutylammonium iodide (370 mg, 1.0 mmol, 0.3 eq.) and saturated $NaHCO_3$ solution (20 ml) were added to the solution. The resulting bi-phasic mixture was stirred vigorously at room temperature over night, before extraction with DCM (2×). The combined organic phases were washed with $NaHCO_3$, water and brine before drying over Na_2SO_4. Evaporation gave a yellow crystalline solid (1.2 g) which was purified by column chromatography (hexane/ethyl acetate: 3/1 → 1/1) to yield 2,3,4,6-tetra-*O*-acetyl-α-D-glucopyranosyl azide (**73**) as white crystalline powder (870 mg, 2.3 mmol, 69%).

Analytical data is in agreement with published data.[238]

Melting point: m.p. 120−121.5 °C (lit. m.p. 129−130 °C).[238]

IR (neat) cm^{-1}: 2117, 1750, 1731, 1368, 1233, 1210, 1057, 1037, 908.

^{1}H-NMR (CD_3OD, 400 MHz): δ 5.29 ('t', ^3J(H3,H4) = 9.5 Hz, ^3J(H3,H2) = 9.1 Hz, 1H, H-3), 5.06 ('t', ^3J(H4,H5) = 10.1 Hz, ^3J(H4,H3) = 9.5 Hz, 1H, H-4), 1H, H-4), 4.91–4.84 (m, 3H, H-1,2), 4.30 (dd, ^2J(H6a,H6b) = 12.5 Hz, ^3J(H6a,H5) = 4.7 Hz, 1H, H-6a), 4.17 (dd, ^2J(H6b,H6a) = 12.5 Hz, ^3J(H6b,H5) = 2.3 Hz, 1H, H-6b), 3.99 (ddd, ^3J(H5,H4) = 10.1 Hz, ^3J(H6a,H5) = 4.7 Hz, ^3J(H6b,H5) = 2.3 Hz, 1H, H-5), 2.07 (s, 3H, CH_3), 2.05 (s, 3H, CH_3), 2.01 (s, 3H, CH_3), 1.97 (s, 3H, CH_3).

^{13}C-NMR (CD_3OD, 100 MHz): δ 168.34 (C=O), 168.08 (C=O), 167.67 (C=O), 167.53 (C=O), 88.89 (C-1), 75.08 (C-5), 74.14 (C-3), 72.20 (C-2), 69.46 (C-4), 62.99 (C-6), 20.66 (CH_3), 20.60 (CH_3), 20.57 (CH_3), 20.53 (CH_3).

NSI-MS *m/z* (%): 769 (12, [2M+Na^+]), 391 (100, [M+NH_4^+]).

HRMS-NSI *m/z*: Calc. for $C_{14}H_{23}N_4O_9$ [M+H^+]: 391.1460; found: 391.1462.

3-(Azidosulfonyl)-3*H*-imidazol-1-ium hydrogen sulfate

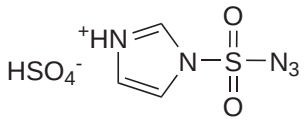

78

Sodium azide (1.3 g, 20 mmol) was taken up in dry acetonitrile (20 ml) under nitrogen atmosphere and cooled to 0 °C on an ice-bath. Sulfuryl chloride (1.6 ml, 20 mmol) was added dropwise to the solution, which was then stirred at room temperature (16 °C) for 16 hours. The solution was cooled to 0 °C, before the addition of imidazole (2.62 g, 38.2 mmol) in 5 portions. Then reaction mixture was allowed to warm and stirred at room temperature for 4 hours, before dilution with ethyl acetate (40 ml). The solution was washed twice each with water, saturated $NaHCO_3$ solution and brine, then dried over Na_2SO_4. The solution was concentrated to 10 ml and cooled to 0 °C. Concentrated sulfuric acid (1.07 ml, 20 mmol) in ethyl acetate (20 ml) was added slowly, the reaction mixture stirred at room temperature for 2 hours. The formed precipitate was collected by vacuum filtration and dried over P_2O_5 *in vacuo* to give 3-(azidosulfonyl)-3*H*-imidazol-1-ium hydrogen sulfate (**78**) as a white powder (3.32 g, 12.2 mmol, 61%).
CAUTION! Imidazole-1-sulfonyl azide and its salts are energetic materials with sensitivities toward shock and friction. Specifically, neat imidazole-1-sulfonyl azide is very sensitive and has to be handled with great care.[230,239,285]

All analytical data is in agreement with published data.[239]

^{1}H-NMR (DMSO−d_6, 400 MHz): δ 14.27 (br s, 1H), 9.09 ('s', 1H), 8.57 ('s', 1H), 7.97 (t, $^{'}J$ = 1.5 Hz 1H), 7.70 (d, $^{'}J$ = 0.8 Hz 1H), 7.32 (d, $^{'}J$ = 0.8 Hz 1H), 6.16 (br s, 11H).

^{13}C-NMR (DMSO−d_6, 100 MHz): δ 137.73, 130.93, 119.36, 118.88.

2-Azido-2-deoxy-D-glucopyranose 1,3,4,6-tetra-*O*-acetate

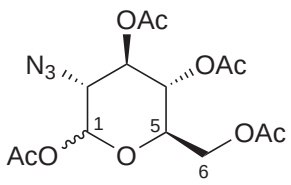

74

Glucosamine hydrochloride (1.14 g, 5.3 mmol), imidazole-1-sulfonyl azide **78** (1.725 g, 6.36 mmol, 1.2 eq.) and K_2CO_3 (2.93 g, 21.2 mmol, 4 eq.) were suspended in methanol (25 ml). $CuSO_4 \cdot 5\,H_2O$ (15 mg, 60 µmol, 11%mol) was added to the solution and the resulting mixture was stirred for 4 days. The solvent was evaporated and residual methanol removed by co-evaporation with toluene (4× 10 ml). The residue was taken up in pyridine (25 ml) and acetic anhydride (10 ml) and stirred for 2 days. The reaction mixture was evaporated and dissolved in water. The solution was extracted with ethyl acetate (3×) and the combined organic phases were washed with brine, then dried over Na_2SO_4 and evaporated to give a brown residue (1.13 g). The crude azide was purified by column chromatography (hexane/ethyl acetate: 10/1 → 3/1) to give 2-azido-2-deoxy-D-glucopyranose 1,3,4,6-tetra-*O*-acetate (**74**) as a colourless wax (458 mg, 1.23 mmol, 23%, α:β 1:2.1).

All analytical data and the assignment of α/β isomers is in good agreement with published data.[286,287]

Melting point: m.p. 70−72 °C (lit. m.p. 80 °C (β anomer)).[287]

IR (neat) cm^{-1}: 2112 (s), 1743, 1367, 1205, 1032.

^{1}H-NMR ($CDCl_3$, 400 MHz): δ 6.30 (d, ^3J(H1,H2) = 3.7 Hz, 1H, α, H-1), 5.56 (d, ^3J(H1, H2) = 8.6 Hz, 2H, β, H-1), 5.46 (dd, ^3J(H3,H2) = 10.6 Hz, ^3J(H3,H4) = 9.4 Hz, 1H, α, H-3), 5.12 (dd, ^3J(H4,H3) = 10.6 Hz, ^3J(H4,H5) = 9.5 Hz, 1H, α, H-4, overlapping with β H-3), 5.09 (dd, ^3J(H3,H2) = 9.9 Hz, ^3J(H3,H4) = 9.3 Hz, 2H, β, H-3, overlapping with α H-4), 5.05 (dd, ^3J(H4,H5) = 9.7 Hz, ^3J(H4,H3) = 9.3 Hz, 2H, β, H-4), 4.31 (dd, ^2J(H6a, H6b) = 12.7 Hz, ^3J(H6a,H5) = 4.4 Hz, 2H, β, H-6a, overlapping with α), 4.29 (dd, ^2J(H6a, H6b) = 12.7 Hz, ^3J(H6a,H5) = 4.2 Hz, 1H, α, H-6a, overlapping with β), 4.11–4.04 (m, 4H, α H-5,6b, β H-6b), 3.81 (ddd, ^3J(H5,H4) = 9.7 Hz, ^3J(H5,H6a) = 4.3 Hz, ^3J(H6b,,) = 2.1 Hz 2H, β, H-5), 3.68 (dd, ^3J(H2,H3) = 10.1 Hz, ^3J(H2,H3) = 8.6 Hz, 2H, β, H-2, overlapping with α), 3.67 (dd, ^3J(H2,H3) = 10.6 Hz, ^3J(H2,H3) = 3.7 Hz, 1H, α, H-2, overlapping with β), 2.20 (s, 9H, β/α, CH_3), 2.11 (s, 3H, α, CH_3), 2.10 (s, 6H, β, CH_3), 2.08 (s, 9H, β/α, CH_3), 2.05 (s, 3H, α, CH_3), 2.03 (s, 6H, β, CH_3).

^{13}C-NMR ($CDCl_3$, 100 MHz): δ 170.71 (β/α, C=O), 170.22 (α, C=O), 169.95 (β, C=O), 169.77 (β/α, C=O), 168.72 (β, C=O), 168.67 (α, C=O), 92.70 (β, C-1), 90.08 (α, C-1), 72.86 (β, C-5), 72.81 (β, C-3), 70.87 (α, C-3), 69.88 (α, C-5), 67.96 (α, C-4), 67.86 (β, C-4), 62.67 (β, C-2), 61.52 (α, C-6), 61.50 (β, C-6), 60.40 (α, C-2), 21.09 (α, CH_3), 21.04 (β, CH_3), 20.85 (α, CH_3), 20.83 (β, CH_3), 20.78 (β, CH_3), 20.71 (β/α, CH_3).

NSI-MS *m/z* (%): 769 (12, [2M+Na^+]), 396 (23, [M+Na^+]), 391 (100, [M+NH_4^+]).

HRMS-NSI *m/z*: Calc. for $C_{14}H_{23}N_4O_9$ [M+NH_4^+]: 391.1460; found: 391.1462.

6-*O*-Trityl-D-glucopyranose

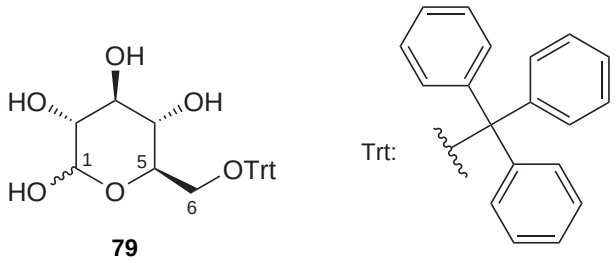

79

Triphenylmethyl chloride (8.5 g, 30.5 mmol, 1.1 eq.) was added to a solution of glucose (5.0 g, 27.8 mmol) in pyridine (60 ml), which was subsequently heated to 75 °C for 14 hours. Volatiles were removed by evaporation and the orange residue dissolved in DCM (75 ml). The solution was washed twice with saturated NH_4Cl and $NaHCO_3$ solutions and brine, before drying over Na_2SO_4. Evaporation gave a yellow foam, which was purified by column chromatography (chloroform/methanol: 100/0→9/1) affording 6-*O*-trityl-D-glucopyranose (**79**) as a yellow foam. (8.4 g, 19.9 mmol, 72%, α:β 1.3:1).

All analytical data is in good agreement with published data.[231]

IR (neat) cm^{-1}: 3337 (br), 2924 (w), 1490, 1448, 1033.

^{1}H-NMR (CD_3OD, 400 MHz): δ 7.39–7.36 (m, 14H, Ar), 7.20–7.16 (m, 14H, Ar), 7.14–7.09 (m, 7H, Ar), 5.07 (d, ^3J(H1,H2) = 3.7 Hz, 1.3H, α, H-1), 4.42 (d, ^3J(H1,H2) = 7.7 Hz, 1H, β, H-1), 3.88 (ddd, ^3J(H5,H4) = 10.1 Hz, ^3J(H5,H6a) = 5.5 Hz, ^3J(H5,H6b) = 2.0 Hz, 1.4H, α, H-5), 3.56 (dd, ^3J(H3,H2) = 9.6 Hz, ^3J(H3,H4) = 8.9 Hz, α, H-3), 3.37 (ddd, 5.8, 3.3, J = 1.7 Hz, 1H, β, H-5), 3.35–3.22 (m, 7.5H, α, H-2, H-4, H-6a; β, H-3, H-4, H-6a), 3.16–3.11 (m, 2.6H, α/β, H-6b), 3.07 (dd, ^3J(H2,H3) = 9.3 Hz, ^3J(H2,H1) = 7.7 Hz, 1H, β, H-2).

^{13}C-NMR (CD_3OD, 100 MHz): δ 145.65 (q, α, Trt C-1), 145.53 (q, β, Trt C-1), 130.03 (α/β, 2 Trt C), 128.69 (β, 2 Trt C), 128.66 (α, 2 Trt C), 127.99 (β, Trt C), 127.96 (α, Trt C), 98.27 (β, C-1), 94.00 (α, C-1), 78.39 (β, C-3), 77.04 (β, C-5), 76.31 (β, C-2), 75.20 (α, C-3), 73.92 (α, C-2), 72.34 (α, C-4), 72.11 (β, C-4), 72.08 (α, C-5), 64.96 (β, C-6), 64.88 (α, C-6).

NSI-MS *m/z* (%): 867 (22, $[2M+Na]^+$), 862 (26, $[2M+NH_4^+]$), 445 (24, $[M+Na^+]$), 243 (100, $[Trt^+]$).

HRMS-NSI *m/z*: Calc. for $C_{25}H_{26}NaO_6$ $[M+Na^+]$: 445.1622, found: 445.1620.

Benzyl 2,3,4-tri-*O*-benzyl-6-*O*-trityl-D-glucopyranoside

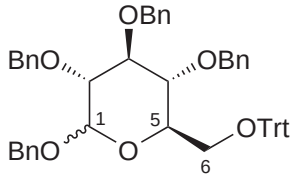

80

6-Trityl glucose **79** (1.5 g, 3.55 mmol) and tetrabutylammonium iodide (133 mg, 0.36 mmol, 10%mol) were dissolved in dry DMF (25 ml) under nitrogen atmosphere, benzyl bromide (2.1 ml, 17.66 mmol, 5 eq. was added then. The solution was cooled on an ice-bath, before addition of sodium hydride (60% suspension, 720 mg, 18 mmol, 5.1 eq.) in portions. The reaction mixture was allowed to slowly warm to room temperature (17 °C) and was stirred for 40 hours before quenching by addition of saturated NH_4Cl solution. The reaction mixture was extracted with ethyl acetate (2× 40 ml) and the organic phase was wased with saturated NH_4Cl solution, water and brine (40 ml each), then dried over Na_2SO_4. Evaporation gave the crude product as thick, yellow oil (3.22 g), which was purified by column chromatography (hexane/ethyl acetate: 2/1) to afford benzyl 2,3,4-tri-*O*-benzyl-6-*O*-trityl-D-glucopyranoside (**80**) as a pale yellow wax (2.12 g, 2.71 mmol, 76%, α:β 1:1.9).

All analytical data is in good agreement with published data.[231]

IR (neat) cm^{-1}: 3062 (w), 3030 (w), 2876 (w), 1494, 1449, 1068.

^{1}H-NMR ($CDCl_3$, 400 MHz): δ 7.56–7.52 (m, 11H, Ar), 7.50–7.43 (m, 13H, Ar), 7.39–7.16 (m, 72H, Ar), 6.88–6.85 (m, 5H, Ar), 5.08 (d, ^2J = 11.8 Hz, 1.9H, β, O−*CH*$_2$−Ph), 5.02 (d, ^2J = 11.0 Hz, 1.9H, β, O−*CH*$_2$−Ph), 4.97 (d, ^2J = 10.7 Hz, 1H, α, O−*CH*$_2$−Ph), 4.95 (d, ^3J(H1,H2) = 3.7 Hz, 1H, α, H-1), 4.90 (d, ^2J = 10.8 Hz, 1H, β, O−*CH*$_2$−Ph), 4.81 (d, ^2J = 11.4 Hz, 1H, α, O−*CH*$_2$−Ph), 4.79 ('d', ^2J = 11.3 Hz, 4.8H, 2β/α, 3 O−*CH*$_2$−Ph), 4.77 (d, ^2J = 11.7 Hz, 1.9H, β, O−*CH*$_2$−Ph), 4.72 (d, ^2J = 11.9 Hz, 1H, α, O−*CH*$_2$−Ph), 4.70 (d, ^2J = 10.3 Hz, 2.9H, β/2α, 3× O−*CH*$_2$−Ph), 4.64 (d, ^2J = 12.2 Hz, 1H, α, O−*CH*$_2$−Ph), 4.63 (d, ^2J = 12.0 Hz, 1H, α, O−*CH*$_2$−Ph), 4.56 (d, ^3J(H1, H2) = 7.4 Hz, 1.9H, β, H-1), 4.37 (d, ^2J = 10.4 Hz, 1.8H, β, O−*CH*$_2$−Ph), 4.30 (d, ^2J = 10.4 Hz, 1H, α, O−*CH*$_2$−Ph), 4.02 ('t', ^3J(H3,H2) = 9.6 Hz, ^3J(H3,H4) = 8.9 Hz, 1H, α, H-3), 3.87 (ddd, ^3J(H5,H4) = 10.4 Hz, ^3J(H5,H6b) = 4.4 Hz, ^3J(H5,H6a) = 1.8 Hz, 1H, α, H-5), 3.83 ('t', ^3J(H4,H5) = 9.9 Hz, ^3J(H4,H3) = 8.5 Hz, 1.8H, β, H-4), 3.67 ('t', ^3J(H4, H5) = 10.2 Hz, ^3J(H4,H3) = 9.1 Hz, 1H, α, H-4), 3.66–3.58 (m, 6.6H, β/α, H-2; β H-3; β, H-6a), 3.46 (dd, ^2J(H6a,H6b) = 10.1 Hz, ^3J(H6a,H5) = 1.9 Hz, 1H, α, H-6a), 3.42 (ddd,

^3J(H5,H4) = 9.9 Hz, ^3J(H5,H6b) = 3.9 Hz, ^3J(H5,H6a) = 1.8 Hz, 2.0H, β, H-5), 3.27 (dd, ^2J(H6b,H6a) = 10.1 Hz, ^3J(H6b,H5) = 4.0 Hz, 1.9H, β, H-6b), 3.19 (dd, ^2J(H6b,H6a) = 10.1 Hz, ^3J(H6b,H5) = 4.4 Hz, 1H, α, H-6b).

^{13}C-NMR ($CDCl_3$, 100 MHz): δ 144.12 (q, α, Trt C-1), 144.09 (q, β, Trt C-1), 138.71 (q, Ar), 138.68 (q, Ar), 138.00 (q, Ar), 137.53 (q, Ar), 129.00 (4 Ar), 128.97 (2 Ar), 128.86 (Ar), 128.59 (2 Ar), 128.57 (2 Ar), 128.55 (2 Ar), 128.52 (2 Ar), 128.36 (2 Ar), 128.32 (3 Ar), 128.27 (Ar), 128.22 (2 Ar), 128.19 (2 Ar), 128.02 (Ar), 127.99 (Ar), 127.96 (4 Ar), 127.94 (2 Ar), 127.88 (Ar), 127.84 (Ar), 127.81 (Ar), 127.13 (2 Ar), 127.10 (Ar), 102.41 (β, C-1), 94.79 (α, C-1), 86.55 (q, β, $-O\underline{C}Ph_3$), 86.47 (q, α, $-O\underline{C}Ph_3$), 84.90 (β, C-3), 82.74 (β, C-2), 82.51 (α, C-3), 80.37 (α, C-2), 78.31 (α, C-4), 78.07 (β, C-4), 76.14 (α, O$-CH_2-$Ph), 76.11 (β, O$-CH_2-$Ph), 75.23 (α, O$-CH_2-$Ph), 75.18 (β, O$-CH_2-$Ph), 75.12 (β, O$-CH_2-$Ph), 74.80 (β, C-5), 73.12 (α, O$-CH_2-$Ph), 70.86 (β, O$-CH_2-$Ph), 70.71 (α, C-5), 68.76 (α, O$-CH_2-$Ph), 62.61 (β/α, C-6).

NSI-MS *m/z* (%): 800 (100, [M+NH_4^+]), 243 ([Trt^+]).

HRMS-NSI *m/z*: Calc. for $C_{53}H_{54}O_6N$ [M+NH_4^+]: 800.3946, found: 800.3925.

Benzyl 2,3,4-tri-*O*-benzyl-D-glucopyranoside

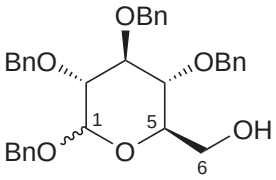

81

To a solution of 6-trityl glucoside **80** (434 mg, 0.56 mmol) in dry DCM (6 ml) was added a solution of $AlCl_3$ (110 mg, 0.833 mmol, 1.5 eq.) in dry Et_2O(2.5 ml). The resulting bright yellow solution was stirred at room temperature for 3 h. The reaction was quenched with saturated $NaHCO_3$ solution and diluted with Et_2O. The aqueous phase was extracted with Et_2O and the combined organic phases washed twice each with saturated $NaHCO_3$, water and then brine. After drying over Na_2SO_4, evaporation gave a yellowish oil which slowly crystallised as a pale yellow solid (418 mg). The crude sugar was purified by column chromatography (hexane/ethyl acetate: 10/0 → 9/1 → 3/1) to give benzyl 2,3,4-tri-*O*-benzyl-D-glucopyranoside (**81**) as a colourless solid (218 mg, 0.40 mmol, 72%, α:β 1:1.3).

All spectroscopic data is in good agreement with published data.[231] Melting point data does not match the melting point of either anomer.[288]

Melting point: m.p. 78−91 °C (lit. m.p. 101−103 °C (β anomer), m.p. 86−87 °C (α anomer)).[288]

IR (neat) cm^{-1}: 3358 (br), 3064 (w), 3030 (w), 2920 (w), 2870 (w), 1497, 1453, 1358, 1066, 1026.

^{1}H-NMR ($CDCl_3$, 400 MHz): δ 7.41–7.28 (m, 44H, Ar), 5.01 (d, ^2J = 10.9 Hz, 1H, α, O−*CH*$_2$−Ph), 4.95 (d, ^2J = 11.0 Hz, 1.3H, β, O−*CH*$_2$−Ph), 4.93 (d, ^2J = 10.8 Hz, 1.3H, β, O−*CH*$_2$−Ph), 4.92 (d, ^2J = 11.9 Hz, 1.3H, β, O−*CH*$_2$−Ph), 4.89 (d, ^2J = 10.9 Hz, 1H, α, O−*CH*$_2$−Ph), 4.86 (d, ^2J = 10.6 Hz, 1.3H, β, O−*CH*$_2$−Ph), 4.84 (d, ^2J = 10.9 Hz, 1H, α, O−*CH*$_2$−Ph), 4.81 (d, ^2J = 10.7 Hz, 1.3H, β, O−*CH*$_2$−Ph), 4.80 (d, ^3J(H1,H2) = 3.7 Hz, 1H, α, H-1), 4.73 (d, ^2J = 10.8 Hz, 1.3H, β, O−*CH*$_2$−Ph), 4.70 (d, ^2J = 11.9 Hz, 1.3H, β, O−*CH*$_2$−Ph), 4.69 (d, ^2J = 11.8 Hz, 1H, α, O−*CH*$_2$−Ph), 4.68 (d, ^2J = 12.1 Hz, 1H, α, O−*CH*$_2$−Ph), 4.64 (d, ^2J = 10.9 Hz, 1H, α, O−*CH*$_2$−Ph), 4.64 (d, ^2J = 10.8 Hz, 1.3H, β, O−*CH*$_2$−Ph), 4.57 (d, ^3J(H1,H2) = 7.8 Hz, 1H, β, H-1), 4.56 (d, ^2J = 11.9 Hz, 1H, α, O−*CH*$_2$−Ph), 4.55 (d, ^2J = 12.1 Hz, 1H, α, O−*CH*$_2$−Ph), 4.07 ('t', ^3J(H3,H2) = 9.6 Hz, ^3J(H3,H4) = 9.4 Hz, 1H, α, H-3), 3.87 (broad d, J = 11.9 Hz, 1.4H, β, H-6a), 3.73–3.65 (m, 5.6H, β, H-3; α, H-5; α, H-6a; β/α, H-6b), 3.57 ('t', ^3J(H4,H5) = 9.7 Hz, ^3J(H4,H3) = 9.1 Hz, 1.3H, β, H-4), 3.54 ('t', ^3J(H4,H3) = 9.4 Hz, ^3J(H4,H5) = 8.9 Hz, 1H, α, H-4), 3.50 (dd, ^3J(H2,H3) = 9.6 Hz, ^3J(H2,H1) = 3.7 Hz, 1H, α, H-2), 3.49 (dd, ^3J(H2,H3) = 9.0 Hz, ^3J(H2,H1) = 7.8 Hz, 1.3H, β, H-2), 3.36 (ddd, ^3J(H5,H4) = 9.7 Hz, ^3J(H5,H6a) = 4.6 Hz, ^3J(H5,H6b) = 2.8 Hz, 1.3H, β, H-5), 1.82 (br, 1H, OH) 1.55 (br s, OH).

^{13}C-NMR ($CDCl_3$, 100 MHz): δ 138.77 (q, Ar), 138.47 (q, Ar), 138.27 (q, Ar), 138.09 (q, Ar), 137.93 (q, Ar), 137.43 (q, Ar), 137.25 (q, Ar), 137.05 (q, Ar), 128.49 (2 Ar), 128.40 (3 Ar), 128.37 (Ar), 128.14 (Ar), 128.10 (Ar), 128.07 (Ar), 127.94 (3 Ar), 127.88 (Ar), 127.80 (Ar), 127.71 (Ar), 127.65 (Ar), 127.60 (Ar), 102.83 (β, C-1), 95.56 (α, C-1), 84.53 (β, C-3), 82.33 (β, C-2), 81.94 (α, C-3), 80.00 (α, C-2), 77.55 (β, C-4), 77.21 (α, C-4), 75.73 (β/α, 2 O−*CH*$_2$−Ph), 75.10 (α, O−*CH*$_2$−Ph), 75.07 (β, O−*CH*$_2$−Ph), 75.02 (β, C-5), 74.99 (β, O−*CH*$_2$−Ph), 73.08 (α, O−*CH*$_2$−Ph), 71.68 (β, O−*CH*$_2$−Ph), 70.95 (α, C-5), 69.26 (α, O−*CH*$_2$−Ph), 62.08 (β, C-6), 61.81 (α, C-6).

NSI-MS *m/z* (%): 1103 (15, [2M+Na^+]), 1098 (15, [2M+NH_4^+]), 563 (37, [M+Na^+]), 558 (100, [M+NH_4^+]).

HRMS-NSI *m/z*: Calc. for $C_{34}H_{40}O_6N$ [M+NH_4^+]: 558.2850, found: 558.2846.

Benzyl 2,3,4-tri-*O*-benzyl-D-glucopyranoside 6-methanesulfonate

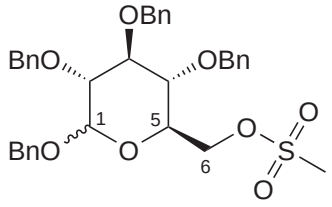

82

Benzyl 2,3,4-tri-*O*-benzyl-D-glucopyranoside (**81**) (162 mg, 0.3 mmol, α:β 1:2.25) was dissolved in dry DCM (1.5 ml) under nitrogen atmosphere and cooled to 0 °C in an ice-bath. Triethylamine (64 µl, 0.45 mmol, 1.5 eq.) was added before addition of methanesulfonyl chloride (28 µl, 0.36 mmol, 1.2 eq.). The reaction was stirred at 0 °C for 35 min before dilution with DCM. The solution was washed twice with water and once with saturated $NaHCO_3$ solution. Drying over Na_2SO_4 and evaporation gave benzyl 2,3,4-tri-*O*-benzyl-D-glucopyranoside 6-methanesulfonate (**82**) as a whitish oil which solidified as a pale yellow solid over night (165 mg, 0.27 mmol, 89%, α:β 1:2.25).

All spectroscopic data is in good agreement with published data.[289] Melting point data does not match the reported melting point for the pure β anomer.[289]

Melting point: m.p. 81−96 °C (lit. m.p. 101−103 °C (β anomer)).[289]

IR (neat) cm^{-1}: 3031 (w), 2935 (w), 1732 (w), 1497 (w), 1455, 1361, 1177, 1059, 990.

^{1}H-NMR ($CDCl_3$, 400 MHz): δ 7.38–7.27 (m, 60H, Ar), 5.03 (d, ^2J = 10.9 Hz, 1H, α, O−*CH₂*−Ph), 4.96–4.88 (m, 10.2H, α, 4× β, O−*CH₂*−Ph), 4.83 (d, ^2J = 10.9 Hz, 1H, α, O−*CH₂*−Ph), 4.82 (d, ^3J(H1,H2) = 3.3 Hz, 1H, α, H-1), 4.80 (d, ^2J = 10.9 Hz, 2.3H, β, O−*CH₂*−Ph), 4.72 (d, ^2J = 10.9 Hz, 2.4H, β, O−*CH₂*−Ph), 4.68 (d, ^2J = 12.1 Hz, 3.3H, α/β, O−*CH₂*−Ph), 4.67 (d, ^2J = 12.0 Hz, 1H, α, O−*CH₂*−Ph), 4.62 (br d, 3.3H, α/β, O−*CH₂*−Ph), 4.58 (d, ^2J = 12.2 Hz, 1H, α, O−*CH₂*−Ph), 4.55 (d, ^2J = 11.3 Hz, 1H, α, O−*CH₂*−Ph), 4.54 (d, ^3J(H1,H2) = 7.7 Hz, 2.5H, β, H-1), 4.47 (dd, ^3J(H6a,H6b) = 11.3 Hz, ^3J(H6a,H5) = 1.2 Hz, 2.4H, β, H-6a), 4.35 ('ddd', ^2J = 11.4 Hz, ^3J = 4.0 Hz, ^3J = 1.8 Hz, 3.3H, β, H-6b; α, H-6a), 4.21 (dd, ^2J(H6b,H6a) = 11.1 Hz, ^3J(H6b,H5) = 1.9 Hz, 1H, α, H-6b), 4.07 (t, ^3J = 9.2 Hz, 1H, β, H-3), 3.86 (ddd, ^3J(H5,H4) = 10.1 Hz, ^3J(H5,H6a) = 4.0 Hz, ^3J(H5,H6b) = 1.8 Hz, 1H, α, H-5), 3.67 (t, ^3J = 8.7 Hz, β, H-3), 3.57–3.47 (m, 8.8H, β, H-2, H-4, H-5; α, H-2, H-4), 3.02 (s, 6.8H, β ,−SO_2CH_3), 2.97 (s, 3H, α ,−SO_2CH_3).

^{13}C-NMR ($CDCl_3$, 100 MHz): δ 138.37 (q, Ar), 138.25 (q, 2 Ar), 138.06 (q, Ar), 137.83 (q, Ar), 137.65 (q, Ar), 137.13 (q, Ar), 137.00 (q, Ar), 128.81 (2 Ar), 128.78 (Ar), 128.74 (2 Ar), 128.68 (4 Ar), 128.63 (2 Ar), 128.40 (3 Ar), 128.38 (2 Ar), 128.34 (Ar), 128.22 (Ar), 128.20 (2 Ar), 128.15 (Ar), 128.11 (Ar), 128.08 (2 Ar), 128.01 (Ar), 128.00 (Ar), 102.65 (β, C-1), 95.86 (α, C-1), 84.49 (β, C-3), 82.24 (β, C-2), 81.97 (α, C-3), 79.92 (α, C-2), 76.94 (α/β, C-4), 75.94 (β, O−*CH₂*−Ph), 75.91 (α, O−*CH₂*−Ph), 75.32 (α/β, 2 O−*CH₂*−Ph), 75.15 (β, O−*CH₂*−Ph), 73.29 (α, O−*CH₂*−Ph), 72.94 (β, C-5), 71.66 (β, O−*CH₂*−Ph), 69.83 (α, O−*CH₂*−Ph), 69.02 (α, C-5), 68.58 (β, C-6), 68.36 (α, C-6), 37.84 (β, $-SO_2CH_3$), 37.68 (α, $-SO_2CH_3$).

NSI-MS *m/z* (%): 1254 (13, [2M+NH_4^+]), 636 (100, [M+NH_4^+]).

HRMS-NSI *m/z*: Calc. for $C_{35}H_{42}O_8SN$ [M+NH_4^+]: 636.2626, found: 636.2620.

Benzyl 6-azido-2,3,4-tri-*O*-benzyl-6-deoxy-D-glucopyranoside

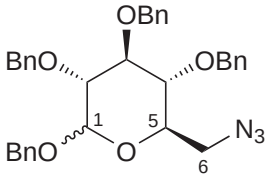

75

Method A – From 6-methanesulfonate: Benzyl 2,3,4-tri-*O*-benzyl-D-glucopyranoside 6-methanesulfonate (**82**) (92 mg, 150 µmol) and sodium azide (31 mg, 480 µmol, 3.2 eq.) were dissolved in non-dry DMF (1.5 ml). The reaction mixture was heated to 110 °C for 15 hours and then diluted with water and extracted with ethyl acetate (3×). The combined organic phases were washed with brine and dried over Na_2SO_4. Evaporation gave benzyl 6-azido-2,3,4-tri-*O*-benzyl-6-deoxy-D-glucopyranoside (**75**) as pale orange solid (77 mg, 136 µmol, 91%, 81% over both steps from **81**).

Method B – One-pot reaction from 6-hydroxy sugar: Benzyl 2,3,4-tri-*O*-benzyl-D-glucopyranoside (**81**) (216 mg, 0.4 mmol) was dissolved in dry DCM (3 ml) and cooled to −10 °C under nitrogen atmosphere. Triethylamine (84 µl, 0.6 mmol, 1.5 eq.) was added and then methanesulfonyl chloride (37 µl, 0.48 µmol, 1.2 eq.) was added slowly to the reaction mixture. The reaction mixture was stirred at −10 °C for 30 min, when TLC (hexane/ethyl acetate: 3/1) showed full conversion of the starting material. The reaction mixture was then evaporated to dryness and re-dissolved in non-dry DMF (3 ml). Sodium azide (130 mg, 2 mmol, 5 eq.) was added and the reaction mixture heated to 120 °C for 17 hours. The reaction mixture was diluted with saturated $NaHCO_3$ and extracted with ethyl acetate.

The organic phase was washed with brine and dried over Na_2SO_4. Evaporation gave a waxy orange solid (215 mg) which was purified by column chromatography (hexane/ethyl acetate: 10/1) to give benzyl 6-azido-2,3,4-tri-*O*-benzyl-6-deoxy-D-glucopyranoside (**75**) as an off-white solid (149 mg, 265 µmol, 66% over two steps).

Melting point: m.p. 60−84 °C.

IR (neat) cm^{-1}: 3066 (w), 3029 (w), 2922, 2856, 2097 ($-N_3$), 1497, 1454, 1358, 1283, 1099, 1067, 1027.

^{1}H-NMR ($CDCl_3$, 400 MHz): δ 7.43–7.22 (m, 65H, Ar), 5.01 (d, ^2J = 10.8 Hz, 1H, α, 3-O−*CH₂*−Ph), 4.97 (d, ^2J = 11.0 Hz, 4.4H, β, 1-O−*CH₂*−Ph, 2-O−*CH₂*−Ph), 4.94 (d, ^2J = 10.6 Hz, 2.4H, β, 3-O−*CH₂*−Ph), 4.90 (d, ^2J = 10.8 Hz, 1H, α, 4-O−*CH₂*−Ph), 4.87 (d, ^2J = 11.5 Hz, 2.4H, β, 4-O−*CH₂*−Ph), 4.84 (d, ^3J(H1,H2) = 3.7 Hz, 1H, α, H-1), 4.81 (d, ^2J = 11.0 Hz, 1H, α, 3-O−*CH₂*−Ph), 4.77 (d, ^2J = 10.8 Hz, 2.4H, β, 3-O−*CH₂*−Ph), 4.72 ('d', ^2J = 12.4 Hz, ^2J = 10.9 Hz, 3.3H, α, 1-O−*CH₂*−Ph; β, 2-O−*CH₂*−Ph), 4.67 (d, ^2J = 11.7 Hz, 2.4H, β, 1-O−*CH₂*−Ph), 4.65 (d, ^2J = 11.9 Hz, 1H, α, 2-O−*CH₂*−Ph), 4.57 ('d', ^2J = 11.9 Hz, ^2J = 10.8 Hz, 2H, α, 1-O−*CH₂*−Ph, 4-O−*CH₂*−Ph), 4.56 (d, ^2J = 11.3 Hz, 2.3H, β, 4-O−*CH₂*−Ph), 4.55 (d, ^3J(H1,H2) = 8.0 Hz, 2.3H, β, H-1), 4.54 (d, ^2J = 11.9 Hz, 1H, α, 2-O−*CH₂*−Ph), 4.04 (t, ^3J(H3,H2,4) = 9.3 Hz, 1H, α, H-3), 3.85 (ddd, ^3J(H5,H4) = 9.7 Hz, ^3J(H5,H6b) = 5.4 Hz, ^3J(H5,H6a) = 2.8 Hz, 1H, α, H-5), 3.65 ('t', ^3J(H3,H2) = 9.2 Hz, ^3J(H3,H4) = 8.5 Hz, 2.4H, β, H-3), 3.54 (dd, ^3J(H2,H3) = 9.2 Hz, ^3J(H2,H1) = 3.8 Hz, 1H, α, H-2), 3.53 (dd, ^3J(H2,H3) = 9.3 Hz, ^3J(H2,H1) = 7.9 Hz, 2.3H, β, H-2), 3.50 (ddd, ^3J(H5,H4) = 9.2 Hz, ^3J(H5,H6b) = 6.3 Hz, ^3J(H5,H6a) = 2.3 Hz, 2.3H, β, H-5), 3.44 ('t', 3.3H, β, ^3J(H4,H2,4) = 9.2 Hz, H-4; α, ^3J(H4,H5) = 9.7 Hz, ^3J(H4,H3) = 9.2 Hz, H-4), 3.39 (dd, ^2J(H6a,H6b) = 13.2 Hz, ^3J(H6a,H5) = 2.4 Hz, 2.3H, β, H-6a), 3.36 (dd, ^2J(H6a,H6b) = 12.9 Hz, ^3J(H6a,H5) = 2.8 Hz, 1H, α, H-6a), 3.33 (dd, ^2J(H6b, H6a) = 13.1 Hz, ^3J(H6b,H5) = 6.3 Hz, 2.3H, β, H-6b), 3.30 (dd, ^2J(H6b,H6a) = 12.8 Hz, ^3J(H6b,H5) = 5.3 Hz, 1H, α, H-6b).

^{13}C-NMR ($CDCl_3$, 100 MHz): δ 138.76 (q, α, Ar), 138.47 (q, β, Ar), 138.36 (q, β, Ar), 138.11 (q, α, Ar), 138.02 (q, α, Ar), 137.80 (q, β, Ar), 137.21 (q, β, Ar), 137.02 (q, α, Ar), 128.64 (2 Ar), 128.61 (Ar), 128.58 (2 Ar), 128.56 (Ar), 128.53 (3 Ar), 128.49 (2 Ar), 128.28 (2 Ar), 128.24 (2 Ar), 128.19 (2 Ar), 128.15 (Ar), 128.11 (Ar), 128.05 (Ar), 128.00 (3 Ar), 127.94 (Ar), 127.84 (Ar), 127.82 (Ar), 127.76 (Ar), 102.33 (β, C-1), 95.31 (α, C-1), 84.57 (β, C-3), 82.38 (β, C-2), 81.95 (α, C-3), 80.08 (α, C-2), 78.51 (α, C-4), 78.48 (β, C-4), 75.85 (α/β, 3-O−*CH₂*−Ph), 75.31 (α, 4-O−*CH₂*−Ph), 75.20 (β, 4-O−*CH₂*−Ph), 75.05 (β, 2-O−*CH₂*−Ph), 74.92 (β, C-5), 73.11 (α, 2-O−*CH₂*−Ph), 71.25 (β, 1-O−*CH₂*−Ph), 70.40 (α, C-5), 69.39 (α, 1-O−*CH₂*−Ph), 51.56 (β, C-6), 51.47 (α, C-6).

NSI-MS *m/z* (%): 624 (42, [M+ACN+NH_4^+]), 604 (17, [M+K^+]), 588 (25, [M+Na^+]), 583 (100, [M+NH_4^+]).

HRMS-NSI *m/z*: Calc. for $C_{34}H_{39}N_4O_5$ [M+NH_4^+]: 583.2915, found: 583.2911.

3-(Benzyloxy)-2-methyl-1-(prop-2-ynyl)pyridin-4(1*H*)-one

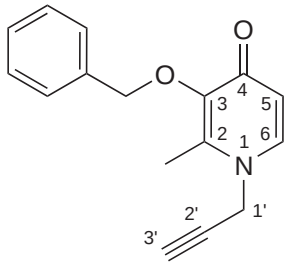

85

Benzyl maltol **33** (216 mg, 1 mmol) and propargylamine (130 µl, 2.0 mmol) were dissolved in a water/methanol mixture (5 ml). Reaction mixture was adjusted to pH 12 with 1M NaOH and then heated to reflux over night. The solution was adjusted to pH 1 with HCl and extracted with Et_2O. The organic phase was discarded and the aqueous phase was adjusted to pH 12, then extracted with DCM. The organic phase was washed with water, then dried over Na_2SO_4. Evaporation gave a brown gum (63 mg), which was a mixture of compounds but did not contain the desired product.

3-(Benzyloxy)-1-(2-hydroxyethyl)-2-methylpyridin-4(1*H*)-one

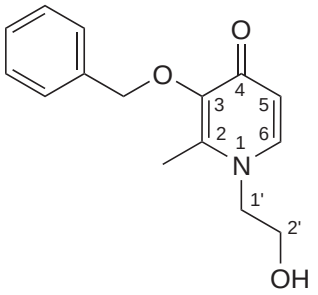

83

Ethanolamine (3 ml, 50 mmol) was added to a solution of benzyl maltol **33** (4.0 g, 18.5 mmol) in methanol (20 ml) and 1M NaOH (10 ml). The reaction mixture was heated to reflux over night (18 hours), then concentrated *in vacuo*. Upon acidifying the solution with HCl, 3-(benzyloxy)-1-(2-hydroxyethyl)-2-methylpyridin-4(1*H*)-one (**83**) precipitated as a cream

coloured powder, which was collected by vacuum filtration. Further product was isolated by concentrating the mother liquor (3.1 g, 10.3 mmol, 56%, as HCl salt).

All analytical data is in agreement with published data.[199,290,291]

Melting point: m.p. 200−202 °C (lit. m.p. 205−206 °C).[199]

IR (neat) cm^{-1}: 3295, 1636, 1519, 1491, 1344, 1266,1241, 1076, 1033, 968.

^{1}H-NMR (CD_3OD, 400 MHz): δ 8.30 (d, ^3J(H6,H5) = 7.1 Hz, 1H, H-6), 7.45–7.41 (m, 2H, Ph H-3,5), 7.40–7.37 (m, 3H, Ph H-2,4,6), 7.20 (d, ^3J(H5,H6) = 7.1 Hz, 1H, H-5), 5.18 (s, 2H, O−*CH*$_2$−Ph), 4.45 (t, ^3J(H1',H2') = 5.0 Hz, 2H, H-1'), 3.87 (t, ^3J(H2',H1') = 5.0 Hz, 2H, H-2'), 2.51 (s, 3H, CH_3).

3-(Benzyloxy)-2-methyl-1-[2-(prop-2-ynyloxy)ethyl]pyridin-4(1*H*)-one

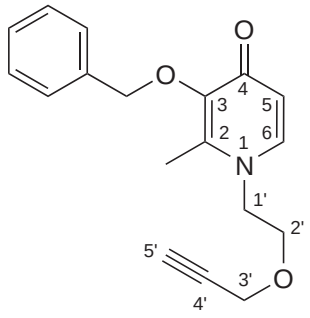

84

Under nitrogen atmosphere, pyridinone **83** (1.18 g, 4 mmol) was dissolved in dry DMF (20 ml). Tetrabutylammonium iodide (148 mg, 0.4 mmol, 10%mol) was added and the cloudy solution cooled to −10 °C, then sodium hydride (60% suspension, 400 mg, 10 mmol, 2.5 eq.) was added in portions and the solution left to stir for 30 min. Propargyl bromide (80% solution in toluene, 560 µl, 5 mmol, 1.25 eq.) was added via a syringe and the reaction mixture was stirred at −10 °C for 1 hour before it was allowed to warm to room temperature and stir over night. The reaction was quenched by addition of saturated NH_4Cl solution and extracted with chloroform (2×). The combined organic phases were washed with water and brine before drying over Na_2SO_4. Evaporation gave a brown oil (900 mg) which was purified by column chromatography (chloroform/methanol: 20/1 → 10/1 → 6/1) to give 3-(benzyloxy)-2-methyl-1-[2-(prop-2-ynyloxy)ethyl]pyridin-4(1*H*)-one (**84**) as a pale brown oil (774 mg, 2.6 mmol, 65%).

IR (neat) cm^{-1}: 3285 (br), 2869 (br), 2109 (w), 1624, 1559, 1520, 1496, 1353, 1248, 1216, 1160, 1098.

^{1}H-NMR ($CDCl_3$, 400 MHz): δ 7.41 ('dd', 2H, Ph H-3,5), 7.35–7.29 (m, 3H, Ph H-2,4,6), 7.24 (d, ^3J(H6,H5) = 7.6 Hz, 1H, H-6), 6.41 (d, ^3J(H5,H6) = 7.6 Hz, 1H, H-5), 5.22 (s, 2H, O−*CH*$_2$−Ph), 4.09 (d, ^4J(H3',H5') = 2.4 Hz, 2H, H-3'), 3.96 (t, ^3J(H1',H2') = 5.2 Hz, 2H, H-1'), 3.69 (t, ^3J(H2',H1') = 5.2 Hz, 2H, H-2'), 2.43 (t, ^4J(H5',H3') = 2.4 Hz, 1H, H-5'), 2.11 (s, 3H, CH_3).

^{13}C-NMR ($CDCl_3$, 100 MHz): δ 173.60 (C-4), 146.10 (C-3), 141.08 (C-2), 138.85 (C-6), 137.85 (Ph C-1), 129.16 (Ph C-3,5), 128.24 (Ph C-2,6), 127.94 (Ph C-4), 117.18 (C-5), 78.59 (C-4'), 75.38 (C-5'), 73.01 (O−*CH*$_2$−Ph), 68.27 (C-2'), 58.65 (C-3'), 52.90 (C-1'), 12.73 (CH_3).

NSI-MS *m/z* (%): 617 (17, [2M+Na^+]), 595 (26, [2M+H^+]), 298 (100, [M+H^+]).

HRMS-NSI *m/z*: Calc. for $C_{18}H_{20}NO_3$ [M+H^+]: 298.1438; found: 298.1438.

1-Benzyl-4-(phenoxymethyl)-1*H*-1,2,3-triazole

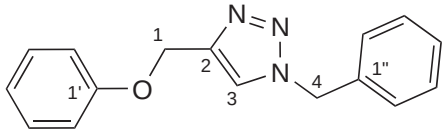

88

Phenyl propargyl ether (128 µl, 1 mmol) and benzyl azide (125 µl, 1 mmol) were dissolved in tBuOH/water (3 ml). Ascorbic acid (20.2 mg, 11.5 µmol, 12%mol), 1M NaOH (100 µl, 100 µmol, 10%mol) and 1M copper sulfate (50 µl, 50 µmol, 5%mol) were added to the reaction mixture, which was heated in a sealed tube at 60 °C for 1 hour. The reaction mixture was diluted with water (10 ml) and 10% aqueous ammonia (2 ml) and stirred for 10 min. The formed precipitate was collected by vacuum filtration and dried over P_4O_{10} to give the desired triazole **88** as olive green powder (224 mg, 0.84 mmol, 84%).

Analytical data is in good agreement with published data.[292]

IR (neat) cm^{-1}: 3134 (w), 2924 (w), 1598, 1585, 1487, 1467, 1457, 1429, 1383, 1332, 1292, 1240, 1219, 1178, 1120, 1054, 1030, 1007, 988.

^{1}H-NMR ($CDCl_3$, 400 MHz): δ 7.53 (s, 1H), 7.40–7.35 (m, 3H), 7.30–7.25 (m, 4H), 6.99–6.94 (m, 3H), 5.53 (s, 2H), 5.19 (s, 2H).

1-(2,3,4,6-Tetra-*O*-acetyl-β-D-glucopyranosyl)-4-(phenoxymethyl)-1*H*-1,2,3-triazole

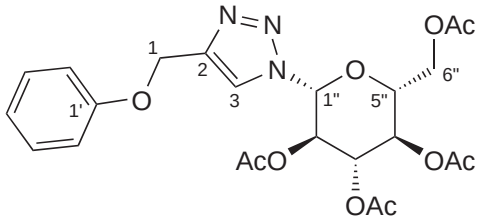

89

Phenyl propargyl ether (31 µl, 250 µmol) and azido glucoside **73** (93 mg, 250 µmol) were dissolved in a tBuOH/water mixture (1.5 ml). Then, ascorbic acid (5 mg, 28 µmol, 11%mol), 1M NaOH (25 µl, 25 µmol, 10%mol) and 1M copper sulfate (12.5 µl, 12.5 µmol, 5%mol) were added to the reaction mixture, which was subsequently heated in a sealed tube at 60 °C for 22 hours. TLC (hexane/ethyl acetate: 5/1) showed full conversion of phenyl propargyl ether. Water (5 ml) was added to the reaction mixture, which led to the formation of a gel. This gel was dissolved with ethyl acetate and partitioned with dilute ammonia. The aqueous phase was extracted twice with ethyl acetate and the combined organic phases were washed with saturated $NaHCO_3$ and brine, then dried over Na_2SO_4. Evaporation gave 1-(2,3,4,6-tetra-*O*-acetyl-β-D-glucopyranosyl)-4-(phenoxymethyl)-1*H*-1,2,3-triazole (**89**) as off-white solid (118 mg, 233 µmol, 93%).

Spectral data is in good agreement with published data.[292]

Melting point: m.p. 106−108 °C (lit. m.p. 142−143 °C).[292]

^{1}H-NMR ($CDCl_3$, 400 MHz): δ 7.86 (s, 1H, H-3), 7.33–7.28 (m, 2H, H-3',5'), 7.01–6.96 (m, 3H, H-2',4',6'), 5.89 (d, ^3J(H1",H2") = 8.8 Hz, 1H, H-1"), 5.48–5.39 (m, 2H, H-2",3"), 5.27–5.20 (m, 3H, H-1, H-4"), 4.30 (dd, ^3J(H6a",H6b") = 12.6 Hz, ^3J(H6a",H5") = 5.0 Hz, 1H, H-6a"), 4.15 (dd, ^3J(H6b",H6a") = 12.6 Hz, ^3J(H6b",H5") = 2.0 Hz, 1H, H-6b"), 4.00 (ddd, ^3J(H5",H4") = 10.1 Hz, ^3J(H5",H6a") = 5.0 Hz, ^3J(H5",H6b") = 2.0 Hz, 1H, H-5"), 2.09 (s, 3H, CH_3), 2.07 (s, 3H, CH_3), 2.03 (s, 3H, CH_3), 1.85 (s, 3H, CH_3).

^{13}C-NMR ($CDCl_3$, 100 MHz): δ 170.49 (C=O), 169.91 (C=O), 169.32 (C=O), 168.89 (C=O), 158.04 (C-1'), 145.11 (C-2), 129.54 (C-3',5'), 121.34 (C-4'), 121.03 (C-3), 114.77 (C-2',6'), 85.73 (C-1"), 75.14 (C-5"), 72.62 (C-3"), 70.19 (C-2"), 67.63 (C-4"), 61.75 (C-1), 61.49 (C-6"), 20.68 (CH_3), 20.52 (CH_3), 20.50 (CH_3), 20.11 (CH_3).

NSI-MS *m/z* (%): 1033 (14, [2M+Na^+]), 1011 (55, [2M+H^+]), 528 (15, [M+Na^+]), 506 (100, [M+H^+]), 331 (28, [PhOCH_2triazolyl]).

HRMS-NSI *m/z*: Calc. for $C_{23}H_{28}N_3O_{10}$ [M+H^+]: 506.1769; found: 506.1770.

4-(Phenoxymethyl)-1*H*-1,2,3-triazole

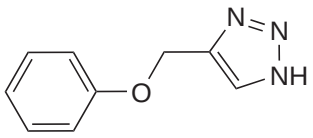

110

Triazole **88** (50 mg, 190 µmol) was dissolved in DCM (5 ml) and boiled with activated charcoal for 10 min, then filtered and evaporated; residual solvent was co-evaporated with methanol. The residue was then dissolved in methanol (5 ml) and Pd/C (10% wt., 5 mg) was added. The suspension was shaken in a Parr shaker under hydrogen atmosphere (2 bar) over night. The reaction mixture was filtered through a pad of celite and evaporated to give the unreacted starting material **88** as off-white solid.

1-{2-[(1-Benzyl-1*H*-1,2,3-triazol-4-yl)methoxy]ethyl}-3-(benzyloxy)-2-methylpyridin-4(1*H*)-one

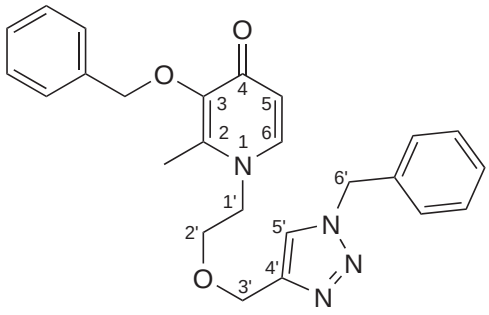

90

Alkyne **84** (149 mg, 0.5 mmol) and benzyl azide (62 µl, 0.5 mmol) were dissolved in a tBuOH/water mixture (1.5 ml). Then, ascorbic acid (9.7 mg, 55 µmol, 11%mol), 1M NaOH (50 µl, 50 µmol, 10%mol) and 1M copper sulfate (25 µl, 25 µmol, 5%mol) were added to the reaction mixture which was subsequently heated in a sealed tube at 60 °C for 20 hours. The reaction mixture was diluted with 5% ammonia and the solution stirred for 5 min, then further diluted with water and extracted with ethyl acetate (2×). The combined organic phases were washed with water and brine, then dried over Na_2SO_4. Evaporation gave the desired triazole **90** as pale tan plates (187 mg, 0.44 mmol, 87%).

Melting point: m.p. 118−121 °C.

IR (neat) cm^{-1}: 3033 (w), 2965 (w), 2926 (w), 1733 (w), 1626, 1570, 1528, 1494, 1455, 1246, 1216, 1123, 1085, 1058.

^{1}H-NMR ($CDCl_3$, 400 MHz): δ 7.42–7.34 (m, 5H, OBn), 7.33–7.26 (m, 5H, ArBn), 7.22 (s, 1H, H-5'), 7.13 (d, ^3J(H6,H5) = 7.5 Hz, 1H, H-6), 6.33 (d, ^3J(H5,H6) = 7.5 Hz, 1H, H-5), 5.51 (s, 2H, H-6'), 5.21 (s, 2H, O−*CH*$_2$−Ph), 4.52 (s, 2H, H-3'), 3.89 (t, ^3J(H1',H2') = 5.1 Hz, 2H, H-1'), 3.68 (t, ^3J(H2',H1') = 5.1 Hz, 2H, H-2'), 2.06 (s, 3H, 2-CH_3).

^{13}C-NMR ($CDCl_3$, 100 MHz): δ 173.50 (C-4), 146.15 (C-3), 144.55 (C-4'), 140.73 (C-2), 138.97 (C-6), 137.65 (OBn C-1), 134.48 (ArBn C-1), 129.16 (OBn C-3,5), 129.08 (OBn C-2,6), 128.82 (OBn C-4), 128.25 (ArBn C-2,3,5,6), 127.97 (ArBn C-4), 122.48 (C-5'), 116.83 (C-5), 72.94 (O−*CH*$_2$−Ph), 68.12 (C-2'), 64.38 (C-3'), 54.25 (C-6'), 53.02 (C-1'), 12.64 (2-CH_3).

1-{2-[(1*H*-1,2,3-Triazol-4-yl)methoxy]ethyl}-3-hydroxy-2-methylpyridin-4(1*H*)-one

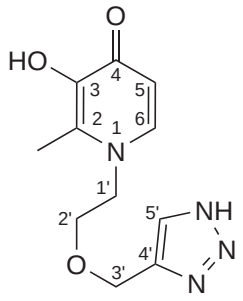

111

Method A: Hydrogenation Triazole **90** (99 mg, 230 µmol) and Pd/C (10% wt., 3 mg) were taken up in methanol (5 ml) and the suspension shaken over night (16 hours) in a Parr shaker under hydrogen atmosphere (2 bar, pressure dropped to 0.5 bar over night). TLC (chloroform/methanol: 6/1) showed no conversion, the reaction mixture was acidified with HCl, then hydrogenated for 20 hours, but no reaction occurred. The reaction mixture was then filtered through a pad of celite (previously washed with HCl) and evaporated to give a pale brown wax, which was redissolved in DCM and boiled with activated charcoal (10 mg) for 15 min. After filtration and evaporation, the residue was dissolved in methanol (5 ml) and Pd/C (10% wt., 5 mg) was added before shaking in a Parr shaker under hydrogen atmosphere (2 bar) for 18 hours. Filtration through a pad of celite and evaporation afforded the unreacted starting material **90**.

Method B: Boron tribromide Triazole **90** (99 mg, 230 µmol) was dissolved in dry DCM (6 ml) under nitrogen atmosphere and cooled in an ice-bath. Boron tribromide (1M solution in DCM, 1.8 ml) was added slowly via a syringe and the reaction mixture stirred for 10 min at 0 °C, then allowed to warm to room temperature and stirred for 2 days. The reaction mixture was quenched by the slow addition of methanol (10 ml) and stirred for 1 hour before evaporation and drying under high vacuum. The residue was purified by reverse phase chromatography (Lichroprep RP-18 resin, gradient 0.05 M TEAB/methanol: 100/0 → 70/30) The product-containing fractions were combined, evaporated *in vacuo* and freeze dried. The residue contained only 3-(benzyloxy)-1-(2-hydroxyethyl)-2-methylpyridin-4(1*H*)-one (**83**).

1-(2-{[1-(2,3,4,6-Tetra-*O*-acetyl-β-D-glucopyranosyl)-1*H*-1,2,3-triazol-4-yl]methoxy}ethyl)-3-(benzyloxy)-2-methylpyridin-4(1*H*)-one

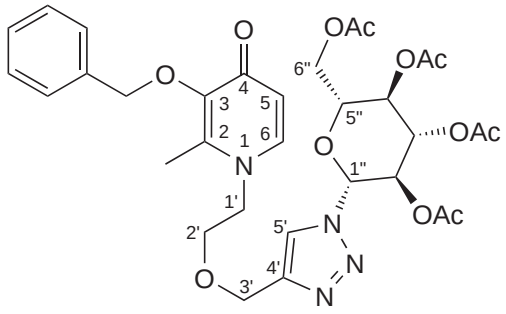

91

Alkyne **84** (358 mg, 1.2 mmol) and 1-azido glucoside **73** (447 mg, 1.2 mmol, 1 eq.) were dissolved in tBuOH (2 ml) and water (1 ml). Ascorbic acid (21.1 mg, 120 µmol), 1M NaOH (120 µl, 120 µmol) and 1M copper sulfate (60 µl, 60 µmol) were added and the reaction mixture was then heated in a sealed tube at 60 °C for 18 hours. Thin layer chromatography (chloroform/methanol: 6/1) showed only one spot with a similar R_f value as the alkyne. This spot did not stain when treated with $KMnO_4$ solution, indicating the consumption of the starting material and formation of a new product. The reaction mixture was diluted with water and then extracted with chloroform (2×). The combined organic phases were washed twice with water and once with brine, before drying over Na_2SO_4. Evaporation gave a brown waxy solid (1.1 g), which was purified by column chromatography (chloroform/methanol: 20/1), yielding 1-(2-{[1-(2,3,4,6-tetra-*O*-acetyl-β-D-glucopyranosyl)-1*H*-1,2,3-triazol-4-yl]methoxy}ethyl)-3-(benzyloxy)-2-methylpyridin-4(1*H*)-one (**91**) as off-white foam (685 mg, 1.04 mmol, 85%).

Melting point: m.p. 72−78 °C.

IR (neat) cm^{-1}: 1745, 1626, 1563, 1366, 1211, 1095, 1034.

^{1}H-NMR ($CDCl_3$, 400 MHz): δ 7.58 (s, 1H, H-5'), 7.43–7.39 (m, 2H, Ph H-3,5), 7.33–7.26 (m, 3H, Ph H-2,4,6), 7.23 (d, ^3J(H6,H5) = 7.5 Hz, 1H, H-6), 6.40 (d, ^3J(H5,H6) = 7.5 Hz, 1H, H-5), 5.81 (d, ^3J(H1",H2") = 9.0 Hz, 1H, H-1"), 5.42 (t, ^3J(H3",H2") = 9.5 Hz, ^3J(H3",H4") = 9.2 Hz, 1H, H-3"), 5.35 (t, ^3J(H2",H3") = 9.5 Hz, ^3J(H2",H1") = 9.0 Hz, 1H, H-2"), 5.30 ('t', ^3J(H4",H5") = 10.1 Hz, ^3J(H4",H3") = 9.2 Hz, 1H, H-4"), 5.23 (s, 2H, O−*CH*$_2$−Ph), 4.58 (s, 2H, H-3'), 4.35 (dd, ^2J(H6a",H6b") = 12.7 Hz, ^3J(H6a",H5") = 5.1 Hz, 1H, H-6a"), 4.20 (dd, ^2J(H6b",H6a") = 12.7 Hz, ^3J(H6b",H5") = 2.0 Hz, 1H, H-6b"), 4.01 (ddd, ^3J(H5",H4") = 10.1 Hz, ^3J(H5",H6a") = 5.1 Hz, ^3J(H5",H6b") = 2.0 Hz, 1H, H-5"), 3.93 (t, ^3J(H1',H2') = 5.2 Hz, 2H, H-1'), 3.69–3.60 (m, 2H, H-2'), 2.10 (s, 3H, 2-CH_3), 2.08 (s, 3H, CH_3), 2.07 (s, 3H, CH_3), 2.03 (s, 3H, CH_3), 1.86 (s, 3H, CH_3).

^{13}C-NMR ($CDCl_3$, 100 MHz): δ 173.48 (C-4), 170.49 (C=O), 169.91 (C=O), 169.33 (C=O), 168.91 (C=O), 145.92 (C-3), 144.93 (C-4'), 140.73 (C-2), 139.04 (Ph C-1), 129.15 (Ph C-3,5), 128.22 (Ph C-2,6), 127.92 (Ph C-4), 121.00 (C-5'), 117.01 (C-5), 85.81 (C-1"), 75.32 (C-5"), 72.97 (O−*CH*$_2$−Ph), 72.43 (C-3"), 70.45 (C-2"), 68.51 (C-2'), 67.70 (C-4"), 64.41 (C-3'), 61.55 (C-6"), 52.91 (C-1'), 20.72 (CH_3), 20.55 (CH_3), 20.52 (CH_3), 20.18 (CH_3), 12.66 (2-CH_3).

NSI-MS *m/z* (%): 1341 (12, [2M+H^+]), 693 (13, [M+Na^+]), 671 (100, [M+H^+]).

HRMS-NSI *m/z*: Calc. for $C_{32}H_{39}N_4O_{12}$ [M+H^+]: 671.2559; found: 671.2553.

3-(Benzyloxy)-1-(2-{[1-(β-D-glucopyranosyl)-1*H*-1,2,3-triazol-4-yl]methoxy}-ethyl)-2-methylpyridin-4(1*H*)-one

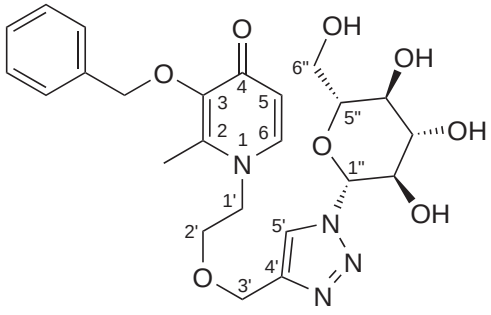

97

Triazole **91** (201 mg, 0.3 mmol) was dissolved in dry methanol (3 ml) and 1M sodium methoxide (800 µl, 0.8 mmol) was added. The reaction progress was complete after 5 min as determined by TLC (chloroform/methanol: 3/1). The reaction mixture was neutralised with 2M HCl (450 ml) and evaporated to dryness. The residue was purified by column chromatography (chloroform/methanol: $20/1 \rightarrow 10/1 \rightarrow 3/1$) to give 3-(benzyloxy)-1-(2-{[1-(β-D-glucopyranosyl)-1*H*-1,2,3-triazol-4-yl]methoxy}ethyl)-2-methylpyridin-4(1*H*)-one (**97**) as off-white foam (153 mg, 0.3 mmol, quantitative).

IR (neat) cm^{-1}: 3252 (br), 2921 (w), 1623, 1546, 1507, 1454, 1404, 1253, 1222, 1093, 1042.

^{1}H-NMR (CD_3OD, 400 MHz): δ 8.05 (s, 1H, H-5'), 7.63 (d, ^3J(H6,H5) = 7.5 Hz, 1H, H-6), 7.41–7.37 (m, 2H, Ph H-3,5), 7.35–7.30 (m, 3H, Ph H-2,4,6), 6.42 (d, ^3J(H5,H6) = 7.5 Hz, 1H, H-5), 5.58 (d, ^3J(H1",H2") = 9.2 Hz, 1H, H-1"), 5.05 (s, 2H, O$-CH_2-$Ph), 4.56 (s, 2H, H-3'), 4.16 (t, ^3J(H1',H2') = 5.0 Hz, 2H, H-1'), 3.88 (dd, ^2J(H6a",H6b") = 12.3 Hz, ^3J(H6a",H5") = 2.0 Hz, 1H, H-6a"), 3.85 ('t', ^3J(H2",H1") = 9.2 Hz, ^3J(H2",H3") = 8.9 Hz, 1H, H-2"), 3.74 (t, ^3J(H2',H1') = 5.0 Hz, 2H, H-2'), 3.71 (dd, ^2J(H6b",H6a") = 12.4 Hz, ^3J(H6b",H5") = 5.5 Hz, 1H, H-6b"), 3.57 (ddd, ^3J(H5",H4") = 9.5 Hz, ^3J(H5",H6b") = 5.4 Hz, ^3J(H5",H6a") = 2.0 Hz, 1H, H-5"), 3.55 ('t', ^3J(H3",H2") = 8.9 Hz, ^3J(H3",H4") = 8.7 Hz, 1H, H-3"), 3.49 ('t', ^3J(H4",H5") = 9.5 Hz, ^3J(H4",H3") = 8.7 Hz, 1H, H-4"), 2.18 (s, 3H, 2-CH_3).

^{13}C-NMR (CD_3OD, 100 MHz): δ 174.00 (C-4), 146.52 (C-3), 146.23 (C-2), 145.39 (C-4'), 142.18 (C-6), 138.23 (Ph C-1), 130.19 (Ph C-3,5), 129.46 (Ph C-2,6), 129.40 (Ph C-4), 124.48 (C-5'), 116.73 (C-5), 89.40 (C-1"), 81.06 (C-5"), 78.34 (C-3"), 74.69 (O$-CH_2-$Ph), 73.99 (C-2"), 70.87 (C-4"), 69.85 (C-2'), 64.82 (C-3'), 62.28 (C-6"), 54.88 (C-1'), 13.31 (2-CH_3).

NSI-MS *m/z* (%): 525 (11, [M+Na^+]), 503 (100, [M+H^+]), 371 (42).

HRMS-NSI *m/z*: Calc. for $C_{24}H_{31}N_4O_8$ [M+H^+]: 503.2136; found: 503.2132.

1-(2-{[1-(2,3,4,6-Tetra-*O*-acetyl-β-D-glucopyranosyl)-1*H*-1,2,3-triazol-4-yl]methoxy}ethyl)-3-hydroxy-2-methylpyridin-4(1*H*)-one

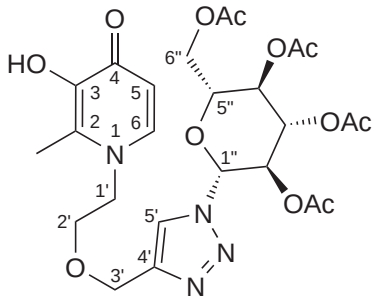

96

To a solution of triazole **91** (101 mg, 150 µmol) in methanol (10 ml) was added Pd/C (10% wt., 3 mg). The suspension was shaken in a Parr shaker under hydrogen atmosphere (2 bar) over night, then filtered through a pad of celite (previously washed with HCl) and evaporated to give a colourless glass. The residue was re-dissolved in dilute methanolic HCl, evaporated and dried under high vacuum to give 1-(2-{[1-(2,3,4,6-tetra-*O*-acetyl-β-D-glucopyranosyl)-1*H*-1,2,3-triazol-4-yl]methoxy}ethyl)-3-hydroxy-2-methylpyridin-4(1*H*)-one (**96**) as colourless glass (62 mg, 108 µmol, 71%).

IR (neat) cm^{-1}: 3265 (br), 2922 (w), 1634, 1506, 1335, 1250, 1092, 1025.

^{1}H-NMR (CD_3OD, 400 MHz): δ 8.10–7.80 (br, 2H, H-6, H-5'), 7.28–7.17 (br, 1H, H-5), 6.06–5.89 (br, 1H, H-1"), 5.50–5.35 (m, 2H, H-2",3"), 5.28 ('t', 1H, H-4"), 4.70–4.60 (br, 2H, H-3'), 4.61–4.45 (br, 2H, H-1'), 4.37–4.29 (m, 1H, H-6a"), 4.28–4.20 (m, 1H, H-6b"), 4.18–4.11 (m, 1H, H-5") 4.10–3.90 (br, 2H, H-2'), 2.62 (br s, 3H, 2-CH_3), 2.09 (s, 3H, CH_3), 2.07 (s, 3H, CH_3), 2.04 (s, 3H, CH_3), 1.88 (s, 3H, CH_3).

^{13}C-NMR (CD_3OD, 100 MHz): δ 170.56 (C=O), 169.87 (C=O), 169.40 (C=O), 169.02 (C=O), 158.49 (C-4), 143.27 (C-3), 142.24 (C-2), 142.21 (C-4'), 138.12 (C-6), 122.16 (C-5'), 112.12 (C-5), 85.77 (C-1"), 75.08 (C-5"), 72.35 (C-3"), 70.50 (C-2"), 67.82 (C-2'), 67.58 (C-4"), 63.77 (C-3'), 61.47 (C-6"), 56.32 (C-1'), 20.75 (CH_3), 20.53 (2x CH_3), 20.24 (CH_3), 13.44 (2-CH_3).

NSI-MS *m/z* (%): 1169 (16), 1127 (27), 1085 (12), 603 (30, [M+Na^+]), 581 (100, [M+H^+]), 539 (55, [M-Ac+H^+]).

HRMS-NSI *m/z*: Calc. for $C_{25}H_{33}N_4O_{12}$ [M+H^+]: 581.2089; found: 581.2082.

1-(2-{[1-(β-D-Glucopyranosyl)-1*H*-1,2,3-triazol-4-yl]methoxy}ethyl)-3-hydroxy-2-methylpyridin-4(1*H*)-one

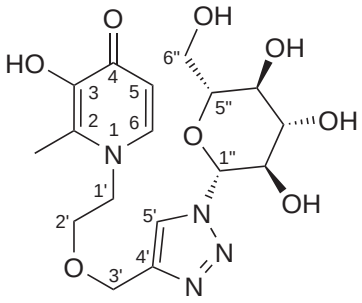

98

In a solution of triazole **97** (130 mg, 260 µmol) in methanol (5 ml) and concentrated hydrochloric acid (7 drops) was suspended Pd/C (10% wt., 3 mg). The reaction mixture was shaken in a Parr shaker under hydrogen atmosphere (2 bar) over night (18 hours), then filtered through a pad of celite (previously washed with HCl) and evaporated and dried under high vacuum to give 1-(2-{[1-(β-D-glucopyranosyl)-1*H*-1,2,3-triazol-4-yl]methoxy}-ethyl)-3-hydroxy-2-methylpyridin-4(1*H*)-one (**98**) as a pale yellow foam (120 mg, 260 µmol, quantitative, as HCl salt).

Melting point: m.p. 61−70 °C.

IR (neat) cm^{-1}: 3264 (w), 2922 (w), 1634, 1537 (w), 1505, 1335, 1250, 1093, 1025.

^{1}H-NMR (CD_3OD, 400 MHz): δ 8.10 (s, 1H, H-5'), 8.01 (d, ^3J(H6,H5) = 7.0 Hz, 1H, H-6), 7.01 (d, ^3J(H5,H6) = 7.0 Hz, 1H, H-5), 5.57 (d, ^3J(H1",H2") = 9.2 Hz, 1H, H-1"), 4.59 (s, 2H, H-3'), 4.57–4.53 (m, 2H, H-1'), 3.95 (t, ^3J(H2',H1') = 4.9 Hz, 2H, H-2'), 3.94 (dd, ^2J(H6a",H6b") = 12.1 Hz, ^3J(H6a",H5") = 2.1 Hz, 1H, H-6a"), 3.84 (t, ^3J(H2",H1") = 9.2 Hz, ^3J(H2",H3") = 9.0 Hz, 1H, H-2"), 3.74 (dd, ^2J(H6b",H6a") = 12.1 Hz, ^3J(H6b",H5") = 5.8 Hz, 1H, H-6b"), 3.60 (ddd, ^3J(H5",H4") = 9.7 Hz, ^3J(H5",H6b") = 5.8 Hz, ^3J(H5", H6a") = 2.1 Hz, 1H, H-5"), 3.56 (t, ^3J(H3",H2") = 9.0 Hz, ^3J(H3",H4") = 8.8 Hz, 1H, H-3"), 3.47 ('t', ^3J(H4",H3") = 9.7 Hz, ^3J(H4",H5") = 8.9 Hz, 1H, H-4"), 2.61 (s, 3H, 2-CH_3).

^{13}C-NMR (CD_3OD, 100 MHz): δ 159.66 (C-4), 145.16 (C-3), 144.74 (C-2), 143.69 (C-4'), 139.75 (C-6), 124.42 (C-5'), 111.34 (C-5), 89.55 (C-1"), 81.16 (C-5"), 78.47 (C-3"), 74.02 (C-2"), 70.97 (C-4"), 69.17 (C-2'), 64.59 (C-3'), 62.45 (C-6"), 57.17 (C-1'), 13.05 (2-CH_3).

NSI-MS *m/z* (%): 435 (17, [M+Na^+]), 413 (92, [M+H^+]), 251 (100, [M-Glc+H^+]).

HRMS-NSI *m/z*: Calc. for $C_{17}H_{25}N_4O_8$ [M+H^+]: 413.1667; found: 413.1662.

1-(2-{[1-(1,3,4,6-Tetra-*O*-acetyl-2-deoxy-D-glucopyranos-2-yl)-1*H*-1,2,3-triazol-4-yl]methoxy}ethyl)-3-(benzyloxy)-2-methylpyridin-4(1*H*)-one

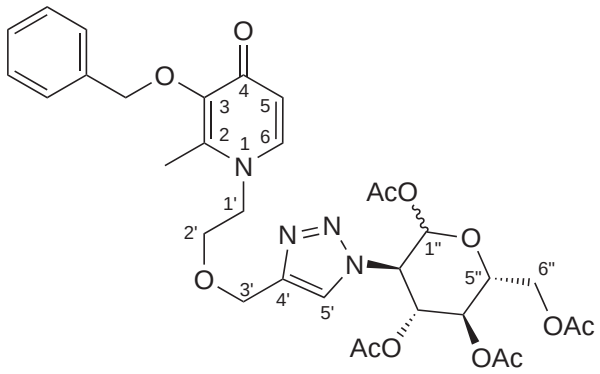

92

The azido sugar **74** (250 mg, 0.67 mmol) and alkyne **84** (230 mg, 0.77 mmol, 1.15 eq.) were each dissolved in tBuOH (1.5 ml), the two solutions were combined and diluted with water (3 ml) to form a pale yellow, cloudy solution. Ascorbic acid (14 mg, 80 µmol, 12%mol), 1M NaOH (80 µl, 80 µmol, 12%mol) and 1M copper sulfate (40 µl, 40 µmol, 6%mol) were added and the reaction mixture was then heated to 60 °C in a sealed tube for 23 hours. The reaction mixture was diluted with water (50 ml) and extracted with chloroform (2× 25 ml). The combined organic phases were washed twice with water and once with brine, then dried over Na_2SO_4. Evaporation gave a brown waxy residue (523 mg), which was purified by column chromatography (first column: chloroform/methanol: 100/0 → 20/1 → 10/1 → 5/1; second column: 100/0 → 50/1 → 20/1) to give 1-(2-{[1-(1,3,4,6-tetra-*O*-acetyl-2-deoxy-D-glucopyranos-2-yl)-1*H*-1,2,3-triazol-4-yl]methoxy}ethyl)-3-(benzyloxy)-2-methylpyridin-4(1*H*)-one (**92**) as white foam (378 mg, 0.56 mmol, 84%, α:β 1:1.8).

Melting point: m.p. 70−77 °C.

IR (neat) cm^{-1}: 1746, 1626, 1564, 1366, 1210, 1034.

^{1}H-NMR ($CDCl_3$, 400 MHz): δ 7.56 (s, 1H, α, H-5'), 7.44 (s, 2H, β, H-5'), 7.36–7.22 (m, 19H, H-6, Ph H-2–6), 6.55 (d, ^3J(H5,H6) = 7.4 Hz, 2H, β, H-5), 6.52 (d, ^3J(H5,H6) = 7.8 Hz, 1H, α, H-5), 6.30 (d, ^3J(H1",H2") = 3.6 Hz, 1H, α, H-1"), 6.10 (d, ^3J(H1",H2") = 8.7 Hz, 2H, β, H-1"), 5.86 (dd, ^3J(H3",H2") = 11.3 Hz, ^3J(H3",H4") = 9.3 Hz, 1H, α, H-3"), 5.60 (dd, ^3J(H3",H2") = 10.7 Hz, ^3J(H3",H4") = 9.3 Hz, 2H, β, H-3"), 5.21 (dd, ^3J = 10.1 Hz, ^3J = 9.5 Hz, 1H, α), 5.17–5.03 (m, 6H, O−CH_2−Ph), 4.63 (dd, ^3J(H2",H3") = 10.7 Hz, ^3J(H2",H1") = 8.7 Hz, 2H, β, H-2"), 4.50 (s, 3H, β/α, H-3'), 4.48 (d, J = 2.6 Hz, 2H), 4.36–4.26 (m, 4H), 4.16 (ddd, J = 10.1 Hz, J = 4.1 Hz, J = 2.0 Hz, 2H), 4.07 (ddd,

J = 12.5 Hz, J = 8.1 Hz, J = 5.2 Hz, J = 2.1 Hz, 3H), 3.98–3.91 (m, 5H, β/α, H-2'), 3.60 (t, ^3J = 5.1 Hz, 5H, β/α, H-1'), 2.10 (s, 6H, β, 2-CH_3), 2.09 (s, 3H, α, 2-CH_3), 2.05 (s, 3H, α, CH_3), 2.04 (s, 5H, β, CH_3), 2.03 (s, 3H, α, CH_3), 2.00 (s, 3H, α, CH_3), 1.96 (s, 5H, β, CH_3), 1.89 (s, 5H, β, CH_3), 1.78 (s, 5H, β, CH_3), 1.77 (s, 3H, α, CH_3).

^{13}C-NMR ($CDCl_3$, 100 MHz): δ 172.88 (β/α, C-4), 170.74 (C=O), 170.70 (C=O), 169.93 (C=O), 169.72 (C=O), 169.69 (C=O), 169.46 (C=O), 169.30 (C=O), 168.20 (C=O), 145.89 (β/α, C-3), 144.93 (β/α, C-4'), 144.71 (β/α, C-2), 139.75 (β or α, C-6), 139.52 (β or α, C-6), 137.57 (β or α, Ph C-1), 137.55 (β or α, Ph C-1), 129.20 (β or α, Ph C-3,5), 129.16 (β or α, Ph C-3,5), 128.47 (β or α, Ph C-2,6), 128.45 (β or α, Ph C-2,6), 128.24 (β/α, Ph C-4), 122.15 (β, C-5'), 122.09 (α, C-5'), 116.74 (β/α, C-5), 91.61 (β, C-1"), 90.10 (α, C-1"), 73.32 (β/α, O−*CH₂*−Ph), 72.98 (β, C-5"), 72.14 (β, C-3"), 70.06 (α, C-3"), 69.05 (α, C-5"), 68.76 (α, C-2') 68.70 (β, C-2'), 68.19 (α, C-4"), 67.88 (β, C-4"), 64.77 (β, C-3'), 64.70 (α, C-3'), 63.32 (β/α, C-2"), 61.48 (β, C-6"), 61.40 (α, C-6") 53.53 (β, C-1'), 53.36 (α, C-1'), 20.89 (β or α, CH_3), 20.87 (β or α, CH_3), 20.83 (β or α, CH_3), 20.69 (β or α, CH_3), 20.68 (β/α, CH_3), 20.47 (β or α, CH_3), 20.39 (β or α, CH_3), 12.97 (β/α, 2-CH_3).

NSI-MS *m/z* (%): 671 (100, [M+H$^+$]), 693 (13, [M-Ac+Na$^+$]).

HRMS-NSI *m/z*: Calc. for $C_{32}H_{39}N_4O_{12}$ [M+H$^+$]: 671.2559; found: 671.2541.

3-(Benzyloxy)-1-(2-{[1-(2-deoxy-D-glucopyranos-2-yl)-1*H*-1,2,3-triazol-4-yl]-methoxy}ethyl)-2-methylpyridin-4(1*H*)-one

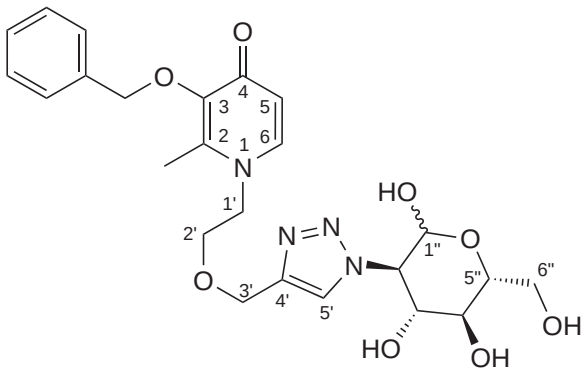

100

The triazole **92** (149 mg, 222 µmol) was dissolved in dry methanol (3 ml), then 1M sodium methoxide (400 µl, 400 µmol) was added and the reaction mixture stirred at room temperature for 30 min. The reaction was quenched by the addition of 2M HCl (200 µl)

and then evaporated to give crude product (137 mg), which was purified by column chromatography (chloroform/methanol: 6/1) to give 3-(benzyloxy)-1-(2-{[1-(2-deoxy-D-glucopyranos-2-yl)-1*H*-1,2,3-triazol-4-yl]methoxy}ethyl)-2-methylpyridin-4(1*H*)-one (**100**) as a colourless glass (30 mg, 60 µmol, 27%).

Melting point: m.p. 95−109 °C.

IR (neat) cm^{-1}: 3252 (br), 1623, 1547, 1506, 1455 (w), 1252, 1220, 1079, 1033.

^{1}H-NMR (CD_3OD, 400 MHz): δ 8.08 (s, 1H, β or α, H-5'), 7.92 (s, 1H, β or α, H-5'), 7.64 (d, ^3J(H6,H5) = 7.4 Hz, 2H, β/α, H-6), 7.41–7.28 (m, 10H, β/α, Ph H-2–6), 6.42 (d, ^3J(H5,H6) = 7.4 Hz, 2H, β/α, H-5), 5.26 (d, ^3J(H1",H2") = 3.3 Hz, 1H, α, H-1"), 5.11 (d, ^3J(H1",H2") = 8.2 Hz, 1H, β, H-1"), 5.05 (s, 4H, O−*CH*$_2$−Ph), 4.64 (dd, ^3J(H2",H3") = 10.9 Hz, ^3J(H2",H1") = 3.4 Hz, 1H, α, H-2"), 4.58–4.52 (m, 4H, β/α, H-3"), 4.19–4.11 (m, 5H, β/α, H-1'; β, H-2"), 3.99–3.78 (m, 6H, α, H-3",4",5",6"; β, H-5",6"), 3.77–3.70 (m, 5H, β/α, H-2',6"), 3.63 (dd, ^3J = 9.8 Hz, ^3J = 8.8 Hz, 1H, α, H-4"), 3.57–3.46 (m, 2H, β, H-3",4"), 2.19 (s, 6H, 2-CH_3).

^{13}C-NMR (CD_3OD, 100 MHz): δ 174.92 (C-4), 146.84 (C-3), 145.52 (β or α, C-4'), 154.50 (β or α, C-4'), 145.01 (C-2), 141.88 (C-6), 138.47 (Ph C-1), 130.21 (Ph C-2,6), 129.41 (Ph C-3,5), 129.31 (Ph C-4), 126.48 (β or α, C-5'), 124.55 (β or α, C-5'), 116.98 (C-5), 96.09 (β, C-1"), 92.55 (α, C-1"), 85.27 (β, C-5"), 81.81 (α, C-5"), 78.12 (β, C-3"), 74.53 (O−*CH*$_2$−Ph), 73.32 (α, C-3"), 72.08 (α, C-4"), 71.92 (β, C-4"), 69.96 (β or α, C-2'), 69.88 (β or α, C-2'), 68.65 (β, C-2"), 65.80 (α, C-2"), 65.07 (β or α, C-3'), 64.99 (β or α, C-3'), 62.45 (β or α, C-6"), 62.21 (β or α, C-6"), 54.64 (C-1'), 13.13 (2-CH_3).

NSI-MS *m/z* (%): 517 (100, [M+14m/z]), 503 (8, [M+H^+]).

HRMS-NSI *m/z*: Calc. for $C_{24}H_{31}N_4O_8$ [M+H^+]: 503.2136; found: 503.2132.

1-(2-{[1-(2-Deoxy-D-glucopyranos-2-yl)-1*H*-1,2,3-triazol-4-yl]methoxy}ethyl)-3-hydroxy-2-methylpyridin-4(1*H*)-one

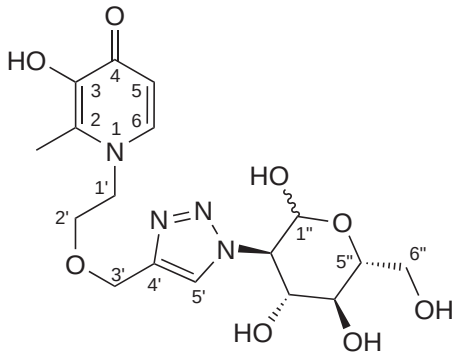

101

The triazole **92** (80 mg, 119 µmol) was dissolved in methanol (5 ml) and acidified with HCl, then Pd/C (10% wt., 7 mg) was added and the suspension was shaken in a Parr shaker under hydrogen atmosphere (2 bar) for 74 hours, then left at room room temperature for 1 day. Filtration through a pad of celite and evaporation gave an off-white residue which was purified by column chromatography over a very short column (chloroform/methanol: 6/1) to give 1-(2-{[1-(2-deoxy-D-glucopyranos-2-yl)-1*H*-1,2,3-triazol-4-yl]methoxy}ethyl)-3-hydroxy-2-methylpyridin-4(1*H*)-one (**101**) as a colourless gummy syrup (49 mg, 109 µmol, 92%).

Melting point: m.p. 54−73 °C.

IR (neat) cm^{-1}: 3219 (br), 2922 (w), 1634, 1535 (w), 1505, 1333, 1251, 1024.

^{1}H-NMR (CD_3OD, 400 MHz): δ 8.22 (s, 1H, β or α, H-5), 8.16 (s, 1H, β or α, H-5), 8.12 (d, ^3J(H6,H5) = 6.9 Hz, 2H, β/α, H-6), 7.12 (d, ^3J(H5,H6) = 6.9 Hz, 2H, β/α, H-5), 5.32 (d, ^3J(H1",H2") = 3.3 Hz, 1H, β/α, H-1"), 5.12 (d, ^3J(H1",H2") = 8.1 Hz, 1H, β/α, H-1"), 4.70–4.64 (m, 5H, β/α, H-3'; α, H-2"), 4.61 ('t', 4H, β/α, H-1'), 4.27 (dd, ^3J(H3",H2") = 10.5 Hz, ^3J(H3",H4") = 8.6 Hz, 1H, α, H-3"), 4.21 (dd, ^3J(H2",H3") = 10.4 Hz, ^3J(H2", H1") = 8.0 Hz, 1H, β, H-2"), 4.11 (dd, ^3J(H3",H2") = 10.4 Hz, ^3J(H3",H4") = 7.9 Hz, 1H, β, H-3"), 3.99–3.91 (m, 6H, β, H-2',6a"; α, H-2',5"), 3.85 (dd, ^3J(H6a",H6b") = 12.0 Hz, ^3J(H6a",H5") = 2.4 Hz, 1H, α, H-6a"), 3.79 (dd, ^3J(H6b",H6a") = 12.0 Hz, ^3J(H6b",H5") = 4.9 Hz, 1H, α, H-6b"), 3.75 (dd, ^3J(H6b",H6a") = 12.0 Hz, ^3J(H6b",H5") = 5.2 Hz, 1H, β, H-6b"), 3.55 (dd, ^3J(H4",H5") = 9.8 Hz, ^3J(H4",H3") = 8.6 Hz, 1H, α, H-4", overlapping), 3.53 (ddd, ^3J(H5",H4") = 9.6 Hz, ^3J(H5",H6b") = 5.3 Hz, ^3J(H5",H6a") = 2.1 Hz, 1H, β, H-5", overlapping), 3.48 (dd, ^3J(H4",H5") = 9.6 Hz, ^3J(H4",H3") = 7.9 Hz, 1H, β, H-4", overlapping), 2.63 (s, 6H, 2-CH_3).

^{13}C-NMR (CD_3OD, 100 MHz): δ 159.76 (β/α, C-4), 144.75 (β/α, C-2,3), 143.79 (β/α, C-4'), 143.75 (β or α, C-4'), 140.01 (β/α, C-6), 127.08 (β or α, C-5'), 125.54 (β or α, C-5'), 111.44 (β or α, C-5), 111.42 (β or α, C-5), 96.03 (β, C-1"), 92.42 (α, C-1"), 78.23 (β, C-5"), 75.40 (β, C-3"), 73.32 (α, C-5"), 72.31 (α, C-4"), 72.11 (β, C-4"), 71.63 (α, C-3"), 70.16 (β, C-2"), 69.38 (β/α, C-2'), 67.46 (α, C-2"), 64.38 (β or α, C-3'), 64.28 (β or α, C-3'), 62.55 (β or α, C-6"), 62.39 (β or α, C-6"), 57.12 (β/α, C-1'), 13.15 (β/α, 2-CH_3).

NSI-MS *m/z* (%): 497 (26, [M+2Ac+H^+]), 455 (100, [M+Ac+H^+]), 413 (67, [M+H^+]).

HRMS-NSI *m/z*: Calc. for $C_{17}H_{25}N_4O_8$ [M+H^+]: 413.1667, found: 413.1661.

1-(2-{[1-(1,2,3,4-Tetra-*O*-benzyl-6-deoxy-D-glucopyranos-6-yl)-1*H*-1,2,3-triazol-4-yl]methoxy}ethyl)-3-(benzyloxy)-2-methylpyridin-4(1*H*)-one

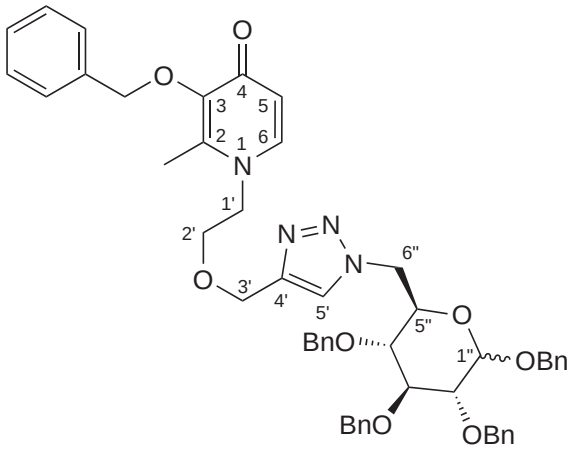

93

Alkyne **84** (89 mg, 0.3 mmol) and 6-azido sugar **75** (170 mg, 0.3 mmol) were dissolved in tBuOH (2 ml) and water (2 ml), then ascorbic acid (5.3 mg, 30 µmol, 10%mol), 1M NaOH (30 µl) and 1M copper sulfate (15 µl, 15 µmol, 5%mol) were added. The reaction mixture was heated to 60 °C in a sealed tube for 20 hours, then diluted with water and extracted with chloroform. The combined organic phases were washed with water, 1M NaOH and brine before drying over Na_2SO_4. Evaporation gave the crude product as brown solid (238 mg) which was purified by column chromatography (chloroform/methanol: 50/1 → 20/1), yielding pure 1-(2-{[1-(1,2,3,4-tetra-*O*-benzyl-6-deoxy-D-glucopyranos-6-yl)-1*H*-1,2,3-triazol-4-yl]methoxy}ethyl)-3-(benzyloxy)-2-methylpyridin-4(1*H*)-one (**93**) as a pale yellow, waxy solid (154 mg, 199 µmol, 66%, α:β 1:1.4).

Melting point: <40 °C.

IR (neat) cm^{-1}: 3030 (w), 2869 (w), 1626, 1571, 1496, 1454, 1322, 1250, 1213, 1068.

^{1}H-NMR ($CDCl_3$, 400 MHz): δ 7.43 (s, 2.7H, H-5'), 7.41–7.24 (m, 67H, Ar), 7.17 (d, ^3J(H6,H5) = 7.5 Hz, 2.5H, H-6), 6.42 (d, ^3J(H5,H6) = 6.4 Hz, 2.4H, H-5), 5.20 (s, 5.1H, 3-O−*CH₂*−Ph), 4.99 (d, ^2J = 10.6 Hz, 1H, α, O−*CH₂*−Ph), 4.92 (d, ^2J = 10.8 Hz, 1H, α, O−*CH₂*−Ph), 4.91 (d, ^2J = 11.0 Hz, 2.4H, β, O−*CH₂*−Ph), 4.86 (d, ^2J = 10.5 Hz, 2.2H, β, O−*CH₂*−Ph), 4.81–4.75 (m, ^3J(H1",H2") = 3.5 Hz, 5.2H, β, 2 O−*CH₂*−Ph; α, O−*CH₂*−Ph, H-1"), 4.73–4.67 (m, 4.1H, α, O−*CH₂*−Ph; β, 2 O−*CH₂*−Ph), 4.65–4.60 (m, 3.5H, α, 2 O−*CH₂*−Ph; β, H-6a") 4.57–4.48 (m, 10.1H, α, O−*CH₂*−Ph, H-3', H-6a"; β, 2 O−*CH₂*−Ph, H-3', H-6b"), 4.46 (d, ^3J(H1",H2") = 7.8 Hz, 1.4H, β, H-1"), 4.43 (dd, ^2J(H6b",H6a") = 14.5 Hz, ^3J(H6b,H5) = 2.9 Hz, 1H, α, H-6b"), 4.31 (d, ^2J = 11.8 Hz, 1H, α, O−*CH₂*−Ph), 4.05 ('t', ^3J(H3",H2") = 9.6 Hz, ^3J(H3",H4") = 8.8 Hz, 1H, α, H-3"), 4.00 (ddd, ^3J(H5",H4") = 9.9 Hz, ^3J(H5",H6a") = 6.0 Hz, ^3J(H5",H6b") = 2.8 Hz, 1H, α, H-5"), 3.91–3.86 (m, 4.7H, H-1'), 3.70 (t, ^3J(H2',H1') = 5.1 Hz, 4.7H, H-2'), 3.68–3.61 (m, ^3J(H5",H4") = 9.7 Hz, ^3J(H3",H2") = 9.2 Hz, ^3J(H3",H4") = 9.0 Hz, ^3J(H5",H6a") = 5.8 Hz, ^3J(H5",H6b") = 2.8 Hz, 3.6H, β, H-3", H-5"), 3.42–3.37 (m, 2.4H, α, ^3J(H2",H3") = 9.6 Hz, ^3J(H2",H1") = 3.4 Hz, H-2"; β, ^3J(H2",H3") = 9.2 Hz, ^3J(H2",H1") = 7.8 Hz, H-2"), 3.18 (dd, ^3J(H4",H5") = 9.6 Hz, ^3J(H4",H3") = 9.0 Hz, 1.5H, β, H-4"), 3.11 (dd, ^3J(H4",H5") = 9.9 Hz, ^3J(H4",H3") = 8.8 Hz, 1.5H, α, H-4"), 2.07 (s, 7.7H, 3-CH_3).

^{13}C-NMR ($CDCl_3$, 100 MHz): δ 171.58 (q, C-4), 145.85 (q, C-3), 143.88 (q, C-4'), 141.06 (q, C-1), 139.06 (C-6), 138.42 (q, Ar), 138.14 (q, Ar), 137.96 (q, Ar), 137.79 (q, Ar), 137.58 (q, Ar), 137.02 (q, Ar), 136.67 (q, Ar), 129.07 (2 Ar), 128.55 (2 Ar), 128.50 (Ar), 128.47 (2 Ar), 128.44 (Ar), 128.40 (Ar), 128.30 (Ar), 128.28 (2 Ar), 128.12 (Ar), 128.08 (2 Ar), 128.04 (Ar), 127.98 (2 Ar), 127.91 (2 Ar), 127.85 (Ar), 127.82 (Ar), 127.80 (Ar), 124.62 (β, C-5'), 124.34 (α, C-5'), 116.74 (C-5), 102.46 (β, C-1"), 95.30 (α, C-1"), 84.44 (β, C-3"), 82.08 (β, C-2"), 81.86 (α, C-3"), 79.93 (α, C-2"), 77.92 (α, C-4"), 77.70 (β, C-4"), 75.81 (O−*CH₂*−Ph), 75.80 (O−*CH₂*−Ph), 75.06 (O−*CH₂*−Ph), 74.98 (O−*CH₂*−Ph), 74.92 (O−*CH₂*−Ph), 73.08 (3-O−*CH₂*−Ph), 73.04 (β, C-5"), 72.99 (O−*CH₂*−Ph), 71.40 (O−*CH₂*−Ph), 69.35 (α, O−*CH₂*−Ph), 69.27 (α, C-5"), 68.37 (α, C-2'), 68.30 (β, C-2'), 64.41 (α, C-3'), 64.31 (β, C-3'), 53.14 (C-1'), 50.65 (β, C-6"), 50.59 (α, C-6"), 12.69 (2-CH_3).

NSI-MS *m/z* (%): 885 (14, [M+Na^+]), 863 (100, [M+H^+]), 355 (13).

HRMS-NSI *m/z*: Calc. for $C_{52}H_{55}N_4O_8$ [M+H^+]: 863.4014, found: 863.4006.

3-(Benzyloxy)-1-(2-{[1-(6-deoxy-D-glucopyranos-6-yl)-1*H*-1,2,3-triazol-4-yl]methoxy}ethyl)-2-methylpyridin-4(1*H*)-one

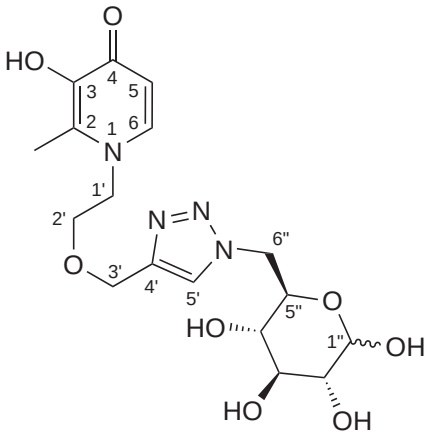

102

Method A: Hydrogenation The triazole **93** (111 mg, 128 µmol) was dissolved in methanol (5 ml) and chloroform (0.5 ml), Pd/C (10%wt., 10 mg) was added and the reaction was shaken under hydrogen atmosphere (2 bar) in a Parr shaker for 17 hours. Filtration of the reaction mixture through a pad of celite and evaporation gave a crude material which was unreacted starting material **112**, as confirmed by NMR.

Method B: Boron tribromide The triazole **93** (111 mg, 128 µmol) was dissolved in dry DCM (3 ml) under nitrogen atmosphere. The solution was cooled on an ice-bath and boron tribromide (1M solution in DCM, 2 ml) was added slowly. The reaction mixture was stirred at 0 °C for 10 min, then at room temperature for 2.5 hours before quenching by addition of methanol (5 ml). The solution was evaporated and dried under high vacuum before purification by reverse phase chromatography (Lichroprep RP-18 resin, gradient 0.05M TEAB/methanol: 100/0→50/50). Multiple fractions were isolated, but none were found to contain the desired product.

7.2 Biological Evaluation

7.2.1 General

Cells. Primary brain endothelial cells (PBEC), previously isolated from fresh pig brains, were stored in liquid nitrogen,[255] and kindly provided by Prof Joan Abbott and Dr Jane Preston (Drug Delivery Group, Institute of Pharmaceutical Science, King's College London).

Reagents. Low glucose Dulbecco's modified Eagle's medium (DMEM, 1 mg/ml glucose, D5546), Hank's balanced salt solution (HBSS, H8264), HBSS with phenol red and without calcium and magnesium ('HBSS red', H9394), fibronectin from bovine plasma (F1141), puromycin (P8833), heparin (H3149), penicillin/streptomycin (P/S, P0781), L-glutamine (G7513), hydrocortisone (H0135), trypsin-EDTA, 8-(4-chlorophenylthio)-cAMP sodium salt (pCPT-cAMP, C3912) and DMSO were obtained from Sigma-Aldrich. Bovine plasma derived serum (BPDS, 10% solution, 60-00-850) was obtained from First Link Ltd (Birmingham, UK), RO-20-1724 (Calbiochem 557502) from Merck KGaA. All other reagents were obtained from major suppliers.

Growth Medium. DMEM containing 1% BDPS, 2 mM glutamine, 125 µg/ml heparin, 100 U/ml penicillin, 100 µg/ml streptomycin.

Induction Medium. DMEM containing 2 mM glutamine, 125 µg/ml heparin, 100 U/ml penicillin, 100 µg/ml streptomycin, 550 nM hydrocortisone, 250 µM pCPT-cAMP, 17.5 µM RO-20-1724.

Assay Buffer. Deionised water containing 135 mM sodium chloride, 25 mM HEPES, 5.4 mM potassium chloride, 1.5 mM calcium chloride, 1.2 mM magnesium chloride and 1 mM pyruvate (added shortly before the experiment) adjusted to pH 7.4 with sodium hydroxide.

Stopping Buffer. Phloretin (100 µM) and mercuric chloride (1 µM) in phosphate buffered saline composed of 137 mM sodium chloride, 10 mM phosphate, 2.7 mM potassium chloride in deionised water.

Transwells and TEER. 'Transwell' inserts (12 mm polycarbonate membrane, 0.4 µm pore size, tissue-culture treated, 3401) were obtained from Corning Lifesciences. Transendothelial electrical resistance (TEER) was measured with a STX100 probe and an EVOM Volt-Ohm meter (World Precision Instruments, Sarasota, FL, USA). All TEER values are given as $\Omega\,cm^2$ and were corrected by the baseline resistance of a collagen-coated filter insert without cells.

Radioisotopes. [^{3}H]3-*O*-Methylglucose (3OMG, 1.0 mCi/ml, specific activity 37 mCi/mmol) was obtained from PerkinElmer and [^{14}C]sucrose (0.1 mCi/ml, specific activity 643 mCi/mmol) from GE Healthcare. A scintillation cocktail liquid (PerkinElmer, Waltham, MA, USA) was added to each of the scintillation vials and samples were counted on a LKB Wallac 1219 Rackbeta liquid scintillation counter (LKB Wallac, Wallac, MD, USA).

Plate Readers. Fluorescence (excitation/emission wavelengths: 485/528 nm) was measured on a BioTek Synergy HT microplate reader (BioTek Instruments, Winooski, VT, USA) and absorption on a MTX Multiskan Ascent microplate reader (MTX Lab Systems, Vienna, VA, USA).

HPLC. Samples were analysed on a Waters HPLC system (600 controller, 626 pump, 996 PDA detector, 717 autosampler; Waters Corp, Milford, MA, USA). A reverse-phase polymer column (PLRP-S 150 x 4.6 mm, pore size 300 Å, particle size 8 µm) with a flow rate of 1 ml/min was used for separation with gradient elution. Acetonitrile, water and 1-heptanesulfonic acid (all HPLC grade) were obtained from Thermo Fisher Scientific. The mobile phase was composed of a buffer (5 mmol 1-heptanesulfonic acid in water, adjusted to pH 2 with HCl) and acetonitrile.
A gradient of 2-35% acetonitrile was run for 20 min, followed by 5 min at 35% acetonitrile and a 5 min post-run period at 2% acetonitrile. The total time per sample was 31 min, samples were injected twice or thrice (100 µl per injection). Sample components were detected by UV absorption at 280 nm. Chromatograms were processed and exported with Millennium32 (Waters Corp).

7.2.2 Thawing and Growth of PBEC

T75 cell-culture flasks were coated at room temperature with lab-made rat-tail collagen (300 µg/ml in sterile water) for at least 2 h , then washed twice with HBSS and coated with fibronectin (7.5 µg/ml in sterile water) for at least 2 h. One vial (microvessels from approx. half of a pig brain) PBECs was thawed and quickly added to 20 ml warmed growth medium including puromycin (4 µg/ml). Puromycin inhibits protein synthesis and serves to remove contaminant cells, but does not affect healthy endothelium with active efflux transporters to exclude the drug. The cell suspension was split evenly between two flasks. Cells were grown in an incubator at 37 °C in 5% CO_2 in air and reached about 70% confluence within 3 days. If the cells had not reached the desired cell density on day 3, they were fed with fresh growth medium and their confluence checked daily.

7.2.3 Harvesting

Flasks that had reached the desired cell density (about 70% confluence) were harvested as follows. The medium was removed by aspiration, and the cells washed twice with 'HBSS red' (without calcium and magnesium, 4 ml each). Trypsin (2 ml) was added and the flasks incubated for 7 min, then – under observation under the microscope – shaken and tapped lightly for 2 min to detach the cells, incubated for a further minute and shaken/tapped for another 2 min. Trypsin was quenched by the addition of growth medium to the flasks (8 ml each), and the contents were transferred to a centrifuge tube. The cells were centrifuged for 5 min at $380g$ and the cell pellet re-suspended in 1 ml growth medium. The cell number was determined using a haemocytometer.

7.2.4 Microplate-based Assays

Cells were seeded in collagen-coated transparent multiwell plates and grown to confluence and fed after 3 days, if necessary. The seeding density for 96-well, 24-well and 12-well plates was 2.5×10^4, 1×10^5 and 2×10^5 cells per well, respectively (1×10^5 cells/ml), whilst only the central 10×6 wells were used in 96-well plates. Cells were supplemented with hydrocortisone, cell permeable cAMP (pCPT-cAMP) and type IV phosphodiesterase inhibitor RO-20-1724 to increase intracellular cAMP levels and facilitate tight junction formation.
Different experiments were performed in this microplate setup:

- The uptake of **CP20**, **Phe**, and **Phe** in the presence of glucose (100 or 500 µM) in 96-well plates (200 µl per well) was evaluated at 1, 4 and 24 hours. At the end of the experiment, cells were washed 3× with PBS and lysed with water (100 µl). The content of triplicate wells was pooled, protein removed by the precipitation with trifluoroactic acid (9% final concentration) and centrifugation (15 min at $5400g$) The samples were then analysed by HPLC.

- Four compounds (**CP20, CP40, Phe, Val**; 0–500 µM) were evaluated for their effect on the uptake of 3OMG (1.5 µCi/ml, 0.3 µCi per well) at 10 and 20 min in 96-well plates (200 µl per well). [^{14}C]Sucrose (0.15 µCi/ml, 0.03 µCi per well) was herein used as extracellular marker. At the end of the experiment, cells were washed 3× with PBS and lysed with 1% Triton X-100 solution (200 µl, 45 min). 100 µl of the lysate were added to scintillation vials and diluted with 3.5 ml scintillation cocktail before analysis in the scintillation counter.

- Cells were pre-incubated with assay buffer 500 µl per well for 30 min. The uptake of 3OMG (1.5 µCi/ml, 0.75 µCi per well) was evaluated at 15 and 60 min in 24-well

plates (500 µl per well) in the presence of **CP20** and **Phe** (500 µM). [^{14}C]Sucrose (0.15 µCi/ml, 0.075 µCi per well) was used as extracellular marker. To stop the experiment, the cells were washed 3× with ice-cold stopping buffer and lysed with 1% Triton X-100 solution (200 µl, 45 min). The lysate was added to a scintillation vial and diluted with 3.5 ml scintillation cocktail before before analysis in the scintillation counter.

- The uptake of 3OMG (1.5 µCi/ml) was evaluated in the presence and absence of 5 mM glucose at 15 seconds in 24- and 12-well plates (500 and 1000 µl per well, respectively). [^{14}C]Sucrose (0.15 µCi/ml) was used as extracellular marker. To stop the experiment, cells were washed 3× with equal volume of ice-cold stopping buffer and lysed for 15 min with 200 µl 0.1 M sodium hydroxide solution (500 µl for 12-well plates). The lysate was added to scintillation vials and diluted with 3.5 ml scintillation cocktail before counting.

7.2.5 Transwell-based Assays

Transwell inserts (12 mm diameter, 1.12 cm^2) were coated with collagen and fibronectin as described for T75 flasks (500 µl per insert). Cells were then seeded onto the inserts at a density of 1×10^5 cells per insert and grown for 3 days (500 µl in the apical compartment, 1.5 ml in the basolateral compartment). On day 3 and every day thereafter, the medium was replaced with induction medium. When treated with induction medium, pCPT-cAMP and RO-20-1724 were added directly to the apical and basolateral compartments, whilst BPDS (50 µl, 1% final concentration) was added only to the apical compartment. TEER values were measured 1 and 2 days after the switch to induction medium and the cells were not manipulated further for at least 2 h after the TEER measurement. Cells were used for experiments after two days of treatment with induction medium.

Inhibition Assay. The inhibition of 3OMG transport by glucose (5 mM), phloretin (250 µM) and HPOs (**CP20**, **26a**, **Val, Phe, M6, M10**; 500 µM) was determined in a Transwell setup. Sample buffers were prepared from the assay buffer and contained 3OMG (1.5 µCi/ml, 0.75 µCi/ml per well) and [^{14}C]sucrose (0.5 µCi/ml, 0.075 µCi/ml per well), as well as a final concentration of 1% DMSO (HPO stocks were 50 mM solutions in 100% DMSO). The sample buffers (500 µl) were added to the apical side of the Transwell, the basolateral side contained assay buffer (1.5 ml) and incubation was performed up to 2 hours in an orbital shaker (300 rpm) at 37 °C. Samples from both compartments (sample size is 10% of the compartment volume) were taken at specific time points and the volume was replaced with fresh assay buffer.

Different experiments were performed based on the described method in this microplate setup:

- The transport of 3OMG across the monolayer was measured at 30 sec, 2 min, 5 min, 1 h and 2 h. The effects glucose, **CP20** and **Phe**, as well as pre-incubation with assay buffer on 3OMG transport were determined. Samples (10% of compartment volume) were taken at each time point from both compartments, diluted with scintillation liquid (3.5 ml) and measured in a scintillation counter.
- The transport of 3OMG at 2, 5, 30, 60 min was investigated after glucose, **CP20** and **Phe** had been added to the apical side, or both sides. Samples from each time point (10% of compartment volume) were analysed by scintillation counting. Samples from the 60 min time point were also analysed by HPLC in order to determine the amount of test compound that had crossed the monolayer.
- The inhibition of 3OMG uptake in the presence of glucose, phloretin and HPOs (**CP20**, **26a**, **Val, Phe**) was measured at 2, 5, 10 and 30 min by scintillation counting. HPLC samples were only taken at the 30 min time point.
- The inhibition of 3OMG uptake in the presence of glucose and HPOs (**CP20**, **26a**, **Phe, M6, M10**) was measured at 2, 5, 10 and 30 min by scintillation counting. HPLC samples were taken at the 30 min time point only. Instead of [^{14}C]sucrose as paracellular marker in every well, sodium fluorescein (7.5 µg/ml final concentration) was used in separate wells. For the fluorescence read-out, 150 µl were sampled from the basolateral side and 50 µl from the apical side, which were diluted to 150 µl with assay buffer.

Permeability Assay. The permeability of HPOs (500 µM) across the BBB was determined by measuring the permeability of the compound across a PBEC monolayer. Sodium fluorescein (7.5 µg/ml final concentration) was used as marker for the paracellular permeability. After 30 min preincubation with assay buffer, fresh buffer was added to the basolateral side (1.5 ml, receiver compartment) and the sample solutions (compound plus sodium fluorescein, 1% DMSO) were added to the apical side (0.5 ml, donor compartment). The inserts were incubated for 60 min in an orbital shaker (300 rpm) in the dark at 37 °C. The incubation was stopped by removing the insert from the receiver compartment. Samples for fluorescence measurement were taken in triplicate from each compartment (10% of compartment volume each). The apical samples (50 µl) were diluted to 150 µl with assay buffer. Samples for HPLC were taken from both sides and measured in duplicate without further work-up.

7.2.6 Calculations and Statistical Analysis.

All calculations were done with Microsoft Excel 2003 or 2010 and statistical test and graphs were done using GraphPad Prism 6 (GraphPad Software, Inc.). milogP values were calculated online on the Molinspiration webpage.[264]

The apparent permeability P_{app} ($\mathrm{cm\,s^{-1}}$) of compounds, which allows the comparison of results with other cell based assays, was calculated using the equation:

$$P_{app} = V_D/(A * M_D) * (\Delta M_R/\Delta t) \tag{7.1}$$

where V_D = apical (donor) volume, A = membrane surface area (1.12 cm^2), M_D = apical (donor) amount (nmol) and $\Delta M_R/\Delta t$ = amount (nmol) of compound transferred to receiver compartment over time in seconds.[263]
For each plate, the P_{app} was also normalised as P_{app} % of CP20 on that plate, in order to account for day-to-day variation between experiments.

Assays were performed on at least two independent days and in duplicate or triplicate on each plate. All data is presented as mean ± SEM. The TEER of batches was compared with 2-way ANOVA, with Sidak's correction for multiple comparisons. P_{app} values from Transwell experiments were compared by one-way ANOVA, with Holm-Sidak's correction for multiple comparisons.

Bibliography

[1] Murthy R.S., The World Health Report: 2001. Mental Health: New Understanding, New Hope. Technical Report, World Health Organization, Geneva, **2001**.

[2] Olesen J. and Leonardi M., The burden of brain diseases in Europe. *European Journal of Neurology*, **2003**, *10* (5), 471–477.

[3] Peden A.H. and Ironside J.W., Molecular Pathology in Neurodegenerative Diseases. *Current Drug Targets*, **2012**, *13* (12), 1548–1559.

[4] Dorsey E.R., Constantinescu R., Thompson J.P., Biglan K.M., Holloway R.G., Kieburtz K., Marshall F.J., Ravina B.M., Schifitto G., Siderowf A. and Tanner C.M., Projected number of people with Parkinson disease in the most populous nations, 2005 through 2030. *Neurology*, **2007**, *68* (5), 384–386.

[5] DiNunzio J.C. and Williams R.O., CNS disorder - Current treatment options and the prospects for advanced therapies. *Drug Development and Industrial Pharmacy*, **2008**, *34* (11), 1141–1167.

[6] Molina-Holgado F., Hider R.C., Gaeta A., Williams R.J. and Francis P., Metals ions and neurodegeneration. *Biometals*, **2007**, *20* (3-4), 639–654.

[7] Dauer W. and Przedborski S., Parkinson's disease: mechanisms and models. *Neuron*, **2003**, *39* (6), 889–909.

[8] Bolognin S., Drago D., Messori L. and Zatta P., Chelation therapy for neurodegenerative diseases. *Medicinal Research Reviews*, **2009**, *29* (4), 547–570.

[9] Parkinson J., An Essay on the Shaking Palsy. *Journal of Neuropsychiatry*, **2002**, *14* (2), 223–236.

[10] de Lau L.M.L. and Breteler M.M.B., Epidemiology of Parkinson's disease. *The Lancet Neurology*, **2006**, *5* (6), 525–535.

[11] Parkinson's UK, Parkinson's prevalence in the United Kingdom (2009). Technical Report, Parkinson's UK, **2009**.

[12] Lesage S. and Brice A., Parkinson's disease: From monogenic forms to genetic susceptibility factors. *Human Molecular Genetics*, **2009**, *18* (1), 48–59.

[13] Checkoway H., Farin F.M., Costa-Mallen P., Kirchner S.C. and Costa L.G., Genetic polymorphisms in Parkinson's disease. *Neurotoxicology*, **1998**, *19* (4-5), 635–643.

[14] Lai B.C.L., Marion S.A., Teschke K. and Tsui J.K.C., Occupational and environmental risk factors for Parkinson's disease. *Parkinsonism & Related Disorders*, **2002**, *8* (5), 297–309.

[15] Duffy P.E. and Tennyson V.M., Phase and Electron Microscopic Observations of Lewy Bodies and Melanin Granules in the Substantia Nigra and Locus Caeruleus in Parkinson's Disease. *Journal of Neuropathology & Experimental Neurology*, **1965**, *24* (3), 398–414.

[16] Davie C.A., A Review of Parkinson's Disease. *British Medical Bulletin*, **2008**, *86* (1), 109–127.

[17] Bernheimer H., Birkmayer W., Hornykiewicz O., Jellinger K. and Seitelberger F., Brain dopamine and the syndromes of Parkinson and Huntington. Clinical, morphological and neurochemical correlations. *Journal of the Neurological Sciences*, **1973**, *20* (4), 415–455.

[18] Obeso J.A., Rodriguez-Oroz M.C., Goetz C.G., Marin C., Kordower J.H., Rodriguez M., Hirsch E.C., Farrer M., Schapira A.H.V. and Halliday G., Missing pieces in the Parkinson's disease puzzle. *Nature Medicine*, **2010**, *16* (6), 653–661.

[19] Crichton R.R., Dexter D.T. and Ward R.J., Metal based neurodegenerative diseases - From molecular mechanisms to therapeutic strategies. *Coordination Chemistry Reviews*, **2008**, *252* (10-11), 1189–1199.

[20] Xu J., Kao S.Y., Lee F.J.S., Song W., Jin L.W. and Yankner B.A., Dopamine-dependent neurotoxicity of alpha-synuclein: a mechanism for selective neurodegeneration in Parkinson disease. *Nature Medicine*, **2002**, *8* (6), 600–606.

[21] Dexter D.T., Wells F.R., Lee A.J., Agid F., Agid Y., Jenner P. and Marsden C.D., Increased Nigral Iron Content and Alterations in Other Metal Ions Occurring in Brain in Parkinson's Disease. *Journal of Neurochemistry*, **1989**, *52* (6), 1830–1836.

[22] Sofic E., Paulus W., Jellinger K., Riederer P. and Youdim M.B.H., Selective Increase of Iron in Substantia Nigra Zona Compacta of Parkinsonian Brains. *Journal of Neurochemistry*, **1991**, *56* (3), 978–982.

[23] Alam Z.I., Daniel S.E., Lees A.J., Marsden D.C., Jenner P. and Halliwell B., A generalised increase in protein carbonyls in the brain in Parkinson's but not incidental Lewy body disease. *Journal of Neurochemistry*, **1997**, *69* (3), 1326–1329.

[24] Ramachandiran S., Hansen J.M., Jones D.P., Richardson J.R. J.R. and Miller G.W., Divergent mechanisms of paraquat, MPP+, and rotenone toxicity: Oxidation of thioredoxin and caspase-3 activation. *Toxicological Sciences*, **2007**, *95* (1), 163–171.

[25] Nicklas W.J., Vyas I. and Heikkila R.E., Inhibition of NADH-linked oxidation in brain mitochondria by 1-methyl-4-phenyl-pyridine, a metabolite of the neurotoxin, 1-methyl-4-phenyl-1,2,5,6-tetrahydropyridine. *Life Sciences*, **1985**, *36* (26), 2503–2508.

[26] Sayre L.M., Biochemical mechanism of action of the dopaminergic neurotoxin 1-methyl-4-phenyl-1,2,3,6-tetrahydropyridine (MPTP). *Toxicology Letters*, **1989**, *48* (2), 121–149.

[27] Cassarino D.S., Parks J.K., Parker W. and Bennett J.P., The parkinsonian neurotoxin MPP+ opens the mitochondrial permeability transition pore and releases cytochrome c in isolated mitochondria via an oxidative mechanism. *Biochimica et Biophysica Acta (BBA) - Molecular Basis of Disease*, **1999**, *1453* (1), 49–62.

[28] Chang G.D. and Ramirez V.D., The mechanism of action of MPTP and MPP+ on endogenous dopamine release from the rat corpus striatum superfused in vitro. *Brain Research*, **1986**, *368* (1), 134–140.

[29] Lotharius J. and O'Malley K.L., The parkinsonism-inducing drug 1-methyl-4-phenylpyridinium triggers intracellular dopamine oxidation. A novel mechanism of toxicity. *The Journal of Biological Chemistry*, **2000**, *275* (49), 38581–8.

[30] Glinka Y., Tipton K.F. and Youdim M.B.H., Nature of Inhibition of Mitochondrial Respiratory Complex I by 6-Hydroxydopamine. *Journal of Neurochemistry*, **2002**, *66* (5), 2004–2010.

[31] Glinka Y., Gassen M. and Youdim M.B.H., Mechanism of 6-hydroxydopamine neurotoxicity. P. Riederer, D.B. Calne, R. Horowski, Y. Mizuno, W. Poewe and M.B.H. Youdim (editors), *Advances in Research on Neurodegeneration*, *Journal of Neural Transmission. Supplementa*, volume 50 (Springer Vienna, Vienna, **1997**), 55–66.

[32] Rodriguez-Pallares J., Parga J.A., Muñoz A., Rey P., Guerra M.J. and Labandeira-Garcia J.L., Mechanism of 6-hydroxydopamine neurotoxicity: The role of NADPH oxidase and microglial activation in 6-hydroxydopamine-induced degeneration of dopaminergic neurons. *Journal of Neurochemistry*, **2007**, *103* (1), 145–156.

[33] Dexter D.T., Wells F.R., Agid F., Agid Y., Lees A.J., Jenner P. and Marsden C.D., Increase Nigral Iron Content in Postmortem Parkinsonian Brain. *The Lancet*, **1987**, *330* (8569), 1219–1220.

[34] Höck A., Demmel U., Schicha H., Kasperek K. and Feinendegen L.E., Trace element concentration in human brain. Activation analysis of cobalt, iron, rubidium, selenium, zinc, chromium, silver, cesium, antimony and scandium. *Brain*, **1975**, *98* (1), 49–64.

[35] Fenton H.J.H., LXXIII. – Oxidation of tartaric acid in presence of iron. *Journal of the Chemical Society, Transactions*, **1894**, *65*, 899–910.

[36] Gaeta A. and Hider R.C., The crucial role of metal ions in neurodegeneration: the basis for a promising therapeutic strategy. *British Journal of Pharmacology*, **2005**, *146* (8), 1041–1059.

[37] Eaton J.W. and Qian M., Molecular bases of cellular iron toxicity. *Free Radical Biology and Medicine*, **2002**, *32* (9), 833–840.

[38] Giasson B.I., Duda J.E., Murray I.V., Chen Q., Souza J.M., Hurtig H.I., Ischiropoulos H., Trojanowski J.Q. and Lee V.M., Oxidative damage linked to neurodegeneration by selective alpha-synuclein nitration in synucleinopathy lesions. *Science*, **2000**, *290* (5493), 985–989.

[39] Uversky V.N., Li J. and Fink A.L., Metal-triggered structural transformations, aggregation, and fibrillation of human alpha-synuclein. A possible molecular link between Parkinson's disease and heavy metal exposure. *The Journal of Biological Chemistry*, **2001**, *276* (47), 44284–44296.

[40] Hider R.C., Roy S., Ma Y.M., Kong X.L. and Preston J.E., The potential application of iron chelators for the treatment of neurodegenerative diseases. *Metallomics*, **2011**, *3* (3), 239–249.

[41] Herz D.M., Haagensen B.N., Christensen M.S., Madsen K.H., Rowe J.B., Lø kkegaard A. and Siebner H.R., The acute brain response to levodopa heralds dyskinesias in Parkinson disease. *Annals of Neurology*, **2014**, *75* (6), 829–836.

[42] Barbeau A., L-DOPA therapy in Parkinson's disease: a critical review of nine years' experience. *Canadian Medical Association Journal*, **1969**, *101* (13), 59–68.

[43] Zheng H., Gal S., Weiner L.M., Bar-Am O., Warshawsky A., Fridkin M. and Youdim M.B.H., Novel multifunctional neuroprotective iron chelator-monoamine oxidase inhibitor drugs for neurodegenerative diseases: in vitro studies on antioxidant activity, prevention of lipid peroxide formation and monoamine oxidase inhibition. *Journal of Neurochemistry*, **2005**, *95* (1), 68–78.

[44] Haavik J. and Toska K., Tyrosine hydroxylase and Parkinson's disease. *Molecular Neurobiology*, **1998**, *16* (3), 285–309.

[45] Dexter D.T., Statton S.A., Whitmore C., Freinbichler W., Weinberger P., Tipton K.F., Della Corte L., Ward R.J. and Crichton R.R., Clinically available iron chelators induce neuroprotection in the 6-OHDA model of Parkinson's disease after peripheral administration. *Journal of Neural Transmission*, **2011**, *118* (2), 223–231.

[46] Molina-Holgado F., Gaeta A., Francis P.T., Williams R.J. and Hider R.C., Neuroprotective actions of deferiprone in cultured cortical neurones and SHSY-5Y cells. *Journal of Neurochemistry*, **2008**, *105* (6), 2466–2476.

[47] Kaur D., Yantiri F., Rajagopalan S., Kumar J., Mo J.Q., Boonplueang R., Viswanath V., Jacobs R., Yang L. and Beal M.F., Genetic or Pharmacological Iron Chelation Prevents MPTP-Induced Neurotoxicity In Vivo: A Novel Therapy for Parkinson's Disease. *Neuron*, **2003**, *37* (6), 899–909.

[48] Devos D., Moreau C., Devedjian J.C., Kluza J., Petrault M., Laloux C., Jonneaux A., Ryckewaert G., Garçon G., Rouaix N., Duhamel A., Jissendi P., Dujardin K., Auger F., Ravasi L., Hopes L., Grolez G., Firdaus W., Sablonnière B., Strubi-Vuillaume I., Zahr N., Destée A., Corvol J.C., Pöltl D., Leist M., Rose C., Defebvre L., Marchetti P., Cabantchik Z.I. and Bordet R., Targeting chelatable iron as a therapeutic modality in Parkinson's disease. *Antioxidants & Redox Signaling*, **2014**, *21* (2), 195–210.

[49] Dexter D.T., Oral Communication. **2014**.

[50] Devos D., Oral Communication. **2014**.

[51] Roy S., Preston J.E., Hider R.C. and Ma Y.M., Glucosylated deferiprone and its brain uptake: implications for developing glucosylated hydroxypyridinone analogues intended to cross the blood-brain barrier. *Journal of Medicinal Chemistry*, **2010**, *53* (15), 5886–5889.

[52] Singh S., Epemolu R.O., Dobbin P.S., Tilbrook G.S., Ellis B.L., Damani L.A. and Hider R.C., Urinary metabolic profiles in human and rat of 1,2-dimethyl- and 1,2-diethyl-substituted 3-hydroxypyridin-4-ones. *Drug Metabolism and Disposition*, **1992**, *20*, 256–261.

[53] Porter J.B., Abeysinghe R.D., Hoyes K.P., Barra C., Huehns E.R., Brooks P.N., Blackwell M.P., Araneta M., Brittenham G., Singh S., Dobbin P.S. and Hider R.C., Contrasting interspecies efficacy and toxicology of 1,2-diethyl-3-hydroxypyridin-4-one, CP94, relates to differing metabolism of the iron chelating site. *British Journal of Haematology*, **1993**, *85* (1), 159–168.

[54] Pontikoglou C. and Papadaki H.A., Idiosyncratic drug-induced agranulocytosis: the paradigm of deferiprone. *Hemoglobin*, **2010**, *34* (3), 291–304.

[55] Pardridge W.M., Blood-brain barrier drug targeting: the future of brain drug development. *Molecular Interventions*, **2003**, *3* (2), 90–105.

[56] Goldmann E.E., *Die äussere und innere Sekretion des gesunden und kranken Organismus im Lichte der "vitalen Färbung"*, volume 64 (H. Laupp, **1909**).

[57] Ghose A.K., Viswanadhan V.N. and Wendoloski J.J., A knowledge-based approach in designing combinatorial or medicinal chemistry libraries for drug discovery. 1. A qualitative and quantitative characterization of known drug databases. *Journal of Combinatorial Chemistry*, **1999**, *1*, 55–68.

[58] Pardridge W.M., Blood-Brain Barrier: Interface Between Internal Medicine and the Brain. *Annals of Internal Medicine*, **1986**, *105* (1), 82–95.

[59] Lipinski C.A., Lead- and drug-like compounds: the rule-of-five revolution. *Drug Discovery Today. Technologies*, **2004**, *1* (4), 337–341.

[60] Norinder U. and Haeberlein M., Computational approaches to the prediction of the blood-brain distribution. *Advanced Drug Delivery Reviews*, **2002**, *54* (3), 291–313.

[61] Abbott N.J., Dynamics of CNS Barriers: Evolution, Differentiation, and Modulation. *Cellular and Molecular Neurobiology*, **2005**, *25* (1), 5–23.

[62] Abbott N.J., Patabendige A., Dolman D.E., Yusof S.R. and Begley D.J., Structure and function of the blood-brain barrier. *Neurobiolology of Disease*, **2010**, *37* (1), 13–25.

[63] Obermeier B., Daneman R. and Ransohoff R.M., Development, maintenance and disruption of the blood-brain barrier. *Nature Medicine*, **2013**, *19* (12), 1584–1596.

[64] Wolburg H., Noell S., Mack A., Wolburg-Buchholz K. and Fallier-Becker P., Brain endothelial cells and the glio-vascular complex. *Cell and Tissue Research*, **2009**, *335* (1), 75–96.

[65] Minn A., Ghersi-Egea J.F., Perrin R., Leininger B. and Siest G., Drug metabolizing enzymes in the brain and cerebral microvessels. *Brain Research Reviews*, **1991**, *16* (1), 65–82.

[66] Lipinski C.A., Lombardo F., Dominy B.W. and Feeney P.J., Experimental and computational approaches to estimate solubility and permeability in drug discovery and development settings. *Advanced Drug Delivery Reviews*, **1997**, *23* (1-3), 3–25.

[67] Jong A. and Huang S.H., Blood-brain barrier drug discovery for central nervous system infections. *Current Drug Targets. Infectious Disorders*, **2005**, *5* (1), 65–72.

[68] Pavan B., Dalpiaz A., Ciliberti N., Biondi C., Manfredini S. and Vertuani S., Progress in Drug Delivery to the Central Nervous System by the Prodrug Approach. *Molecules*, **2008**, *13* (5), 1035–1065.

[69] Habgood M.D., Begley D.J. and Abbott N.J., Determinants of passive drug entry into the central nervous system. *Cellular and Molecular Neurobiology*, **2000**, *20* (2), 231–253.

[70] Fischer H., Gottschlich R. and Seelig A., Blood-Brain Barrier Permeation: Molecular Parameters Governing Passive Diffusion. *The Journal of Membrane Biology*, **1998**, *165* (3), 201–211.

[71] Lieb W.R. and Stein W.D., Non-stokesian nature of transverse diffusion within human red cell membranes. *The Journal of Membrane Biology*, **1986**, *92* (2), 111–119.

[72] Sutherland W., LXXV. A dynamical theory of diffusion for non-electrolytes and the molecular mass of albumin. *Philosophical Magazine Series 6*, **1905**, *9* (54), 781–785.

[73] Hitchcock S.A. and Pennington L.D., Structure-brain exposure relationships. *Journal of Medicinal Chemistry*, **2006**, *49* (26), 7559–7583.

[74] Oldendorf W.H., Lipid Solubility and Drug Penetration of the Blood Brain Barrier. *Experimental Biology and Medicine*, **1974**, *147* (3), 813–816.

[75] Frimurer T.M., Bywater R., Naerum L., Lauritsen L.N. and Brunak S., Improving the odds in discriminating "drug-like" from "non drug-like" compounds. *Journal of Chemical Information and Computer Sciences*, **2000**, *40* (6), 1315–1324.

[76] Habgood M.D., Liu Z.D., Dehkordi L.S., Khodr H.H., Abbott N.J. and Hider R.C., Investigation into the correlation between the structure of hydroxypyridinones and blood-brain barrier permeability. *Biochemical Pharmacology*, **1999**, *57* (11), 1305–1310.

[77] Anderson B.D., Prodrugs for improved CNS delivery. *Advanced Drug Delivery Reviews*, **1996**, *19* (2), 171–202.

[78] Rautio J., Laine K., Gynther M. and Savolainen J., Prodrug approaches for CNS delivery. *The AAPS Journal*, **2008**, *10* (1), 92–102.

[79] Kageyama T., Nakamura M., Matsuo A., Yamasaki Y., Takakura Y., Hashida M., Kanai Y., Naito M., Tsuruo T., Minato N. and Shimohama S., The 4F2hc/LAT1 complex transports L-DOPA across the blood-brain barrier. *Brain Research*, **2000**, *879* (1-2), 115–21.

[80] Burkhard P., Dominici P., Borri-Voltattorni C., Jansonius J.N. and Malashkevich V.N., Structural insight into Parkinson's disease treatment from drug-inhibited DOPA decarboxylase. *Nature Structural Biology*, **2001**, *8* (11), 963–967.

[81] Zlokovic B.V., The blood-brain barrier in health and chronic neurodegenerative disorders. *Neuron*, **2008**, *57* (2), 178–201.

[82] King A., Breaking Through the Barrier. *Chemistry World*, **2011**, *8* (6), 36–39.

[83] Lee G., Dallas S., Hong M. and Bendayan R., Drug transporters in the central nervous system: brain barriers and brain parenchyma considerations. *Pharmacological Reviews*, **2001**, *53* (4), 569–596.

[84] Pardridge W.M., Drug transport across the blood-brain barrier. *Journal of Cerebral Blood Flow and Metabolism*, **2012**, *32* (11), 1959–72.

[85] Begley D.J., Delivery of therapeutic agents to the central nervous system: the problems and the possibilities. *Pharmacology & Therapeutics*, **2004**, *104* (1), 29–45.

[86] Pialoux G., Fournier S., Moulignier A., Poveda J.D., Clavel F. and Dupont B., Central nervous system as a sanctuary for HIV-1 infection despite treatment with zidovudine, lamivudine and indinavir. *AIDS (London, England)*, **1997**, *11* (10), 1302–3.

[87] Pan G., Giri N. and Elmquist W.F., Abcg2/Bcrp1 mediates the polarized transport of antiretroviral nucleosides abacavir and zidovudine. *Drug Metabolism and Disposition*, **2007**, *35* (7), 1165–73.

[88] Sai Y. and Tsuji A., Transporter-mediated drug delivery: recent progress and experimental approaches. *Drug Discovery Today*, **2004**, *9* (16), 712–720.

[89] Sadeque A.J., Wandel C., He H., Shah S. and Wood A.J., Increased drug delivery to the brain by P-glycoprotein inhibition. *Clinical Pharmacology and Therapeutics*, **2000**, *68* (3), 231–7.

[90] Lajoie P. and Nabi I.R., Lipid rafts, caveolae, and their endocytosis. *International Review of Cell and Molecular Biology*, **2010**, *282*, 135–63.

[91] Parton R.G. and Simons K., The multiple faces of caveolae. *Nature Reviews. Molecular Cell Biology*, **2007**, *8* (3), 185–94.

[92] Pardridge W.M., Vector-mediated drug delivery to the brain. *Advanced Drug Delivery Reviews*, **1999**, *36* (2-3), 299–321.

[93] Yan F., Wang Y., He S., Ku S., Gu W. and Ye L., Transferrin-conjugated, fluorescein-loaded magnetic nanoparticles for targeted delivery across the blood-brain barrier. *Journal of Materials Science. Materials in Medicine*, **2013**, *24* (10), 2371–9.

[94] Niewoehner J., Bohrmann B., Collin L., Urich E., Sade H., Maier P., Rueger P., Stracke J.O., Lau W., Tissot A.C., Loetscher H., Ghosh A. and Freskgard P.O., Increased brain penetration and potency of a therapeutic antibody using a monovalent molecular shuttle. *Neuron*, **2014**, *81* (1), 49–60.

[95] Tamai I. and Tsuji A., Transporter-mediated permeation of drugs across the blood-brain barrier. *Journal of Pharmaceutical Sciences*, **2000**, *89* (11), 1371–1388.

[96] Adkison K.D. and Shen D.D., Uptake of valproic acid into rat brain is mediated by a medium-chain fatty acid transporter. *The Journal of Pharmacology and Experimental Therapeutics*, **1996**, *276* (3), 1189–1200.

[97] Ylikangas H., Malmioja K., Peura L., Gynther M., Nwachukwu E.O., Leppänen J., Laine K., Rautio J., Lahtela-Kakkonen M., Huttunen K.M. and Poso A., Quantitative Insight into the Design of Compounds Recognized by the L-Type Amino Acid Transporter 1 (LAT1). *ChemMedChem*, **2014**.

[98] Gomes P. and Soares-da Silva P., L-DOPA transport properties in an immortalised cell line of rat capillary cerebral endothelial cells, RBE 4. *Brain Research*, **1999**, *829* (1-2), 143–150.

[99] Walker I., Nicholls D., Irwin W.J. and Freeman S., Drug delivery via active transport at the blood-brain barrier: affinity of a prodrug of phosphonoformate for the large amino acid transporter. *International Journal of Pharmaceutics*, **1994**, *104* (2), 157–167.

[100] Wang Y. and Welty D.R., The Simultaneous Estimation of the Influx and Efflux Blood-Brain Barrier Permeabilities of Gabapentin Using a Microdialysis-Pharmacokinetic Approach. *Pharmaceutical Research*, **1996**, *13* (3), 398–403.

[101] Dickens D., Webb S.D., Antonyuk S., Giannoudis A., Owen A., Rädisch S., Hasnain S.S. and Pirmohamed M., Transport of gabapentin by LAT1 (SLC7A5). *Biochemical Pharmacology*, **2013**, *85* (11), 1672–1683.

[102] Cornford E.M., Young D., Paxton J.W., Finlay G.J., Wilson W.R. and Pardridge W.M., Melphalan Penetration of the Blood-Brain Barrier via the Neutral Amino Acid Transporter in Tumor-bearing Brain. *Cancer Research*, **1992**, *52* (1), 138–143.

[103] Hokari M., Wu H.Q., Schwarcz R. and Smith Q.R., Facilitated brain uptake of 4-chlorokynurenine and conversion to 7-chlorokynurenic acid. *Neuroreport*, **1996**, *8* (1), 15–8.

[104] Cheeseman C.I., Hexose Transport Across Mammalian Epithelia. G.A. Gerencser (editor), *Epithelial Transport Physiology* (Humana Press, Totowa, NJ, **2010**), 323–352.

[105] Bell G.I., Burant C.F., Takeda J. and Gould G.W., Structure and function of mammalian facilitative sugar transporters. *The Journal of Biological Chemistry*, **1993**, *268* (26), 19161–19164.

[106] Wood I.S. and Trayhurn P., Glucose transporters (GLUT and SGLT): expanded families of sugar transport proteins. *The British Journal of Nutrition*, **2003**, *89* (1), 3–9.

[107] Kalaria R.N., Gravina S.A., Schmidley J.W., Perry G. and Harik S.I., The glucose transporter of the human brain and blood-brain barrier. *Annals of Neurology*, **1988**, *24* (6), 757–764.

[108] Carruthers A., DeZutter J., Ganguly A. and Devaskar S.U., Will the original glucose transporter isoform please stand up! *American Journal of Physiology. Endocrinology and Metabolism*, **2009**, *297* (4), E836–E848.

[109] Pardridge W.M., Boado R.J. and Farrell C.R., Brain-type glucose transporter (GLUT-1) is selectively localized to the blood-brain barrier. Studies with quantitative western blotting and in situ hybridization. *The Journal of Biological Chemistry*, **1990**, *265* (29), 18035–18040.

[110] Baldwin S.A., Mammalian passive glucose transporters: members of an ubiquitous family of active and passive transport proteins. *Biochimica et Biophysica Acta*, **1993**, *1154* (1), 17–49.

[111] Kumagai A.K., Glucose transport in brain and retina: implications in the management and complications of diabetes. *Diabetes/Metabolism Research and Reviews*, **1999**, *15* (4), 261–273.

[112] Agus D.B., Gambhir S.S., Pardridge W.M., Spielholz C., Baselga J., Vera J.C. and Golde D.W., Vitamin C crosses the blood-brain barrier in the oxidized form through the glucose transporters. *The Journal of Clinical Investigation*, **1997**, *100* (11), 2842–2848.

[113] Rose R.C., Transport of ascorbic acid and other water-soluble vitamins. *Biochimica et Biophysica Acta*, **1988**, *947* (2), 335–366.

[114] Thorens B. and Mueckler M., Glucose transporters in the 21st Century. *American Journal of Physiology. Endocrinology and Metabolism*, **2010**, *298* (2), E141–E145.

[115] Thorens B. and Joost H.G., The extended GLUT-family of sugar/polyol transport facilitators: nomenclature, sequence characteristics, and potential function of its novel members. *Molecular Membrane Biology*, **2001**, *18* (4), 247–256.

[116] Manolescu A.R., Witkowska K., Kinnaird A., Cessford T. and Cheeseman C.I., Facilitated hexose transporters: new perspectives on form and function. *Physiology*, **2007**, *22*, 234–240.

[117] Foster D.L., Boublik M. and Kaback H.R., Structure of the lac carrier protein of Escherichia coli. *The Journal of Biological Chemistry*, **1983**, *258* (1), 31–34.

[118] Maiden M.C., Davis E.O., Baldwin S.A., Moore D.C. and Henderson P.J., Mammalian and bacterial sugar transport proteins are homologous. *Nature*, **1987**, *325* (6105), 641–3.

[119] Yan N., Structural advances for the major facilitator superfamily (MFS) transporters. *Trends in Biochemical Sciences*, **2013**, *38* (3), 151–9.

[120] Mueckler M., Caruso C., Baldwin S., Panico M., Blench I., Morris H., Allard W., Lienhard G. and Lodish H., Sequence and structure of a human glucose transporter. *Science*, **1985**, *229* (4717), 941–945.

[121] Salas-Burgos A.M., Iserovich P., Zuniga F., Vera J.C. and Fischbarg J., Predicting the three-dimensional structure of the human facilitative glucose transporter Glut1 by a novel evolutionary homology strategy: insights on the

molecular mechanism of substrate migration, and binding sites for glucose and inhibitory molecules. *Biophysical Journal*, **2004**, *87* (5), 2990–2999.

[122] Sun L., Zeng X., Yan C., Sun X., Gong X., Rao Y. and Yan N., Crystal structure of a bacterial homologue of glucose transporters GLUT1-4. *Nature*, **2012**, *490* (7420), 361–366.

[123] Quistgaard E.M., Löw C., Moberg P., Trésaugues L. and Nordlund P., Structural basis for substrate transport in the GLUT-homology family of monosaccharide transporters. *Nature Structural & Molecular Biology*, **2013**, *20* (6), 766–768.

[124] Deng D., Xu C., Sun P., Wu J., Yan C., Hu M. and Yan N., Crystal structure of the human glucose transporter GLUT1. *Nature*, **2014**, *510* (7503), 121–125.

[125] Blodgett D.M. and Carruthers A., Quench-flow analysis reveals multiple phases of GluT1-mediated sugar transport. *Biochemistry*, **2005**, *44* (7), 2650–2660.

[126] Barnett J.E., Holman G.D. and Munday K.A., An explanation of the asymmetric binding of sugars to the human erythrocyte sugar-transport systems. *The Biochemical Journal*, **1973**, *135* (3), 539–541.

[127] Pardridge W.M. and Oldendorf W.H., Kinetics of blood-brain barrier transport of hexoses. *Biochimica et Biophysica Acta - Biomembranes*, **1975**, *382* (3), 377–392.

[128] Barnett J.E., Holman G.D. and Munday K.a., Structural requirements for binding to the sugar-transport system of the human erythrocyte. *The Biochemical Journal*, **1973**, *131* (2), 211–221.

[129] Barnett J.E., Holman G.D., Chalkley R.A. and Munday K.A., Evidence for two asymmetric conformational states in the human erythrocyte sugar-transport system. *The Biochemical Journal*, **1975**, *145* (3), 417–429.

[130] Takakura Y., Kuentzel S.L., Raub T.J., Davies A., Baldwin S.A. and Borchardt R.T., Hexose uptake in primary cultures of bovine brain microvessel endothelial cells. I. Basic characteristics and effects of D-glucose and insulin. *Biochimica et Biophysica Acta*, **1991**, *1070* (1), 1–10.

[131] Serrano I.D., Ribeiro M.M.B. and Castanho M.A.R.B., A Focus on Glucose-Mediated Drug Delivery to the Central Nervous System. *Mini Reviews in Medicinal Chemistry*, **2012**, *12* (4), 301–312.

[132] Polt R., Dhanasekaran M. and Keyari C.M., Glycosylated neuropeptides: a new vista for neuropsychopharmacology? *Medicinal Research Reviews*, **2005**, *25* (5), 557–585.

[133] Guo X., Geng M. and Du G., Glucose Transporter 1, Distribution in the Brain and in Neural Disorders: Its Relationship With Transport of Neuroactive Drugs Through the Blood-Brain Barrier. *Biochemical Genetics*, **2005**, *43* (3-4), 175–187.

[134] Bardají E., Torres J.L., Clapés P., Albericio F., Barany G., Rodríguez R.E., Sacristán M.P. and Valencia G., Synthesis and biological activity of O-glycosylated morphiceptin analogues. *Journal of the Chemical Society, Perkin Transactions 1*, **1991**, (7), 1755–1759.

[135] Biondi L., Filira F., Gobbo M., Scolaro B. and Rocchi R., Synthesis of glycosylated tuftsins and tuftsin-containing IgG fragment undecapeptide. *International Journal of Peptide and Protein Research*, **1991**, *37* (2), 112–121.

[136] Drouillat B., Kellam B., Dekany G., Starr M.S. and Toth I., Solid phase synthesis of C-terminal carbohydrate modified enkephalins. *Bioorganic & Medicinal Chemistry Letters*, **1997**, *7* (17), 2247–2250.

[137] Egleton R.D., Mitchell S.A., Huber J.D., Janders J., Stropova D., Polt R., Yamamura H.I., Hruby V.J. and Davis T.P., Improved bioavailability to the brain of glycosylated Met-enkephalin analogs. *Brain Research*, **2000**, *881* (1), 37–46.

[138] Egleton R.D., Mitchell S.A., Huber J.D., Palian M.M., Polt R. and Davis T.P., Improved blood-brain barrier penetration and enhanced analgesia of an opioid peptide by glycosylation. *The Journal of Pharmacology and Experimental Therapeutics*, **2001**, *299* (3), 967–972.

[139] Horvat J., Horvat v., Lemieux C. and Schiller P.W., Synthesis and biological activity of [Leu5]enkephalin derivatives containing D-glucose. *International Journal of Peptide and Protein Research*, **1988**, *31* (5), 499–507.

[140] Horvat v., Varga L., Horvat J., Pfützner A., Suhartono H. and Rübsamen-Waigmann H., [5-Leucin]enkephalin-Related Glycoconjugates: Structurally Novel Agents Effective against HIV-1. *Helvetica Chimica Acta*, **1991**, *74* (5), 951–955.

[141] Horvat v., Horvat J., Varga-Defterdarović L., Pavelić K., Chung N.N. and Schiller P.W., Methionine-enkephalin related glycoconjugates. Synthesis and biological activity. *International Journal of Peptide and Protein Research*, **1993**, *41* (4), 399–404.

[142] Kellam B., Drouillat B., Dekany G., Starr M.S. and Toth I., Synthesis and in vitro evaluation of lipoamino acid and carbohydrate-modified enkephalins as potential antinociceptive agents. *International Journal of Pharmaceutics*, **1998**, *161* (1), 55–64.

[143] Kriss C.T., Lou B.S., Szabó L.Z., Mitchell S.a., Hruby V.J. and Polt R., Enkephalin-based drug design: conformational analysis of O-linked glycopeptides by NMR and molecular modeling. *Tetrahedron: Asymmetry*, **2000**, *11* (1), 9–25.

[144] Masand G., Hanif K., Sen S., Ahsan A., Maiti S. and Pasha S., Synthesis, conformational and pharmacological studies of glycosylated chimeric peptides of Met-enkephalin and FMRFa. *Brain Research Bulletin*, **2006**, *68* (5), 329–334.

[145] Negri L., Lattanzi R., Tabacco F., Scolaro B. and Rocchi R., Glycodermorphins: Opioid peptides with potent and prolonged analgesic activity and enhanced blood-brain barrier penetration. *British Journal of Pharmacology*, **1998**, *124* (7), 1516–1522.

[146] Negri L., Lattanzi R., Tabacco F., Orrù L., Severini C., Scolaro B. and Rocchi R., Dermorphin and deltorphin glycosylated analogues: Synthesis and antinociceptive activity after systemic administration. *Journal of Medicinal Chemistry*, **1999**, *42* (3), 400–404.

[147] Palian M.M., Boguslavsky V.I., O'Brien D.F. and Polt R., Glycopeptide-membrane interactions: glycosyl enkephalin analogues adopt turn conformations by NMR and CD in amphipathic media. *Journal of the American Chemical Society*, **2003**, *125* (19), 5823–5831.

[148] Polt R., Porreca F., Szabó L.Z. and Hruby V.J., Synthesis of Glycosyl-Enkephalin Analogues which Rapidly Cross the Blood-Brain Barrier to Produce Analgesia in Mice. An Entirely New Class of "Designer Drugs". *Glycoconjugate Journal*, **1993**, *10* (4), 261.

[149] Polt R., Porreca F., Szabó L.Z., Bilsky E.J., Davis P., Abbruscato T.J., Davis T.P., Horvath R., Yamamura H.I. and Hruby V.J., Glycopeptide enkephalin analogues produce analgesia in mice: evidence for penetration of the blood-brain barrier. *Proceedings of the National Academy of Sciences of the United States of America*, **1994**, *91* (15), 7114–7118.

[150] Rodríguez R.E., Rodriguez F.D., Sacristán M.P., Torres J.L., VALENCIA G. and García-Antón J.M., New glycosylpeptides with high antinociceptive activity. *Neuroscience Letters*, **1989**, *101* (1), 89–94.

[151] Tomatis R., Marastoni M., Balboni G., Guerrini R., Capasso A., Sorrentino L., Santagada V., Caliendo G., Lazarus L.H. and Salvadori S., Synthesis and pharmacological activity of deltorphin and dermorphin-related glycopeptides. *Journal of Medicinal Chemistry*, **1997**, *40* (18), 2948–2952.

[152] Torres J.L., Reig F., Valencia G., Rodríguez R.E. and García-Antón J.M., [d-Met2, Pro5] enkephalin [N1.5-β-d-glucopyranosyl] amide: a glycosylpeptide with high antinociceptive activity. *International Journal of Peptide and Protein Research*, **2009**, *31* (5), 474–480.

[153] Varga-Defterdarović L., Horvat v., Chung N.N. and Schiller P.W., Glycoconjugates of opioid peptides. *International Journal of Peptide and Protein Research*, **2009**, *39* (1), 12–17.

[154] Wong A.K., Ross B.P., Chan Y.N., Artursson P., Lazorova L., Jones A. and Toth I., Determination of transport in the Caco-2 cell assay of compounds varying in lipophilicity using LC-MS: Enhanced transport of Leu-enkephalin analogues. *European Journal of Pharmaceutical Sciences*, **2002**, *16* (3), 113–118.

[155] Mahraoui L., Rodolosse A., Barbat A., Dussaulx E., Zweibaum A., Rousset M. and Brot-Laroche E., Presence and differential expression of

SGLT1, GLUT1, GLUT2, GLUT3 and GLUT5 hexose-transporter mRNAs in Caco-2 cell clones in relation to cell growth and glucose consumption. *The Biochemical Journal*, **1994**, *298 Pt 3*, 629–633.

[156] Williams S.A., Abbruscato T.J., Szabó L.Z., Polt R., Hruby V.J. and Davis T.P., The Effect of Glycosylation on the Uptake of an Enkephalin Analogue into the Central Nervous System. P.O. Couraud and D. Scherman (editors), *Biology and Physiology of the Blood-Brain Barrier*, *Advances in Behavioral Biology*, volume 46 (Springer US, Boston, MA, **1996**), 69–77.

[157] Thompson K.A., Cherry C.L., Bell J.E. and McLean C.A., Brain cell reservoirs of latent virus in presymptomatic HIV-infected individuals. *American Journal of Pathology*, **2011**, *179*, 1623–1629.

[158] Bonina F., Puglia C., Rimoli M.G., Avallone L., Abignente E., Boatto G., Nieddu M., Meli R., Amorena M. and de Caprariis P., Synthesis and in vitro chemical and enzymatic stability of glycosyl 3'-azido-3'-deoxythymidine derivatives as potential anti-HIV agents. *European Journal of Pharmaceutical Sciences*, **2002**, *16* (3), 167–174.

[159] Rouquayrol M., Gaucher B., Greiner J., Aubertin A.M., Vierling P. and Guedj R., Synthesis and anti-HIV activity of glucose-containing prodrugs derived from saquinavir, indinavir and nelfinavir. *Carbohydrate Research*, **2001**, *336* (3), 161–180.

[160] Rouquayrol M., Gaucher B., Roche D., Greiner J. and Vierling P., Transepithelial transport of prodrugs of the HIV protease inhibitors saquinavir, indinavir, and nelfinavir across Caco-2 cell monolayers. *Pharmaceutical Research*, **2002**, *19* (11), 1704–1712.

[161] Jacob J.N. and Tazawa M.J., Glucose-aspirin: Synthesis and in vitro anti-cancer activity studies. *Bioorganic & Medicinal Chemistry Letters*, **2012**, *22* (9), 3168–3171.

[162] Chen Q., Gong T., Liu J., Wang X., Fu H. and Zhang Z., Synthesis, in vitro and in vivo characterization of glycosyl derivatives of ibuprofen as novel prodrugs for brain drug delivery. *Journal of Drug Targeting*, **2009**, *17* (4), 318–328.

[163] Gynther M., Ropponen J., Laine K., Leppänen J., Haapakoski P., Peura L., Järvinen T. and Rautio J., Glucose promoiety enables glucose transporter mediated brain uptake of ketoprofen and indomethacin prodrugs in rats. *Journal of Medicinal Chemistry*, **2009**, *52* (10), 3348–3353.

[164] Halmos T., Santarromana M., Antonakis K. and Scherman D., Synthesis of O-methylsulfonyl derivatives of D-glucose as potential alkylating agents for targeted drug delivery to the brain. Evaluation of their interaction with the human erythrocyte GLUT1 hexose transporter. *Carbohydrate Research*, **1997**, *299* (1-2), 15–21.

[165] Halmos T., Santarromana M., Antonakis K. and Scherman D., Synthesis of glucose-chlorambucil derivatives and their recognition by the human GLUT1 glucose transporter. *European Journal of Pharmacology*, **1996**, *318* (2-3), 477–484.

[166] Uriel C., Egron M.J., Santarromana M., Scherman D., Antonakis K. and Herscovici J., Hexose keto-C-glycoside conjugates: design, synthesis, cytotoxicity, and evaluation of their affinity for the glucose transporter Glut-1. *Bioorganic & Medicinal Chemistry Letters*, **1996**, *4* (12), 2081–2090.

[167] Borst P., Evers R., Kool M. and Wijnholds J., A family of drug transporters: the multidrug resistance-associated proteins. *Journal of the National Cancer Institute*, **2000**, *92* (16), 1295–1302.

[168] Joyce H., McCann A., Clynes M. and Larkin A., Influence of multidrug resistance and drug transport proteins on chemotherapy drug metabolism. *Expert Opinion on Drug Metabolism & Toxicology*, **2015**, *1*, 1–15.

[169] Zhang X., Dong D., Wang H., Ma Z., Wang Y. and Wu B., Stable Knock-down of Efflux Transporters Leads to Reduced Glucuronidation in UGT1A1-Overexpressing HeLa Cells: The Evidence for Glucuronidation-Transport Interplay. *Molecular Pharmaceutics*, **2015**, *12* (4), 1268–78.

[170] Wei Y., Wu B., Jiang W., Yin T., Jia X., Basu S., Yang G. and Hu M., Revolving door action of breast cancer resistance protein (BCRP) facilitates or controls the efflux of flavone glucuronides from UGT1A9-overexpressing HeLa cells. *Molecular Pharmaceutics*, **2013**, *10* (5), 1736–50.

[171] Chang J.H. and Benet L.Z., Glucuronidation and the transport of the glucuronide metabolites in LLC-PK1 cells. *Molecular Pharmaceutics*, **2005**, *2* (5), 428–34.

[172] Mulder G.J., Pharmacological effects of drug conjugates: Is morphine 6-glucuronide an exception? *Trends in Pharmacological Sciences*, **1992**, *13* (8), 302–304.

[173] Wu D., Kang Y.S., Bickel U. and Pardridge W.M., Blood-Brain Barrier Permeability to Morphine-6-Glucuronide is Markedly Reduced Compared with Morphine. *Drug Metabolism and Disposition*, **1997**, *25* (6), 768–771.

[174] Stachulski A.V., Scheinmann F., Ferguson J.R., Law J.L., Lumbard K.W., Hopkins P., Patel N., Clarke S., Gloyne A. and Joel S.P., StructureâĂŞactivity relationships of some opiate glycosides. *Bioorganic & Medicinal Chemistry Letters*, **2003**, *13* (6), 1207–1214.

[175] Arsequell G., Salvatella M., Valencia G., Fernández-Mayoralas A., Fontanella M., Venturi C., Jiménez-Barbero J., Marrón E. and Rodríguez R.E., Synthesis, conformation, and biological characterization of a sugar derivative of morphine that is a potent, long-lasting, and nontolerant antinociceptive. *Journal of Medicinal Chemistry*, **2009**, *52* (9), 2656–2666.

[176] Bourasset F., Cisternino S., Temsamani J. and Scherrmann J.M., Evidence for an active transport of morphine-6-β-d-glucuronide but not P-glycoprotein-mediated at the blood-brain barrier. *Journal of Neurochemistry*, **2003**, *86* (6), 1564–1567.

[177] Sattari M., Routledge P. and Mashayekhi S., The influence of active transport systems on morphine -6-glucuronide transport in MDCKII and MDCK-PGP cells. *Daru : Journal of Pharmaceutical Sciences*, **2011**, *19* (6), 412–416.

[178] Battaglia G., La Russa M., Bruno V., Arenare L., Ippolito R., Copani A., Bonina F. and Nicoletti F., Systemically administered D-glucose conjugates of 7-chlorokynurenic acid are centrally available and exert anticonvulsant activity in rodents. *Brain Research*, **2000**, *860* (1-2), 149–156.

[179] Speizer L., Haugland R. and Kutchai H., Asymmetric transport of a fluorescent glucose analogue by human erythrocytes. *Biochimica et Biophysica Acta - Biomembranes*, **1985**, *815* (1), 75–84.

[180] Barros L.F., Bittner C.X., Loaiza A., Ruminot I., Larenas V., Moldenhauer H., Oyarzún C. and Alvarez M., Kinetic validation of 6-NBDG as a probe for the glucose transporter GLUT1 in astrocytes. *Journal of Neurochemistry*, **2009**, *109 Suppl*, 94–100.

[181] Bonina F., Puglia C., Rimoli M.G., Melisi D., Boatto G., Nieddu M., Calignano A., La Rana G. and De Caprariis P., Glycosyl derivatives of dopamine and L-dopa as anti-Parkinson prodrugs: synthesis, pharmacological activity and in vitro stability studies. *Journal of Drug Targeting*, **2003**, *11* (1), 25–36.

[182] Fernández C., Nieto O., Rivas E., Montenegro G., Fontenla J.A. and Fernández-Mayoralas, Synthesis and biological studies of glycosyl dopamine derivatives as potential antiparkinsonian agents. *Carbohydrate Research*, **2000**, *327* (4), 353–365.

[183] Fernández C., Nieto O., Fontenla J.A., Rivas E., de Ceballos M.L. and Fernández-Mayoralas A., Synthesis of glycosyl derivatives as dopamine prodrugs: interaction with glucose carrier GLUT-1. *Organic & Biomolecular Chemistry*, **2003**, *1* (5), 767–771.

[184] García-Alvarez I., Garrido L. and Fernández-Mayoralas A., Studies on the uptake of glucose derivatives by red blood cells. *ChemMedChem*, **2007**, *2* (4), 496–504.

[185] Storr T., Merkel M., Song-Zhao G.X., Scott L.E., Green D.E., Bowen M.L., Thompson K.H., Patrick B.O., Schugar H.J. and Orvig C., Synthesis, characterization, and metal coordinating ability of multifunctional carbohydrate-containing compounds for Alzheimer's therapy. *Journal of the American Chemical Society*, **2007**, *129* (23), 7453–7463.

[186] Schugar H.J., Green D.E., Bowen M.L., Scott L.E., Storr T., Bohmerle K., Thomas F., Allen D.D., Lockman P.R., Merkel M., Thompson K.H.,

Orvig C. and Böhmerle K., Combating Alzheimer's disease with multifunctional molecules designed for metal passivation. *Angewandte Chemie (International ed. in English)*, **2007**, *46* (10), 1716–1718.

[187] Scott L.E., Telpoukhovskaia M., Rodríguez-Rodríguez C., Merkel M., Bowen M.L., Page B.D.G., Green D.E., Storr T., Thomas F., Allen D.D., Lockman P.R., Patrick B.O., Adam M.J. and Orvig C., N-Aryl-substituted 3-(β-D-glucopyranosyloxy)-2-methyl-4(1H)-pyridinones as agents for Alzheimer's therapy. *Chemical Science*, **2011**, *2* (4), 642–648.

[188] Green D.E., Bowen M.L., Scott L.E., Storr T., Merkel M., Böhmerle K., Thompson K.H., Patrick B.O., Schugar H.J. and Orvig C., In vitro studies of 3-hydroxy-4-pyridinones and their glycosylated derivatives as potential agents for Alzheimer's disease. *Dalton Transactions*, **2010**, *39* (6), 1604–1615.

[189] Blanksby S.J. and Ellison G.B., Bond dissociation energies of organic molecules. *Accounts of Chemical Research*, **2003**, *36* (4), 255–63.

[190] Kürti L. and Czakó B., *Strategic Applications of Named Reactions in Organic Synthesis : Background and Detailed Mechanisms* (Elsevier Academic Press, Amsterdam, Boston, **2005**), 1st edition.

[191] Roslund M.U., Tähtinen P., Niemitz M. and Sjöholm R., Complete assignments of the (1)H and (13)C chemical shifts and J(H,H) coupling constants in NMR spectra of D-glucopyranose and all D-glucopyranosyl-D-glucopyranosides. *Carbohydrate Research*, **2008**, *343* (1), 101–112.

[192] Saghaie L. and Hider R.C., Synthesis and physico-chemical properties of a series of bidentate 3-hydroxypyridin-4-ones iron chelating agents. *Research in Pharmaceutical Sciences*, **2008**, *3* (April), 21–30.

[193] Klapars A. and Buchwald S.L., Copper-Catalyzed Halogen Exchange in Aryl Halides: An Aromatic Finkelstein Reaction. *Journal of the American Chemical Society*, **2002**, *124* (50), 14844–14845.

[194] Clarke E.T. and Martell A.E., Stabilities of 1,2-dimethyl-3-hydroxy-4-pyridinone chelates of divalent and trivalent metal ions. *Inorganica Chimica Acta*, **1992**, *191* (1), 57–63.

[195] El-Jammal A., Howell P.L., Turner M.A., Li N. and Templeton D.M., Copper Complexation by 3-Hydroxypyridin-4-one Iron Chelators: Structural and Iron Competition Studies. *Journal of Medicinal Chemistry*, **1994**, *37* (4), 461–466.

[196] Kalchhauser H. and Robien W., CSEARCH: A computer program for identification of organic compounds and fully automated assignment of carbon-13 nuclear magnetic resonance spectra. *Journal of Chemical Information and Computer Sciences*, **1985**, *25* (2), 103–108.

[197] NMR Predict. Modgraph Consultants, Ltd., Welwyn, Herts., UK. **2014**.

[198] ACD/NMR Predictors. Advanced Chemistry Development, Inc. (ACD/Labs), Toronto, ON, Canada. **2014**.

[199] Dobbin P.S., Hider R.C., Hall A.D., Taylor P.D., Sarpong P., Porter J.B., Xiao G. and van der Helm D., Synthesis, physicochemical properties, and biological evaluation of N-substituted 2-alkyl-3-hydroxy-4(1H)-pyridinones: Orally active iron chelators with clinical potential. *Journal of Medicinal Chemistry*, **1993**, *36* (17), 2448–2458.

[200] Chen Y.L., Barlow D.J., Kong X.L., Ma Y.M. and Hider R.C., Prediction of 3-hydroxypyridin-4-one (HPO) hydroxyl pKa values. *Dalton Transactions*, **2012**, *41* (21), 6549–6557.

[201] Bartulin J., Belmar J., Gallardo H. and Leon G., Syntheses of 2-acetyl-3-hydroxy-1-n-propylpyrrole from isomaltol and 1-n-alkyl-3-hydroxy-2-methyl-4-pyridones from maltol. *Journal of Heterocyclic Chemistry*, **1992**, *29* (4), 1017–1019.

[202] Elkaschef M.A.F. and Nosseir M.H., The 4-Pyrones. Part I. Reactions of Some 4-Pyrones and 4-Thiopyrones Involving the Ring Oxygen. *Journal of the American Chemical Society*, **1960**, *82* (16), 4344–4347.

[203] Liu Z.D., Khodr H.H., Liu D.Y., Lu S.L. and Hider R.C., Synthesis, physicochemical characterization, and biological evaluation of 2-(1'-hydroxyalkyl-3-hydroxypyridin-4-ones: Novel iron chelators with enhanced pFe3+ values. *Journal of Medicinal Chemistry*, **1999**, *42*, 4814–4823.

[204] Piyamongkol S., Liu Z.D. and Hider R.C., Novel Synthetic Approach to 2-(1'-Hydroxyalkyl)- and 2-Amido-3-hydroxypyridin-4-ones. *Tetrahedron*, **2001**, *57* (16), 3479–3486.

[205] Pace P., Nizi E., Pacini B., Pesci S., Matassa V., De Francesco R., Altamura S. and Summa V., The monoethyl ester of meconic acid is an active site inhibitor of HCVNS5B RNA-dependent RNA polymerase. *Bioorganic & Medicinal Chemistry Letters*, **2004**, *14* (12), 3257–3261.

[206] Kulangara V.R.K. and Raj T.T., Process for the preparation of substituted pyridone carboxylic acids. **2010**.

[207] Shi G. and Ji X., New ways to derivatize at position 6 of 7,7-dimethyl-7,8-dihydropterin. *Tetrahedron Letters*, **2011**, *52* (46), 6174–6176.

[208] Wang Y.F., Zhang F.L. and Chiba S., Copper-Catalyzed Aerobic Methyl/-Methylene Oxygenation and C-H Formylation with a DABCO-DMSO System for the Synthesis of Carbonyl Indoles and Pyrroles. *Synthesis*, **2012**, *44* (10), 1526–1534.

[209] Bergmann M. and Zervas L., Synthesen mit Glucosamin. *Berichte der Deutschen Chemischen Gesellschaft*, **1931**, *64*, 975–980.

[210] Myszka H., Bednarczyk D., Najder M. and Kaca W., Synthesis and induction of apoptosis in B cell chronic leukemia by diosgenyl 2-amino-2-deoxy-beta-D-glucopyranoside hydrochloride and its derivatives. *Carbohydrate Research*, **2003**, *338* (2), 133–141.

[211] Wuts P.G.M. and Greene T.W., *Greene's Protective Groups in Organic Synthesis* (John Wiley & Sons, Inc., Hoboken, New Jersey, **2007**), 4th edition.

[212] Fieser M., Fieser L.F., Toromanoff E., Hirata Y., Heymann H., Tefft M. and Bhattacharya S., Synthetic Emulsifying Agents. *Journal of the American Chemical Society*, **1956**, *78* (12), 2825–2832.

[213] Owen L.N., Peat S. and Jones W.J.G., 65. Furanose and pyranose derivatives of glucurone. *Journal of the Chemical Society (Resumed)*, **1941**, 339–344.

[214] Csuk R., Müller N. and Weidmann H., Vollständige 13C-NMR-Zuordnung von gluco- und idokonfigurierten 1,2-O-Alkyliden-furanurono-6,3-lactonen durch 2D-1H-13C-korrelierte NMR-Spektroskopie. *Monatshefte für Chemie*, **1984**, *115* (1), 93–99.

[215] Weymouth-Wilson A.C. and Fleet G.W.J., Stereospecific Synthesis of Iduronic Acid Derivatives, Deoxynojirimycin and Deoxyidonojirimycin. **2010**.

[216] Jenkinson S.F., Best D., Weymouth-Wilson A.C., Clarkson R.A., Fleet G.W.J. and Watkin D.J., (1S)-1,2-O-Benzylidene-α-d-glucurono-6,3-lactone. *Acta Crystallographica. Section E, Structure Reports Online*, **2009**, *65* (Pt 2), o414–o415.

[217] Li Y., Manickam G., Ghoshal A. and Subramaniam P., More Efficient Palladium Catalyst for Hydrogenolysis of Benzyl Groups. *Synthetic Communications*, **2006**, *36* (7), 925–928.

[218] Huisgen R., 1.3-Dipolare Cycloadditionen Rückschau und Ausblick. *Angewandte Chemie*, **1963**, *75* (13), 604–637.

[219] Tornoe C.W., Christensen C. and Meldal M., Peptidotriazoles on Solid Phase: [1,2,3]-Triazoles by Regiospecific Copper(I)-Catalyzed 1,3-Dipolar Cycloadditions of Terminal Alkynes to Azides. *The Journal of Organic Chemistry*, **2002**, *67* (9), 3057–3064.

[220] Rostovtsev V.V., Green L.G., Fokin V.V. and Sharpless K.B., A stepwise huisgen cycloaddition process: copper(I)-catalyzed regioselective "ligation" of azides and terminal alkynes. *Angewandte Chemie (International ed. in English)*, **2002**, *41* (14), 2596–2599.

[221] Meldal M. and Tornoe C.W., Cu-catalyzed azide-alkyne cycloaddition. *Chemical Reviews*, **2008**, *108* (8), 2952–3015.

[222] Moses J.E. and Moorhouse A.D., The growing applications of click chemistry. *Chemical Society Reviews*, **2007**, *36* (8), 1249–1262.

[223] McNulty J., Keskar K. and Vemula R., The first well-defined silver(I)-complex-catalyzed cycloaddition of azides onto terminal alkynes at room temperature. *Chemistry (Weinheim an der Bergstrasse, Germany)*, **2011**, *17* (52), 14727–14730.

[224] McNulty J. and Keskar K., Discovery of a Robust and Efficient Homogeneous Silver(I) Catalyst for the Cycloaddition of Azides onto Terminal Alkynes. *European Journal of Organic Chemistry*, **2012**, *2012* (28), 5462–5470.

[225] Gao M., He C., Chen H., Bai R., Cheng B. and Lei A., Synthesis of pyrroles by click reaction: silver-catalyzed cycloaddition of terminal alkynes with isocyanides. *Angewandte Chemie (International ed. in English)*, **2013**, *52* (27), 6958–6961.

[226] Baskin J.M., Prescher J.A., Laughlin S.T., Agard N.J., Chang P.V., Miller I.A., Lo A., Codelli J.A. and Bertozzi C.R., Copper-free click chemistry for dynamic in vivo imaging. *Proceedings of the National Academy of Sciences of the United States of America*, **2007**, *104* (43), 16793–16797.

[227] Liu P.N., Li J., Su F.H., Ju K.D., Zhang L., Shi C., Sung H.H.Y., Williams I.D., Fokin V.V., Lin Z. and Jia G., Selective Formation of 1,4-Disubstituted Triazoles from Ruthenium-Catalyzed Cycloaddition of Terminal Alkynes and Organic Azides: Scope and Reaction Mechanism. *Organometallics*, **2012**, *31* (13), 4904–4915.

[228] Boren B.C., Narayan S., Rasmussen L.K., Zhang L., Zhao H., Lin Z., Jia G. and Fokin V.V., Ruthenium-catalyzed azide-alkyne cycloaddition: scope and mechanism. *Journal of the American Chemical Society*, **2008**, *130* (28), 8923–8930.

[229] Zhang L., Chen X., Xue P., Sun H.H.Y., Williams I.D., Sharpless K.B., Fokin V.V. and Jia G., Ruthenium-catalyzed cycloaddition of alkynes and organic azides. *Journal of the American Chemical Society*, **2005**, *127* (46), 15998–15999.

[230] Goddard-Borger E.D. and Stick R.V., An efficient, inexpensive, and shelf-stable diazotransfer reagent: imidazole-1-sulfonyl azide hydrochloride. *Organic Letters*, **2007**, *9* (19), 3797–3800.

[231] Amigues E.J., Greenberg M.L., Ju S., Chen Y. and Migaud M.E., Synthesis of cyclophospho-glucoses and glucitols. *Tetrahedron*, **2007**, *63* (40), 10042–10053.

[232] Halcomb R.L. and Danishefsky S.J., On the direct epoxidation of glycals: application of a reiterative strategy for the synthesis of beta-linked oligosaccharides. *Journal of the American Chemical Society*, **1989**, *111* (17), 6661–6666.

[233] Gilbert J.C. and Weerasooriya U., Diazoethenes: Their attempted synthesis from aldehydes and aromatic ketones by way of the Horner-Emmons modification of the Wittig reaction. A facile synthesis of alkynes. *The Journal of Organic Chemistry*, **1982**, *47* (10), 1837–1845.

[234] Leeuwenburgh M.A., Timmers C.M., van der Marel G.A., van Boom J.H., Mallet J.M. and Sinaÿ P.G., Stereoselective Synthesis of α-C-(alkynyl)-glycosides via Ring-opening of α-1,2-Anhydrosugars. *Tetrahedron Letters*, **1997**, *38* (35), 6251–6254.

[235] Leeuwenburgh M.A., van der Marel G.A., Overkleeft H.S. and van Boom J.H., From α-1,2-Anhydrosugars to C-Glycosides: The Influence of Lewis Acids and Nucleophiles on the Stereochemistry. *Journal of Carbohydrate Chemistry*, **2003**, *22* (7-8), 549–564.

[236] Kuijpers B.H.M., Groothuys S., Keereweer a.B.R., Quaedflieg P.J.L.M., Blaauw R.H., van Delft F.L. and Rutjes F.P.J.T., Expedient synthesis of triazole-linked glycosyl amino acids and peptides. *Organic Letters*, **2004**, *6* (18), 3123–3126.

[237] Richards S.J., Jones M.W., Hunaban M., Haddleton D.M. and Gibson M.I., Probing bacterial-toxin inhibition with synthetic glycopolymers prepared by tandem post-polymerization modification: Role of linker length and carbohydrate density. *Angewandte Chemie (International ed. in English)*, **2012**, *51* (31), 7812–6.

[238] Sirion U., Kim H.J., Lee J.H., Seo J.W., Lee B.S., Lee S.J., Oh S.J. and Chi D.Y., An efficient F-18 labeling method for PET study: Huisgen 1,3-dipolar cycloaddition of bioactive substances and F-18-labeled compounds. *Tetrahedron Letters*, **2007**, *48* (23), 3953–3957.

[239] Fischer N., Goddard-Borger E.D., Greiner R., Klapötke T.M., Skelton B.W. and Stierstorfer J., Sensitivities of some imidazole-1-sulfonyl azide salts. *The Journal of Organic Chemistry*, **2012**, *77* (4), 1760–1764.

[240] Tagmose T.M. and Bols M., Synthesis of the 2-Deoxyisomaltose Analogue of Acarbose by an Improved Route to Chiral Valieneamines. *Chemistry - A European Journal*, **1997**, *3* (3), 453–462.

[241] Li S.C., Meng X.B., Cai M.S. and Li Z.J., Optimized Procedure for the Synthesis of 6-Azido-6-deoxy-galactopyranosides From 6-O-Tosyl-galactopyranosides. *Synthetic Communications*, **2006**, *36* (5), 637–643.

[242] Sharpless W.D., Wu P., Hansen T.V. and Lindberg J.G., Just click it: undergraduate procedures for the copper(I)-catalyzed formation of 1,2,3-triazoles from azides and terminal acetylenes. *Journal of Chemical Education*, **2005**, *82* (12), 1833–1836.

[243] Creary X., Anderson A., Brophy C., Crowell F. and Funk Z., Method for assigning structure of 1,2,3-triazoles. *Journal of Organic Chemistry*, **2012**, *77* (19), 8756–8761.

[244] Negrón-Silva G.E., González-Olvera R., Angeles-Beltrán D., Maldonado-Carmona N., Espinoza-Vázquez A., Palomar-Pardavé M.E., Romero-Romo M.a. and Santillan R., Synthesis of new 1,2,3-triazole derivatives of uracil and thymine with potential inhibitory activity against acidic corrosion of steels. *Molecules*, **2013**, *18* (4), 4613–4627.

[245] Toppet S., Wouters G. and Smets G., 1H and 13C NMR study of the prototropic tautomerism of 4(5)-vinyl-1,2,3-triazole in dimethylformamide as solvent. *Organic Magnetic Resonance*, **1978**, *11* (11), 578–579.

[246] Kann N., Johansson J.R. and Beke-Somfai T., Conformational properties of 1,4- and 1,5-substituted 1,2,3-triazole amino acids âĂŞ building units for peptidic foldamers. *Organic & Biomolecular Chemistry*, **2015**, *13* (9), 2776–2785.

[247] Zhou T., Neubert H., Liu D.Y., Liu Z.D., Ma Y.M., Kong X.L., Luo W., Mark S. and Hider R.C., Iron binding dendrimers: A novel approach for the treatment of haemochromatosis. *Journal of Medicinal Chemistry*, **2006**, *49* (14), 4171–82.

[248] Naik P. and Cucullo L., In vitro blood-brain barrier models: Current and perspective technologies. *Journal of Pharmaceutical Sciences*, **2012**, *101* (4), 1337–1354.

[249] de Boer A. and Gaillard P., In Vitro Models of the Blood-Brain Barrier: When to Use Which? *Current Medicinal Chemistry - Central Nervous System Agents*, **2002**, *2* (3), 203–209.

[250] Deli M.A., Abrahám C.S., Kataoka Y. and Niwa M., Permeability studies on in vitro blood-brain barrier models: Physiology, Pathology, and Pharmacology. *Cellular and Molecular Neurobiology*, **2005**, *25* (1), 59–127.

[251] Garberg P., Ball M., Borg N., Cecchelli R., Fenart L., Hurst R.D., Lindmark T., Mabondzo A., Nilsson J.E., Raub T.J., Stanimirovic D., Terasaki T., Oberg J.O. and Osterberg T., In vitro models for the blood-brain barrier. *Toxicology in vitro*, **2005**, *19* (3), 299–334.

[252] Gumbleton M. and Audus K.L., Progress and limitations in the use of in vitro cell cultures to serve as a permeability screen for the blood-brain barrier. *Journal of Pharmaceutical Sciences*, **2001**, *90* (11), 1681–98.

[253] Reichel A., Begley D.J. and Abbott N.J., An overview of in vitro techniques for blood-brain barrier studies. *Methods in Molecular Medicine*, **2003**, *89*, 307–24.

[254] Weksler B., Romero I.A. and Couraud P.O., The hCMEC/D3 cell line as a model of the human blood brain barrier. *Fluids and Barriers of the CNS*, **2013**, *10* (1), 16.

[255] Patabendige A., Skinner R.A., Morgan L. and Abbott N.J., A detailed method for preparation of a functional and flexible blood-brain barrier model using porcine brain endothelial cells. *Brain Research*, **2013**, *1521*, 16–30.

[256] Warren M.S., Zerangue N., Woodford K., Roberts L.M., Tate E.H., Feng B., Li C., Feuerstein T.J., Gibbs J., Smith B., de Morais S.M., Dower W.J. and Koller K.J., Comparative gene expression profiles of ABC transporters in brain microvessel endothelial cells and brain in five species including human. *Pharmacological Research*, **2009**, *59*, 404–413.

[257] Patabendige A., Skinner R.A. and Abbott N.J., Establishment of a simplified in vitro porcine blood-brain barrier model with high transendothelial electrical resistance. *Brain Research*, **2013**, *1521*, 1–15.

[258] Neuwelt E.A., Bauer B., Fahlke C., Fricker G., Iadecola C., Janigro D., Leybaert L., Molnár Z., O'Donnell M.E., Povlishock J.T., Saunders N.R., Sharp F., Stanimirovic D., Watts R.J. and Drewes L.R., Engaging neuroscience to advance translational research in brain barrier biology. *Nature Reviews. Neuroscience*, **2011**, *12* (3), 169–182.

[259] Malina K.C.K., Cooper I. and Teichberg V.I., Closing the gap between the in-vivo and in-vitro blood-brain barrier tightness. *Brain Research*, **2009**, *1284*, 12–21.

[260] Butt A.M., Jones H.C. and Abbott N.J., Electrical resistance across the blood-brain barrier in anaesthetized rats: a developmental study. *The Journal of Physiology*, **1990**, *429*, 47–62.

[261] Hawkins B.T. and Egleton R.D., Fluorescence imaging of blood-brain barrier disruption. *Journal of Neuroscience Methods*, **2006**, *151* (2), 262–7.

[262] Nag S., Blood-brain barrier permeability using tracers and immunohistochemistry. *Methods in Molecular Medicine*, **2003**, *89*, 133–44.

[263] Youdim K.A., Dobbie M.S., Kuhnle G., Proteggente A.R., Abbott N.J. and Rice-Evans C., Interaction between flavonoids and the blood-brain barrier: in vitro studies. *Journal of Neurochemistry*, **2003**, *85* (1), 180–192.

[264] Molinspiration miLogP http://www.molinspiration.com/services/logp.html.

[265] Enanga B., Burchmore R.J.S., Stewart M.L. and Barrett M.P., Sleeping sickness and the brain. *Cellular and Molecular Life Sciences*, **2002**, *59*, 845–858.

[266] Wolburg H., Mogk S., Acker S., Frey C., Meinert M., Schönfeld C., Lazarus M., Urade Y., Kubata B.K. and Duszenko M., Late stage infection in sleeping sickness. *PLoS ONE*, **2012**, *7* (3), e34304.

[267] Gottlieb H.E., Kotlyar V. and Nudelman A., NMR Chemical Shifts of Common Laboratory Solvents as Trace Impurities. *The Journal of Organic Chemistry*, **1997**, *62* (21), 7512–7515.

[268] Himanen J.A. and Pihko P.M., Synthesis of Trisaccharides by Hetero-Diels-Alder Welding of Two Monosaccharide Units. *European Journal of Organic Chemistry*, **2012**, *2012* (20), 3765–3780.

[269] Bartlett M.J., Turner C.A. and Harvey J.E., Pd-catalyzed allylic alkylation cascade with dihydropyrans: Regioselective synthesis of furo[3,2-c]pyrans. *Organic Letters*, **2013**, *15* (10), 2430–2433.

[270] Scott L.E., Page B.D.G., Patrick B.O. and Orvig C., Altering pyridinone N-substituents to optimise activity as potential prodrugs for Alzheimer's disease. *Dalton Transactions*, **2008**, (45), 6364–6367.

[271] Telpoukhovskaia M.A., Rodríguez-Rodríguez C., Scott L.E., Page B.D.G., Patrick B.O. and Orvig C., Synthesis, characterization, and cytotoxicity studies of Cu(II), Zn(II), and Fe(III) complexes of N-derivatized 3-hydroxy-4-pyridiones. *Journal of Inorganic Biochemistry*, **2014**, *132*, 59–66.

[272] Zhang Z., Rettig S.J. and Orvig C., Lipophilic coordination compounds: Aluminum, gallium, and indium complexes of 1-aryl-3-hydroxy-2-methyl-4-pyridinones. *Inorganic Chemistry*, **1991**, *30* (3), 509–515.

[273] Ciupa A., De Bank P.A. and Caggiano L., Multicellular aggregation of maltol-modified cells triggered by Fe(3+) ions. *Chemical Communications*, **2013**, *49* (86), 10148–10150.

[274] Kröger L. and Thiem J., Convenient Multigram Scale Glycosylations of Scented Alcohols Employing Phase-Transfer Reactions. *Journal of Carbohydrate Chemistry*, **2003**, *22* (1), 9–23.

[275] Yasue M., Kawamura N. and Sakakibara J., Syntheses of N-substituted-3-glucosyloxy-2-methyl-4-pyridones and their aglycones. *Yakugaku Zasshi*, **1970**, *90* (10), 1222–1225.

[276] Nunes A., Marques S.M., Quintanova C., Silva D.F., Cardoso S.M., Chaves S. and Santos M.A., Multifunctional iron-chelators with protective roles against neurodegenerative diseases. *Dalton transactions (Cambridge, England : 2003)*, **2013**, *42* (17), 6058–73.

[277] Johns B.A., Duan M. and Hakogi T., Processes and Intermediated for Carbamoylpyridone HIV Integrade Inhibitors. **2010**.

[278] Xie Y.Y., Liu M.S., Hu P.P., Kong X.L., Qiu D.H., Xu J.L., Hider R.C. and Zhou T., Synthesis, physico-chemical properties, and antimicrobial evaluation of a new series of iron(III) hexadentate chelators. *Medicinal Chemistry Research*, **2013**, *22* (5), 2351–2359.

[279] Mulard L., Boutet J., Guerreiro C., Nato F., Sansonetti P. and Phalipon A., Glycoconjugates and use thereof as vaccine against shigella flexneri serotype 3a and x. **2010**.

[280] Xu Y., Choi S.R., Kung M.P. and Kung H.F., Synthesis of radioiodinated 1-deoxy-nojirimycin derivatives: novel glucose analogs. *Nuclear Medicine and Biology*, **1999**, *26* (7), 833–839.

[281] Macher I., Dax K., Wanek E. and Weidmann H., Synthesis of l-idofuranurono-6,3-lactone and its derivatives via hexodialdodifuranoses. *Carbohydrate Research*, **1980**, *80* (1), 45–51.

[282] Ma Y.M., Luo W., Quinn P.J., Liu Z.D. and Hider R.C., Design, synthesis, physicochemical properties, and evaluation of novel iron chelators with fluorescent sensors. *Journal of Medicinal Chemistry*, **2004**, *47* (25), 6349–62.

[283] Gehrke S.S., Pinto E.G., Steverding D., Pleban K., Tempone A.G., Hider R.C. and Wagner G.K., Conjugation to 4-aminoquinoline improves the anti-trypanosomal activity of Deferiprone-type iron chelators. *Bioorganic & Medicinal Chemistry*, **2013**, *21* (3), 805–13.

[284] Mendoza-Ferri M.G., Hartinger C.G., Mendoza M.A., Groessl M., Egger A.E., Eichinger R.E., Mangrum J.B., Farrell N.P., Maruszak M., Bednarski P.J., Klein F., Jakupec M.A., Nazarov A.A., Severin K. and Keppler B.K., Transferring the concept of multinuclearity to ruthenium complexes for improvement of anticancer activity. *Journal of Medicinal Chemistry*, **2009**, *52* (4), 916–925.

[285] Goddard-Borger E.D. and Stick R.V., An Efficient, Inexpensive, and Shelf-Stable Diazotransfer Reagent: Imidazole-1-sulfonyl Azide Hydrochloride - Addition and Correction. *Organic Letters*, **2011**, *13* (9), 2514–2514.

[286] Vasella A., Witzig C., Chiara J.L. and Martin-Lomas M., Convenient Synthesis of 2-Azido-2-deoxy-aldoses by Diazo Transfer. *Helvetica Chimica Acta*, **1991**, *74* (8), 2073–2077.

[287] Lei Z., Wang J., Mao G., Wen Y., Tian Y., Wu H., Li Y. and Xu H., Glucose positions affect the phloem mobility of glucose-fipronil conjugates. *Journal of Agricultural and Food Chemistry*, **2014**, *62* (26), 6065–6071.

[288] Fokt I., Skora S., Conrad C., Madden T., Emmett M. and Priebe W., D-Glucose and D-mannose-based metabolic probes. Part 3: Synthesis of specifically deuterated D-glucose, D-mannose, and 2-deoxy-D-glucose. *Carbohydrate Research*, **2013**, *368*, 111–119.

[289] Berkowitz D.B., Eggen M., Shen Q. and Sloss D.G., Synthesis of (alpha,alpha-difluoroalkyl)phosphonates by displacement of primary triflates. *The Journal of Organic Chemistry*, **1993**, *58* (23), 6174–6176.

[290] Barral K., Balzarini J., Neyts J., De Clercq E., Hider R.C. and Camplo M., Synthesis and antiviral evaluation of cyclic and acyclic 2-methyl-3-hydroxy-4-pyridinone nucleoside derivatives. *Journal of Medicinal Chemistry*, **2006**, *49* (1), 43–50.

[291] Mawani Y., Cawthray J.F., Chang S., Sachs-Barrable K., Weekes D.M., Wasan K.M. and Orvig C., In vitro studies of lanthanide complexes for the treatment of osteoporosis. *Dalton transactions (Cambridge, England : 2003)*, **2013**, *42* (17), 5999–6011.

[292] Sirion U., Lee B.S. and Chi D.Y., Ionic Polymer Supported Copper(I): A Reusable Catalyst for Huisgen's 1,3-Dipolar Cycloaddition. *Synlett*, **2008**, *2008* (15), 2326–2330.